Development of Tailorable Electrically Conductive Thermal Control Material Systems

M.S. Deshpande and Y. Harada
IIT Research Institute, Chicago, IL

National Aeronautics and
Space Administration

Marshall Space Flight Center • MSFC, Alabama 35812
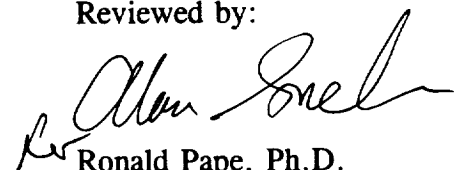
June 1998

Available from:

FOREWORD

This Final Report No. IITRI-C06804-97 under Contract No. NAS8-40580, entitled "Development of Tailorable Electrically Conductive Thermal Control Material Systems", summarizes work initiated in April 1995 and concluded in April 1997. The bulk of the work was performed by August 1996; subsequent work consisted of laboratory studies for formulating candidate thermal control material system (TCMS) to tailor target resistivities using concepts suggested in IIT Research Institute (IITRI) Proposal No. IITRI-94-578AC and space environment simulations studies. These studies have resulted in screening and ranking of developmental electrically conductive thermal control material systems (TCMS) concepts for future scaleup and validation and use on space hardware/space structures.
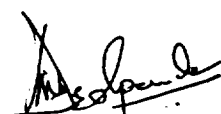
Personnel at IITRI who contributed to this program include: Messrs. T. J. Curtis, W. Sabato, A. Ray, and D. Jones. Mr. G. Sresty acted as Manager of this program. The screening space simulation studies were carried out at the Aerospace Corporation by Dr. M. Meshishnek and at Goddard Space Flight Center (GSFC) by Ms. Wanda Peters and Dr. L. Kauder. Dr. L. Kauder also performed Electro Static Discharge (ESD) testing on candidate materials. Their valuable support, technical input, advice and guidance has helped this program considerably. The continuous encouragement and interest shown in this work by Mr. Pat Carlin (Air Force Materials Laboratory) and Mr. Cliff Cerbus (UDRI) was also valuable. Their efforts in testing a few concepts to typical GEO conditions through space simulation studies at SPECTRE are acknowledged. Lastly, the patient guidance and advice of Mr. Jason Vaughn, Contracting Officer's Representative, are gratefully acknowledged.

The report has been reviewed and found to be in compliance with contract requirements and our internal quality system.

Respectfully submitted,
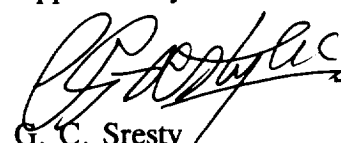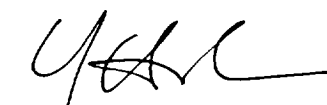IIT RESEARCH INSTITUTE

M. S. Deshpande
Sr. Research Engineer

Reviewed by:

Ronald Pape, Ph.D.
Manager
Chemical Technology Division

Y. Harada
Sr. Materials Scientist

Approved by:

G. C. Sresty
Division Manager
Chemical Technology Division

EXECUTIVE SUMMARY

The optical characteristics of surfaces on spacecraft are fundamental parameters in controlling its temperature. Passive thermal control coatings with designed solar absorptance and infrared emittance properties have been developed and have been in use for some time. In this total space environment, the coating must be stable and maintain its desired optical properties as well as mechanical properties for the course of the mission lifetime. The mission lifetimes are increasing and in our quest to save weight, newer substrates are being integrated which limit electrical grounding schemes. All of this has added to already existing concerns about spacecraft charging and related spacecraft failures or operational failures. The concern is even greater for thermal control surfaces that are very large. One way of alleviating such concerns is to design new thermal control material systems (TCMS) that can help to mitigate charging via providing charge leakage paths.

The objective of this program was to develop two types of passive electrically conductive TCMS. The first was a highly absorbing/emitting black surface and the second was a low (α_S/ϵ_N) type white surface. The surface resistance goals for the black absorber was 10^4 to 10^9 $\Omega/\square$, and for the white surfaces it was 10^6 to 10^{10} $\Omega/\square$. Several material system concepts were suggested and evaluated for space environment stability and electrical performance characterization.

Our efforts in designing and evaluating these material systems have resulted in several developments. New concepts, pigments and binders have been developed to provide new engineering quality TCMS. Some of these have already found application on space hardware, some are waiting to be recognized by thermal designers, and some require further detailed studies to become state-of-the-are for future space hardware and space structures.

Our studies on baseline state-of-the-art materials and conductive concepts have resulted in several important of findings that are of interest to all thermal designers and systems integrators. Some of the important conclusions are as follows:

- All conductive TCMS designs proposed for high absorptivity applications met the program goals of space environment stability and acceptable ESD behavior.

- Studies of the nonconducting state-of-the-art reformulated TCMS showed that:

  (1) S13GP/LO-1 and S13GP/LO-41 show excellent stability to a simulated space environment, approaching that of Z-93P.

  (2) Reformulated YB-71P has essentially the same stability as YB-71.

  (3) Surface resistance of exposed YB-71 and YB-71P are 5.90E+07 to 8.0E+08 $\Omega/\square$.

  (4) Zn_2TiO_4 (ZOT) based TCMS showed a reversal in degradation with UV intensity. This is an interesting finding and needs further conformation study because it may have consequences in material selection for high electron flux orbits.

- Studies of the electrically conductive TCMS concepts showed that:

  (1) The electrically conductive TCMS concepts, Z-93CXY, Z-93SCXY and Z-9SCLMXY, demonstrated the required stability and acceptable ESD performance.

  (2) ZOT/Phos Sol and ZOT/DHS-2 met program goals for stability in the space environment along with required electrical properties. Similar success was also noted for Eu_2O_3-based TCMS. The conductive ZOT-based formulations also showed reversal in degradation with UV intensity as was observed for the nonconducting state-of-the-art systems (Item 4 under last bullet). This is interesting and can have consequences in conductive material selection for high electron flux orbits.

  (3) Two material technologies, doped silicate binder and doped silicate binder based encapsulation, are now available to design the required electrical resistances in the passive TCMS.

  (4) DS13N/LO-XY, flexible conductive TCMS showed acceptable space environment stability, but showed limited success in ESD behavior. Future development steps have been identified as a result of this program.

  (5) Promising electrically conductive passive TCMS have been identified for future investment in scaleup and validation as a result of these efforts. They are listed in the tables provided on the next three pages for ready reference along with their space environment effects' performance. Their ESD performance was considered to be acceptable for use on space hardware.

Typical Performance of Promising Conductive Absorber Optical Coatings						
Material	Pre-exposure α_S	Post-exposure α_S	$\Delta\alpha_S$	Surface Resistivity $\Omega/\square$	Charged to (V)[a]	Remarks
Inorganic-Conductive						
MH55-ICP	0.940	0.938	-0.001	10^8-10^9	<60	b
MH55-ICP	0.942	0.941	-0.001	10^8-10^9	<60	b
MH55-IC	0.928	0.938	0.010	10^8-10^9	<60	c
DBG-IP	0.974	0.975	0.001	10^8-10^9	<80	b
DBG-IP	0.973	0.974	0.001	10^8-10^9	<80	b
DBG-IP	0.957	0.951	-0.006	10^8-10^9	<80	c
DBG-IP	0.970	0.978	0.008	10^8-10^9	<80	d
DBG-DHS	0.958	0.957	-0.001	10^7-10^9	<50	b
DBG-DHS	0.956	0.956	0	10^7-10^9	<50	b
Organic-Flexible-Conductive						
D21S/LO	0.980	0.980	0	10^{10}-10^{11}	N/A	b
D21SC/LO	0.956	0.957	0.001	10^4-10^9	N/A	b
D21SC/LO	0.955	0.956	0.001	10^4-10^9	N/A	b
MH21SC/LO	0.963	0.964	0.001	10^5-10^9	<200	b
MH21SC/LO	0.965	0.965	0	10^5-10^9	<200	b
MH41SCB/LO	0.951	0.950	-0.001	10^8-10^9	<75	b
D36SCB/LO	0.962	0.967	0.005	$<10^3$	<70	c
D36SCBLO	0.966	0.956	-0.010	$<10^3$	<60	d
MH41SCB/LO	0.939	0.947	0.008	10^8-10^9	<75	c
MH21SC/LO	0.951	0.955	0.004	10^5-10^9	<200	c

Remarks:

a = Charged to <50 volts at room temperature; indicated voltages are maximum observed at cryogenic temperatures.
b = Tests performed at Aerospace Corporation
c = Tests performed at GSFC
d = Tests performed at AMCL/SCEPTRE

All tests at GSFC involved exposure to 1000 ESH of UV and Vacuum.

All tests carried out at Aerospace Corporation involved exposure to 2000 ESH of UV + 8.26 x 10^{13} é/cm² [100 KeV] + 5.18 x 10^{13} é/cm² [35 KeV] (typical DMSP orbit) and vacuum.

All tests at AFML/SCEPTRE involved exposure at 2.0 Suns of EUV and 6.78 x 10^{15} e'/cm² (1 KeV) + 3.39 x 10^{15} e'/cm² (10 KeV).

Typical Performance of Promising Conductive White Thermal Control Coatings						
TCMS	**Pre-exposure** α_S	**Post-exposure** α_S	$\Delta\alpha_S$	**Surface Resistivity** $\Omega/\square$	**Charged to V** [a]	**Remarks**
Concept:	Flash Calcination of ZnO (SP-500) to retain controlled Zn interstitials, and stabilization with doped hybrid, silicate binder.					
ZnO(FC)/DHS-2	0.139	0.141	0.002	10^8-10^9	<60	b
ZnO(FC)/DHS-2	0.146	0.146	0.000	10^8-10^9	<60	b
ZnO(FC)/DHS-2	0.168	0.168	0.010	10^8-10^9	<60	c*
ZnO(FC)/DHS-2	0.143	0.225	0.082	10^8-10^9	<60	d[1]
Concept:	Z-93SC55 - Stabilization of Zn interstitials via microencapsulation and incorporation in hybrid silicate and doped hybrid silicate binders.					
S13GP/DHS-1	0.147	0.153	0.006	10^9-10^{10}	<200	b
S13GP/DHS-1	0.142	0.148	0.006	10^9-10^{10}	<200	b
S13GP/SS-55	0.125	0.140	0.015	10^9-10^{10}	N/A	b
S13GP/SS-55	0.127	0.137	0.010	10^9-10^{10}	N/A	b
S13GP/SS-55	0.140	0.177	0.037	10^9-10^{10}	N/A	c**
S13GP/SS-55	0.151	0.206	0.055	10^9-10^{10}	N/A	c**
S13N/DHS-2	0.13	0.196	0.066	10^9-10^{10}	<200	d[1]
Concept:	Z-93SCLMXY - Stabilization of Zn interstitials via microencapsulation using doped hybrid silicate binders and incorporation in hybrid silicate binder or doped hybrid silicate binder.					
DS13N/SS-55	0.136	0.173	0.037	10^8-10^9	N/A	b
DS13N/SS-55	0.137	0.153	0.016	10^8-10^9	N/A	b
DS13N/DHS-2	0.124	0.161	0.037	10^8-10^9	<200	b
DS13N/DHS-2	0.122	0.128	0.006	10^8-10^9	<200	b
DS13N/DHS-2	0.148	0.154	0.006	10^8-10^9	<200	c*
DS13N/DHS-2	0.12	0.24	0.120	10^8-10^9	<200	d[2]
DS13N/SS-55	0.16	0.27	0.11	10^8-10^9	N/A	d[3]

Typical Performance of Promising Conductive White Thermal Coatings (Continued)						
TCMS	Pre-exposure α_S	Post-exposure α_S	$\Delta\alpha_S$	Surface Resistivity $\Omega/\square$	Charged to V[a]	Remarks
Concept:	**Flexible Conductive White TCC with DS13N in stripped silicone**					
DS13N/LO-41	0.161	0.278	0.117	$10^9\text{-}10^{10}$	<800	b
DS13N/LO-41	0.163	0.239	0.076	$10^9\text{-}10^{10}$	N/A	b
DS13N/LO-41	0.210	0.430	0.22	$10^9\text{-}10^{10}$	N/A	c*
DS13N/LO-51	0.193	0.423	0.230	$10^9\text{-}10^{10}$	N/A	d[3]
Conductive Concepts with Other Candidate Pigments						
ZOT/Phos. Sol.	0.131	0.149	0.018	$10^8\text{-}10^9$	<200	b
ZOT/Phos. Sol.	0.128	0.151	0.023	$10^8\text{-}10^9$	<200	b
ZOT/SS-55	0.117	0.156	0.039	$10^9\text{-}10^{10}$	N/A	b
ZOT/SS-55	0.112	0.156	0.044	$10^9\text{-}10^{10}$	N/A	b
ZOT/SS-55	0.129	0.180	0.051	$10^9\text{-}10^{10}$	N/A	b
Eu_2O_3/SS-55	0.087	0.138	0.051	$10^9\text{-}10^{10}$	N/A	b
Eu_2O_3/SS-55	0.100	0.126	0.028	$10^9\text{-}10^{10}$	N/A	b
Eu_2O_3/DHS-2	0.093	0.158	0.065	$10^8\text{-}10^9$	<200	b
Eu_2O_3/DHS-2	0.076	0.108	0.032	$10^8\text{-}10^9$	<200	b
Eu_2O_3/SS-55	0.096	0.129	0.033	$10^9\text{-}10^{10}$	N/A	c*
Eu_2O_3/SS-55	0.076	0.161	0.085	$10^9\text{-}10^{10}$	N/A	d[2]

Remarks:

a = Charged to <50 volts at room temperatures; indicated voltages are maximum observed at cryogenic temperatures.
b = Tests performed at Aerospace Corporation
c = Tests performed at GSFC
d = Tests performed at AMCL/SCEPTRE

*GSFC test involved exposure to 1000 ESH of UV-Vacuum.
**This GSFC test involves exposure to 4300 ESH of UV-Vacuum.

All tests carried out at Aerospace Corp. involved exposure to 2000 ESH of UV + 8.26×10^{13} e'/cm^2 (100 KeV) + 5.18×10^{13} e'/cm^2 (35 KeV) (typical DMSP orbit) and vacuum.

(1) Test at AFML/SCEPTRE involved exposure at 1 Sun of EUV-Vacuum (for Z-93CXY and Z-93SCXY) + 6.78×10^{15} e'/cm^2 (1 KeV) + 3.39×10^{15} e'/cm^2 (10 KeV).

(2) Test at AFML/SCEPTRE involved exposure at 3.3 to 3.6 Suns of EUV-Vacuum (for DS13N/DHS-2 and Eu_2O_3*/SS-55) + 6.78×10^{15} e'/cm^2 (1 KeV) + 3.39×10^{15} e'/cm^2 (10 KeV).

(3) The in situ test at AFML/SCEPTRE involved exposure at 1.6 to 2.1 Suns of EUV-Vacuum + 6.78×10^{15} e'/cm^2 (1 KeV) + 3.39×10^{15} e'/cm^2 (10 KeV).

TABLE OF CONTENTS

TABLE OF CONTENTS (CONCLUDED)

LIST OF TABLES

LIST OF TABLES (CONCLUDED)

LIST OF FIGURES

LIST OF FIGURES (CONCLUDED)

LIST OF ACRONYMS

AFML	Air Force Materials Laboratory
AO	Atomic oxygen
ASTM	American Society for Testing of Materials
BCC	Body centered cubic
BG	Black Glass
BOL	beginning of life
BRDF	Bi-directional reflectance distribution function
CVCM	Collectable Volatile Condensable Material
DoD	Department of Defense
ESD	Electrical static discharge
ESH	Equivalent sun hours
GEO	Geosynchronous Orbit
GPS	Global positioning satellite
GSFC	Goddard Space Flight Center
HTMIAC	High Temperature Materials Information Analysis Center
IR&D	Internal Research and Development
IITRI	IIT Research Institute
JPL	Jet Propulsion Laboratory
LEO	Low Earth Orbit
NASA	National Aeronautics and Space Administration
PBR	Pigment-to-binder ratio
SBIR	Small Business Independent Research
SEE	Space Environmental Effects
TCMS	Thermal control material system
TML	Total mass loss
UV	Ultraviolet
UV/Vis	Ultraviolet and Visible
Vac	Vacuum

1. INTRODUCTION

The temperature control of satellites and spacecraft is one of the most fundamental engineering problems confronting spacecraft designers and materials engineers. The ultimate objective of the thermal design is to ensure that the spacecraft operates within a prescribed temperature range defined by the temperature limitations of the vehicle's material and components.

One of the primary and successfully used methods to achieve the required thermal control has been the use of coatings with high reflectance or low solar absorptance (α_s) that are resistant to degradation in vacuum-ultraviolet and particulate radiation environment. Several National Aeronautics and Space Administration (NASA) and Department of Defense (DoD) cooperative efforts[1,2,3] have reviewed the state-of-the-art carefully and pointed out deficiencies in the data available for existing materials as well as new material needs. This report summarizes successful efforts over the past two and a half years carried out to meet the need of electrically conductive passive thermal control material systems (TCMS).

The ultimate goal was to develop engineering quality tailorable electrically conductive, TCMS for coating space hardware and space structures. This was achieved via performing the following two tasks:

Task A. This task was to develop electrically conductive optically absorbing passive TCMS. The required properties goals were as follows:

- $\alpha_s \geq 0.90$
- $\epsilon_N \geq 0.90$
- Adhesion, thermal shock - satisfactory for long term use, ASTM-D-3359A (4A or better)
- Space environment stable - satisfactory in 1000 ESH UV-vacuum test
- Surface resistivity $\simeq 10^6$ to 10^9 $\Omega/\square$

Task B. This task was to develop white, electrically conductive, passive (low α_s/ϵ_N) TCMS. The required properties goals were as follows:

- α_s - Achieve minimum (≤ 0.18, comparable to the state-of-the-art Z-93P)
- $\epsilon_N \geq 0.88$
- Adhesion, thermal shock - satisfactory for long term use, ASTM-D-3359A (4A or better)

- Space environment stable - satisfactory in 1000 ESH UV-vacuum test
- Surface resistivity $\simeq 10^6$ to 10^{10} $\Omega/\square$

These two tasks have benefited enormously through Internal Research and Development (IR&D) efforts at IITRI and partially funded program for the GPS-Block IIR hardware. In the next section, we summarize past efforts that guided us for selection of product concepts for material design, followed by a results section that first summarizes physical, optical and electrical properties data generated for each concept, followed by results from space environment simulation studies carried out at Aerospace Corporation [Dr. M. Meshishnek], Goddard Space Flight Center (GSFC) [Dr. L. Kauder/Ms. W. Peters], and Air Force Materials Laboratory [Messrs. P. Carlin/C. Cerbus]. The data generated in ESD testing carried out at GSFC [Dr. L. Kauder] for the selected concepts are also presented here.

The studies conducted on the selected concepts and new pigments have provided new conductive engineering TCMS. Some of them have already found applications on space hardware, some are waiting to be noticed by thermal designers, and some require further detailed studies to become the state-of-the-art for future space structures and hardware. A qualitative discussion is also presented at the end of this report on integration of electrically conductive thermal control coatings on space structures and space hardware.

2. TECHNICAL BACKGROUND

Several NASA and Department of Defense cooperative efforts have reviewed the state-of-the-art carefully and pointed out deficiencies in data available for existing spacecraft materials as well as the need for development of new coating materials. (See NASA-CP-3035)[1] A particular need identified by the Space Environments and Effects Project (SEE) was for electrically conductive coating which could be tailored to different property requirements to meet different mission needs. The following summary covers past as well as IR&D efforts at IITRI which have resulted in performing this current program.

2.1 PAST RESEARCH AND DEVELOPMENT ACTIVITIES

2.1.1 Electrically Conductive Absorbing TCMS. The need for electrically conductive absorbing TCMS is not new. The very early efforts were more devoted to absorbing TCMS mainly because of ease and availability of conductive phases. The modification of space environment stable nonconducting cosmic black based D111 silicate binder based TCMS to MH11Z was carried out for the Jet Propulsion Laboratory (JPL) in the early '80s. This experience was achieved to add needed conductive phase (graphite) to the material system to tailor volumetric resistivity of $\leq 1 \times 10^6$ $\Omega \cdot$cm. As expected, there were penalties to the solar absorptance value due to usage of conductive phases. JPL's in-house work concentrated on iron titanate as a pigment and was more resistive than the MH11Z formulation.

In the mid '80s under an Air Force funded program, Black Glass (BG: a carbon doped silica) was developed as atomic oxygen (AO) resistant pigment for baffle applications. These efforts demonstrated that the BG is not only AO resistant, but provides an opportunity to tailor very flat bi-directional reflectance distribution function (BRDF) response that is needed for baffle applications. Based on these efforts, two nonconducting formulations, MH21-I and MH21S/LO, were developed and are in use for baffle applications as well as absorbing TCMS with $\alpha_S =$ 0.97 to 0.98 and $\epsilon_N = 0.90 \pm 0.03$. MH21-I uses an inorganic silicate binder whereas MH21S/LO uses stripped polydimethyl siloxane polymer, meeting necessary outgassing requirements of Total Mass Loss (TML) $< 1.0\%$ and Collectable Volatile Condensable Material (CVCM) $< 0.1\%$. The typical values are TML = 0.15%, CVCM = 0.03. These developments

provided opportunities to tailor electrical conductivities using MH21-I and MH21S/LO as base nonconducting phases. Again, graphite, milled graphite fibers, SiC whiskers and B_4C, were among the candidates for the conductive phases. The experience gained in the early '80s was applied to develop formulations MH55IC and MH21-IC as electrically conductive inorganic TCMS, and MH21SC/LO as an electrically conducting flexible thermal control material system. The typical properties of these TCMS are given in Table 2-1. Our recent communications with NASA-Lewis Research Center's Dr. Purvis[2] provided the most general criteria: Coating system with differential charging up to 10 volts (conservatively) and leakages current < 10 nanoamperes (1 nA preferable). This translates into the resistivity requirement being on the order of 10^9 $\Omega/\square$.

Based on the defined goals, Internal Research and Development (IR&D) work was first undertaken to tailor the electrical resistivity of black TCMS. The scientific basis of this work is best described in a review article by McLachlan et al.[17], who has provided guidance in designing the composite material systems. This work at IITRI used AO resistant BG as a pigment for the required stable optical properties, stripped polydimethyl siloxane (CVCM <0.1% and Total Mass Loss [TML] <1.0%) as a binder, and graphite fiber, graphite, and semiconductor grade boron carbide as conductive phases. Experiments were carried out to build a database to define threshold conductive phase weight fraction requirements and to select optimized processing requirements for each coating concept with desired optimum properties. This work was extended further in a program to develop conductive thermal control coating for GPS Block IIR hardware.[18] The coating systems that have been developed and have shown great potential are: MH55IC, MH21SC/LO, and MH41SCB/LO. The details of the typical properties of these coatings are listed in reference (3). Since each system of these material systems have been known to be space environment stable, the resultant conductive tailored formulations can be considered space environment stable. All of the above materials have tailorable electrical resistivity $\simeq$ 10^6 to 10^9 $\Omega/\square$, α_s $\geq$ 0.90, ϵ_T $\geq$ 0.90 $\pm$ 0.03, and meet adhesion, thermal shock and thermal cycling requirements.

2.1.2 Electrically Conductive Low (α_s/ϵ_N) White TCMS. Our quest for electrically conductive TCMS is not new. Efforts in this area at IITRI date back to the early '70s. Initial efforts were to characterize the electrical resistivity of current state-of-the-art thermal control

	Table 2-1. Summary of Black Thermal Control/Optical Coatings at AMCL/IITRI				
Coating System	Pigment	Binder	α_S	ϵ_T	Comments
D-111P	Carbon black WB-225	Kasil 2130	≈ 0.95	0.90 ± 0.02	Stable, LDEF data. Not recommended for AO resistance.
MH11-ZP	WB-225 graphite	Kasil 2130	0.89 to 0.91	0.90 ± 0.02	Electrically conductive $\leq 10^6 \ \Omega \cdot$cm stable. (JPL)
MH21-IP	Black glass	Kasil 2130	0.95 to 0.02	0.90 ± 0.02	AO-resistant; stable.
MH55-ICP	Black glass	Kasil 2130	0.90 to 0.93	0.90 ± 0.02	Electrically conductive 10^6-$10^9 \ \Omega/\square$
MH21S/LO	Black glass	MHS/LO stripped polydimethyl siloxane	0.95 to 0.98	0.90 ± 0.02	Stable, NASA-TM-100768, recommended for AO resistance.
MH21SC/LO	Black glass graphite fiber	MHS/LO stripped polydimethyl siloxane	0.90 to 0.93	0.90 ± 0.02	Electrically conductive 10^4-$10^9 \ \Omega/\square$

materials such as Z-93 (a calcined ZnO pigmented potassium silicate), S13G/LO-1 (reactively encapsulated ZnO in stripped polydimethyl siloxane) and YB-71 (flash calcined zinc orthotitanate [ZOT] pigmented potassium silicate). Due to the use of YB-71 in Geosynchronous Orbit (GEO), much attention has been devoted to the non-contact measurements of charge developed on such thermal control surfaces. Such studies were carried out at Aerojet[4], JPL[5], and similar measurements were carried out for Z-93 at the NASA-Lewis Research Center, first in 1979[6] and more recently[7] in comparing Z-93 and Z-93P electrical resistivity values. In these studies, the electrical resistivity of silicate coatings was reported, along with contributions from moisture due to their porous nature. It was noted that complete removal of moisture requires about two weeks in vacuum of 10^{-7} to 10^{-8} Torr to achieve artifact-free resistance measurements.[8] In R&D efforts at IITRI, we have developed sample preparation and drying methods to measure surface and volumetric resistivities using a HP-4329 and HP-4339 resistivity meter.[9] The measurement procedure provided resistivity values that agreed well with measurements conducted with exhaustive efforts to remove moisture via exposure to vacuum.[8] Accordingly, the surface resistivity values for current state-of-the-art materials Z-93 and YB-71 are on the order of 10^{13} Ω/□ and for S13G/LO-1 is on the order of 10^{13} to 10^{14} Ω/□.

The earliest program to develop electrically conductive thermal control material was funded through the U.S. Air Force Materials Laboratory (AFML) and was concluded in 1976 at IITRI.[10] These early efforts used sodium and lithium silicate as binders and also evaluated their Ultraviolet/Vacuum (UV/VAC) stability for 1,000 ESH. Efforts were also made to evaluate antimony-doped SnO_2 pigmented potassium silicate coatings. The results of these efforts are summarized in Table 2-2, and UV/VAC stability results are given in Figures 2-1 to 2-3.

There were no additional systematically funded efforts for the development of conductive thermal control coatings until the very recent efforts at JPL for the Cassini Project; at AZ-Technology for Tethered Satellite; and at IITRI for GPS Block IIR (during 1993, 1994). The interplanetary mission of the Cassini Project required the material system to meet the criteria of ρ_v x t $<$ 2 x 10^{10} Ω•cm² (ρ_v = volume resistivity in Ω•cm, t = thickness in cm). The coating also must meet non-contact charging criteria of 10 volts, when samples were irradiated with 10 KeV electron at a flux of 0.5 nA/cm². Solar absorptance (α_s) needed to be kept as low as
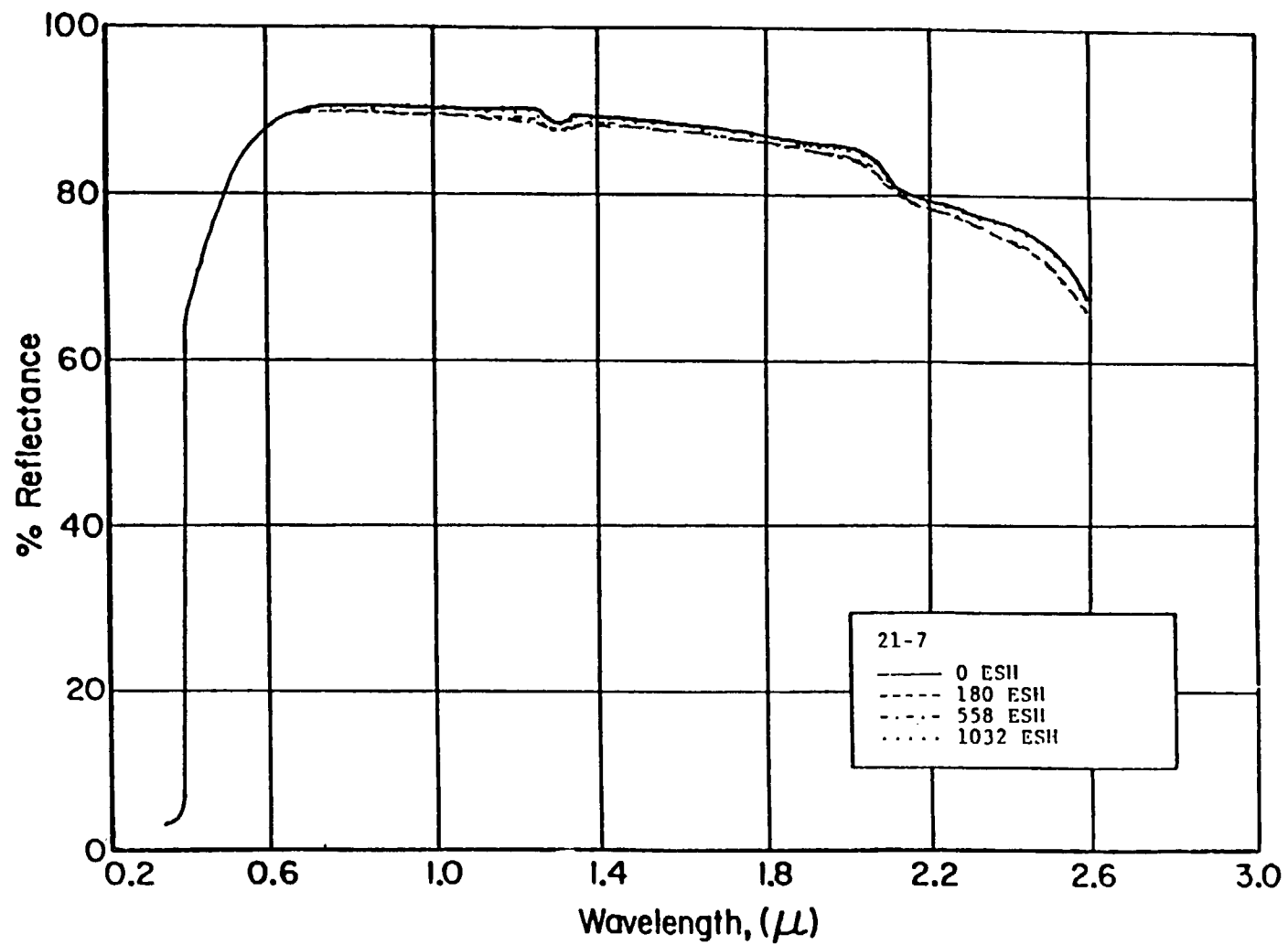
Figure 2-1. Reflectance of ZnO/Lithium Silicate.

% Reflectance vs **Wavelength, (μ)**

21-10

— 0 ESH
----- 180 ESH
-·-·- 558 ESH
····· 1032 ESH
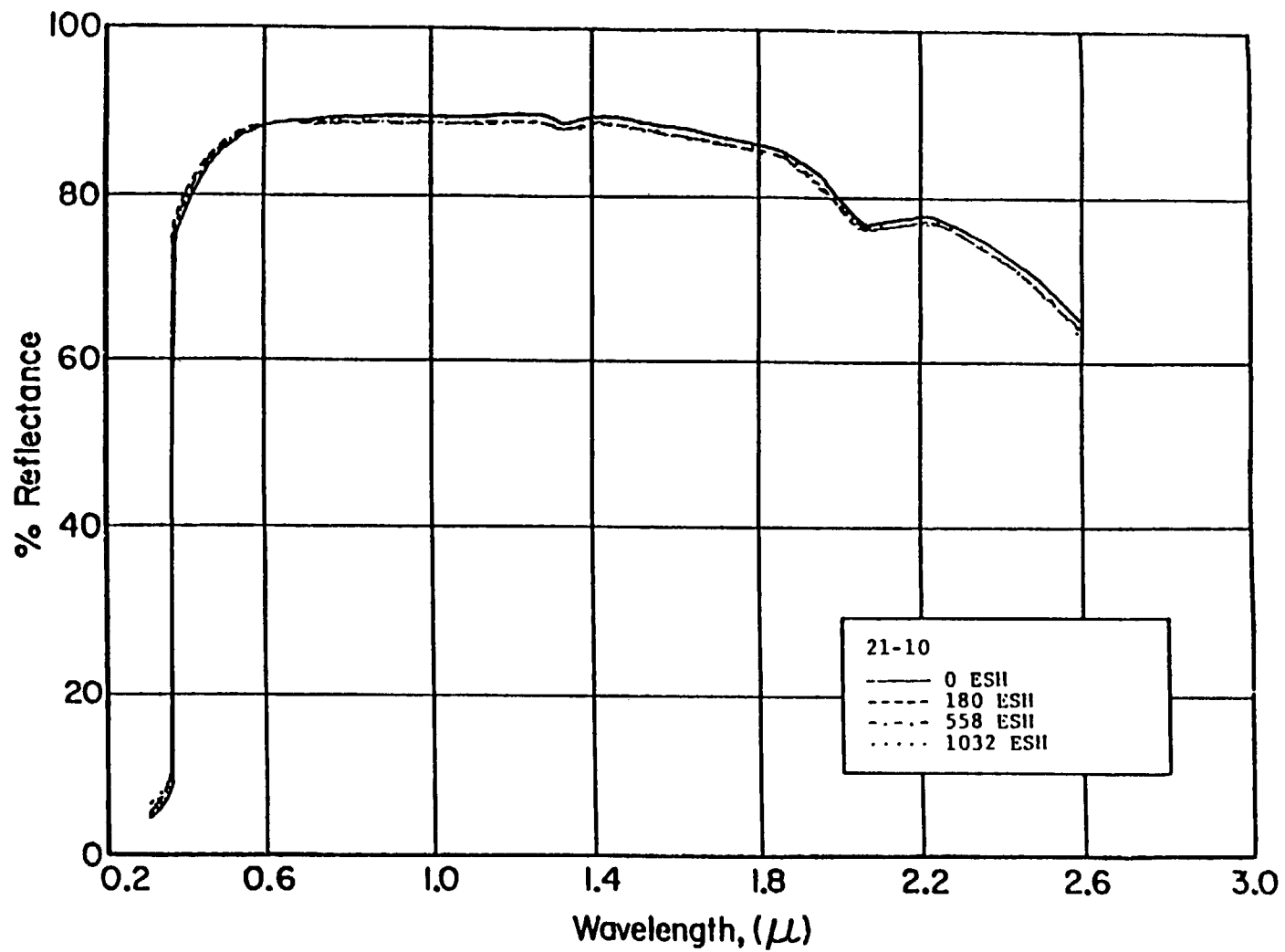
Figure 2-2. Reflectance of ZnO (Calcined)/Lithium Silicate.
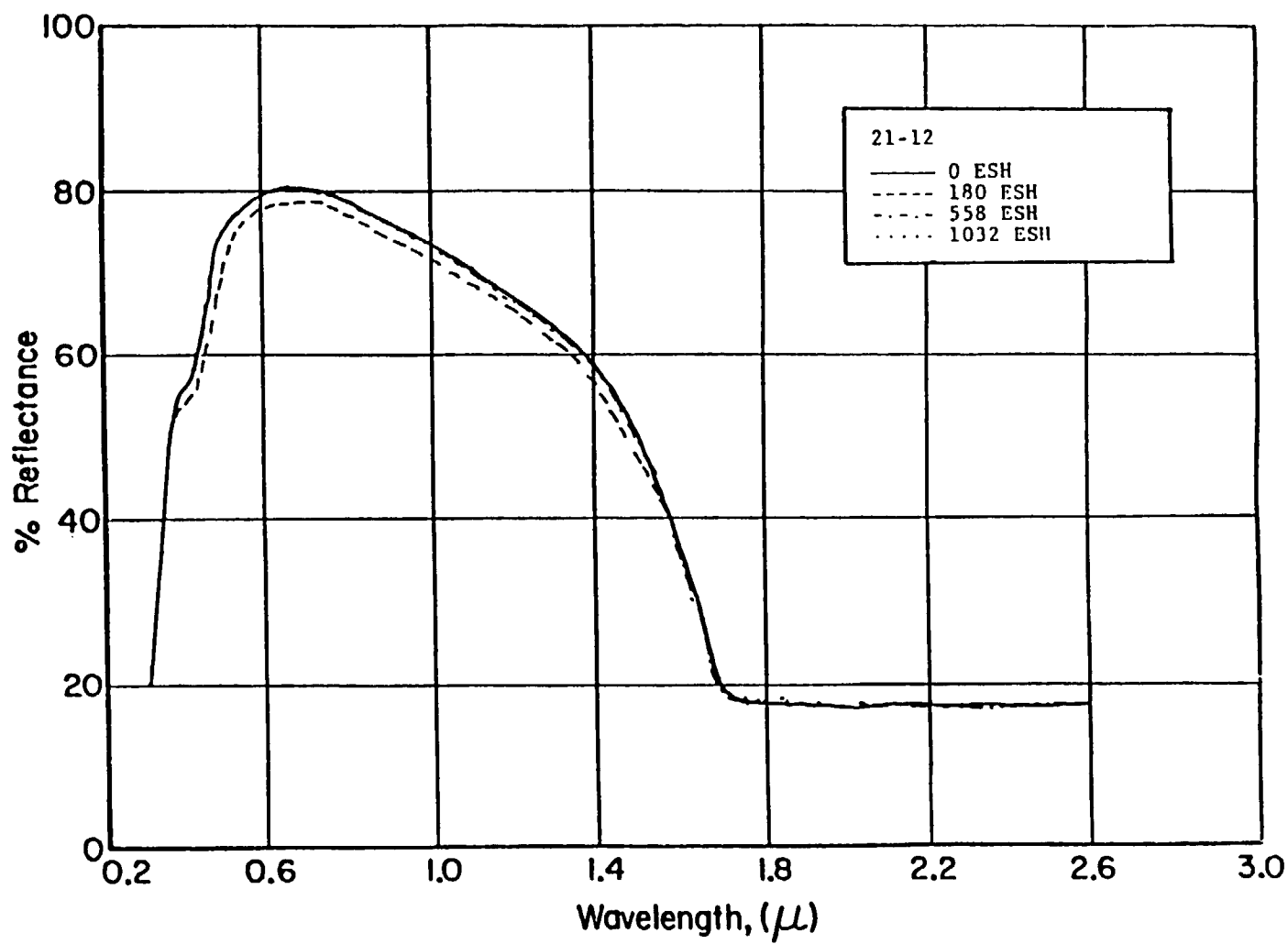
Figure 2-3. Reflectance of Sb:SnO$_2$/PS-7.

Table 2-2. AFML-TR-76-232/IITRI Work (1976)	
Inorganic Binder	**Surface Resistance, Ω**
ZnO/N_2SiO_3 ZnO/Li_2SiO_3	8.0×10^8 1.5×10^9
ZOT/K_2SiO_3 ZOT/Na_2SiO_3 ZOT/Li_2SiO_3	2.5×10^9 1.7×10^9 3.8×10^9
$SnO_2:SB/PS-7$ (High PBR) $SnO_2:SB/PS-7$ (Low PBR)	2.1×10^7 1.2×10^8

Antimony doped SnO_2 pigment was supplied by AFML.

possible with thermal emittance $\epsilon_T \simeq 0.90 \pm 0.02$. In the recently concluded program, material systems considered were Al doped ZnO pigment from Union Miniere, Brussels, Belgium, and NS43G (ZnO with 1% Al_2O_3) yellow pigment from Space Craft Coatings, Inc. of Gambrills, Maryland. (ZnO with 1% Al_2O_3) yellow pigment from Space Craft Coatings, Inc. of Gambrills, Maryland. The French product PCB-Z flexible white conductive thermal control coating was also included in this study. None of these material systems met the required goals.[11] Based on these findings, it was recommended by JPL that some of the requirements be relaxed for the conductive thermal control coatings.[12] The work continued with charging criteria relaxed to 20 volts and α_s (Beginning of Life [BOL]) = 0.22. The resultant coating is now based on a 50:50 mix of NS43G and doped ZnO pigment, the details of which can be found in JPL Spec BS516165A, Rev. A.[13]

The conductive coating used on the Tethered Satellite was developed based on indium stannate as the pigment, and has an α_s (BOL) $\simeq 0.28$ (<0.30). The electrical conductivity of such a system is considered tailorable and will depend on the pigment-to-binder ratio. The Phase I development is proceeding at AZ Technology under an SBIR Phase I contract. The coating system can provide a viable conductive coating, if a compromise on α_s (BOL) can be made, and if (the change in α_S $\Delta\alpha_S$) due to the space environment effects is shown to be acceptable.

Other efforts made at JPL during Cassini project studies[14] involved controlled doping of ZnO with various dopants and treatments. Among these candidates, the Indium-doped ZnO showed a greater potential in charging tests, but α_s (BOL) was near a relatively high 0.29. The electrical resistivity of such silicate binder material systems was on the order of 10^6 to 10^7 $\Omega/\square$.[11,14] Efforts in this direction as well as with different doping approaches were suspended mainly due to high α_s (BOL) and program limitations.[14]

Recent efforts at IITRI date back to 1989.[15] We first proposed the concepts of stable, reliable electrical properties development through careful combination of conductive and insulative phases to build a reliable TCMS. Research and development to build reliable microstructurally engineered resistors (during the early '80s) was the basis of this work. The percolation theories, requirements of percolation threshold, morphologies and distribution of conductive phases and their effects on resultant resistor properties and reliability, were the heart of these efforts. The electrical resistivity goals for coatings have not received complete attention. In practice, they are mission dependent, and material system design lacked needed directions from the mission office. The designer often attempted to work with available state-of-the-art materials rather than engaging in the concurrent engineering exercise of developing much needed new materials. We, at IITRI, have more recently received needs related input for various situations. As iterated in Section 2.1.1, the recent communications with NASA-Lewis Research Center's Dr. Purvis[16] provided the most general criteria: Coating system with differential charging up to 10 volts (conservatively) and leakages current < 10 nanoamperes (1 nA preferable). This translates into the resistivity requirement as on the order of 10^9 $\Omega/\square$.

Based on the defined goals, an IITRI IR&D project was first undertaken to tailor the electrical resistivity of black TCMS. The scientific basis of this work is best described in a review article by McLachlan et al.[17], who has provided guidance in designing the composite material systems. The IR&D for white thermal control coating proved that doping of the existing stable pigments like S13GP and ZOT (zinc ortho titanate) is a must.

Before going into a summary of the IR&D efforts and studies conducted during a recent program for GPS hardware needs for white (low α_s/ϵ_T) thermal control coatings, we need to discuss the reliability and coating needs as applied to conduction mechanisms. The charging of spacecraft surfaces as modelled by the NASCAP computational code, need input on material

properties/parameters. There are 19 input variables. One needs to know the following input parameters that are related to the material properties:

1. Relative dielectric constant
2. Bulk conductivity (volumetric conductivity/resistivity)
3. Atomic number
4. Maximum secondary yield due to electron impact
5. Primary electron energy that produces maximum secondary yield
6. Range of electrons and energy dependence
7. $R = P_7E^{P8} + P_9E^{P10}$ - related parameters
8. Secondary yield due to 1 KeV protons
9. Incident proton energy that products maximum secondary yield
10. Photo electron yield for normal incident sun light
11. Surface resistivity (surface conductivity)
12. Maximum (absolute) potential attainable before a discharge can occur
13. Radiation-induced conductivity (K)
14. Radiation-induced conductivity power (A)
15. Material density

Other parameters deal with thickness of the coating and physical shape and boundary conditions. These input parameters also define some of the characterization needs for the candidate coating material system.

To the best of our knowledge, no systematic effort has been made to measure critical dielectric properties. The charging computational code (NASCAP) needs photo emission and secondary emission properties of a variety of materials. The related databases on materials and coatings have not been systematically assembled. The sensitivity of the NASCAP code output is also very crucial for designing tailorable conductive TCMS. Such sensitivity analyses for chosen orbits have not been performed or published. According to our communications with Dr. Purvis[19], some attempts were made, but results were not published for GEO conditions. The NASCAP charging calculations cannot rank the importance of individual mechanisms. It is apparent that the most important properties will be volumetric and surface resistivity of the coating. The next will be secondary emission yield. Since the thermal control materials are essentially dielectric in nature, they will exhibit leakage current. Since our goal is to limit leakage current (< 10 nanoamperes) under differential charging in orbit, they will be maximum in the portions of the orbit where flux currents are maximum (anti-solar side of the orbit). We know these currents are high, and therefore, for materials with high resistivity, one needs to have additional means to manipulate leakage currents. The only available process then, to

control leakage current is <u>secondary emission</u>. The coating material system needs to have the availability of conductive leaky percolation paths and also should have appropriate secondary emission properties to limit the leakage current. Again, for such a dielectric, the maximum differential potential will be induced, when mean <u>energy</u> encountered is at a maximum. This will be found on the solar side of the orbit, i.e., along with photo emission.

Garrett[20] has discussed the use of emissions (photo electron, secondary electron emission, back scattered electrons) as current mechanisms for charging control. Such emissions do not reduce charge deposition in dielectrics. They can, depending on the grounding scheme, lead to multipacting and preferential deposition of contaminants. Another effect is pinhole formulation and focussing of electrons to cause punctures in coating systems.[20] Due to these concerns the secondary emissions to manipulate leakage current should be used prudently.

In view of the qualitative inputs from spacecraft charging studies summarized here, a survey was carried out to choose possible candidates. The input provided by the High Temperature Materials Information Analysis Center (HTMIAC) at Purdue University[21] is provided here in tabular form, along with comments on potential pigment materials (Tables 2-3 and 2-4). The current state-of-the-art pigments and coatings, that are proven stable in space environment were also tested for volumetric resistivity (ρ_v). The product $\rho_v$xt was calculated as an indicator of possible surface resistivity values. These values are also listed in Table 2-5. These data, when considered with prior work in Europe[26,27,28] to develop stable electrically conductive coatings, points us toward a more successful selection of concepts. The following discussion from our report for the GPS hardware[18] is provided here to illustrate the care taken in selection of concepts during the recent work that was initiated for GPS hardware.

From the available data in Tables 2-3, 2-4 and 2-5, pigments which can exhibit conductive behavior are ZnO, SnO_2, InSnOx, Zn_2SnO_4 and Zn_2TiO_4. Of these, ZnO, SnO_2, Zn_2SnO_4, and Zn_2TiO_4 have been studied as potential pigments for TCMS by Zerlaut et al.[22] and Harada[22,30] during initial development of Z-93 and YB-71 thermal control coatings, the current state-of-the-art materials. Coatings incorporating the pigments SnO_2 or Zn_2SnO_4 were not as stable as Z-93 and YB-71.[22,29] It is also noted that the systems based on the pigments SnO_2, Zn_2SnO_4 or InSnOx, are conductive due to an oxygen deficient defect structure, and the

Table 2-3. Literature Review Summary[21]				
Material	Density, gms/cc	Volumetric Resistivity ($\Omega \cdot cm$)	Relative Dielectric Const. ϵ_r at 1 MHz	Comments
SnO_2	6.993	1.0E+00	9.0	*
SiO_2	2.800	1.0E+13	--	
$ZnAl_2O_4$	4.608	1.9E+03	--	
TiO_2	4.245	2.13E+09	78.90	
$ZnWO_4$	7.872	--	16.10	
Zn_2SiO_4	4.251	3.6E+07	7.70	
ZnO	5.676	1 to 10	12.00	T. K. Gupta (1990)
ZnO-doped (Al)		0.1 to 1		
ZnO (gb)		1.0E+12		

*Becomes conductive with defect structures.

Table 2-4. Other Potential Pigments	
Material	**Comments**
SnO_2	-vc TCR, conductivity-defect structure dependent, e.g., vac. (10^{-7} TORR) baking at 100°C. Needs sealing. Gives ρ_v = 50 Ω·cm. Doped SnO_2 = 50 K 50 Ω·cm (P.Q. Corp. developmental sol) no sealing needed.
$InSO_x$	Conductivity-defect structure dependent. Thick paste - developmental thick paste. (ESL) ρ_v = 10^3-10^7 Ω·cm as polycrystal.
$InSnO_x$	-vc TCR, ρ_v = 10^3-10^9 Ω·cm as polycrystals. $\alpha_{S/BOL} \rightarrow 0.18$ to 0.22 (French Data). French and Canadian flight data available, $\Delta\alpha_S$ - low. $> \Delta\alpha_S/Z$-93.
$ZnTiO_4$	-vc TCR, semiconductor ρ_v = 10^8 Ω·cm as polycrystal. $\alpha_{S/BOL} \rightarrow 0.11$ to 0.13, can be doped to improve ρ_v. Data available on simulation and synergism. (French) CNES efforts devoted to doped ZOT.

Material	ρ, $\Omega \cdot cm$	ρ, x t, $\Omega \cdot cm^2$	Comments
ZOT (1000°C, 24 hrs)	1.27×10^{10} to 3.15×10^{10}	3.23×10^{8} to 8.0×10^{8}	t = 10 mils, $\alpha_{sBOL} \rightarrow 0.10$
ZOT (1000°C, 24 hrs)	2.4×10^{10} to 3.9×10^{10}	6.01×10^{8} to 7.84 10^{8}	t = 10 mils, $\alpha_{sBOL} \rightarrow 0.10$
Calcined ZnO, SP-500 (990°C, 16 hrs)	<0.5 z 10^{6} to 1.5×10^{6}	--	Yellowish t = 10 mils, $\alpha_{sBOL} \rightarrow 0.2$
S13G (950°C, 16 hrs)	3.7×10^{11} to 6.0×10^{10}	5.07×10^{9} to 1.03×10^{9}	$\alpha_{sBOL} \rightarrow 0.15$
S13G (950°C, 16 hrs)	8.4×10^{11} to 1.6×10^{11}	1.07×10^{9} to 2.15×10^{9}	$\alpha_{sBOL} \rightarrow 0.15$
Z-93, 5 mils (100°C, 4 days)	3.65×10^{14} to 9.26×10^{13}	1.23×10^{13} to 9.2×10^{12}	$\alpha_{sBOL} \rightarrow 0.15$
YB-71, 10 mils (100°C, 4 days)	9.0×10^{11} to 9.8×10^{11}	1.17×10^{10} to 1.34×10^{10}	$\alpha_{sBOL} \rightarrow 0.15$
S13GP/LO-1 8 mils	10^{13} to 10^{14}	$\sim 10^{13}$	t = 8 mils $\alpha_{sBOL} \rightarrow 0.15$

ZOT, S13G, Z-93 are all stable to UV-Vac 1,000 ESH exposures.

stability of electrical properties depends on the stability of these oxygen deficient defect structures.[21,24,25]

Vardin and Duck's[27] efforts in experimental verification of charging provides a good insight into the stability of electrical properties of coatings based on these defect structure oxides. This work involved conductive oxide mixtures with a resistive matrix (polyamide) which were irradiated to 5 to 20 KeV (in steps of 5 KeV) electrons for different oxide loadings. The oxides used in this study were Al_2O_3, Ga_2O_3, In_2O_3, In_2SnOx, and ZnO. The charge build-up for these coatings was tested at room temperature and at $-180°C$. The comparison of In_2O_3 and InSnOx (In_2O_3:SnO_2) made by Vardin and Duck[27] is interesting. They argued that the function of SnO_2 in InSnOx coating is to provide conductive paths through the defect structure. We believe In_2O_3 alone can provide such conductive paths, and it may not be necessary to provide such defect structure paths. Another valuable input is that indium alone is responsible for the secondary emission with a yield of 4.8.[20] The difference in the resultant conductivities depends on oxide loading. For equal oxide loadings, InSnOx is slightly more conductive than In_2O_3 alone, e.g., for a PBR of 4:1 InSnOx-based coating exhibited an electrical resistivity of 2.7 x 10^5 Ω•m versus In_2O_3-based coating having resistivity of 1.4 x 10^6 Ω•m. The space environment stability of such coatings on second surface mirrors for thick films (several microns) was also studied by Dutat et al.[28] who reported $\Delta\alpha_s$ (InSnOx) $\approx$ 0.15, whereas $\Delta\alpha_s$ (In_2O_3) $\approx$ 0.03 for an equivalent exposure of 3 sun years.

Vardin and Duck's[27] observations in charging experiments involving ZnO are also interesting. They observed that for electrons >20 KeV, the charging was only a few volts (< 150 V) whereas at low energies, the surfaces charged to thousands of volts. This is consistent with values shared by other researchers. These results suggest an adjustment of the solid-state chemistry of ZnO pigment by incorporating enough Zn interstitials in the ZnO matrix, so as to increase carrier concentrations to tailor in the required conductivity value. The coating made from such pigment may provide enough conductivity to mitigate charge dissipation. One needs to stabilize the Zn interstitials incorporated in the ZnO matrix, and the early work of Harada[29] sheds some light on this concept. The available data on ZnO pigmented potassium silicates suggests that such systems have been studied up to 270 ESH, and do show the space environment stability (Table 2-6). Let us call this candidate treatment concept Z-93CXY. The

Table 2-6. Conductive Thermal Control Material Systems Z-93CXY and Z-93SCXY			
(A) Z-93SXY:	Z-93C06, Z-93C55, Z-93C05 treated ZnO/Kasil 2130 (propriety formulation) $\alpha_s \leq 0.20$, $\epsilon_T = 0.90 \pm 0.03$ Electricity resistivity = 10^9 $\Omega/\square$ (Tailorable) $\Delta\alpha_s$ - Per IITRI-C207-25 Adhesion - Satisfactory to Al substrates/graphite epoxy substrates.		
Exposure, ESH	Solar Factor	Reflectance, %	
		440 nm	600 nm
0		89.0	95.5
270	3	85.5	94.0
(B) Z-93SCXY:	Z-93SC55, treated ZnO/Kasil 2130 (propriety formulation) $\alpha_s \leq 0.18$, $\epsilon_T = 0.90 \pm 0.03$ Electricity resistivity = 10^9 $\Omega/\square$ (Tailorable) $\Delta\alpha_s$ (for 1,000 ESH exposure) = 0.01 (See Figure 2-4) Adhesion - Satisfactory to Al substrates/graphite epoxy substrates.		

concept was further evaluated to verify feasibility during the GPS program.[18] The typical values achieved for surface and volume resistivity listed in Table 2-4 are encouraging. (See Reference 18 for details.)

Stabilization of Zn interstitial in a ZnO matrix is not a new subject. We, at IITRI, have done this routinely for decades using the method reported and for the S13G pigments. (See Zerlaut et al.[22]) The use of such treated ZnO pigments that have been proven stable in 1,000 ESH exposures can also be used to form coatings with silicate binders. Let us call this approach Z-93SCXY. Work was undertaken recently at IITRI as part of the GPS program[18] to verify the feasibility of this concept. The typical values observed are listed in Figure 2-4. The results obtained for surface resistivity measurements[9,18] are encouraging.
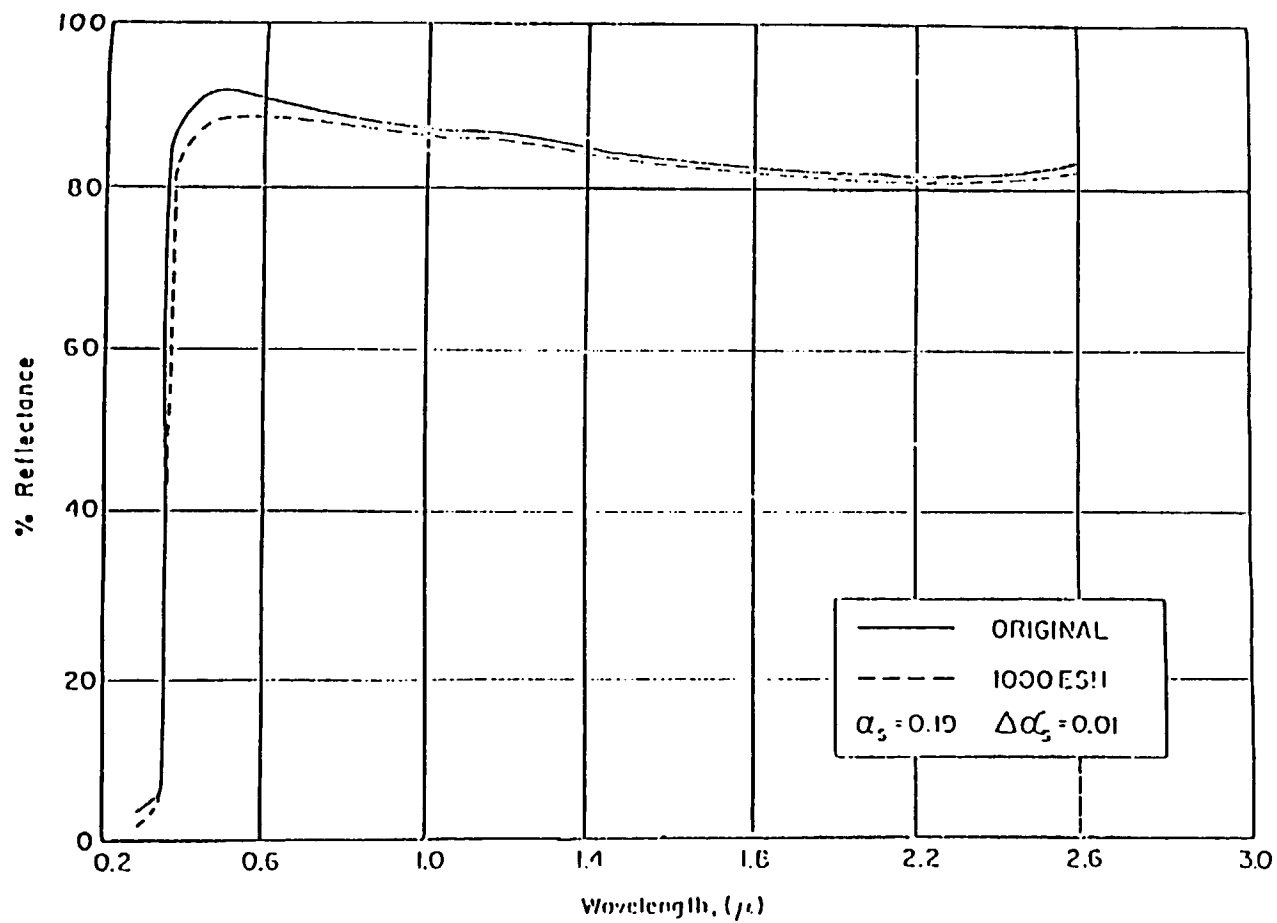
Figure 2-4. 1,000 ESH UV-Vac Stability of Z-93SC55.

The GPS hardware needs[18] are unique. Due to the proximity of the hardware to the communication equipment, there is an added requirement that the electrical resistivity of the coating material system should not drop below 10^7 Ω•cm to prevent interference in transmission. Due to this condition, it was decided that the candidate material system should have a BOL resistivity of the order of 10^9 Ω•cm or slightly higher. The only data available on the space simulation testing on oxygen deficient defect structured oxides was by Dutat et al.[28] It indicates that all oxides that depend on a defect structure for electrical conductivity exhibited a lowering of electrical resistance on the order of 2 to 3 decades due to a space environment (UV + electrons). A conscious decision was made to avoid candidate oxides that depend on oxygen deficient defect structures. This conservative approach thus reduces the probability of the coating system becoming too conductive during the lifetime of the space hardware.

Feasibility studies were also undertaken during the program[18]. Efforts were directed towards concepts based on the experience of Vardin and Duck[27], Dutat et al.[28], and the JPL work.[11,12,13,14] The qualitative discussion provided here earlier for the choice of conduction mechanisms and feedback from Garrett[20] on mitigation strategies clearly indicates that the ideal material system should provide percolation paths, as provided in Z-93CXY and Z-93SCXY with dependence on proven stabilized solid-state chemistry of pigments, along with the secondary emission provided at an optimum level. The concept is to dope the S13G pigment with a dopant that can provide maximum needed secondary emission yield at required optimum low concentration. This concept can help us to design inorganic and organic flexible thermal control coating material systems. Indium was selected as the dopant, and doped S13GPSC pigments were prepared at three candidate dopant concentrations. Three different process routes were used to check feasibility of this concept. Typical values for these doped materials are summarized in Table 2-7, indicating excellent tailorability for an inorganic coating system: Z-93SCLMXY, and for an organic coating system: S13GCLM/LO-XY. Both concepts showed excellent BOL, α_s, ϵ_T and resistivity values. The UV-vacuum stability of these concepts awaits verification.

Due to the complexity and cost of In doping of S13G pigments, a simple approach was also used for preparing "silicated indium." These trials are reported in detail in Reference 18. Such processing helps to reduce processing losses of costly indium, but demands higher

Table 2-7. Typical Properties of Concepts S13GC/LO-XY and Z-93SCLMXY			
Concept	Typical Emittance* (ϵ_T)	Typical Solar Absorptance** (α_s)	Typical Surface Resistivity*** $(\Omega/\square)$
S13GIS/LO-41	0.90 ± 0.03	<0.18	$<10^9$
S13GC16/LO-41 (t= 4.8)	0.90 ± 0.03	0.17 ± 0.03	$<10^9$
S13GC16/LO-41 (t= 6.1)	0.90 ± 0.03	0.16 ± 0.03	$<10^9$
S13GC16/LO-41 (t= 7.0)	0.90 ± 0.03	0.16 ± 0.03	$<10^9$
Z-93SC1605	0.90 ± 0.03	<0.18	$<10^6$
Z-93SC1255	0.90 ± 0.03	<0.18	$<10^9$

t   Is the thickness of the coating in mils

*   Measurements were performed using Gier-Dunkel DB-100 infrared reflectometer.

**   Measurements were performed using Lambda 19 UV-Vis-NIR spectrophotometer. With < signs, the values are approximate.

***   Measurements were performed on HP-4329A High Resistance Meter, following sample preparation method (19).

"silicated indium" loading in the coating to achieve similar resistivity values in the coating material system. Future validation efforts are needed in this area for evaluating the impact of cost versus property tradeoffs. The feasibility study results indicate that property goals are achievable economically for the concepts selected here for screening study.

In view of the GPS hardware program goals, the concept Z-93SCXY was considered to be an established concept. It meets the required conductivity needs of the mission, and required space environment stability data is also at hand. The concept needs to be optimized to minimize cost, or tailor the electrical properties to desired values with ease.

2.2   CONDUCTIVE MATERIAL SYSTEMS: CONCEPTUAL DESIGNS

A summary of the literature review and past efforts in the area of conductive thermal control coatings were presented in the previous section. This summary clearly indicates the need for further efforts on microstructurally engineered material designs evaluated in recent feasibility studies.[18]   In this section, we shall discuss the TCMS conceptual design selected for the screening study. The conceptual designs were carried out in two areas. The first one is related to the area of black conductive thermal control coatings, and the second is related to low α_s/ϵ_T reflector, white conductive thermal control coatings.

2.2.1   Black Tailorable Conductive TCMS Conceptual Design

In the area of conductive optical blacks, our recent work[18] has resulted in the development of coating systems: MH55-IC, MH21SC/LO, D36SCB/LO, D21S/LO, D21SC/LO, and MH41SCB/LO. Typical properties of these coatings systems were given in an earlier section. They all meet the required property goals of this screening study, hence these material designs are the best candidates.

Apart from concepts from already developed in a previous study[18], this study also included conductive thermal control material designs that depend on the concept of doping. IR&D studies at IITRI have resulted in doped B.G. and several doped "leaky" silicate binder systems. They provide unique material design opportunity to tailor electrical performance characteristics without compromise of absorption properties or penalties to the emittance. This approach can provide several material design concepts that depend on combinations of doped

pigment and doped binders. The screening study concentrated on formulations listed above from the study[18], and only a couple concept formulations that can give feedback about doping.

2.2.2 Low α_s/ϵ_T, White Tailorable Conductive Thermal Control Coating Systems: Conceptual Design

In the area of low α_s/ϵ_T coatings, we have investigated concepts that showed potential in a prior study[18]. All proposed concepts used ZnO (SP-500) as a basic pigment material, based on the conservative rationale discussed and justified in an earlier section. The following conceptual material designs were evaluated in the screening study. The description of each material design (pigment concept) and the processes are discussed here.

A. **Concept Z-93CXY**: This coating system used treated ZnO as the pigment and Kasil 2130 potassium silicate as a binder system. The goal of this pigment treatment was to stabilize the required concentration of Zn interstitials in ZnO matrix to meet the conductivity needs of the coating. Harada[29] has listed these treatments as Z-36 and Z-52 in his original work. The goal of this work was to define a processing window for the treatment so that the resultant ZnO (SP-500) has enough required interstitials remaining in ZnO without presenting any penalties in the BOL value of α_s of the resultant coating. Thus, the work involved was developing a treatment parameter matrix of calcination temperature and calcination time during the required flash calcination to control the solid-state chemistry of ZnO. Based on the work done on this concept[18], we anticipate that for each pair of processing parameters, a different optimized pigment-to-binder ratio (PBR) is needed to tailor optical performance. The database was also developed to tailor the electrical resistivity values. This material design, due to its simplicity, offered be the most cost-effective and consistent solution.

B. **Concept Z-93CXY(IS)**: This concept used experimental data generated for an earlier concept along with the addition of silicated indium (In), with Kasil 2130 as a binder. The feasibility study[18] has identified In as one of the desirable ingredients. We also found that silicated In does not provide any additional absorption in the Ultraviolet/Visible (UV/Vis) region as long as the silicated indium concentration is kept low enough and silication is carried out prudently.[18]

Efforts were made in two areas. First, to develop and optimize silicated In oxide processing. The processing route described in Reference 18 provided a good starting point. In the second area, efforts were made to determine optimum concentration of silicated indium in Z-93CXY(IS). This work involved preparing a database on resistivity versus concentration of silicated indium, and a database on α_s (BOL) versus concentration of silicated indium in the Z-93CXY(IS) coating. Silica is usually considered a strong degradable component. [See Zerlaut and Harada[29]] Hence, this material concept was to receive attention only if the need arose. Thus, very little effort was devoted to this material design.

C. **Concept S13GCLM:** This pigment concept deals with development of In-doped microencapsulated ZnO pigment. The study has listed two sol-gel based process routes that need optimization. Efforts were made, first, to determine the optimum dopant level (LM), by choosing three different dopant levels. Recommendations given in Reference 18 were used to economize processing. The doped pigment was processed via two routes. The first one was high temperature (1000°C) doping. Enough IR&D efforts were done on this and were summarized in the section on IR&D efforts. The second one follows the S13G route with use of doped binders.

C-1. **Z-93SCXY-LM:** This concept used S13GCLM pigment with Kasil 2130 and other candidate doped binders for candidate dopant levels. The database of coating properties versus PBR was prepared for determining optimum formulation and optimum dopant levels.

C-2. **S13GCLM/LO-XY:** This concept used S13GCLM pigment with stripped polydimethyl siloxane as binder for the candidate doping levels. The coating properties were measured by selecting optimum PBR formulation and the optimum dopant levels for this flexible system. This concept is named DS13N/LO-XY in the results section.

C-3. **Z-93SCXY:** This concept used only the S13G and S13N pigments with Kasil 2130 and the candidate sodium silicate (SS-55) as the binder systems. The data

for this concept is available and is reported in Reference 18. The work on this concept provided a baseline database, and is presented in the results section.

2.3 CHARACTERIZATION NEEDS

2.3.1 Non-Contact Charging Tests and Needs

Brief efforts were devoted in initial IR&D during an earlier program[18] and during screening studies to understand practices used for space charging experiments. Our efforts revealed that insufficient documentation is available. Documented test procedures were shared by only JPL[11] as an appendix to material specifications. Most of the test practices that are currently in use are based on experience with conductive materials. The usual methods to measure charge developed need to be augmented with data on charge dissipation. Such data then can help in deriving the value of conductivity in the coating due to percolation paths. The desired method would be to use existing static charge development setups to measure voltage dissipated. It is also referred to as the surface voltage decreasing method in the literature. (See Levy et al.[26]) This approach is as follows:

The sample is first exposed to charging by the means of an electron beam. Sample irradiation is then interrupted and its surface is then continuously monitored by a trek voltage probe. Data are collected for surface potential versus time. The following simple analysis then applies.

The thermal control conductive coating applied on the metallic substrate is considered as a capacitor. Then the capacitance of the sample is written as:

$$C = \epsilon_o \epsilon_r \, (A/t)$$

C = capacitance, A = area, t = thickness of coating, ϵ_o and ϵ_r = usual dielectric constants for material system. The capacitor is considered discharging into its own resistance (the leakage resistance built in the thermal control system due to percolation paths)

$$R = \rho \, (t/A)$$

R = resistance, ρ = resistivity of TCMS. If V_s is the surface voltage, then

$$V_s = -R \, (dQ/dt) = -RC \, (dV_s/dt)$$

$$V_s = -\rho\epsilon_o\epsilon_r \, (dV_s/dt)$$

$$\rho = 1/\sigma = -\epsilon_o\epsilon_r \, (dV_s/dt)/V_s$$

Note that the conduction is not ohmic and R is dependent on voltage. The practical fallout is to present results as plot of log (resistivity) versus V_s^2 as a straight line, indicating that conduction is of the Pool-Frankel type and field assisted.

The current practices are also limited in measuring the secondary emissions. The problem of measuring the secondary emission on a dielectric material is complicated by the fact that the surface under measurement becomes charged during the measurement. This creates two problems:

(1)   Target/substrate surface potential must be accounted for to correct the electron energy at the sample level.

(2)   Barrier effects are associated with positively built surface potentials. These barrier voltage prevents the low E secondaries to reach measurement electrodes. This must be controlled to have valid measurements. Thus, the static method that provides charge and secondary emission input for conductive samples cannot give the same reliable information on the dielectric surfaces. One needs to use a dynamic method with pulsed electron techniques. The pulse duration of such a source is critical. Pulse duration should be no longer than a threshold to be determined. To limit the barrier effects in dynamic testing, one may further have to limit peak-to-peak time in consecutive pulses to measure true material properties.

At the present time, no one in the U.S. is actively pursuing dynamic testing. The small amount of data available in literature[26] is for 10 μsec pulses with pulse-to-pulse time of the order of 0.2 millisecond. The current practices used at IITRI are summarized in the form of an overview in the IITRI document.[9] The procedure requires sample conditioning to minimize moisture contributions. The HP-4339 also collects voltage versus time data, but we have reported only steady-state resistance numbers are reported here using the method.[9] These resistance values are representative of material formulation and microstructures and are considered adequate to carry out the material design exercise for this screening study.

3. RESULTS AND DISCUSSION

3.1 BASELINE MATERIALS AND RELEVANT DATA

For the evaluation of selected conductive concepts for material systems, the engineering assessment can only be fruitfully made by comparing the new suggested concepts with carefully prepared "heritage" materials that are currently being used as state-of-the-art materials. Although most of them are nonconducting, their optical, physical and mechanical performance are known with acceptable certainty. Since newer concepts are designed as the variations on the existing base materials and processes, the baseline TCMS manufacturing, sample preparation and characterization were first undertaken.

Baseline formulations were also the subject of recent requalification studies (see AMFL-TR-94-4126) to qualify new sources of raw materials. The findings from that study were to be revisited, so baseline material were prepared very carefully. Care was taken to avoid contamination during manufacturing of material systems and during their deposition as well, as during characterization. The use of newly made fresh materials was emphasized.

The following is a summary of the nonconducting baseline concepts that were selected for screening study for comparison purposes. Another motive was to learn more about reproducibility-related issues raised during the requalification efforts by comparing data that gets generated on these carefully prepared batches of baseline materials. A wide latitude was taken in selecting the baseline material systems, so that selected candidate can help in fruitful comparison during the study of their conductive counterparts.

The baseline material selection for Task A - black thermal control materials systems was straightforward. The concepts selected as a baseline were MH21-IP, MH21S/LO and a new system, D21S/LO, that used cosmic black in stripped polydimethyl siloxane polymer. The wider selection of black candidate pigments in silicate and stripped polydimethyl siloxane was the subject of investigation during recent small programs here at IITRI for GPS Block IIR.[18] The pigments included in those studies were TiC, B_4C, CuO, MnO, and FeO. A mixture of CuO, MnO and FeO is currently being used in formulation MH2200. It was not considered as a baseline material due to its outgassing properties and also due to the fact that it uses unstripped

siloxanes. All of the above mentioned pigment materials are semiconducting in nature, hence, they can also help to formulate conductive versions. For this reason, the baseline nonconducting materials for black TCMS were limited to the three listed candidates.

The nonconducting baseline white (low α_S/ϵ_N) formulation selection was also straightforward. All of the formulations that were reformulated per AFML-TR-94-4126 were considered as baseline. The baseline candidates included are: Z-93P, S13GP/LO-1, YB-71, YB-71P, S13GP/LO-41, ZOTS/LO-41, and a ZOT pigment pellet. These candidates were selected to revisit issues from the reformulation studies such as degradation of YB-71P versus YB-71. ZOT from one freshly prepared batch was selected. A sample of ZOT in pellet form was used to evaluate behavior of pigment alone. The behavior of pigment in stripped polydimethyl siloxanes was also considered as baseline candidate per recommendation from the initial studies carried out at IITRI by Zerlaut and Gilligan.[31] Two other pigments synthesized at IITRI through IR&D studies were also added to the list of baseline candidates. They were doped zinc silicate (DZS) and Europium oxide (Eu_2O_3). Both were selected based on results from the IR&D studies that indicated that a TCMS based on these pigments is capable of providing beginning of life (BOL) solar absorptance (α_S) values less than 0.10. It is important to point out that based on past studies (AFML-TR-71-246) the Eu_2O_3 based TCMS can be acceptably stable to UV-e'-Vac type environment. The choice of Eu_2O_3 was also initiated due to the fact that Eu_2O_3 has body center cubic (BCC) structure. This fact helps in use of conductive binder systems that are doped. It presents electro-ceramists a new regime to tailor conductivity values. Thus, to evaluate conductive concepts, its use as a baseline material was an obvious choice. The pigment/binder couples considered as baseline are listed in Table 3-1.

3.1.1 Material Processing

The baseline materials were prepared using 1 lb batch of pigment and required binder for the chosen pigment-to-binder ratios (PBRs) listed in Table 3-1. Each batch formulation was sprayed onto samples of various sizes for the required thickness to obtain maximum reflectance (minimum α_S). Ten one-inch discs, eight (2"x2") plates and two (4"x4") plates were coated for each formulation and cured per the best practices developed at IITRI. All inorganic coatings need a high humidity (>50%) and ambient temperature conditions during deposition and initial cure of one day. These are then cured at ambient laboratory clean environment for 14 days.

Table 3-1. Description of Concepts and Material Parameters for Formulations in Screening Test			
Concept Name	Pigment	Binder	PBR
Nonconducting Black Baseline Coatings:			
MH21IP	Black glass	Kasil 2130	2:1
MH21S/LO	Black glass	MHS/LO stripped polydimethyl siloxane	2:1
D21S/LO	Cosmic black, WB-500	MHS/LO stripped polydimethyl siloxane	2:1
Nonconducting White Baseline Coatings:			
ZOT (Pellet)	ZOT # 98790	Pressed and fired at 1000°C	
Z-93P	ZnO (Calcined 625°C, 16-18 hrs)	Kasil 2130	4.3
YB-71	ZOT # 98790	PS-7	7.1
YB-71P	ZOT # 98790	Kasil 2130	7.1
S13GP/LO-1	S13GP	MHS/LO stripped polydimethyl siloxane	2.1:1
S13GP/LO-41	S13GP	MHS/LO stripped polydimethyl siloxane	4:1
DZSS/LO-41	DZS	MHS/LO stripped polydimethyl siloxane	4:1
ZOT/LO-41	ZOT # 98790	MHS/LO stripped polydimethyl siloxane	4:1
Eu_2O_3/2130	Eu_2O_3[A]	Kasil 213-	5.5
EOS/LO-41	Eu_2O_3	MHS/LO stripped polydimethyl siloxane	4:1

All organic flexible baseline candidates use stripped polydimethyl siloxanes as a vehicle. These coatings used the process developed for S13GP/LO-1 and documented in processing specifications IITRI-MD-C06788-SP1 and IITRI-MD-C06788-SP2, and were cured for 14 days. All baseline material processing records are available in IITRI files.

3.1.2 Materials Characterization

The samples were then characterized for optical and electrical performance. The optical properties were characterized by measuring the total hemispherical spectral reflectance and the total normal thermal emittance. The measurement method followed the best practices listed as standard operating procedures (SOPs) at IITRI. The measurement of total hemispherical spectral reflectance at IITRI was carried out on a Lambda-19 spectrophotometer, using an integrating sphere. Care was taken for installation of sphere, calibration and data collection following the guidelines given by ASTM-E-903. The spectral reflectance data was then used to calculate solar absorptance following solar spectral weighted average method recommended by ASTM, using the solar air mass zero spectral irradiance curve (ASTM-E-490). The total normal thermal emittance was measured using DB-100 reflectometer. The reported emittance was calculated by subtracting the observed DB-100 reading from one.

The resistivity values reported herewith were measured with high resistance meters provided by Hewlitt Packard. Two different models were available at IITRI. The first one, HP-4329A, represented an older model. This model of resistivity cell used an old design of spring-loaded sample clamping. The sample pressure was not known and one cannot zero out air gap contact resistance. The new high resistance meter, HP-4339A, with the new resistance cell provided the opportunity to clamp the sample at constant selected pressure by dialing dead weight pressure. It also provided the ability to zero out air gas resistances in the cell along with the ability to set limits on leakage current to protect fuses. It also collects voltage and current data as a function of time, and stores the data on computer. The steady-state resistance value for given applied voltages is displayed digitally. Only steady-state values were reported for this screening study. For the interest of this program, the baseline thermal control coatings have surface resistance $> 10^{12}$ $\Omega/\square$, and are inherently porous in nature. Reduction of moisture contributions to the observed resistance values and selection of proper measurement procedure was key to this program. Our IR&D efforts indicated that overnight bake-out of samples at

100°C and measurement of sample surface resistivity on samples that were carefully stored in desiccant before transferring to the resistivity cell provided surface resistance values comparable to the surface resistance values observed on Z-93/Z-93P by Hamburger et al.[8] at Cleveland State University. Their efforts were more exhaustive, where samples were left in vacuum for at least two weeks to remove moisture. The screening study needed a representative surface resistance value for comparison purposes and for designing compositions. The HP-4339 with sample with bake-out approach was used to generate the representative surface resistance values. This practice was consistent with the recommendations provided for surface resistance measurement practices used in the paper industry that produces leaky, high-resistance coated paper products. [Kiethley Instruments - (Private Communications)[32]] An important factor was to use the correct isolator material to isolate the coated sample. We attempted measurements with Kapton 6H, clear Tedlar (2 mils) and Hewlett-Packard provided polyethylene sheet. The resistance numbers vary for a given coating for each isolator, but all of them fall within half to one decade. There are no ASTMs or guidelines available in this area. Help was sought from aerospace industry representatives on these issues. It was recommended that one needs to stay away from Kapton isolators, since they can introduce errors.[33] All reported numbers were obtained by using the polyethylene isolator sheet provided with the meter for consistency.

The data generated on optical and electrical properties for the baseline materials were measured and are provided in Table 3-2. The detailed reflectance curve generated for each formulation are also provided in Figures 3-1 through 3-13. For traceability purposes, each formulation has a batch number and sample series code provided in the data tables, so that the fruitful comparison can be carried out.

Table 3-2. Results of Optical and Electrical Characterization for Baseline Concepts					
Screening Study	Batch #	Alpha	Emittance	Surface Resistance Ω/□	
				HP-4329A	HP-4339A
Black Nonconducting Baseline Coatings:					
MH21-IP	U-284/289(GZ)	0.98	0.90	1.00E+14	1.00E+13
MH21S/LO	U-360(HZ)	0.98	0.90	1.00E+14	1.00E+13
D21S/LO	T-023(BA)	0.98	0.91	1.00E+10	2.00E+10
White Nonconducting Baseline Coatings:					
ZOT(pigment/pellet)	ZOT #98790	0.08	0.78	5.00E+08	9.00E+07
Z-93P	U-347(HX)	0.12	0.92	1.00E+14	11.00E+13
YB-71	U-348(HW)	0.10	0.89	1.00E+14	1.00E+13
YB-71P	U-376(IM)	0.11	0.90	1.00E+14	1.00E+13
S13GP/LO-1	U-310(HY)	0.17	0.91	1.00E+14	1.00E+13
S13GP/LO-41	U-276(HD,D)	0.16	0.91	1.00E+14	1.00E+13
DZSS/LO-41	U208(GI,H)	0.07	0.88	1.00E+14	1.00E+13
ZOTS/LO-41	U-343	0.13	0.85	1.00E+14	1.00E+13
Eu_2O_3/2130	U-352(IF)	0.08	0.92	1.00E+14	1.00E+13
Eu_2O_3/LO-41	U-403(IS)	0.14	0.90	1.00E+14	1.00E+13
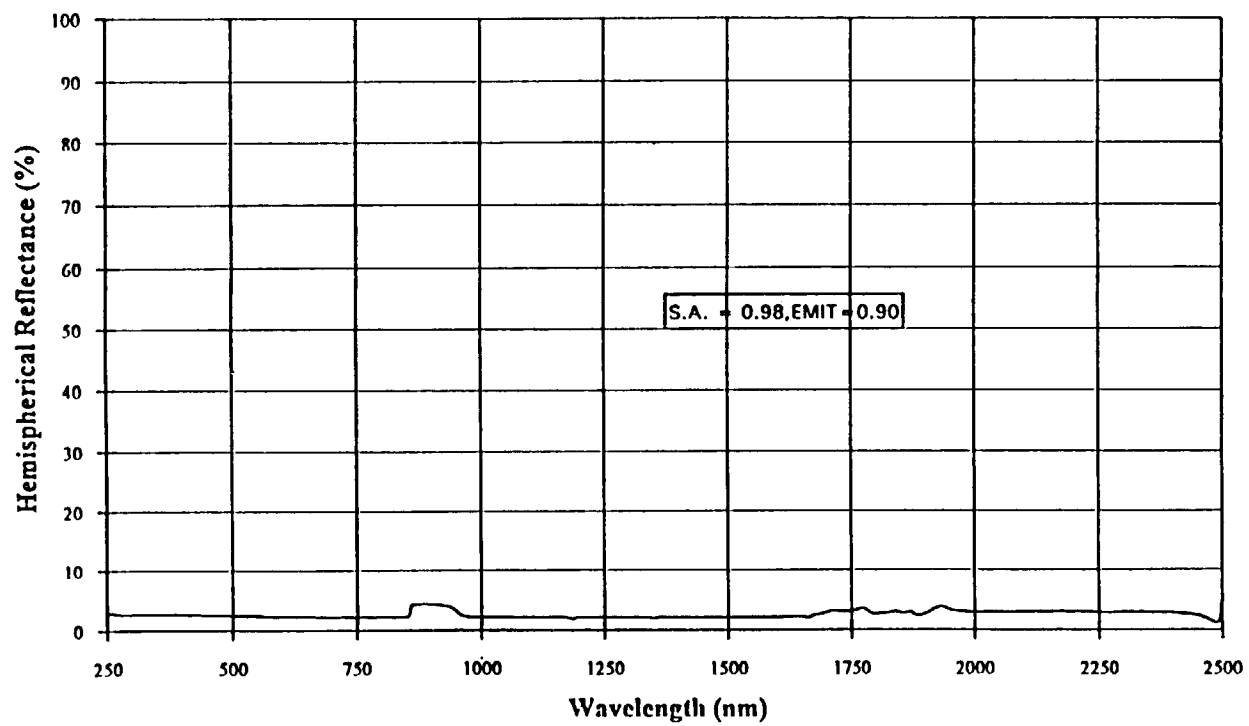
Figure 3-1.   Reflectance Spectrum of MH21-IP Sample #GZM-24, Batch #U-284/289.
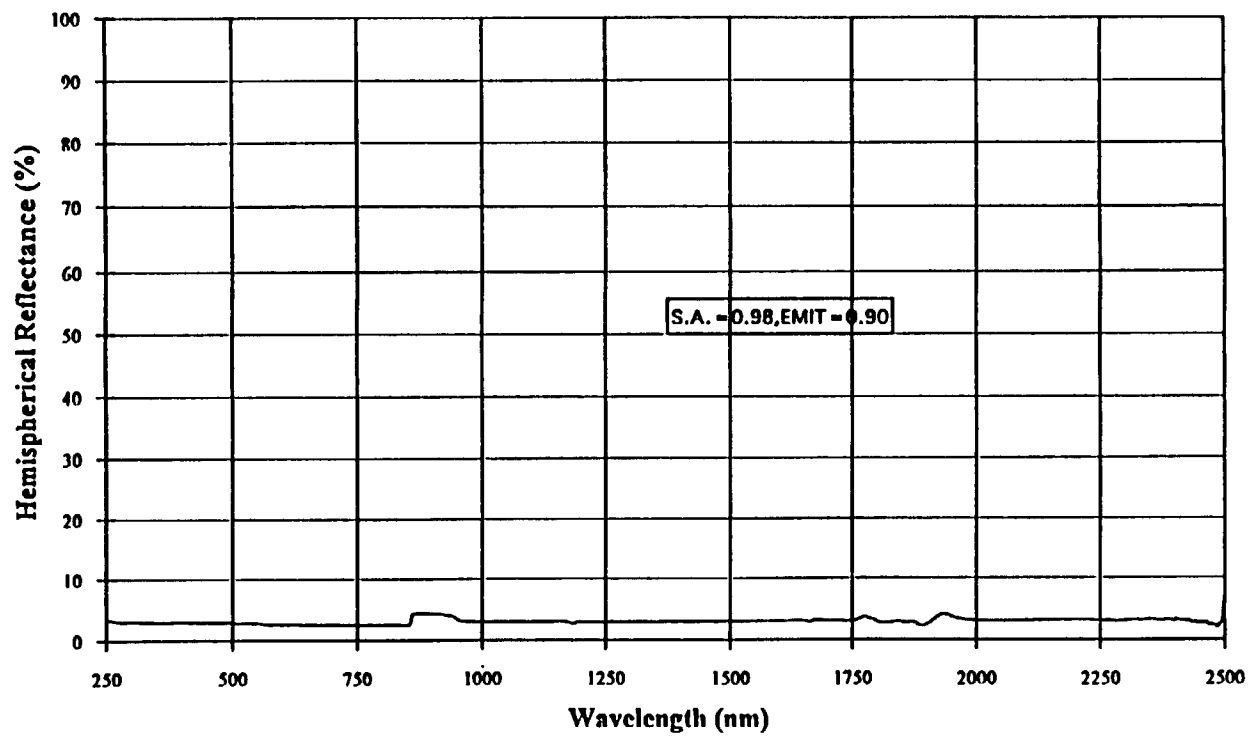
Figure 3-2. Reflectance Spectrum of MH21S/LO Sample #HZ-16, Batch #U-360.
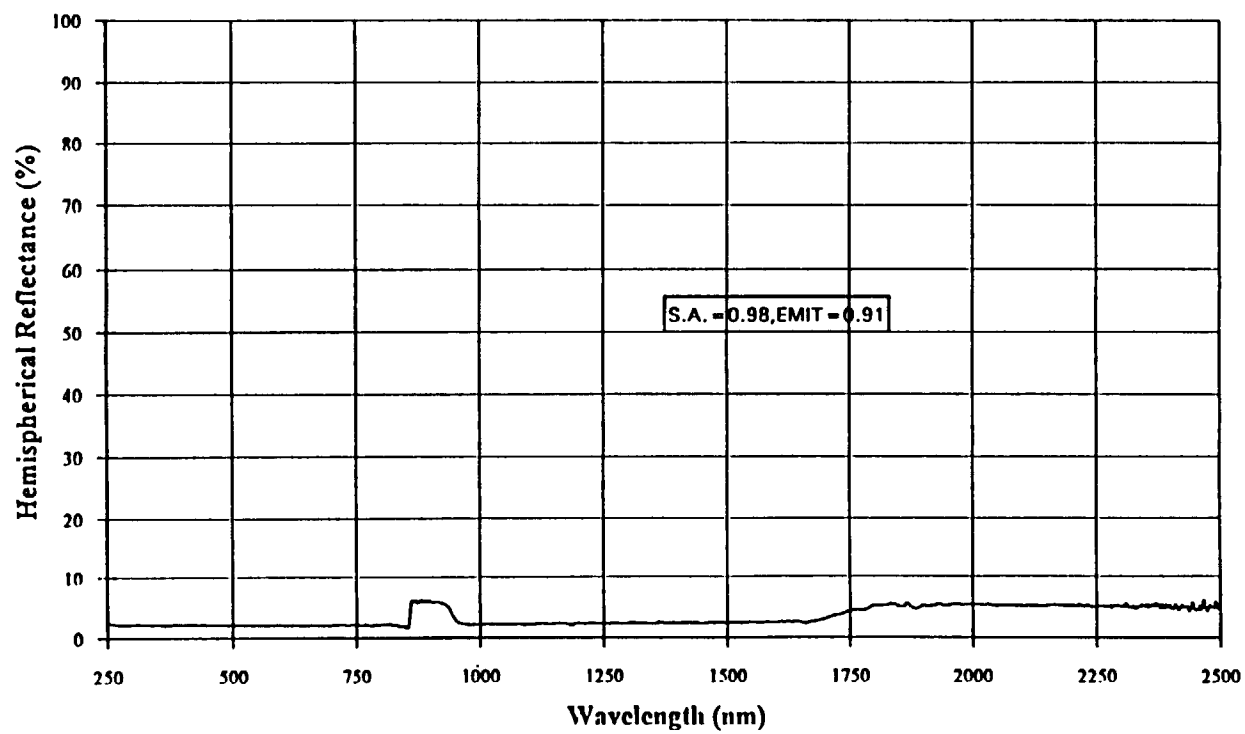
Figure 3-3. Reflectance Spectrum of D21S/LO Sample #BA-7, Batch #T-023.
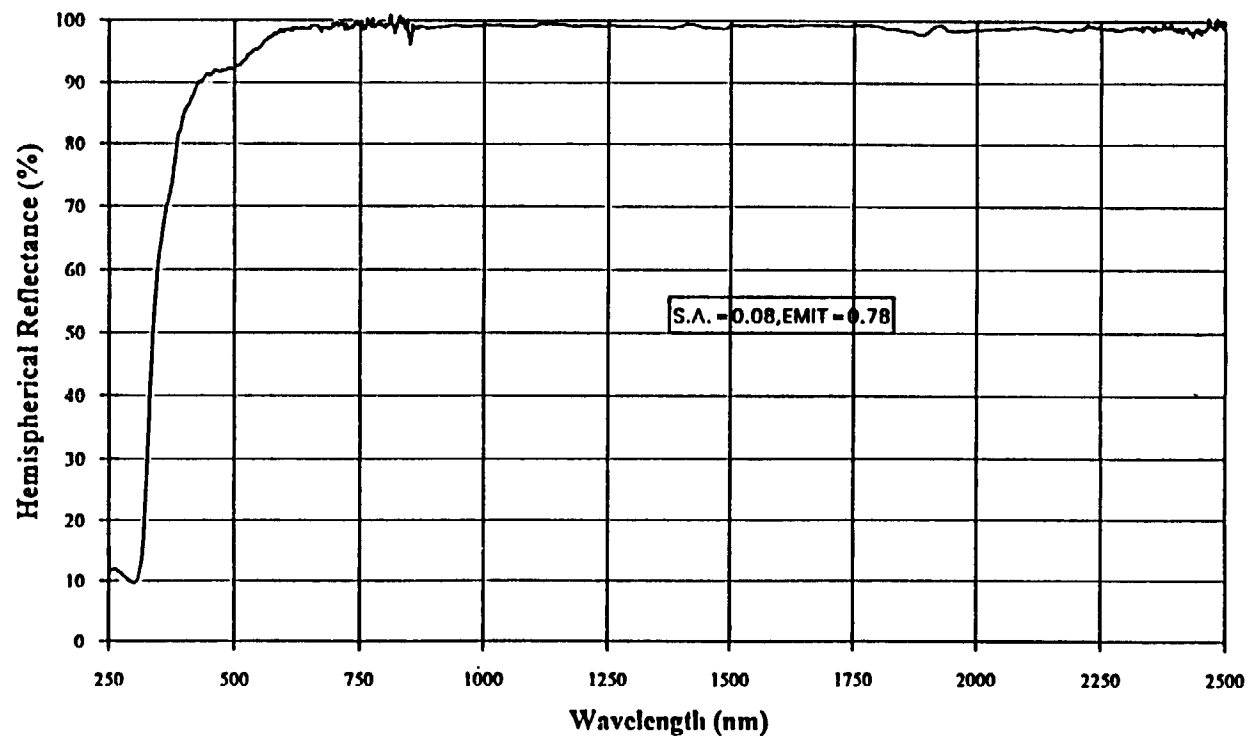
Figure 3-4. Reflectance Spectrum of ZOT/Pigment ZOT #98790.
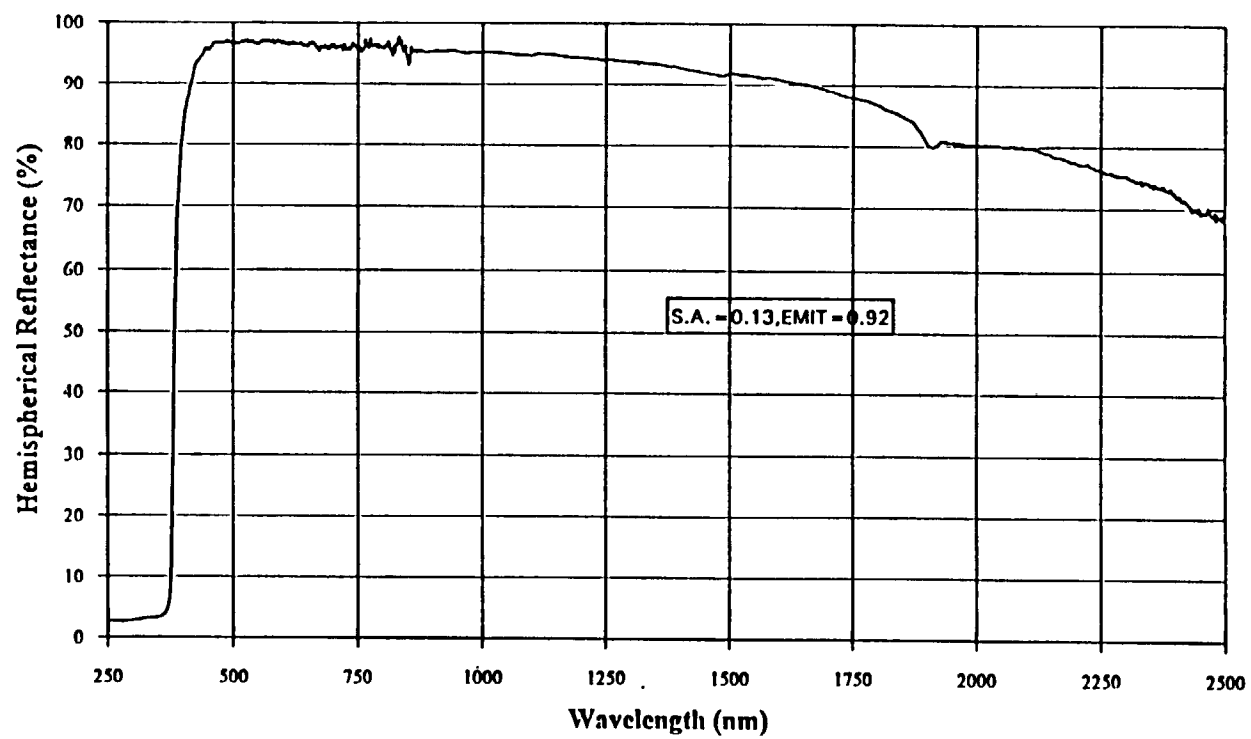
Figure 3-5. Reflectance Spectrum of Z-93P Sample #HX-14, Batch #U-347.
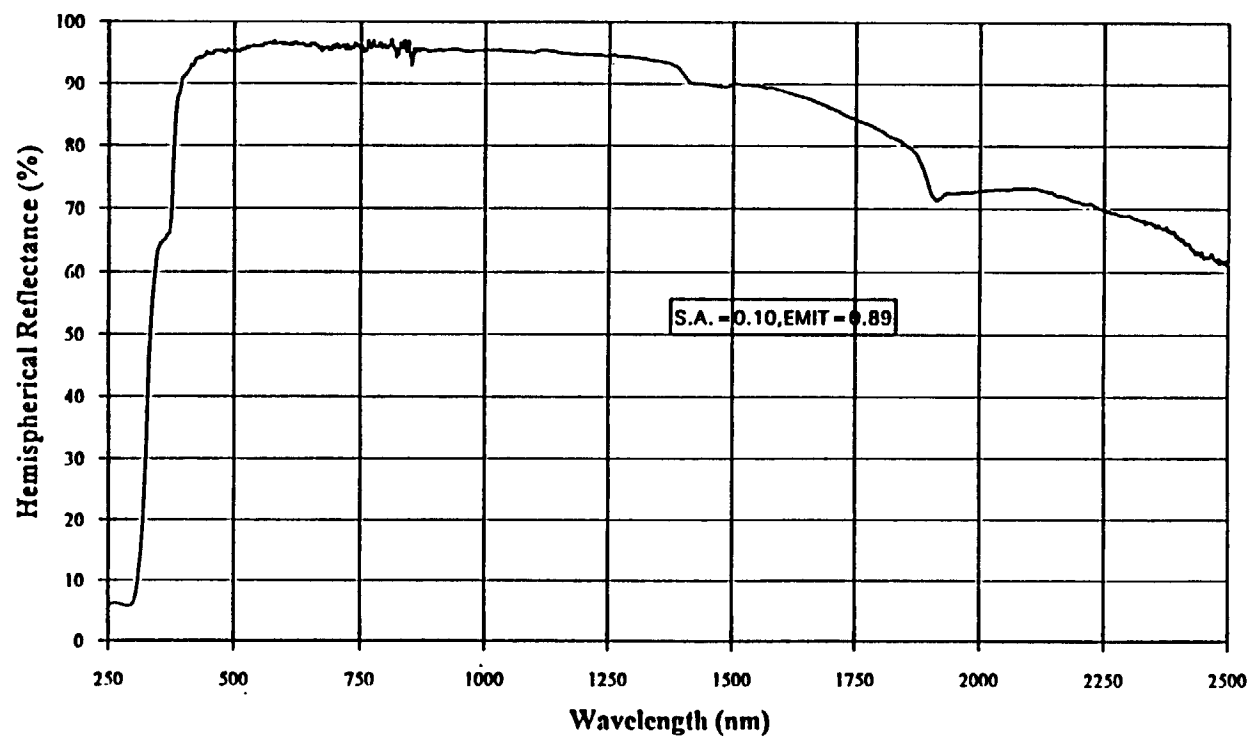
Figure 3-6. Reflectance Spectrum of YB-71 Sample #HW-7, Batch #U-348.
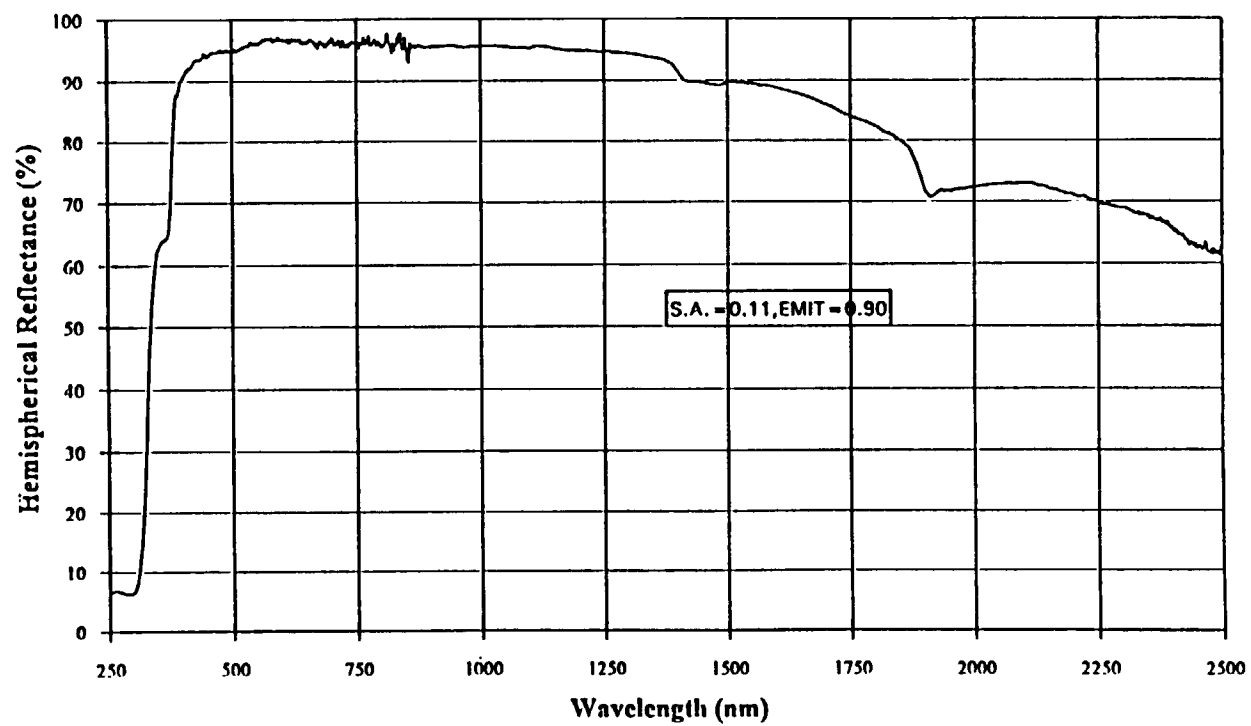
Figure 3-7. Reflectance Spectrum of YB-71P Sample #IM-25, Batch #U-376.
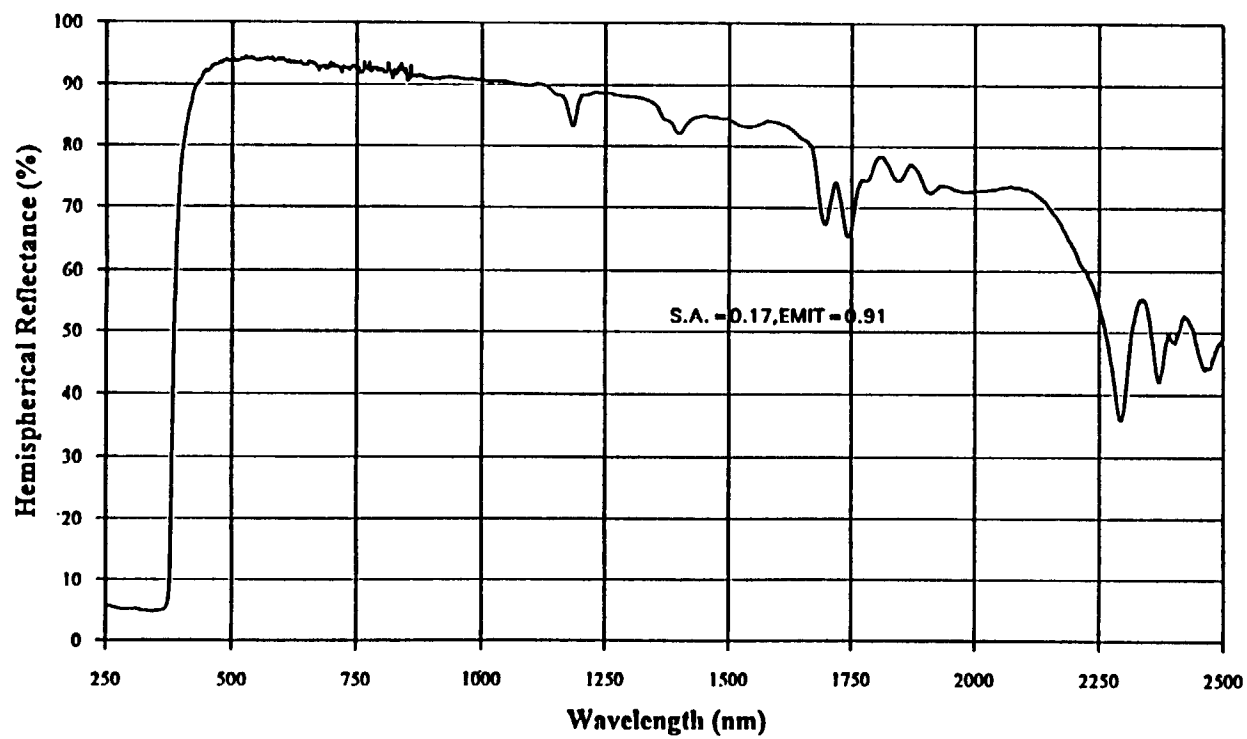
Figure 3-8. Reflectance Spectrum of S13GP/LO-1 Sample #HY-20, Batch #U-310.
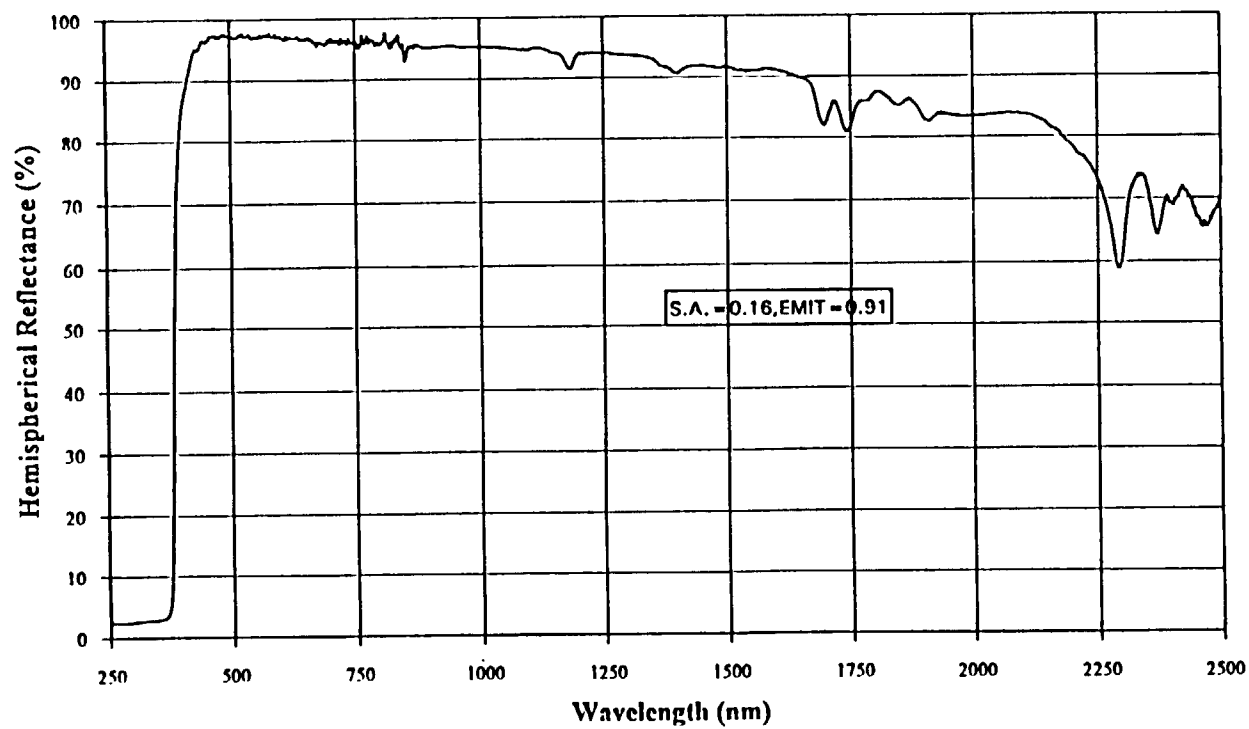
Figure 3-9. Reflectance Spectrum of S13GP/LO-41 Sample #HD-16, Batch #U-276.

S.A. = 0.07, EMIT = 0.88
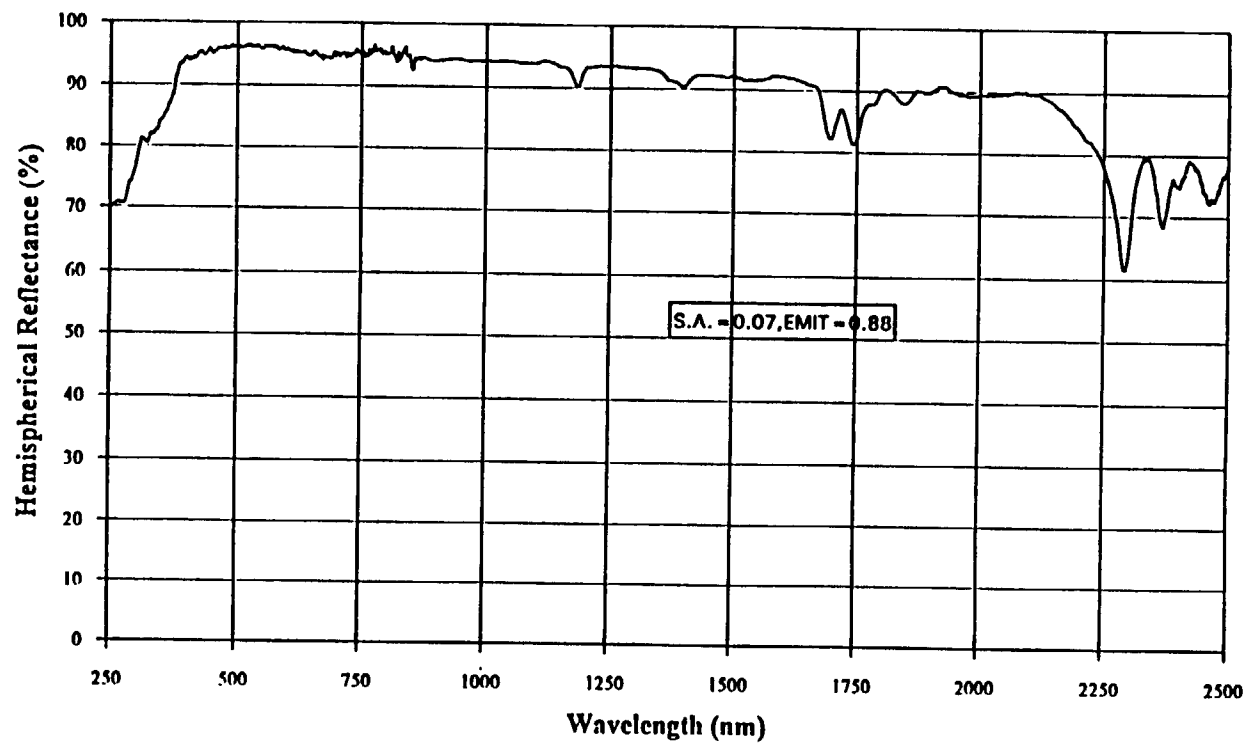
Figure 3-10.   Reflectance Spectrum of DZSS/LO-41 Sample #GI-9, Batch #U-208.
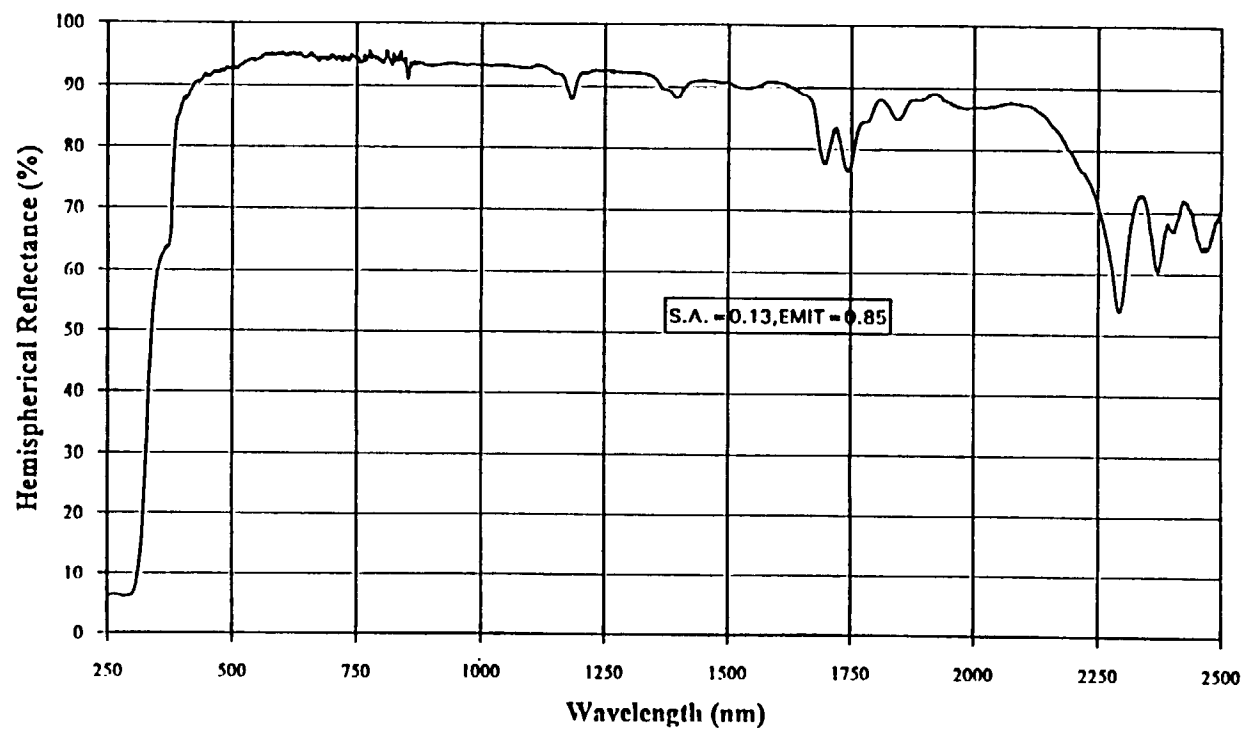
Figure 3-11. Reflectance Spectrum of ZOTS/LO-41 Sample #30, Batch #U-343.
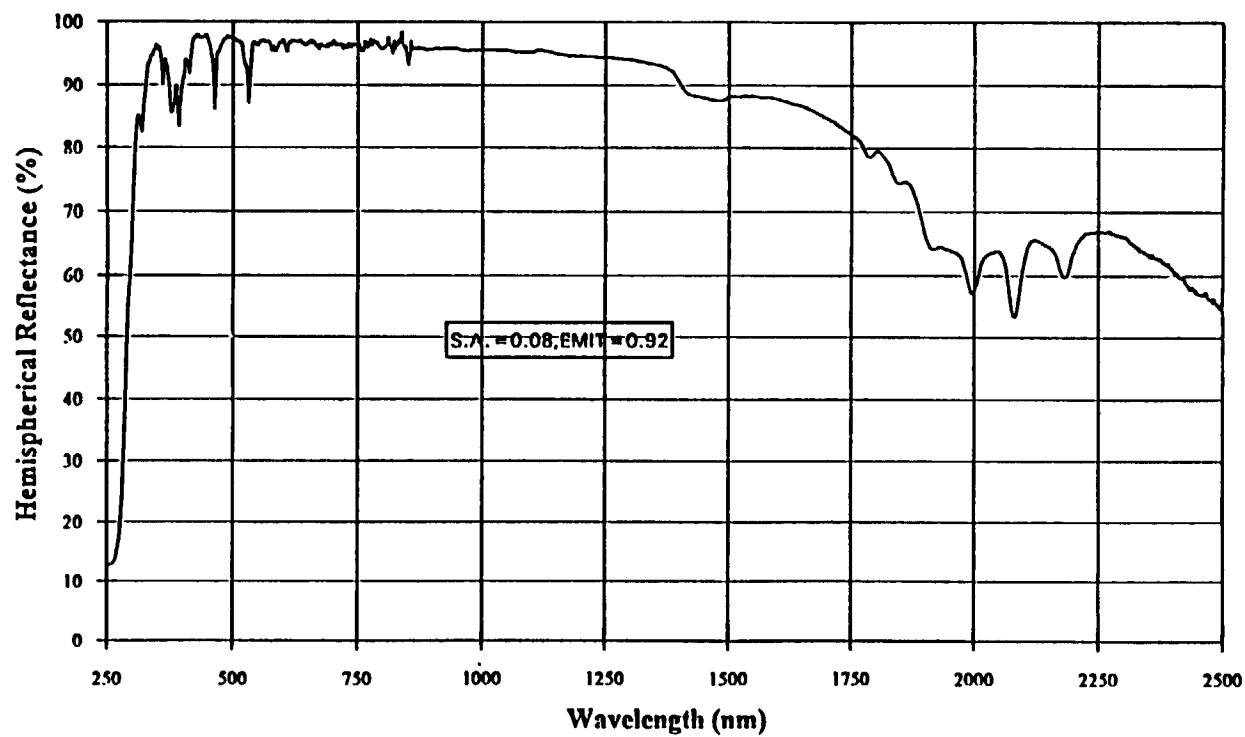
Figure 3-12. Reflectance Spectrum of $Eu_2O_3/2130$ Sample #IF-18, Batch #U-352.
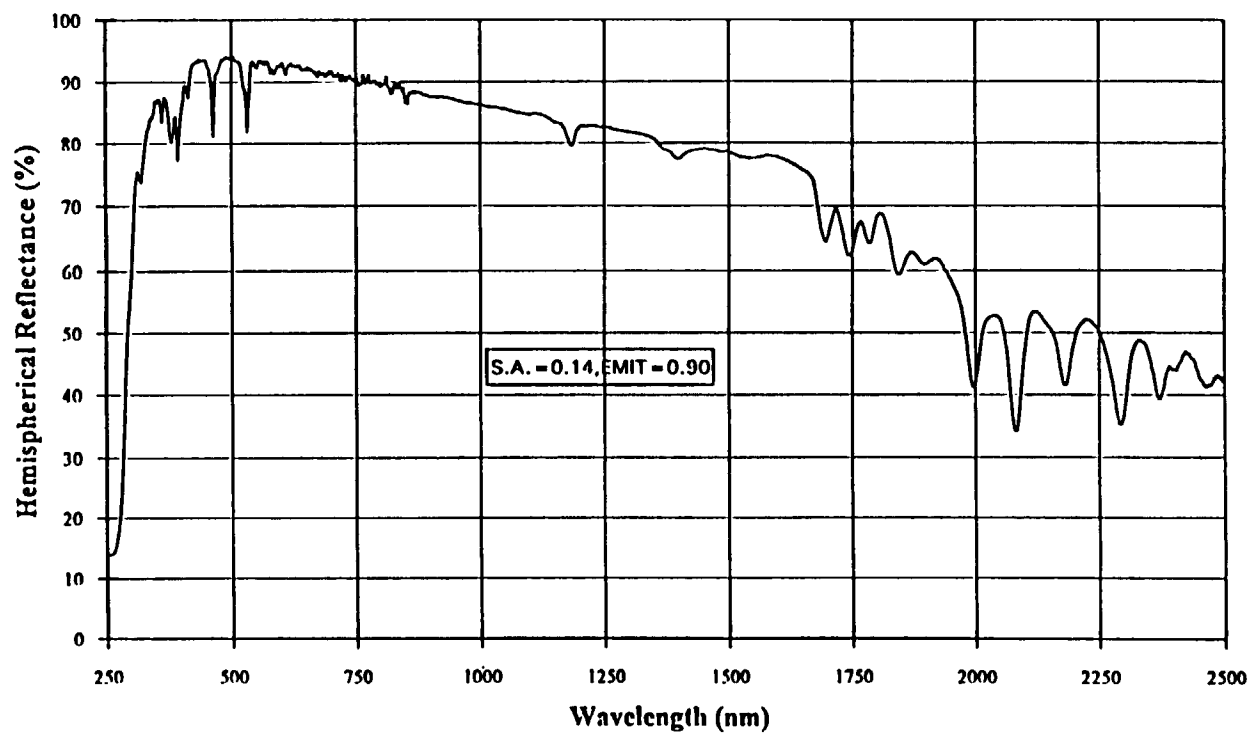
Figure 3-13. Reflectance Spectrum Eu$_2$O$_3$/LO-41 Sample #IS-17, Batch #U-403.

3.2 SELECTED CANDIDATE BINDERS AND PIGMENTS: [IR&D EFFORTS SUMMARY]

3.2.1 Binders. In this section first we describe efforts that were carried out prior to this screening study initiated at IITRI. The efforts started as early as 1991 during the reformulation efforts to replace potassium silicate binder (PS-7) used in the IITRI formulations. Most of these efforts were of short duration and were carried out as IR&D.

Sodium silicate was an obvious alternate for the potassium silicate. It was also used as a binder in very early studies funded by the Jet Propulsion Laboratory (JPL) for development of Z-93[6,29]. Sodium silicate was proven to be a suitable binder for space environment stability, but was not used because of its possible interaction with CO_2 in the atmosphere during storage to form carbonates, which can cause cracking in the coating. [See Zerlaut and Harada and [29]]. In view of these results, attempts were made to incorporate carbonate formation inhibitors to soda silicate sols to provide an alternate binder system. It was observed that the commercially available soda silicate are not pure or of electronic grade. Most of them are of industrial grade. The PQ Corporation provides soda silicate sols either too silicious for thermal control needs or with high alkali oxide content which makes them unsuitable for use in TCMS as binders. The available soda silicate sol thus needs to be considered as just precursors. The formulation of soda silicate sol was prepared using proprietary carbonate inhibitor additives (2% by weight) at IITRI via mixing and warming processes. The derived sol is named as SS-55.

<u>Soda Silicate Sol: SS-55</u>. The typical properties of SS-55 are as follows:

$$pH = 11.0 \text{ to } 11.5$$
$$\% \text{ solid} = 35\%$$
$$Na_2O:SiO_2 = 1:3.33$$

These key properties compare very well with the properties of PS-7 that are known to provide optimum adhesion and transmittance for use as a binder in TCMS. (See AFML-TR-94-4126) Availability of the binder system SS-55 aided this feasibility study significantly, since soda silicate provides flexibility in tailoring electrical conductivity.[6] The inherent small size of sodium ion compared to potassium ion may possibly make it easier for the binder system to participate in charge transfer, thus providing an additional mechanism for leakage in dielectric silicate.

The efforts in the binder area also were extended in doping the binder when it was realized that the presence of sodium alone can provide only limited flexibility in tailoring the surface resistance values. These efforts were initiated as IR&D during the GPS Block IIR study,[18] but were shelved because of their inherent defect structure dependent solid-state chemistry. The dopant used can only provide a defected oxide structure. The reliability of the defected structure was not known fully. This screening study provided the opportunity to investigate the two doped hybrid silicate binder systems named DHS-1 and DHS-2 prepared under IITRI's IR&D efforts. They are described here as follows:

- DHS: 50:50 mixture of Kasil 2130 and SS-55
  Addition of required dopant precursor; mixing/warming

- DHS-1: Maximum dopant level to achieve the highest surface resistance in the desired range

- DHS-2: Minimum dopant level to achieve the highest surface resistance in the desired range.

It was observed that the reproducibility of surface resistance values for the DHS-1 was better than for the DHS-2 formulation. Both were candidates for the feasibility study along with SS-55 to correlate the role of dopant in space environment induced degradation.

3.2.2 Pigments

3.2.2.1 Doped Black Glass. IR&D efforts were also made in the pigment area to enhance their conductivity. These efforts were made prior to initiation of this screening program. One of the remarkable achievements of this IR&D effort was doping black glass. Doped black glass was produced by using fumed silica or Si-backbone organic polymer as Si-precursors, Carbowax as carbon precursor, and Indium (In) precursor salts for doping. The black glass was derived following pyrolysis processing methods to yield the doped version. It was anticipated that incorporation of such a doped black glass in silicate or doped silicate binder would allow us to tailor electrical surface resistance of the coating without compromising either absorptance or emittance values.

Other IR&D efforts were in the area of white pigments. They were essentially focussed on processing aspects of pigment manufacturing. The white pigments that received attention were as follows:

- DZS: High temperature doping of Zn_2SiO_4 (Indium as dopant)

- Preparation of Eu_2O_3 from organometallic precursors of Europium

- Synthesis of Sb doped Zn_2SnO_x

The brief description of these IR&D efforts are given herewith. One to two pound batches of these pigments were processed and made available to this screening study to evaluate other defected oxide-based conductive concepts. We have included them in this study as other promising approaches.

3.2.2.2 DZS: Doped Zn_2SiO_4. The IR&D processing studies made to synthesize doped zinc silicate consisted of preparation of zinc precursor (ZOX) salt zinc oxalate and use of M-5 (Cab-O-Sil) fumed silica as precursor along with In precursor salts. The schedule to control grain size and morphology for tailoring maximum reflectance calls for processing the pigment as follows:

(1)   Mix precursors by dry milling 16 to 18 hrs

(2)   Precursor Decomposition/Firing: 625°C, 4 hrs

(3)   Flash calcine: 1000°C, 4 hrs

It was noted that dopant chemistry is not compatible with the high temperature firing. The retained dopant levels in pigment for tailoring targeted resistivity value demand very high usage of costly In precursor salts. The process route is an expensive route. Over all, two 1-lb batches were processed. The powders were included in the screening study evaluation to prepare coatings and data on the same are provided herewith in Section 3.3.

3.2.2.3 Europium Oxide (Eu_2O_3). The IR&D efforts made to prepare this pigment can be summarized briefly as follows:

(1)   Acquisition of Eu_2O_3

(2)   Precursor Decomposition/Firing: 625°C, 4 hrs

(3)   Flash calcination: 1000°C, 4 hrs

Eu_2O_3 (<400) mesh was also acquired for comparison purposes. It was found that use of <-400 mesh oxide powders provide similar optical properties as powders fired following the above schedule. The samples prepared for this study were all from europium oxide processed using the pigment synthesis steps summarized above. The powders were included in the feasibility study evaluation to prepare coatings and data on the same is provided herewith in Section 3.3.

3.2.2.4 Antimony Doped Zn_2SnO_x ($Sb:Zn_2SnO_x$).

The IR&D processing synthesis studies carried out to prepare this pigment were based on earlier results in space environment stability of Zn_2SnO_4 reported by Zerlaut and Harada[31], and to exploit economic doping approaches presented by the antimony chemistry. It is expected that the Zn_2SnO_4 invariably appears as defected oxide on the surface of pigment. SnO_2 and its defect structure has also been utilized by the semiconductor industry to develop sensing product.[25] The antimony provides an ability to stabilize the defect structures with proper and prudent use of multiple valance nature of its ion at high pH used in precursor sol chemistry, during the synthesis.

Since this pigment synthesis was an IR&D effort, a limited attempt was made to produce Sb-doped Zn_2SnO_x. The precursors used were: (1) ZOX, zinc oxalate synthesized by IITRI following methods listed in Reference 30; (2) Sb:doped tin sol provided to IITRI by P.Q. R&D Division as an experimental product.[24] The P.Q. R&D provided data for solids content (% solids) and the thermo gravimetric analysis (TGA). These data were used to calculate proper mixing ratio to prepare precursor mixtures, which were slowly dried over 2 days at 40°C. The precursor powder mixtures were then fired following firing schedules that were known to provide needed morphology and grain size distribution for maximum reflectance. The firings were carried out as follows:

(1)   625°, 4 hrs

(2)   1000°C, 4 hrs - flash calcination.

The powders were included in the screening study for evaluation of pigments. Various samples were prepared using this pigment and mixing Sb:Zn_2SnO_x with ZnO or DZS. The data obtained on the same are provided in Section 3.3

3.3 SELECTED CONCEPTS AND THEIR OPTICAL AND ELECTRICAL PERFORMANCE PROPERTIES

The conductive concepts considered in this study were based on two types of resistivity tailoring approaches. The first one treated TCMS as a composite. The current state-of-the-art TCMS was considered as a nonconducting component of the composite, and various candidate conductive phases were considered for addition to the nonconductive phase. An extraordinary volume of literature is available to provide guidance for tailoring composite resistance. The subject has received theoretical, numerical and quantitative modeling support, especially because of the discovery of superconductors. McLatchlan et al.[17] have reviewed the subject in depth and have provided guidance to selection of microstructural features in using conductive material as second phase to keep threshold value of volume fraction of conductive phase to a minimum and to acquire required percolation paths for achieving the target conductivity values.

Among the uses of high absorptivity material systems for space application, the electrical surface resistance needs change significantly from hardware to hardware. Tailoring high absorptance with low to moderate surface resistance have been done in the past (e.g., MH11Z at IITRI developed during 1984-1985), but such efforts have exacted penalties to absorptance and emittance values due the second conductive phase (of the order of 2 to 3%). Their RF properties also are lossy. Despite these penalties, the ease of formulating conductive high absorptivity coatings have a role to play for space hardware, because such an approach can offer an economic solution.

Some of the concepts that follow such an approach and were studied during this screening study are listed in Table 3-3. Among the conductive concepts listed in Table 3-3, the first two do not depend on the concept of tailoring conducting paths in TCMS using a second conductive phase. The first two essentially use In as a dopant in glass to provide a leaky dielectric. The two candidates considered can inform us about the role of binders, based on their space environment degradation behavior. These two cases can also provide input on the role that

Table 3-3. Candidate Concepts for Conductive High Absorptivity TCMS			
Concept Name	Pigment	Binder	PBR
Conducting Black Coatings:			
DBG-IP	Doped black glass (Indium doped)	Kasil 2130	2:1
DBG/DHS-1	Doped black glass	DHS-1	2:1
MH55IC	Black glass, Graphite 9035, ZnO	Kasil 2130	5.5
MH21SC/LO	Black glass, graphite fiber,	MHS/LO stripped polydimethyl siloxane	2.1
MH41SCB/LO	Black glass/B$_4$C	MHS/LO stripped polydimethyl siloxane	4:1
D21SC/LO	Cosmic black WB-500, Graphite 9035	MHS/LO stripped polydimethyl siloxane	2:1
MH11Z	Cosmic black WB-500 Graphite 9035, ZnO	Kasil 2130	1.1:1
D36SCB/LO	Cosmic black WB-500 Graphite 9035, B$_4$C	MHS/LO stripped polydimethyl silicone	3.6:1

secondary emissions properties can play in tailoring surface resistances. Unfortunately, graphite and In have similar secondary emission yields, so it may not be feasible to rank the concepts easily. One can make use of RuO_2 as one more conductive phase and tailor optical properties to design new formulations and alter secondary emissions further. The importance of "secondary emissions" mechanisms and their impact on space environment stability can thus be studied. However, the cost of RuO_2 and advanced level of electro-ceramic processing required to manipulate optimized microstructures to develop conductive percolating paths, forced us to shelve this concept due to the limited scope of this screening study.

Overall eight conductive concepts listed in Table 3-4 were used to prepare a batch of conductive TCMS. Each batch was then sprayed on the Al-6061-T6 samples of various sizes (1.0" disc, 2"x2" plates, and 4"x4" plates) for optical and electrical performance characterization. The total hemispherical spectral reflectance, total normal emittance and surface electrical resistances were measured following the same methods that were used for characterizing baseline nonconducting material systems, described earlier in Section 3.1. The observed data are presented here in Table 3-4. The detailed total hemispherical spectral reflectance curves for these concepts are given in Figures 3-14 through 3-19.

3.3.1 Conductive Thermal Control Material Systems for Low (α_S/ϵ_N) Applications

The second task of these efforts was devoted to the study of conductive concepts for which conceptual material design was already carried out and reported in Section 2.3. Pigment and binder concepts discussed in the section on IR&D studies were also included in this task as other concepts. The following section describes studies carried out for each concept along with results of the material and process characterization studies.

3.3.1.1 Concept Z-93CXY. Although the rationale of this concept was discussed in detail in Section 2.3, it may be noteworthy to revisit the same along with a discussion on processing. From the studies on ZnO variators, it is known that the Zn interstitial concentration in ZnO grain control the resistivity value. Zerlaut and Harada[29] showed that removal of Zn interstitial from the grains via annealing provides space environment stability. While studying annealing parameters of temperature and time in this study[29], several schedules were attempted. The schedule picked for Z-93 provided material with the best stability to space environment.

Table 3-4. Summary of Optical and Electrical Properties of Conductive Black Coatings					
	Batch #	Alpha	Emittance	Surface Resistance (Ω/□)	
				HP4329A	HP4339A
Conductive Black Coatings:					
DBG-IP	U-021(EO)	0.97	0.90	2.00E+08	1.00E+08
MH55-ICP	S-204(Z,AC)	0.94	0.88	1.00E+09	1.00E+09
DBG/DHS	U-283(GT,GU)	0.96	0.90	8.00E+08	1.00E+09
MH21SC/LO	U-166(FD-1)	0.96	0.86	1.00E+06	7.00E+05
MH41SCB/LO	U-053(FD)	0.96	0.87	1.00E+09	1.00E+09
D21SC/LO	T-026(BJ)	0.95	0.88	1.00E+06	C/M
D36SCB/LO	T-027	0.95	0.91	1.00E+06	C/M
MH11Z	*	0.89	0.90	1.00E+05	1.00E+04

* From report to JPL.

C/M = Cannot be measured (i.e., resistance is less than 1.00E+03).
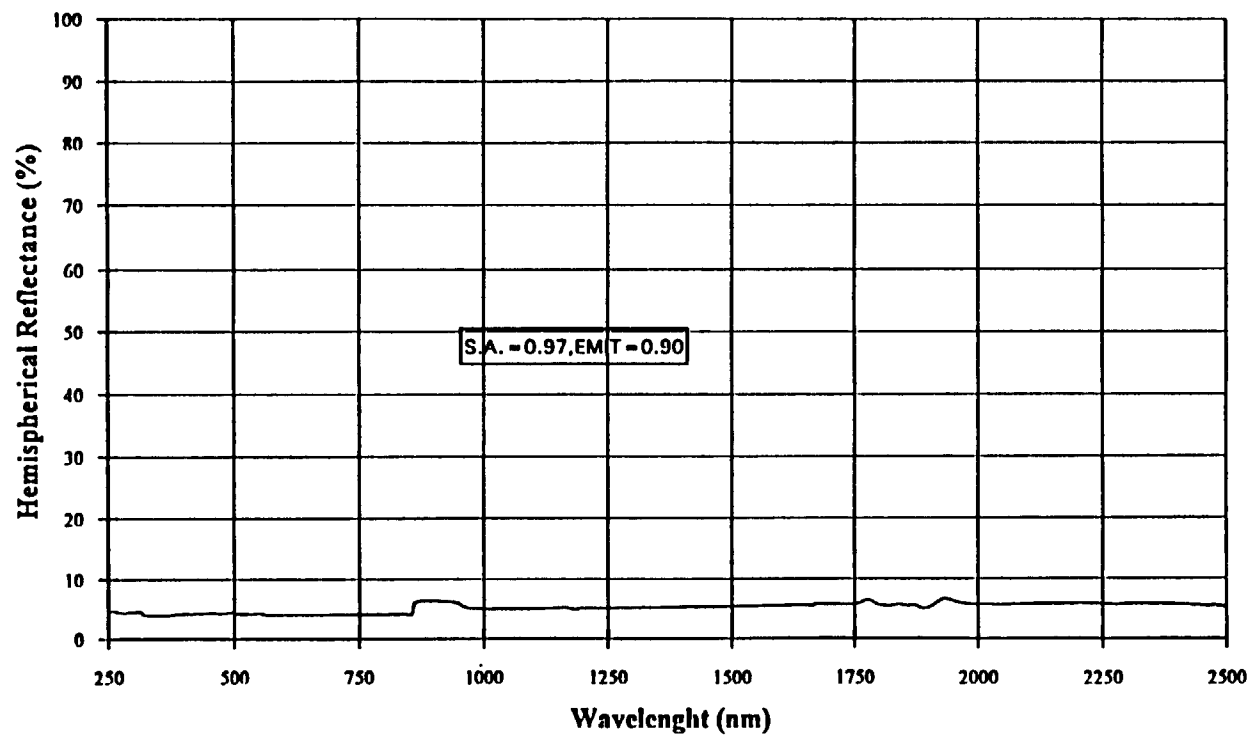
Figure 3-14. Reflectance Spectrum of DBG-IP Sample #EO-6, Batch #U-021.
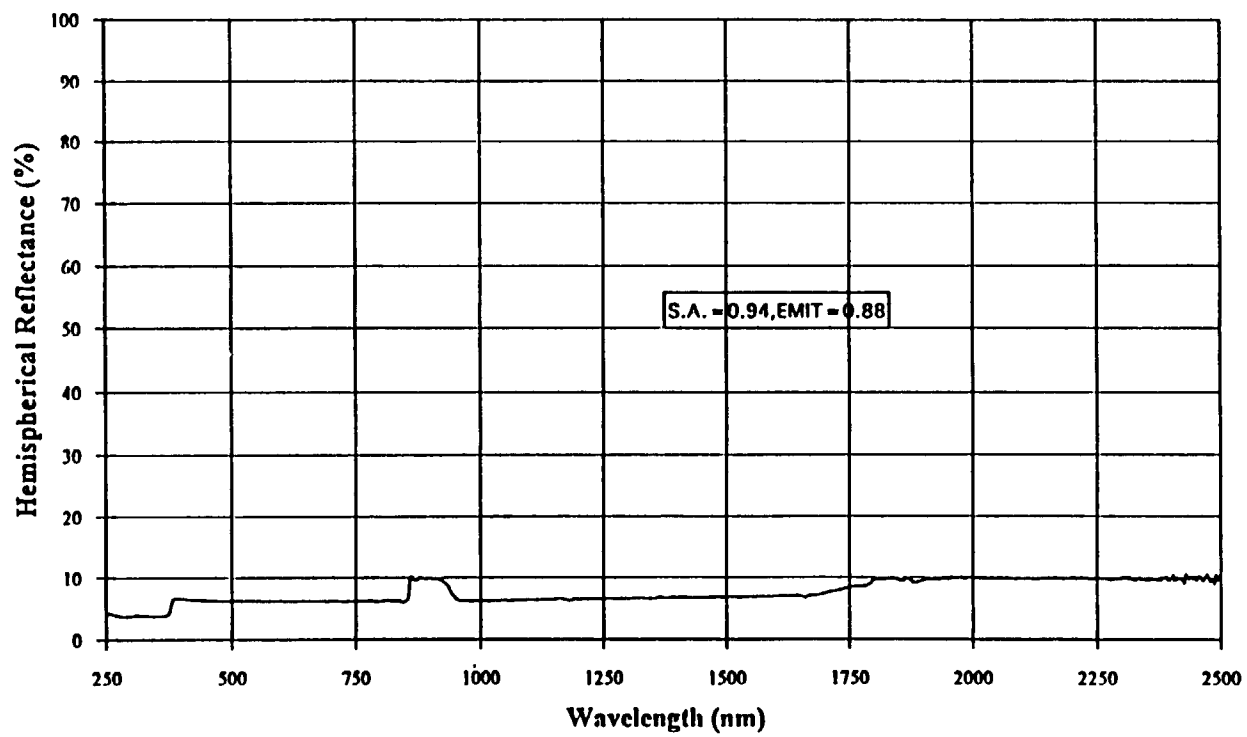
Figure 3-15.   Reflectance Spectrum of MH55-IC Sample #AC-33, Batch #S-204.
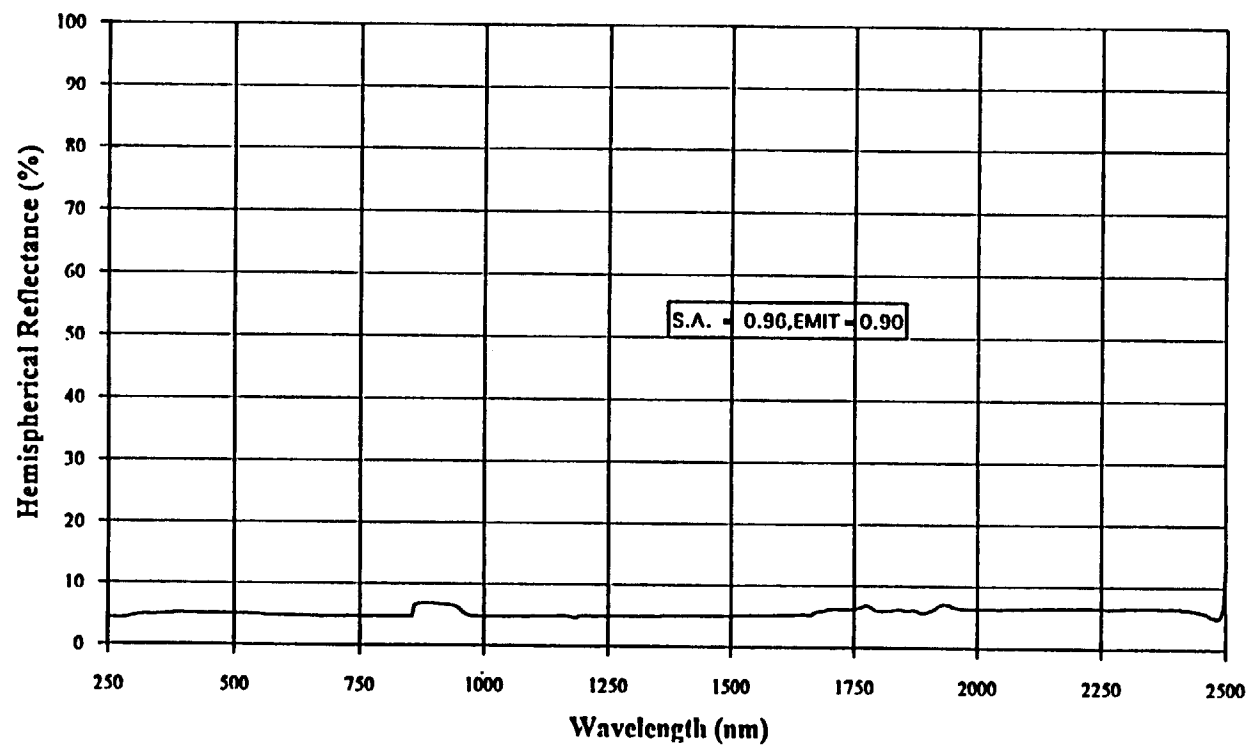
Figure 3-16. Reflectance Spectrum of DBG/DHS Sample #GU-2.
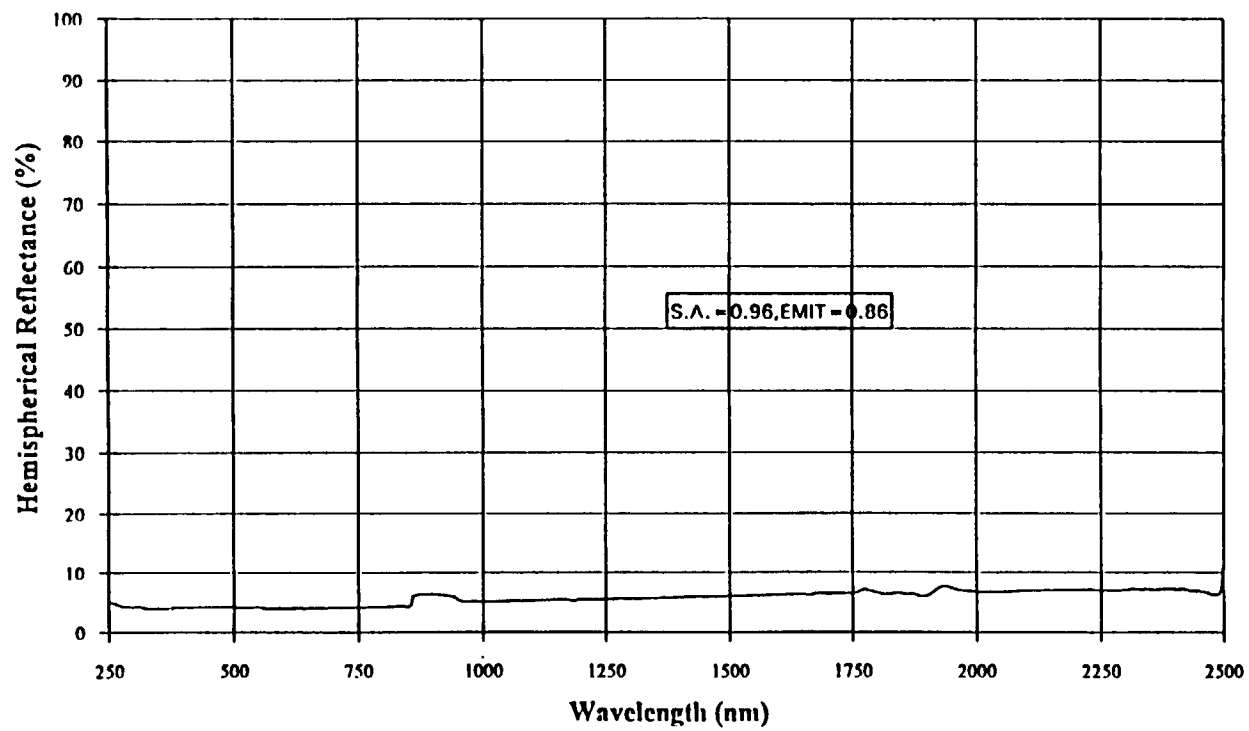
Figure 3-17.   Reflectance Spectrum of MH21SC/LO Sample #FD1-15, Batch #U-166.

The chart shows "Hemispherical Reflectance (%)" on the Y-axis (0 to 100) versus "Wavelength (nm)" on the X-axis (250 to 2500). A label reads "S.A. = 0.96, EMIT = 0.87".
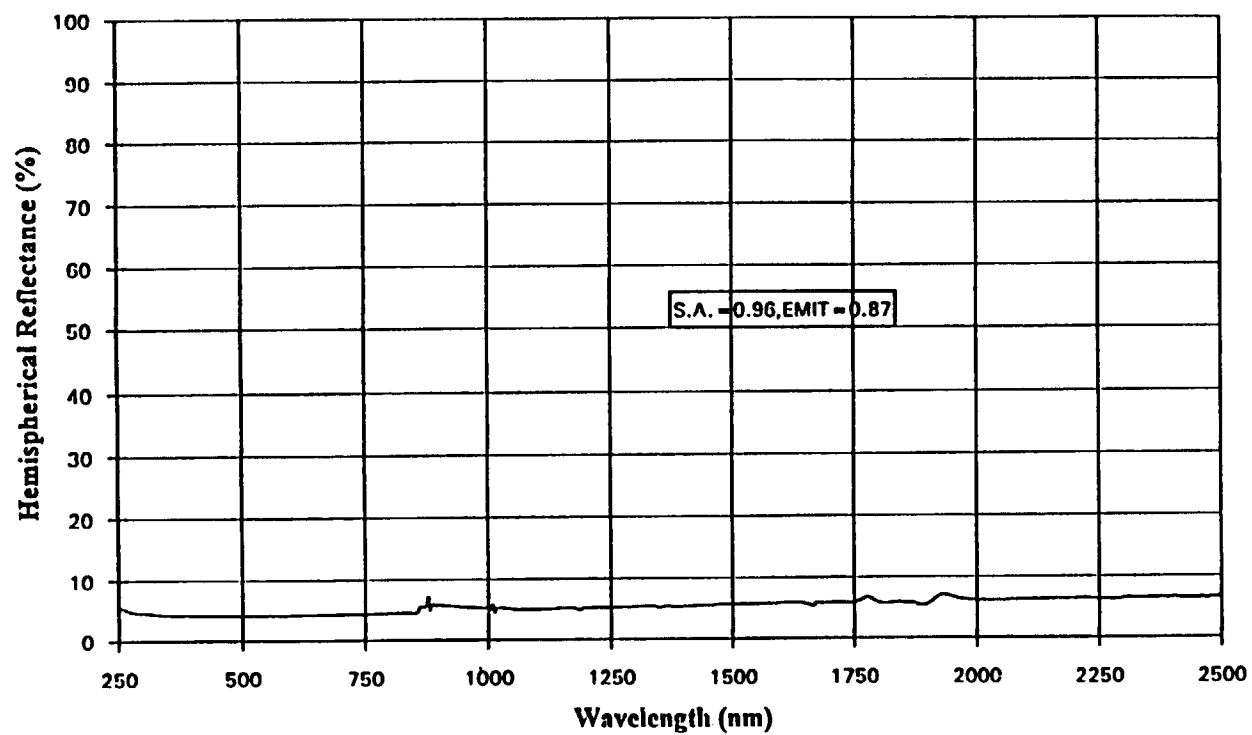
Figure 3-18.   Reflectance Spectrum of MH41SCB/LO-1 Sample #FD-2, Batch #U-053.
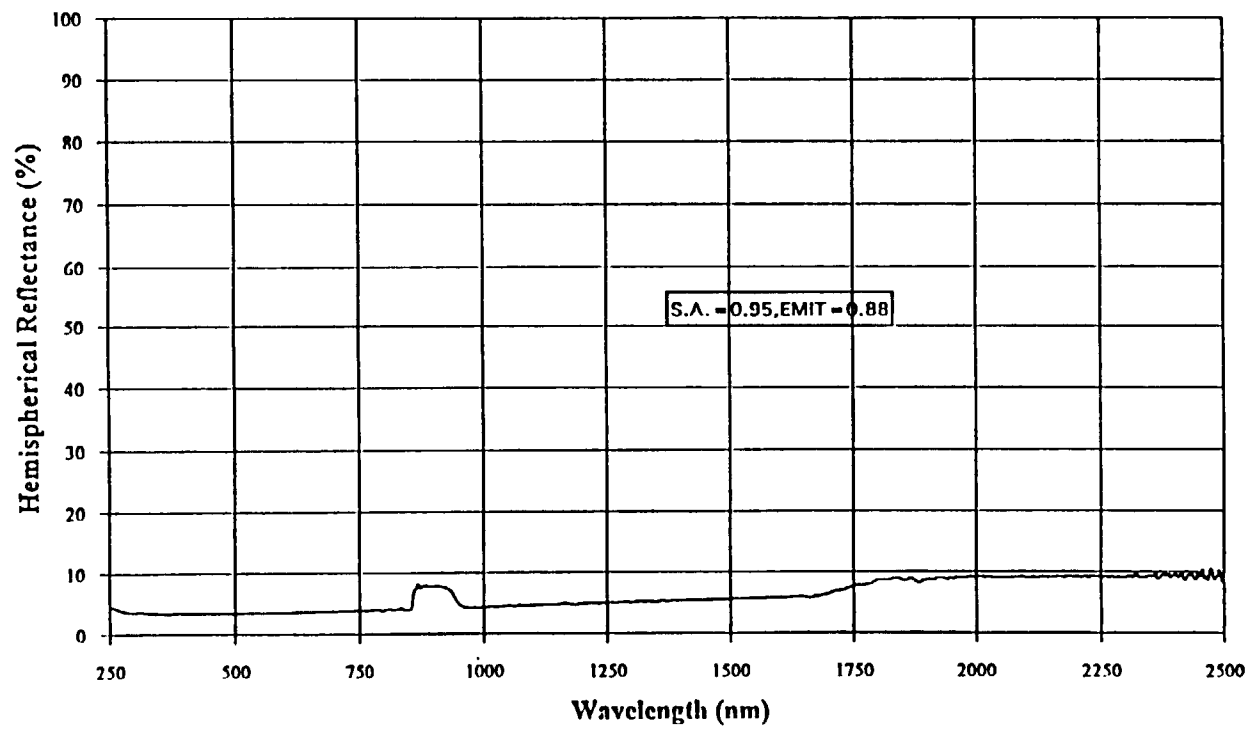
Figure 3-19. Reflectance Spectrum of D21SC/LO Sample #BJ-8, Batch #T-026.

The retention of Zn interstitials to tailor required resistivity values without compromising optical performance was the goal. ZnO (SP-500) of Zinc Corporation of America was used as source and was flash calcined at selected temperatures. Overall three temperatures ($800°$, $900°$ and $1000°C$) were picked for processing trial batches and flash calcinations were carried out in quartz beakers for time periods of 15 minutes, 30 minutes, 1 hour, and 4 hours. A charge of 900 grams was used for each run. Each pigment was then mixed with Kasil 2130 as a binder for preparing samples to measure α_S, ϵ_N. Based on the data collected for a calcination temperature of $900°C$, a flash calcination time of 15 minutes was selected for the screening studies. A flash calcined batch (900 grams, $900°C$, 15 minutes) was prepared and used in four different binder systems. The candidate binder systems used are: Kasil 2130, SS-55 (soda silicate sol), DHS-1 and DHS-2 (both doped hybrid silicate sols developed at IITRI). The description of candidate concepts and material parameters are listed in Table 3-5.

Table 3-5. Conductive Concept Z93CXY			
Z93CXY: Flash calcined (FC), control of Zn interstitials for required conductivity in silicate binders and doped silicate binders.			
Concept: Z-93CXY	Pigment	Binder	PBR
Pigment/Binder			
ZnO (FC)/2130	Zno Flash Calcined (FC)	Kasil 2130	5.5
ZnO (FC)/SS-55	ZnO (FC)	SS-55	5.5
ZnO (FC)/DHS-1	ZnO (FC)	DHS-1	5.5
ZnO (FC)/DHS-2	ZnO (FC)	DHS-2	5.5

A batch of each material formulation was prepared for the above formulations and sprayed onto various substrates of 1.0 inch diameter discs, 2"x2" plates, 4"x4" plates for optical and electrical performance characterization. The total hemispherical spectral reflectance, total normal thermal emittance and surface resistivity were measured following the same methods that were used to characterize baseline nonconducting material described earlier in Section 3.1. The observed data are presented in Table 3-6 and the detailed reflectance curves are presented in Figures 3-20 through 3-23. All data was taken for coating thickness of 5.0 mils (nominal).

Figure 3-20.   Reflectance Spectrum of ZnO(FC)/2130 Sample #HM-21, Batch #U-321.

Figure 3-21. Reflectance Spectrum of ZnO(FC)/SS-55 Sample #HF-16, Batch #U-322.

Figure 3-22.   Reflectance Spectrum of ZnO(FC)/DHS-1 Sample #HG-16, Batch #U-323.

Figure 3-23. Reflectance Spectrum of ZnO(FC)/DHS-2 Sample #HL-25, Batch #U-327.

Table 3-6. Z-93CXY: Properties of Candidate Pigment/Binder Couples					
Concept: Z-93CXY	Batch #	Alpha	Emittance	Surface Resistivity ($\Omega/\square$)	
Pigment/Binder				HP4329A	HP4339A
ZnO(FC)/2130	U-321(HM)	0.14	0.92	1.00E+14	
ZnO(FC)/SS-55	U-322(FH)	0.14	0.91	1.00E+08	6.00E+08
ZnO(FC)/DHS-1	U-323(HG)	0.15	0.92	2.00E+09	2.00E+08
ZnO(FC)/DHS-2	U-327(HL)	0.15	0.91	1.00E+09	1.00E+09

The resistivity values reported in Table 3-6 are the values observed immediately after 14 days of cure at ambient conditions. The coating deposition was carried out similar to Z-93P processing, and curing was carried out using high humidity environment. The samples were then conditioned to avoid moisture contribution to measurement, by purging them in dry desiccant with nitrogen. It was observed that storage of the samples using silicate binders (Kasil 2130, soda silicate SS-55) exposed to ambient conditions causes surface resistivity values to increase in the range of 10^{12} to 10^{13} $\Omega/\square$ after 6 to 8 months. This effect was not observed for doped silicate binders even after two years. All four concepts were submitted to the space environment simulation, but only reliable resistivity concepts were submitted for ESD testing and Goddard Space Flight Center (GSFC). The results are discussed here in corresponding chapters. The results show that flash calcination alone cannot stabilize resistivity. One can speculate that dopant in binder may be helping to stabilize electrical performance of the coating via carrying out in situ doping of ZnO on grain surface. Thus, it will be interesting to review results of the space environment simulation for these candidates, which are presented in the next chapter.

3.3.1.2 Concept Z-93SCXY. The rationale for this concept still lies in control of Zn interstitials in ZnO to impart required resistivity in pigment grains. Here a material technology employs encapsulation approach to stabilize interstitials inside the grain. Our quest for such stability to space environment is not new. We have pursued such stabilization via microencapsulation routinely for S13GP pigment, with ZnO (SP-500) as the starting material.

In providing candidate material concept samples for this evaluation study, microencapsulation of ZnO (SP-500) (uncalcined) was carried out following the SOP for reactive encapsulation using Kasil 2130 as the binder system. The processing steps reported in AFML-TR-94-4126 were used, and the resultant pigment is designated S13GP. Similar processing was carried out on a bench scale setup using newly developed soda silicate sol (SS-55). This pigment was named as S13N. Both these pigments were used with two silicate binders (Kasil 2130 and SS-55) and two doped hybrid silicate binders (DHS-1 and DHS-2) to process candidate conductive TCMS. The description of material parameters is given in Table 3-7.

Table 3-7. Conductive Concept Z93SCXY			
Z93SCXY: Microencapsulated pigments in silicate binders and doped silicate binders.			
Concept: Z-93SCXY	Pigment	Binder	PBR
Pigment/Binder			
S13GP/2130	S13GP	Kasil 2130	5.5
S13GP/SS-55	S13GP	SS-55	5.5
S13GP/DHS-1	S13GP	DHS-1	5.5
S13GP/DHS-2	S13GP	DHS-2	5.5
S13N/SS-55	S13N	SS-55	5.5
S13N/DHS-1	S13N	DHS-1	5.5
S13N/DHS-2	S13N	DHS-2	5.5

A batch of each material formulation was prepared for the above formulations and sprayed onto various substrates of 1.0 inch diameter discs, 2"x2" plates, 4"x4" plates for optical and electrical performance characterization. The total hemispherical spectral reflectance, total normal thermal emittance and surface resistivity were measured following the same methods that were used to characterize baseline nonconducting material described earlier in Section 3.1. The observed data are presented in Table 3-8 and the detailed reflectance curves are presented in Figures 3-24 through 3-30. All data were for a coating thickness of 5.0 mils (nominal).
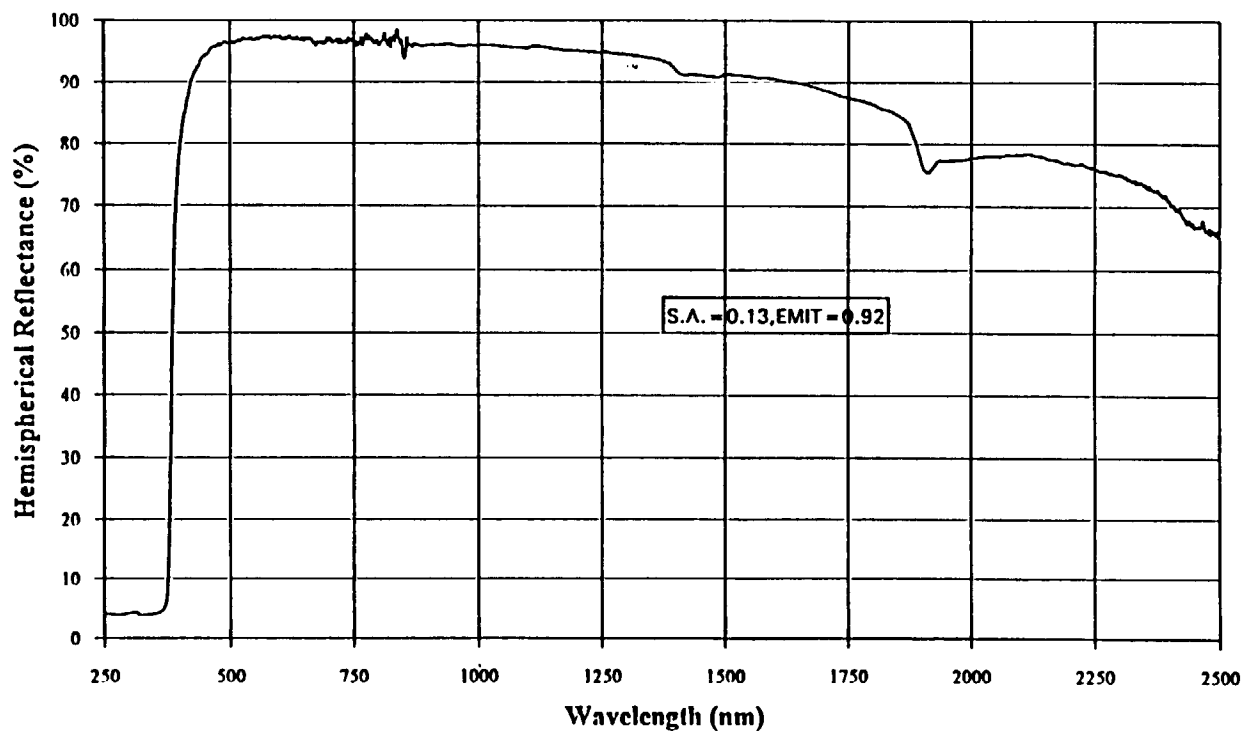
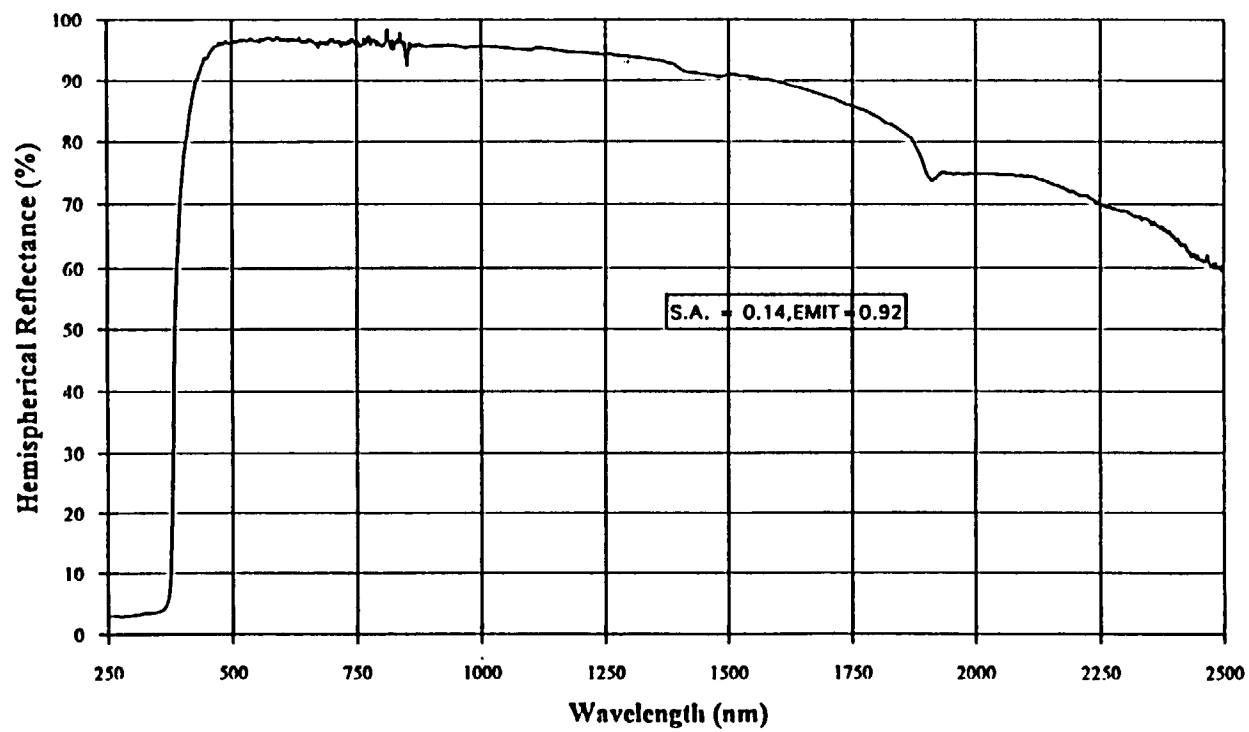Figure 3-24. Reflectance Spectrum of S13GP/2130 Sample #FM-17.
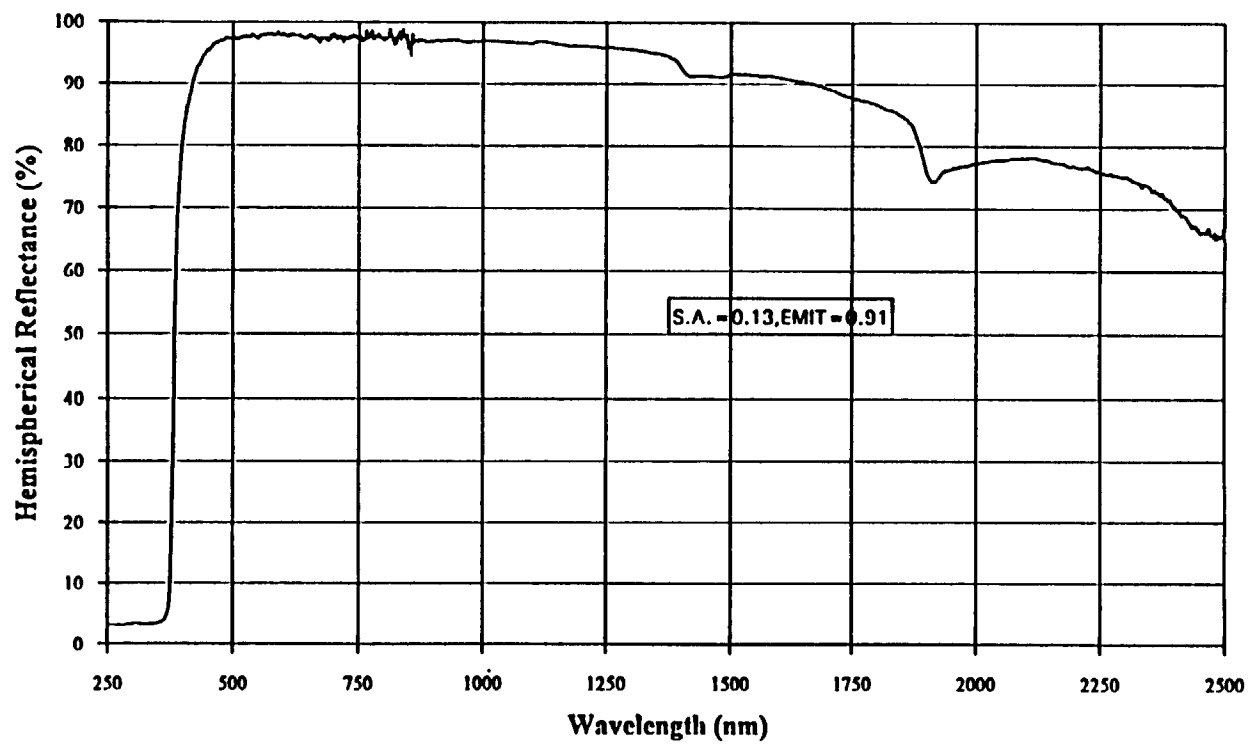
Figure 3-25. Reflectance Spectrum of S13GP/SS-55 Sample #IU-21, Batch #U-405.
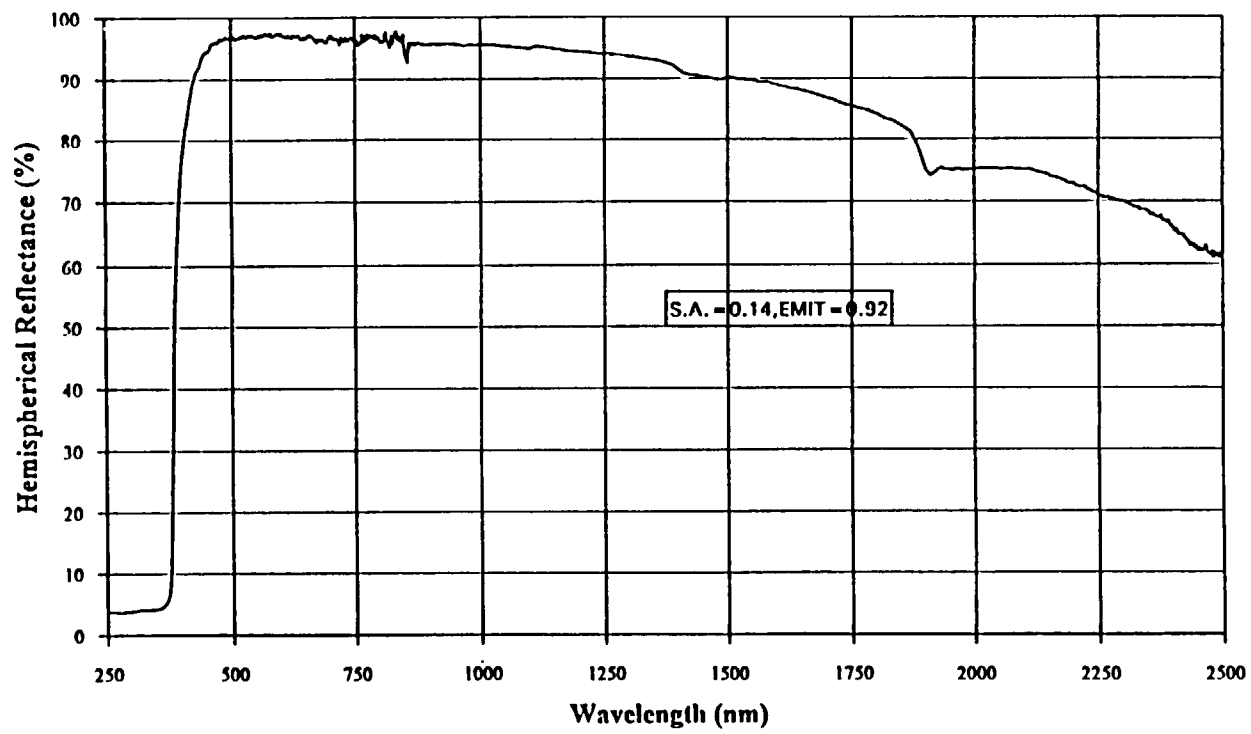
Figure 3-26. Reflectance Spectrum of S13GP/DHS-1 Sample #GS-4, Batch #U-279.

S.A. = 0.13, E = 0.92
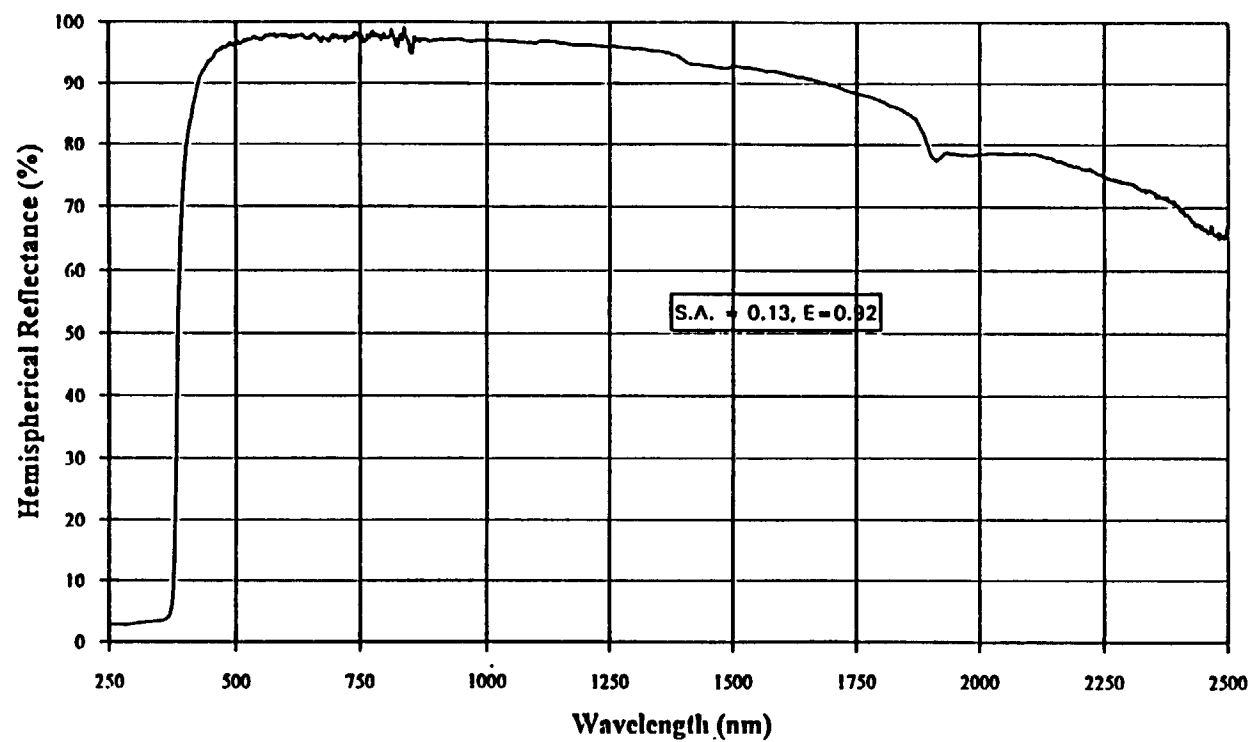
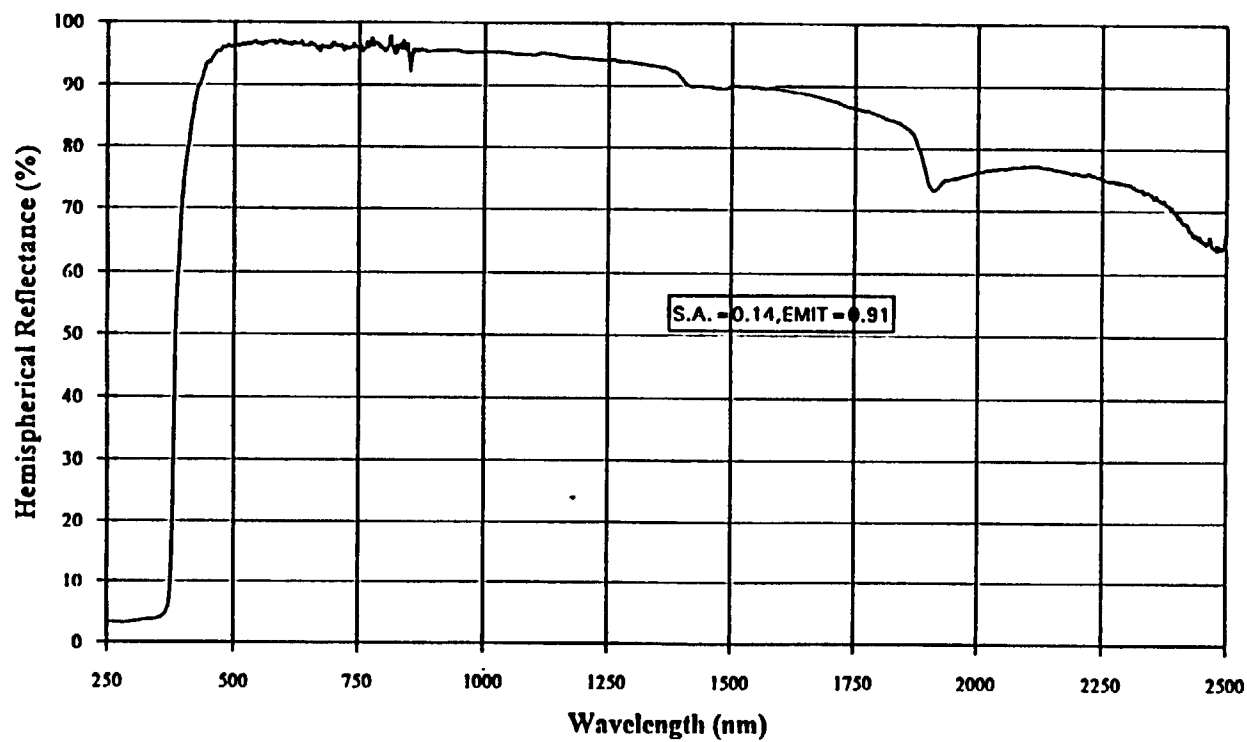Figure 3-27.   Reflectance Spectrum of S13GP/DHS-2 Sample #HH-20, Batch #U-328.
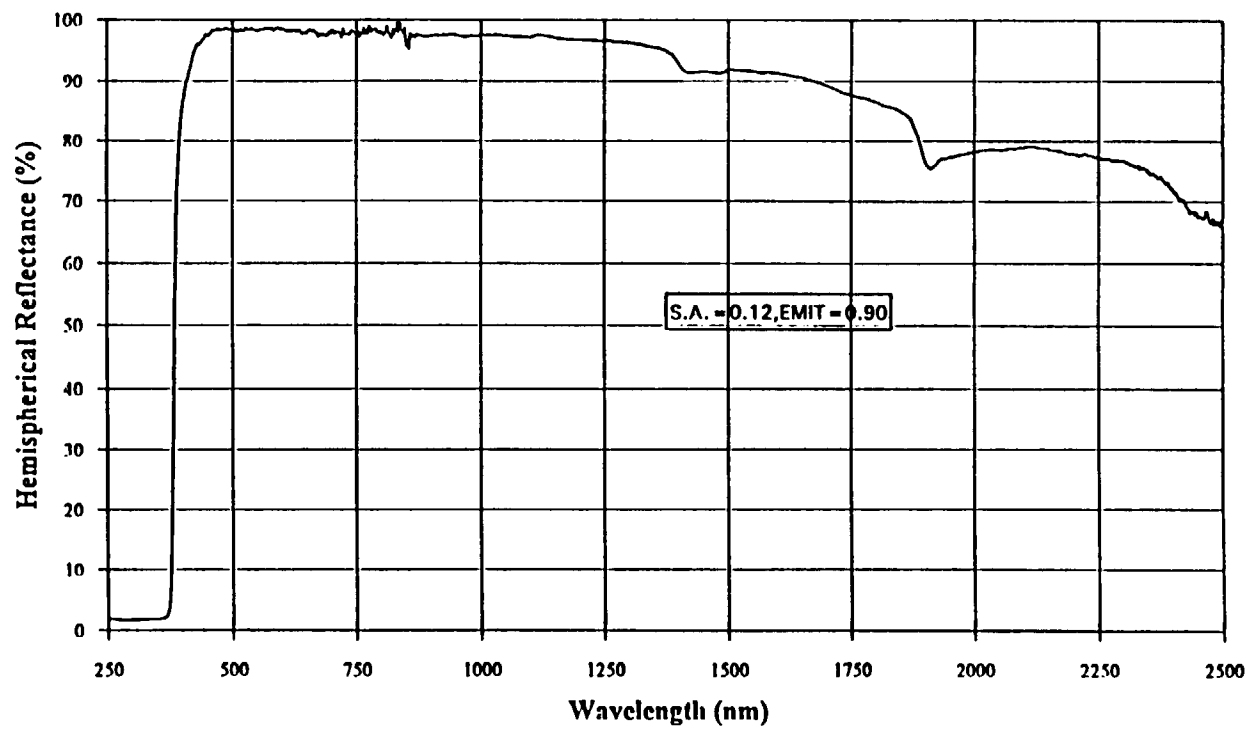
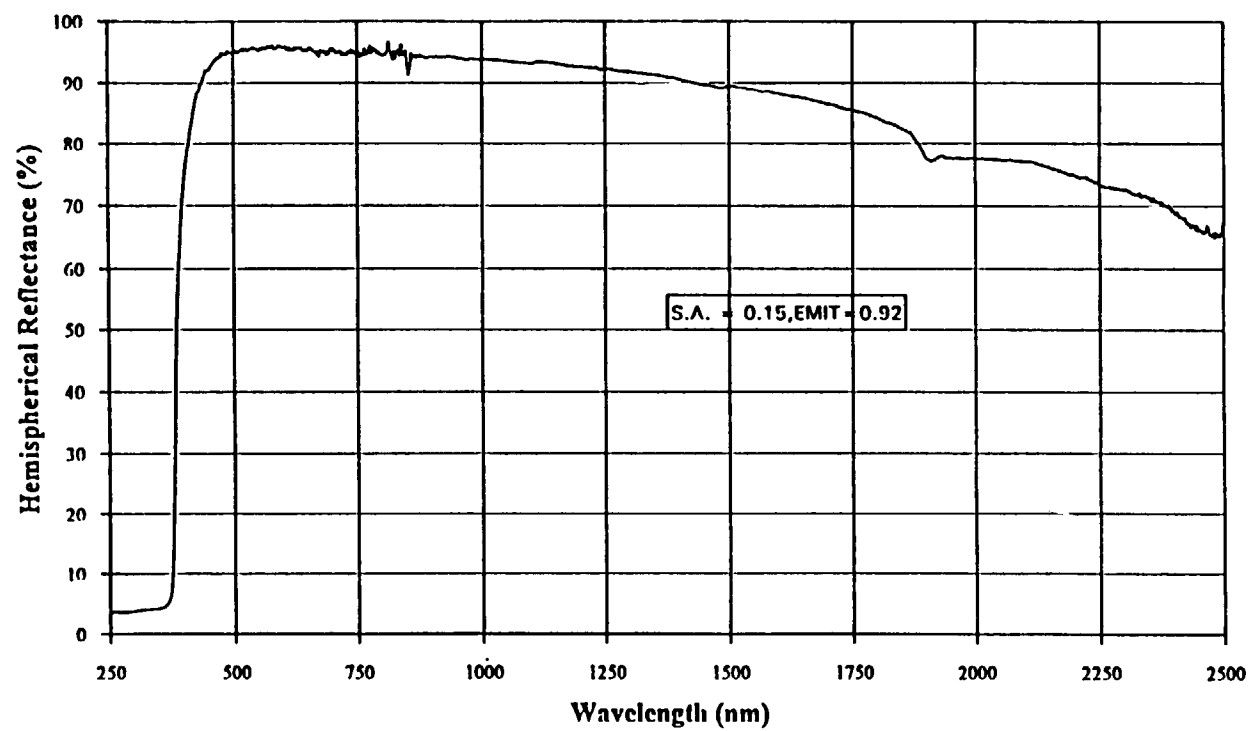Figure 3-28. Reflectance Spectrum of S13N/SS-55 Sample #GR-7, Batch #U-260.
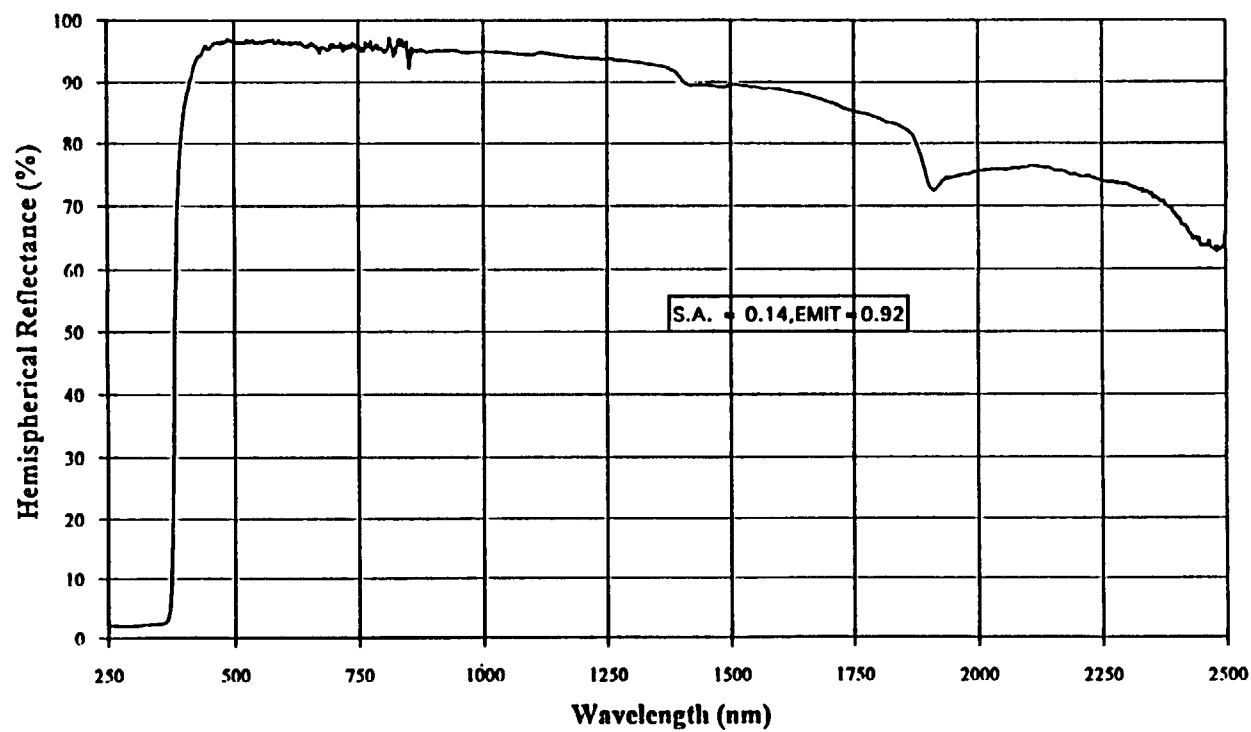
Figure 3-29. Reflectance Spectrum of S13N/DHS-1 Sample #HE-8, Batch #U-317.

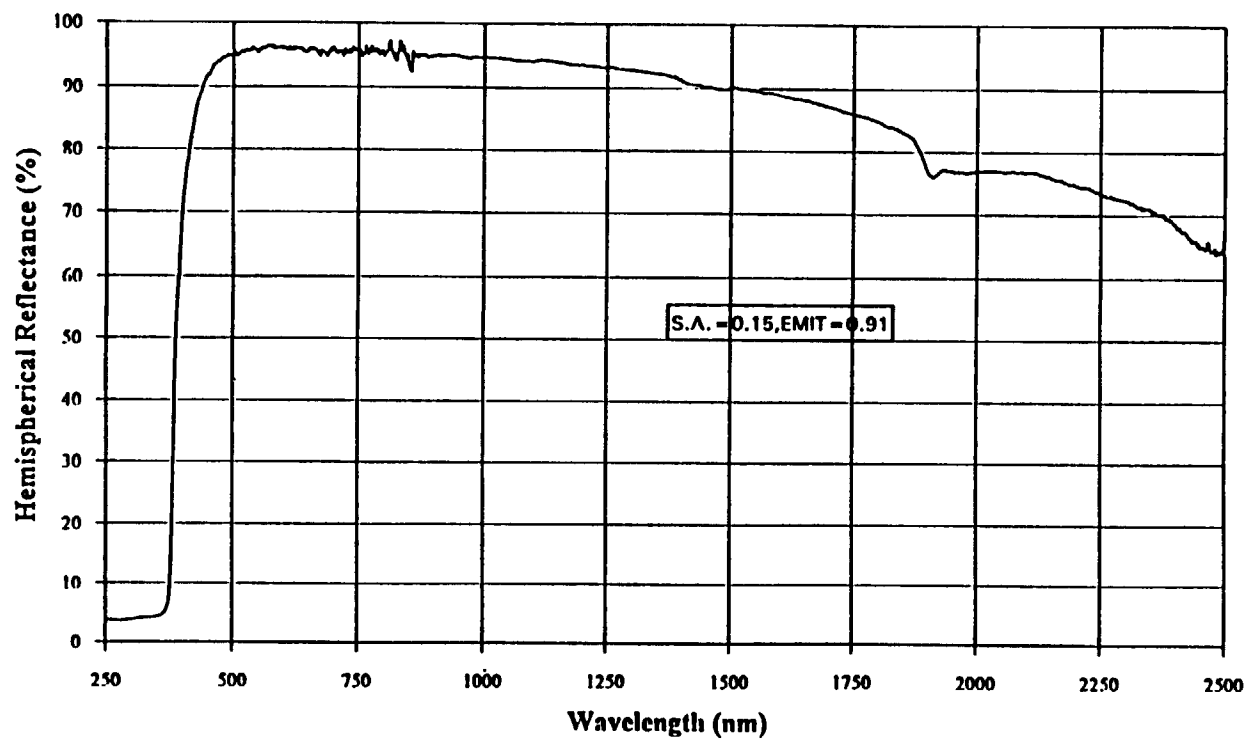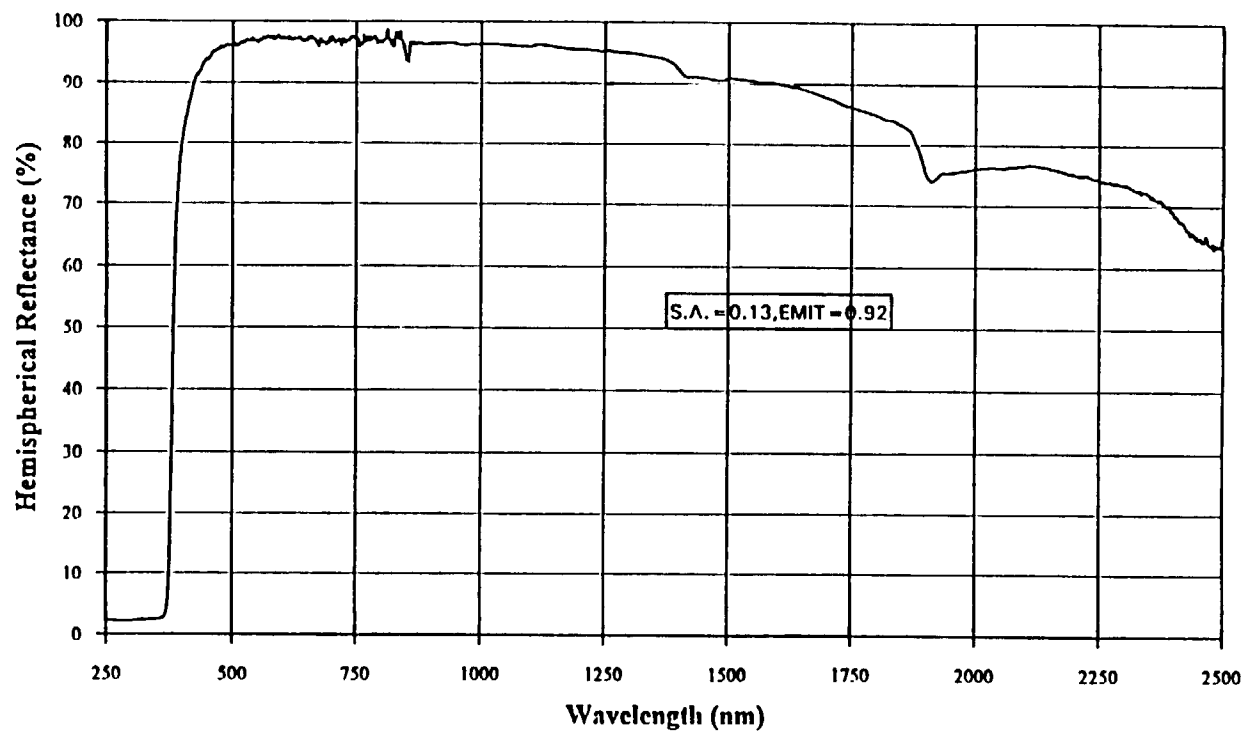Figure 3-30. Reflectance Spectrum of S13N/DHS-2 Sample# HI-27, Batch #U-329.

Chart axes: Hemispherical Reflectance (%) vs Wavelength (nm)

S.A. = 0.13, EMIT = 0.92

Table 3-8. Z-93SCXY: Properties of Candidate Pigment/Binder Couples					
Concept: Z-93SCXY	Batch #	Alpha	Emittance	Surface Resistivity ($\Omega/\square$)	
Pigment/Binder				HP4329A	HP4339A
S13GP/2130	(FM)	0.13	0.92	1.00E+09	5.00E+09
S13GP/SS-55	U-405(IU)	0.13	0.91	8.00E+09	5.00E+09
S13GP/DHS-1	U-279(GS)	0.14	0.92	8.00E+07	1.00E+09
S13GP/DHS-2	U-328(HH)	0.13	0.92	4.70E+08	1.00E+09
S13N/SS-55	U-260(GR)	0.12	0.90	2.00E+08	1.00E+09
S13N/DHS-1	U-317(HE)	0.14	0.92	4.00E+08	1.00E+09
S13N/DHS-2	U-329(HI)	0.13	0.92	5.60E+08	5.00E+09

It is important to report that storage and exposure to ambient conditions do not affect the surface electrical resistance of these formulations. Thus, the microencapsulation can help in tailoring stability as well as the electrical response. We anticipate excellent stability to space environment for this concept and await results for doped binder systems that provide excellent reproducibility in the electrical surface resistance properties of the candidate TCMS pigment/binder couples.

The concept S13GP/hybrid silicate without dopants has already found applications on the GPS-Block II hardware and has been integrated on sunshades of E-Glass/Epoxy composites. The binder system for this hardware did not use dopant to avoid defect structure dependent conduction mechanisms, since we do not know enough of their behavior in extended space exposure environment. The resultant surface resistance for such systems was also 1.0E+09 as measured by HP-4339A. The $\alpha_S \simeq 0.14$ and $\epsilon_N = 0.90$ are typical values for S13GP/hybrid silicate (50/50 mixture of Kasil 2130 and SS-55 without dopants) formulation.

3.3.1.3 Concept Z-93SCLMXY. The rationale for this concept is very much similar to the earlier concept of Z-93SCXY, where control of Zn interstitials was considered as a key to tailor the required resistances in pigment grains. In the earlier concept, microencapsulation of the pigment was considered as the route to stabilize the Zn interstitials in the ZnO grain. The overall process also limits the ability to tailor surface resistances, since each grain is covered

with a dielectric silicate layer. The ability to tailor resistance then is limited by our ability to subsequently leach out the dielectric silicate layer. The process of pigment surface phosphatization to make pigment compatible with the polydimethyl/siloxane also limits the ability to tailor surface resistance values of concept Z-93SCXY. The microstructural parameter that governs this ability is thickness of dielectric layer that encompasses the ZnO grain.

The concept Z-93SCLMXY was studied to relax this limit on the ability to tailor surface resistances. The goal was to provide the ability to manipulate pigments such that the dielectric silicate layer and the phosphatized layer are doped and act as a "leaky" dielectric film, which will also show the ability to protect against space environment irradiation.

To achieve this goal, we have approached "S13GP" pigment design following two paths. In the first one, we used the dopant precursor salts and doped the pigment at high temperatures using precursors of ZnO and silica (SiO_2). The related efforts have been already reported in Section 3.2.2.2 for pigment DZS developed via high temperature doping. We expect that Zn_2SiO_4 formation in such a high temperature route is unavoidable. The pigment DZS developed during IR&D also provides the ability to tailor total hemispherical solar absorptance to values less than 0.10. Thus, the pigment was incorporated in all candidate silicate binders as well as in stripped polydimethyl siloxane to prepare samples for the screening study.

The second path taken was to design a process for doping operation very much like the microencapsulation process. The uncalcined ZnO (SP-500) was reactively encapsulated into doped silicate binder. Since sodium silicate provides the flexibility in providing leaky dielectric silicate, SS-55 was doped with the dopant levels of DHS-1 and was used as a microencapsulants. The microencapsulation process reported in AFML-TR-94-4126 was followed using ZnO (SP-500) and doped hybrid silicate binder DHS-1 to produce the required candidate pigment for this screening study. The pigments produced following the second path were designated as DS13N. The resultant pigment, DS13N, was then incorporated in all candidate silicate binders as well as in the stripped polydimethyl siloxane to prepare samples for the screening study.

The description of the TCMS prepared for study can be summarized briefly in Table 3-9.

Table 3-9. Description of Concepts and Material Parameters for Formulations in Screening Test			
Z-93SCLMXY:	Doped zinc silicate (high temperature doping) in silicate binders and doped silicate binders; and doped microencapsulated pigments (low temperature doping) in silicate binders and doped silicate binders.		
Concept: Z-93SCLMXY	Pigment	Binder	PBR
Pigment/Binder			
DZS/2130	DZS	Kasil 2130	5.5
DZS/SS-55	DZS	SS-55	5.5
DZS/DHS-1	DZS	DHS-2	5.5
DZS/DHS-2	DZS	DHS-2	5.5
DS13N/SS-55	DS13N	SS-55	5.5
DS13N/DHS-1	DS13N	DHS-1	5.5
DS13N/DHS-2	DS13N	DHS-1	5.5
Flexible White Conductive Coating:			
DS13NSC/LO-41	DS13N	MHS/LO stripped polydimethyl siloxane	4.0

Before going to the results obtained for the optical and electrical performance of these coatings, it may be worthwhile to visit the issue of involved costs of doping for each path evaluated here.

For the first path of high temperature doping of the pigment, the costs involved are dominated by the cost of dopant precursor salts and labor costs. The most desirable dopant for white (low α_s/ϵ) TCMS is In. The In precursor salts are very costly, and they are volatile at high temperatures selected for doping. Thus, high temperature doping is a costly approach for doping. The use of high temperature also causes precursor loss, which made the process very difficult to reproduce. The only advantage observed for such a processing route was its ability to provide a total hemispherical solar absorptance of less than 0.10 (as BOL α_s).

For the second path of low temperature doping following the "S13G" type microencapsulation process used in doped silicate binder of high pH, the requirement of the dopant salts per batch to produce the target resistivity was markedly less. It was approximately 1/15th of the dopant precursor salt required in the high temperature doping path. The precursor losses in the microencapsulation process were observed only during the leaching process. The dopant losses for each step of processing were not completely characterized. Analysis of "In" in collected washed fluid after leaching indicated that very minute In losses had occurred. Thus, the second process route was found to be economical. However, this approach cannot yield total hemispherical solar reflectance of less than 0.10. This is very clear from the candidate sample characterization efforts described below.

A batch of each material formulation was prepared for the candidates listed in Table 3-9 and sprayed onto various substrates of 1.0 inch diameter discs, 2"x2" plates, 4"x4" plates for optical and electrical performance characterization. The total hemispherical spectral reflectance, total normal thermal emittance and surface resistance were measured following the same methods that were used to characterize baseline nonconducting material described earlier in Section 3.1. The observed data are presented in Table 3-10 and the detailed reflectance curves are presented in Figures 3-31 through 3-38. All data was recorded for coating thickness of 5.0 mils (nominal).

It is important to report that storage and exposure to ambient conditions have not altered electrical surface resistance values over a two-year period. The conductive white flexible TCMS received a very favorable response from various industrial design engineers, who asked for samples to evaluate RF properties and inquired about the measurement methods. Although no RF properties were communicated back to us, it was apparent from the comments made by the end users that the TCMS with doped silicate binder are less lossy than doped pigment in stripped polydimethyl siloxane polymer. The feedback was received that the flexible conductive TMCS and its baseline counterpart (S13GP/LO-1) are both electroluminescent under UV-exposure. These comments are revisited in the "results and discussion" chapter.
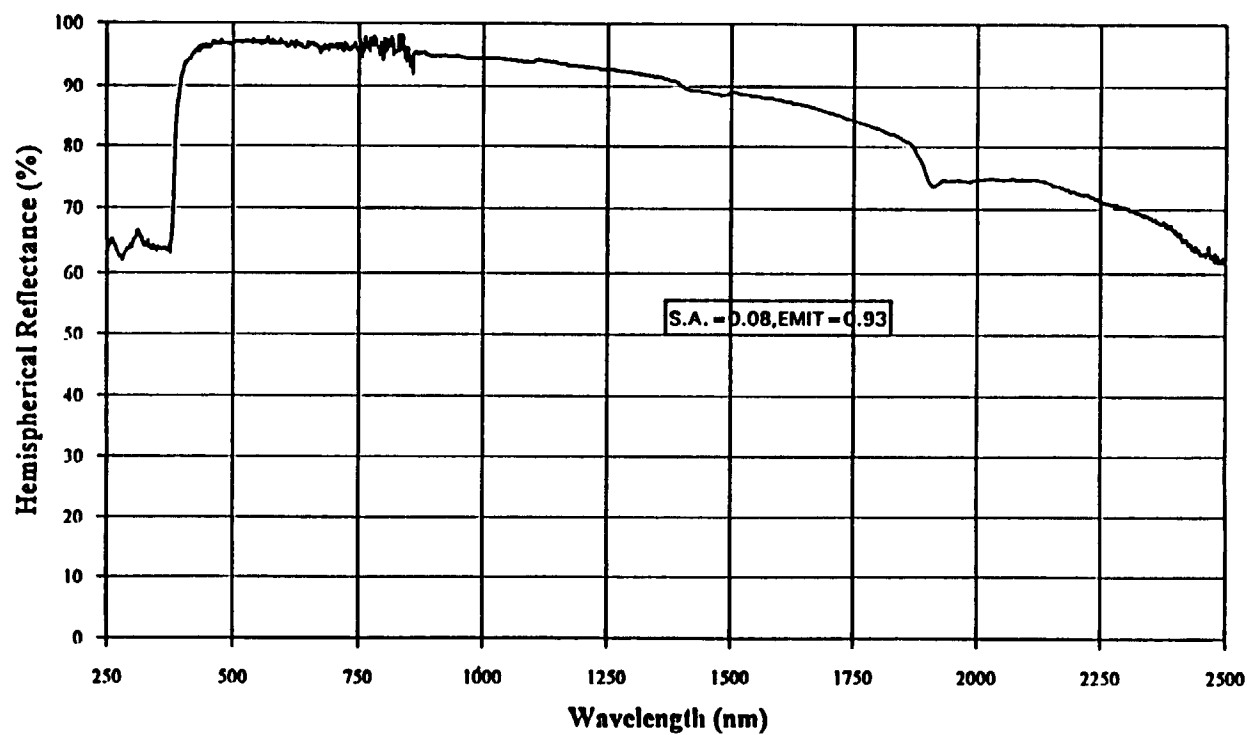
Figure 3-31. Reflectance Spectrum for DZS/2130 Sample #DK-20, Batch #T-244.
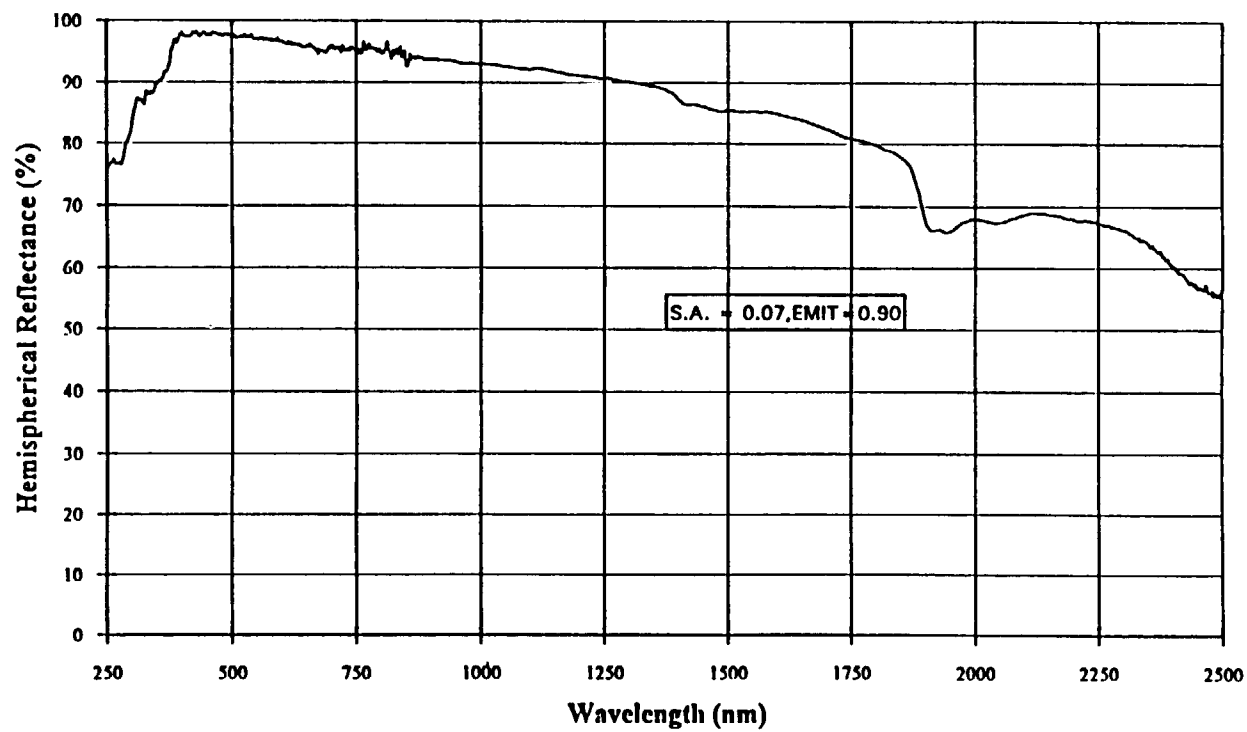
Figure 3-32. Reflectance Spectrum for DZS/SS-55 Sample #FO-4, Batch #U-206.
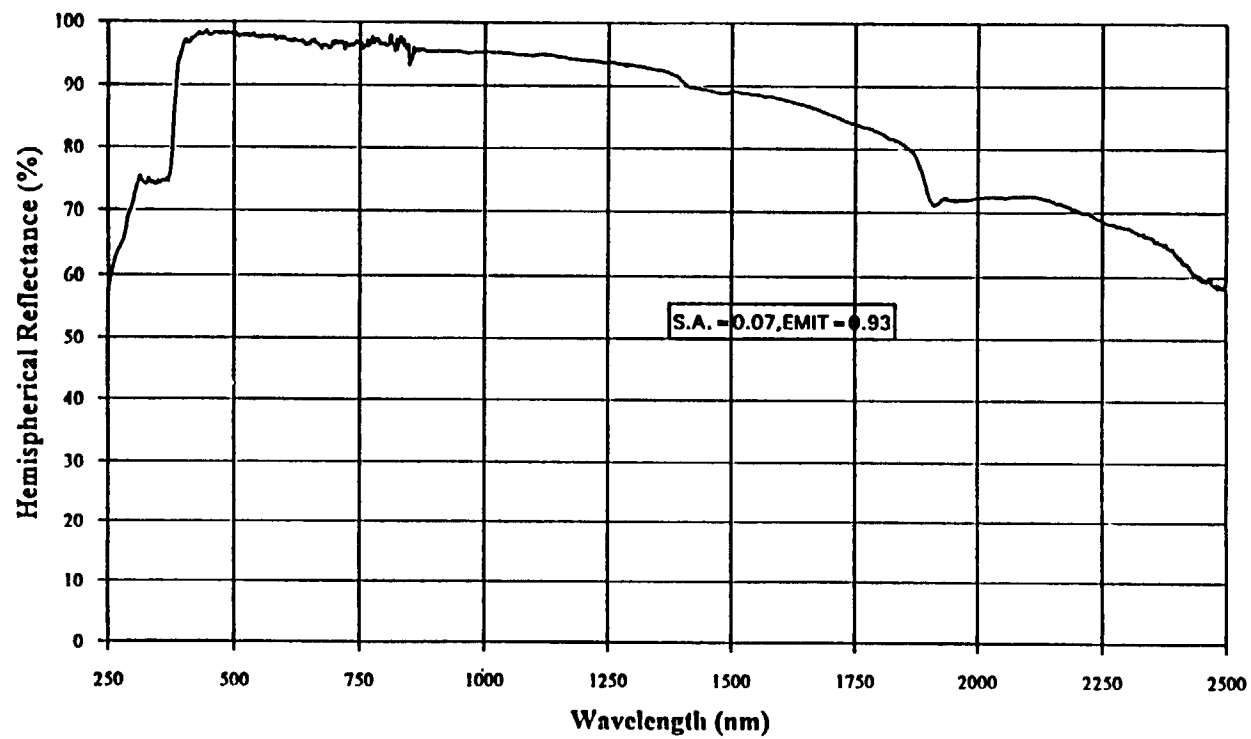
Figure 3-33. Reflectance Spectrum for DZS/DHS-1 Sample #GQ-6, Batch #U-267.
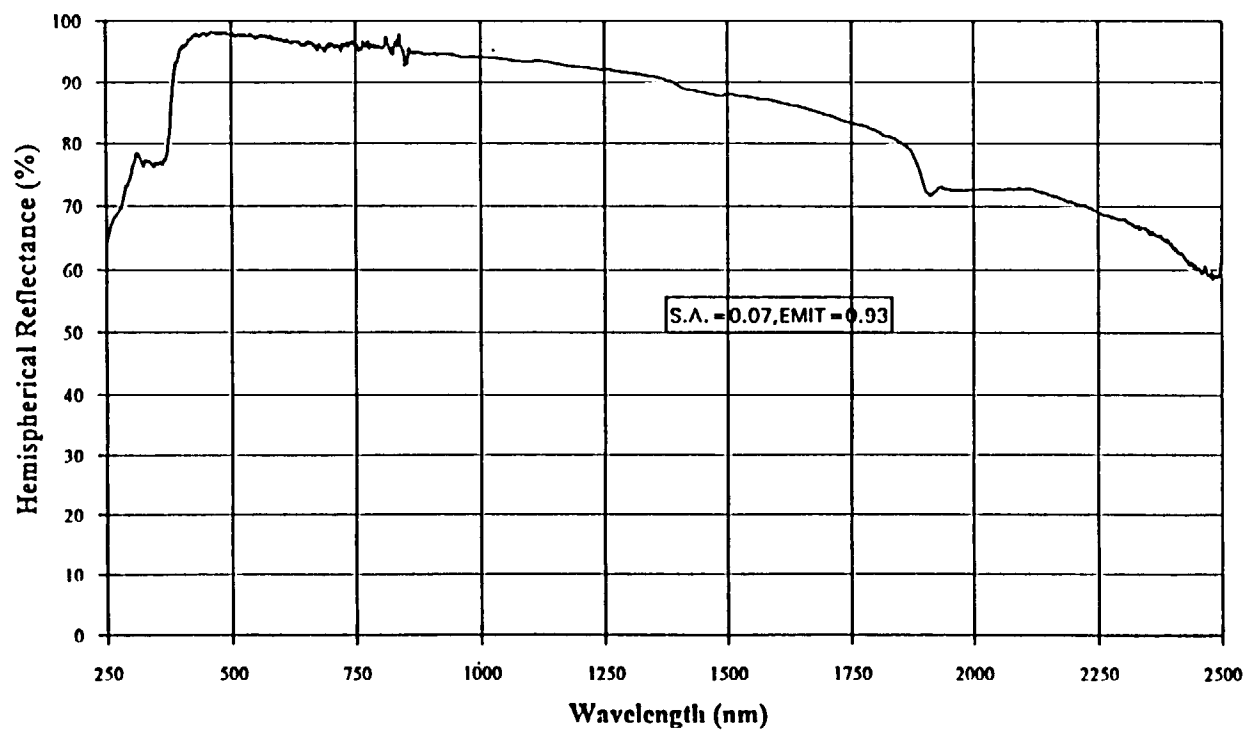
Figure 3-34. Reflectance Spectrum for DZS/DHS-2 Sample #HK-27, Batch #U-331.
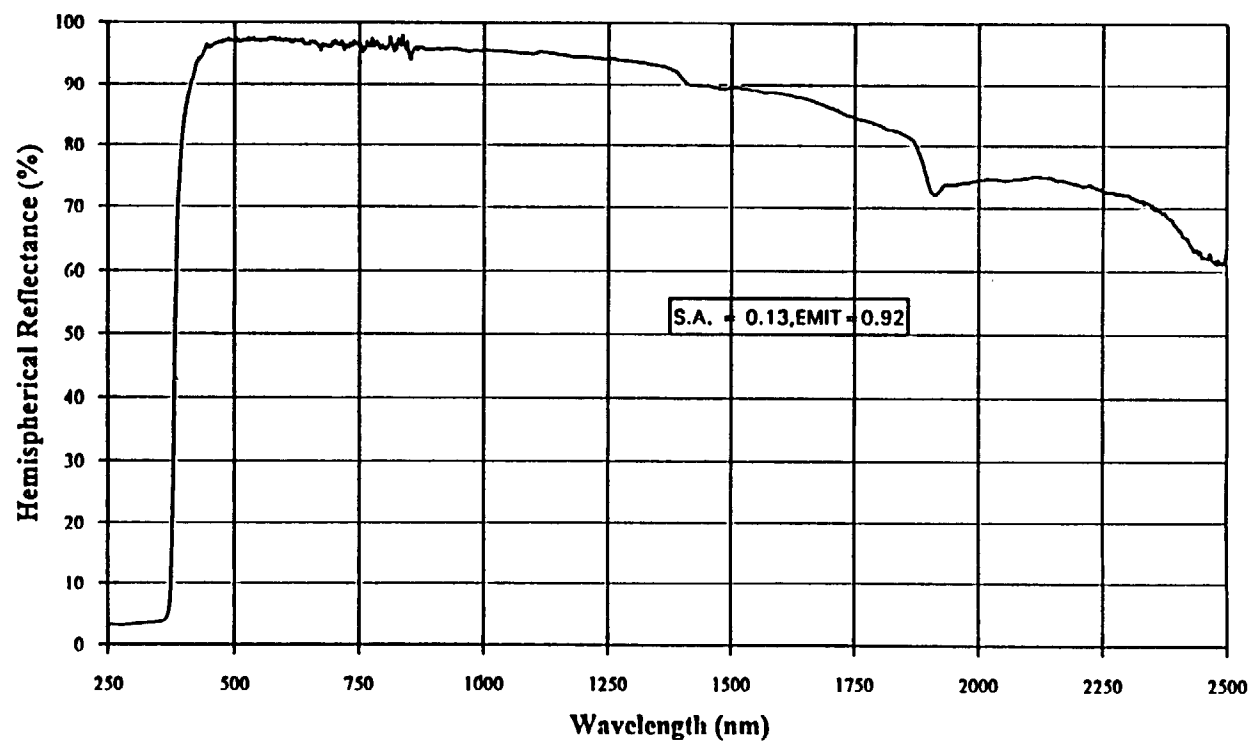
Figure 3-35.   Reflectance Spectrum of DS13N/SS-55 Sample #P-1, Batch #U-315.
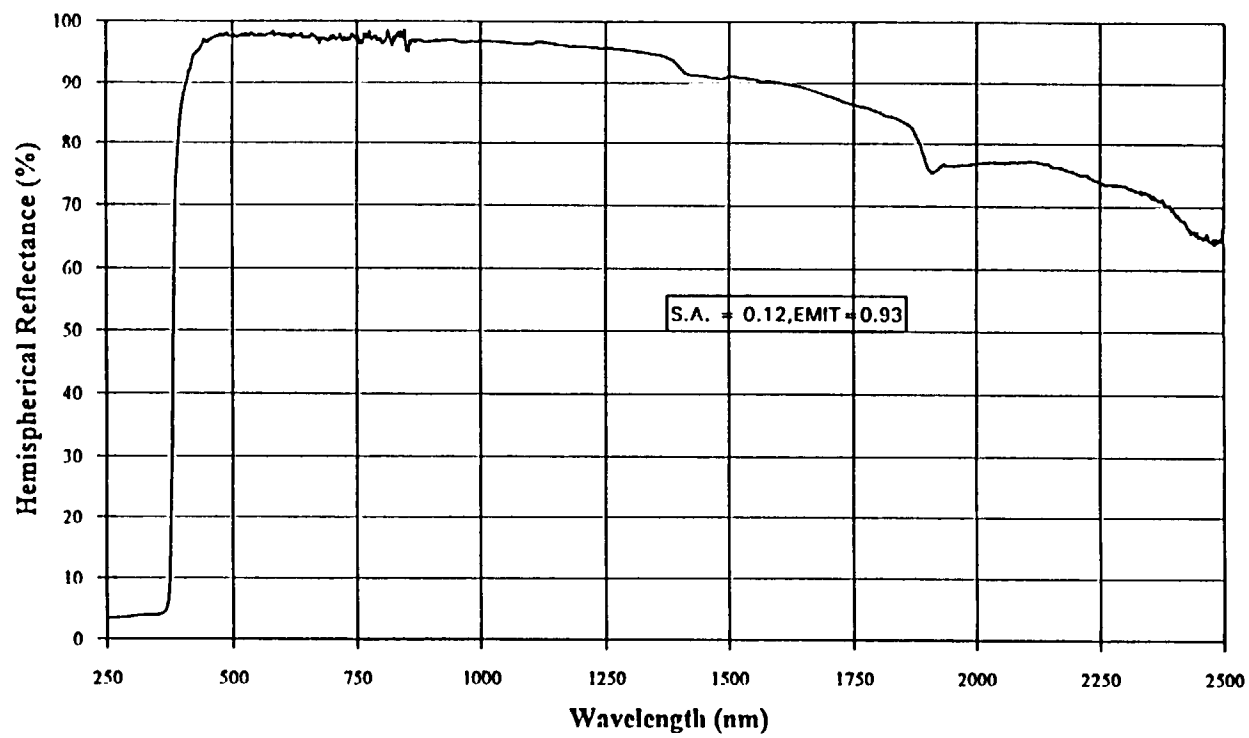
Figure 3-36. Reflectance Spectrum of DS13N/DHS-1 Sample #S, Batch #U-316.
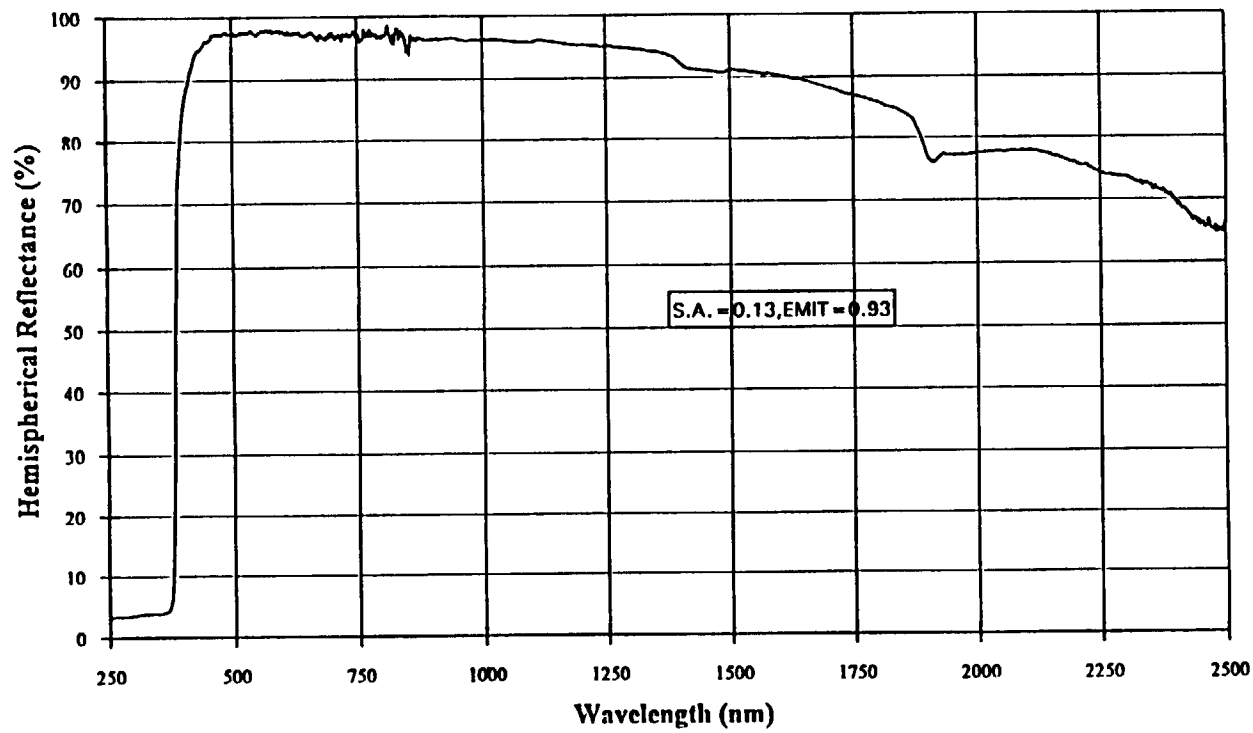
Figure 3-37.   Reflectance Spectrum for DS13N/DHS-2 Sample #HJ-27, Batch #U-330.
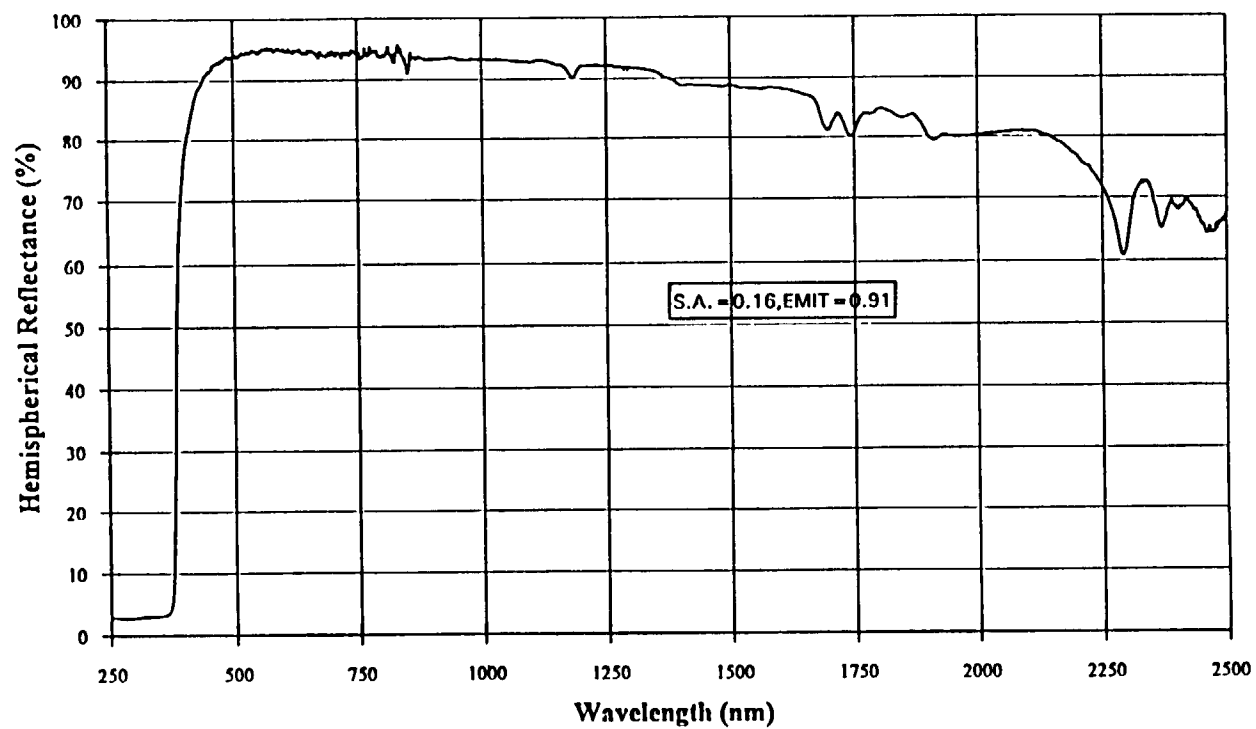
Figure 3-38. Reflectance Spectrum for DS13NSC/LO-41 Sample #HV-12, Batch #U-335.

Table 3-10. Z-93SLMCXY: Properties of Candidate Pigment/Binder Couples					
Concept: **Z-93SCLMXY** **Pigment/Binder**	**Batch #**	**Alpha**	**Emittance**	**Surface Resistivity ($\Omega/\square$)**	
				HP4329A	**HP4339A**
DZS/2130	T-244(DK)	0.08	0.93	1.00E+13	NA
DZS/SS-55	U-207(FO)	0.07	0.90	2.00E+10	1.00E+09
DZS/DHS-1	U-267(GQ)	0.07	0.93	6.00E+07	2.00E+08
DZS/DHS-2	U-331(HK)	0.07	0.93	1.00E+08	7.00E+08
DS13N/SS-55	U-315(P)	0.13	0.92	9.00E+08	1.00E+08
DS13N/DHS-1	U-316(S)	0.12	0.93	2.00E+08	6.00E+08
DS13N/DHS-2	U-330(HJ)	0.13	0.93	3.00E+08	1.00E+09
Flexible White Conductive Coating:					
DS13NSC/LO-41 (5 mils)	U-334(HV)	0.16	0.91	1.00E+09	1.00E+10

3.3.1.4 Other White (Low α_S/ϵ_N) Conductive Concepts. In this section, we present other conductive thermal control design concepts that can help us to achieve our screening program's material performance goals for tailoring electrical resistivity without loss of optical performance. In selecting such other concepts, an attempt was made to emphasize selection of alternate conduction mechanisms or materials that provide advantages.

The first obvious choice was the use of available semiconducting pigment zinc ortho-titanate (ZOT) developed at IITRI.[30,31] The ZOT pigment was also used to prepare baseline samples of TCMS YB-71 and YB-71P with potassium silicate binders PS-7 and Kasil 2130. It was decided to use ZOT from the same batches to prepare samples using the binder systems designed to achieve the target conductivity values. For this purpose, binders SS-55 and DHS-2 were selected. In earlier study of requalification efforts (AFML-TR-94-4126), some anomalous degradation of ZOT was observed with Kasil 2130 for one batch at 900 nanometers. This was discussed at length during earlier efforts along with strategies to mitigate such degradation. Among the strategies discussed, the microencapsulation and ZOT surface defect structure protonation via selection of binders promised possible success. The doped binders also present another option. The dopants can chemically stabilize defect structures present on the ZOT

surface if proper dopant chemistry is made available. Such doping has an added advantage of providing ZOT with required surface resistance. The titanate processing literature is filled with input from such studies. French efforts have been in the area of doping semiconducting Zn_2TiO_4 with lanthanum.[23] The scope of this work requires attention to tailoring electrical surface resistance, so ZOT defect structure stabilization issue were visited here in a limited way. We have provided candidate material designs without any manipulation of pigment surface chemistry here. The ZOT from the same batch that was used to prepare baseline samples has been used to provide conductive TCMS with binders like those sol, SS-55 and DHS-2.

These efforts are also important from the comments made on YB-71 formulation by Garrett[20], which reflects on why it has been used in GEO orbit often. It is anticipated[20] that a coating made up of ZOT as the pigment may charge up only once, and may not charge again. Thus, electrical performance of ZOT based formulations after irradiation also need to be tested.

The second choice was the use of europium oxide. Europium oxide was used strictly because of its body center cubic structure. This aspect provides the ability to withstand diffusion of dopant from binder into pigment without forming defects that can be optically absorbing in nature, or can cause alterations in conduction band to cause deleterious effects on electrical properties. Such flexibility does not exist in semiconducting ZnO or ZOT. Thus, Eu_2O_3 can represent a different regime of conductive TCMS to address the chemical compatibility issues of pigments and doped silicate binders. The Eu_2O_3 was also of interest because of its ability to provide a reflective concept that can help to tailor total hemispherical solar absorptance less than 0.10. Because of these advantages, Eu_2O_3 was prepared for IR&D studies (Section 3.2.2.3) and was used to provide candidate conductive concepts as well as new baseline nonconductive versions.

The third choice was to evaluate a cheaper doping concept, where one avoids use of costly In precursor salts that are used in doping. Antimony-doped tin oxide sol available form P.Q. R&D Division as experimental material provided an excellent opportunity to evaluate this in the screening program. Our IR&D efforts provided antimony-doped Zn_2SnO_x [$Sb:Zn_2SO_x$]. Although we have not perfected or carried out efforts for synthesis of this pigment, the small amount of processed (bench scale) material was used to tailor required optical and electrical performance characteristics. From earlier work carried out by Zerlaut et al.[31] and Gilligan et

al.[6] at IITRI that antimony doping usually results in an absorbing pigment; hence, the resultant optical and electrical performance was tailored via manipulation of TCMS's composition. Calcined ZnO (pigment for Z-93P) was used as a second desirable pigment to provide optical required properties.

The last concept, using Ta_2O_5 as a pigment, was revisited during this screening study. Ta_2O_5 was studied as a candidate pigment during very initial pigment screening studies carried out by Zerlaut and Harada.[29] The $\Delta\alpha_s$ for the Ta_2O_5 available was found to be unacceptable.[29] No further investigations have taken place since then. We also know that Ta_2O_5 is usually added to glasses (e.g., solar panel transparent glass cover sheet) to provide required leaky dielectric response for the glass. In view of the proven use of Ta_2O_5 in transparent glasses in orbit, it was decided to purchase purest Ta_2O_5 available, calcine at 1000°C, and use the pigment with silicate and doped silicate binders (Kasil 2130, SS-55 and DHS-2). The prepared samples were submitted as room temperature cured and heat treated. It was interesting to note that Ta_2O_5 pigmented <u>undoped</u> version met the target surface resistance goal even in resistive silicate binders (i.e., Kasil 2130 and SS-55) for PBR of 5.5.

All of the above selected concepts can be summarized in tabular form to list these other candidate material designs that were considered in this screening study. (See Table 3-11) Their nonconducting versions have already been listed in Section 3.1.

A batch of each candidate material formulation was prepared for the candidates listed in Table 3-11 and sprayed onto various substrates of 1.0 inch diameter discs, 2"x2" plates, 4"x4" plates for optical and electrical performance characterization. The total hemispherical spectral reflectance, total normal thermal emittance and surface resistance were measured following the same methods that were used to characterize baseline nonconducting material described earlier in Section 3.1. The observed data are summarized here in Table 3-12 and the reflectance curves are presented in Figures 3-39 through 3-50. All data were measured for coating thickness of 5.0 mils (nominal).

Table 3-11. Other Conductive Material Design Concepts			
Material Concept	**Pigment**	**Binder**	**PBR**
Pigment/Binder			
Other White Conductive Coatings:			
ZOT/Phos sol	ZOT #98790	Phos sol	5.5
ZOT/SS-55	ZOT # 98790	SS-55	5.5
ZOT/DHS-2	ZOT # 98790	DHS-2	5.5
Eu_2O_3/SS-55	Eu_2O_3	SS-55	5.5
Eu_2O_3/DHS-2	Eu_2O_3	DHS-2	5.5
Ta_2O_5/2130 (RT Cured)	Ta_2O_5	2130	5.5
Ta_2O_5/SS-55 (RT Cured)	Ta_2O_5	SS-55	5.5
Ta_2O_5/DHS-2 (RT Cured)	Ta_2O_5	DHS-2	5.5
Ta_2O_5/2130 (HT Cured)	Ta_2O_5	2130	5.5
Ta_2O_5/SS-55 (HT Cured)	Ta_2O_5	SS-55	5.5
Ta_2O_5/DHS-2 (HT Cured)	Ta_2O_5	DHS-2	5.5
Composite White Conductive Coatings:			
Sb Doped	ZnO + Sb Doped Zn_2SnO_x	2130	5.5
Sb Doped	ZnO + Sb Doped Zn_2SnO_x	MHS/LO stripped polydimethyl siloxane	4:1

Table 3-12. Other Conductive Material Concepts: Properties of Candidate Pigment/Binder Couples					
Material Concept	**Batch #**	**Alpha**	**Emittance**	**Surface Resistance ($\Omega/\square$)**	
Pigment/Binder				**HP-4329A**	**HP-4339A**
Other White Conductive Coatings:					
ZOT/Phos. Sol.	U-377(HT)	0.14	0.89	1.40E+10	5.00E+09
ZOT/SS-55	U-379(IN)	0.12	0.87	2.10E+08	8.90E+08
ZOT/DHS-2	U-378(IO)	0.13	0.88	2.40E+08	2.20E+08
Eu_2O_3/SS-55	U-353(ID)	007	0.92	8.50E+09	1.50(E+09)
Eu_2O_3/DHS-2	U-381(II)	0.08	0.91	2.10E+07	1.50E+09
Ta_2O_5/2150 (RT Cure)	U-358(IG)	0.18	0.90	1.70E+09	4.30E+09
Ta_2O_5/SS-55 (RT Cure)	U-359(IH)	0.17	0.88	5.60E+09	2.20E+09
Ta_2O_5/DHS-2 (RT Cure)	U-364 (IB)	0.13	0.88	5.60E+09	4.00E+09
Ta_2O_5/2130 (HT Cure)	U-358(IG)	0.16	0.90	3.00E+09	3.00E+09
Ta_2O_5/SS-55 (HT Cure)	U-359(IH)	0.15	0.88	1.60E+10	5.00E+09
Ta_2O_5/DHS-2 (HT Cure)	U-364(IB)	0.18	0.87	1.50E+10	8.00E+09
Composite CTG White Conductive Concepts:					
Sb Doped	U-252(GE)	0.13	0.90	8.50E+10	1.50E+09
Sb Doped (Flexible)	U-377(HT)	0.18	0.90	3.00E+09	3.00E+09
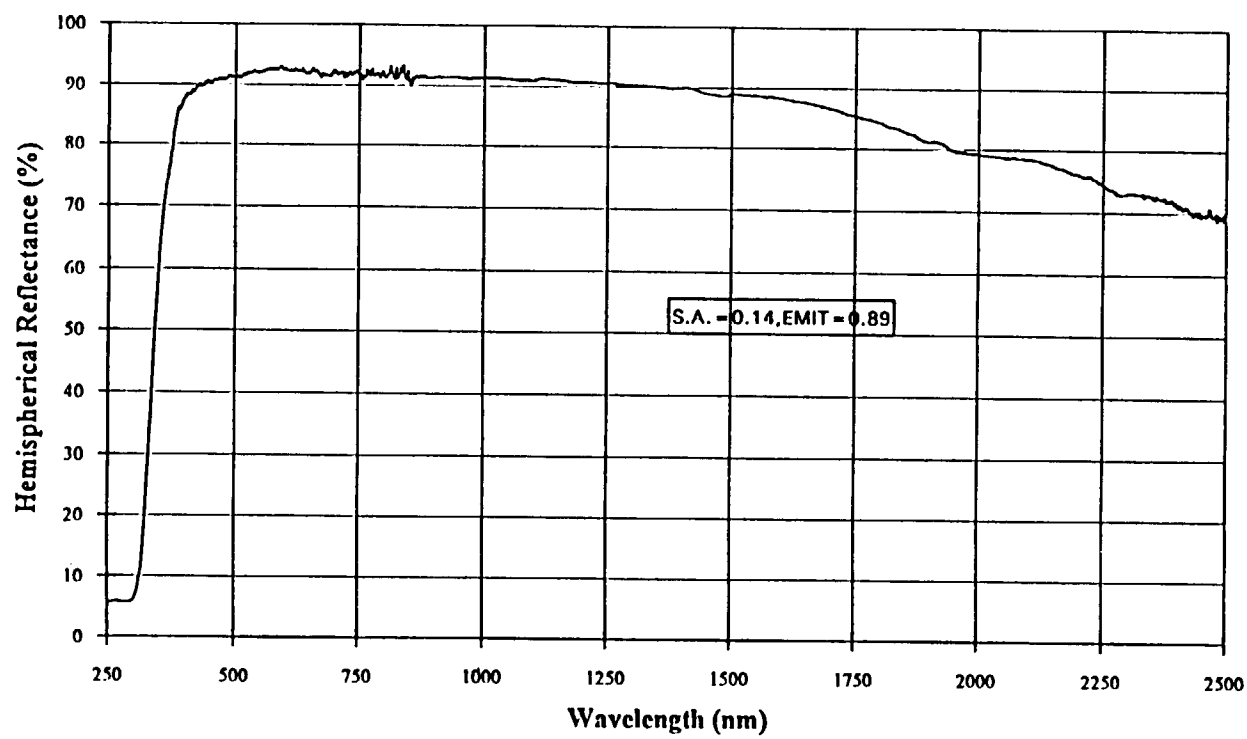
Figure 3-39. Reflectance Spectrum of ZOT/Phos. Sol. Sample #HT-14, Batch #U-377.
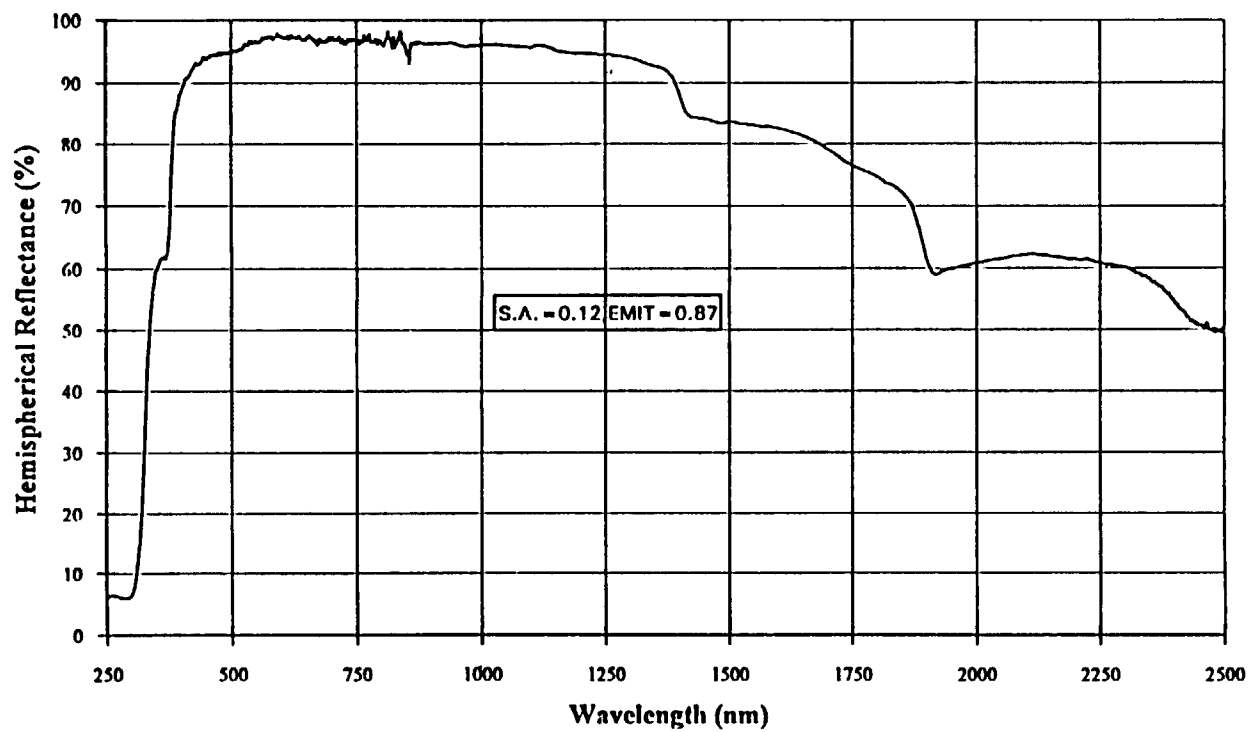
Figure 3-40. Reflectance Spectrum of ZOT/SS-55 Sample #IN-25, Batch #U-379.
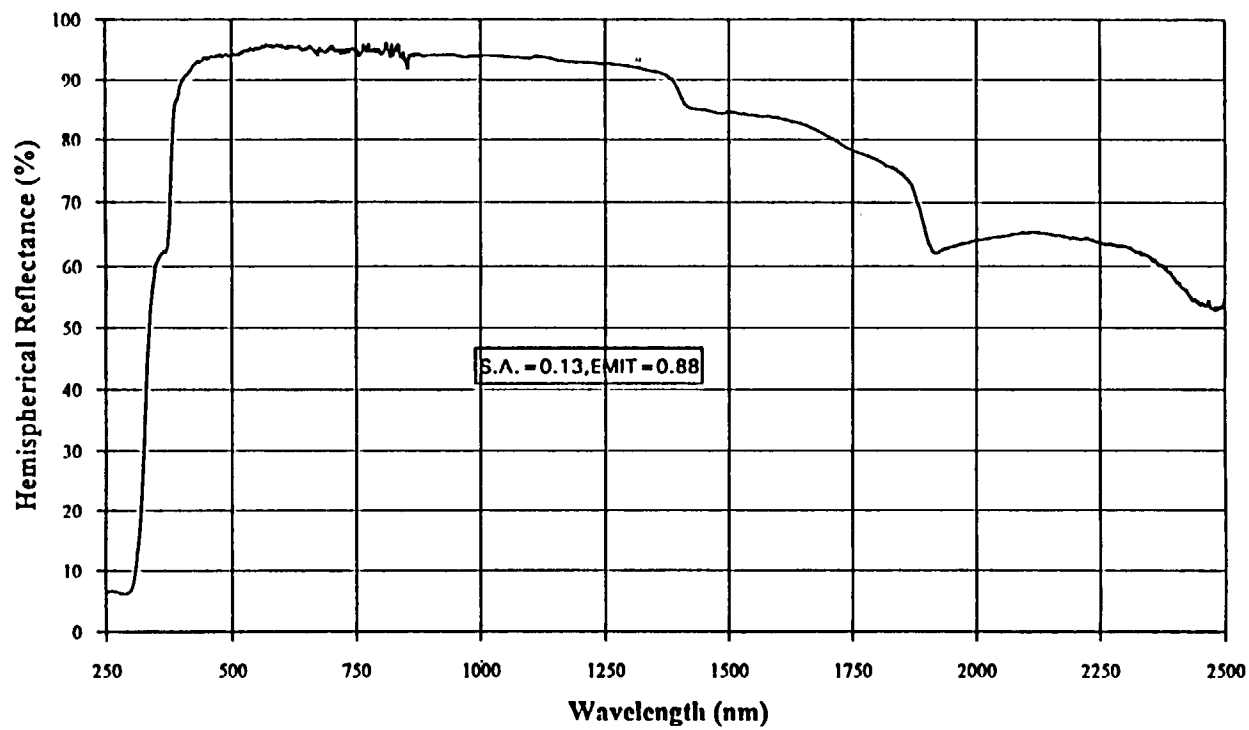
Figure 3-41. Reflectance Spectrum of ZOT/DHS-2 Sample #IO-28, Batch #U-378.
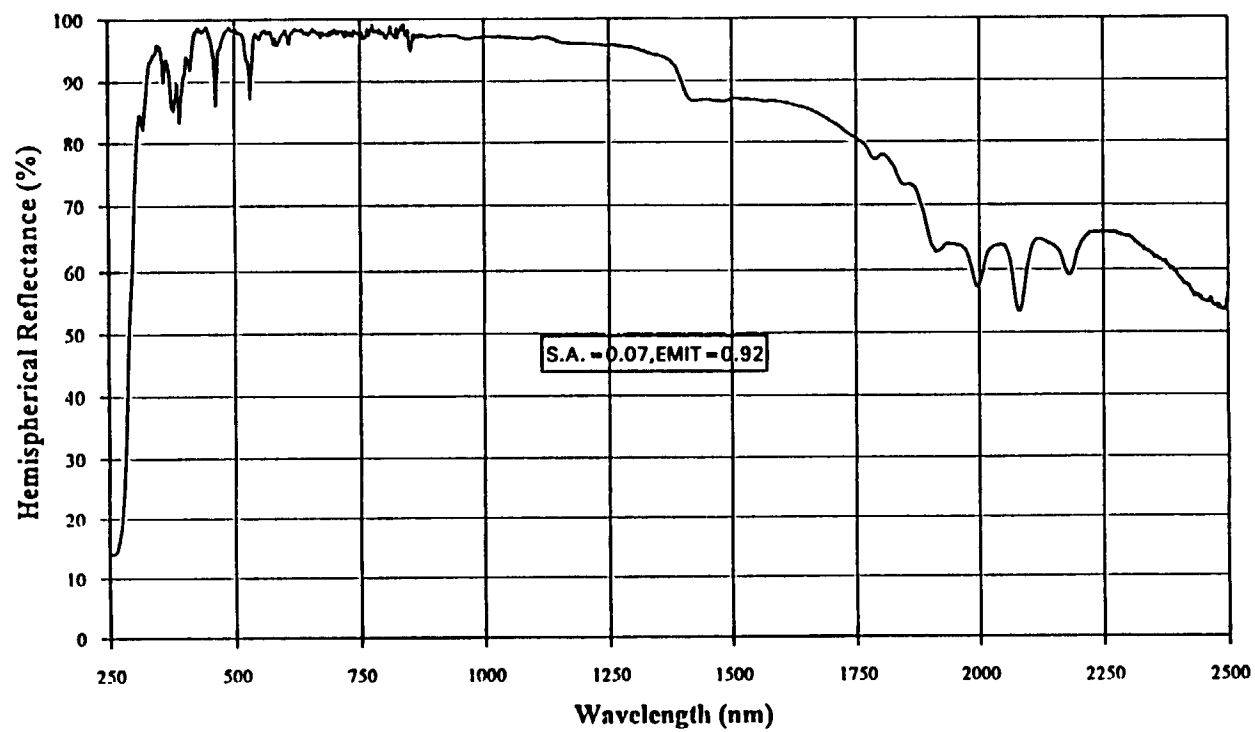
Figure 3-42.   Reflectance Spectrum of Eu$_2$O$_3$/SS-55 Sample #ID-20, Batch #U-353.
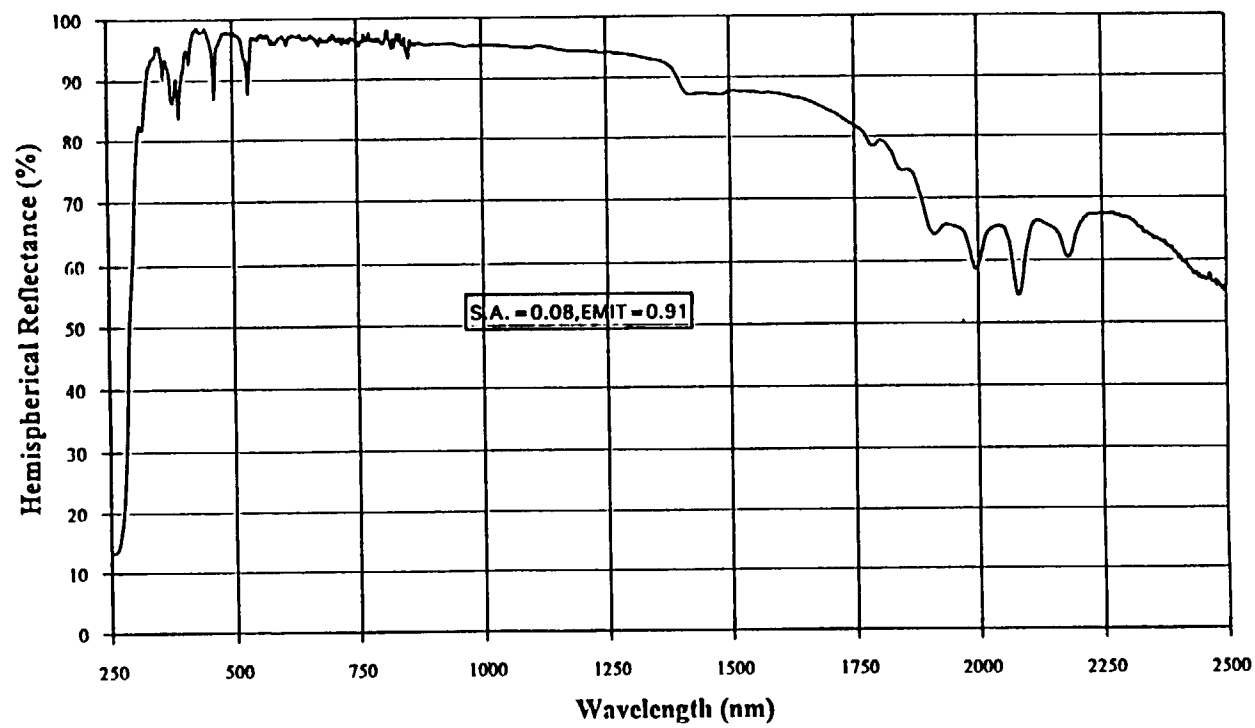
Figure 3-43. Reflectance Spectrum of E_2O_3/DHS-2 Sample #II-17, Batch #U-381.
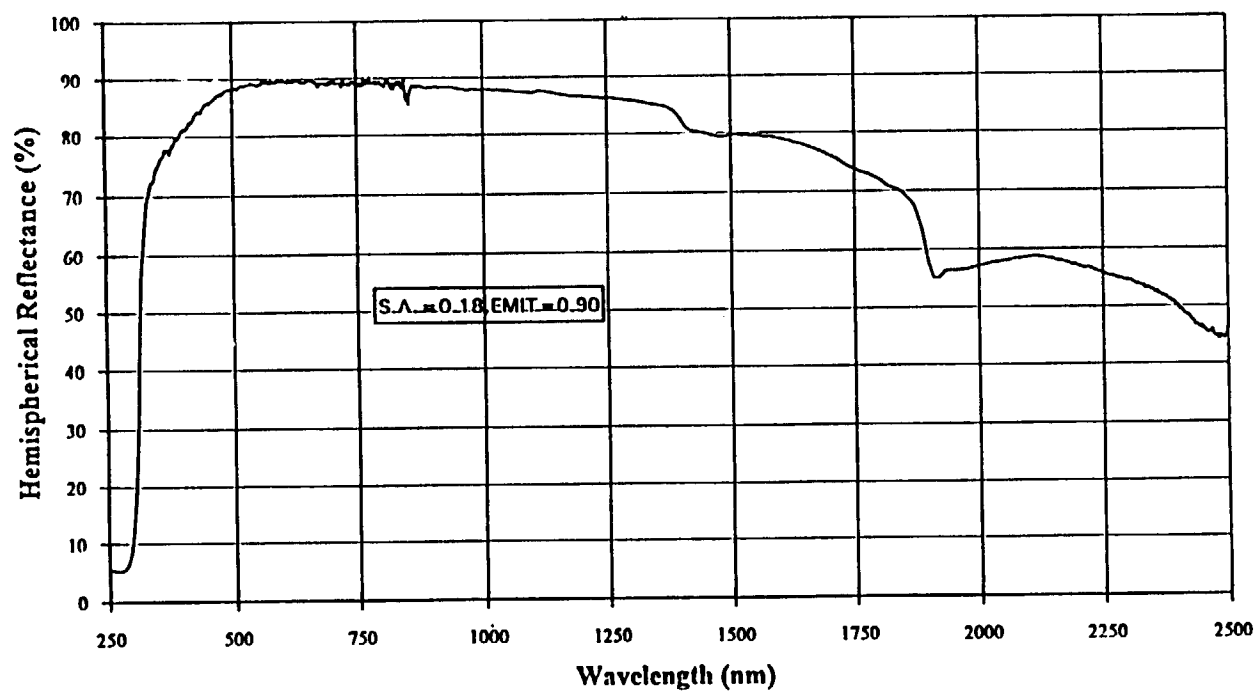
Figure 3-44. Reflectance Spectrum of Ta$_2$O$_5$/2130 (RT Cure) Sample #IG-15, Batch #U-358.
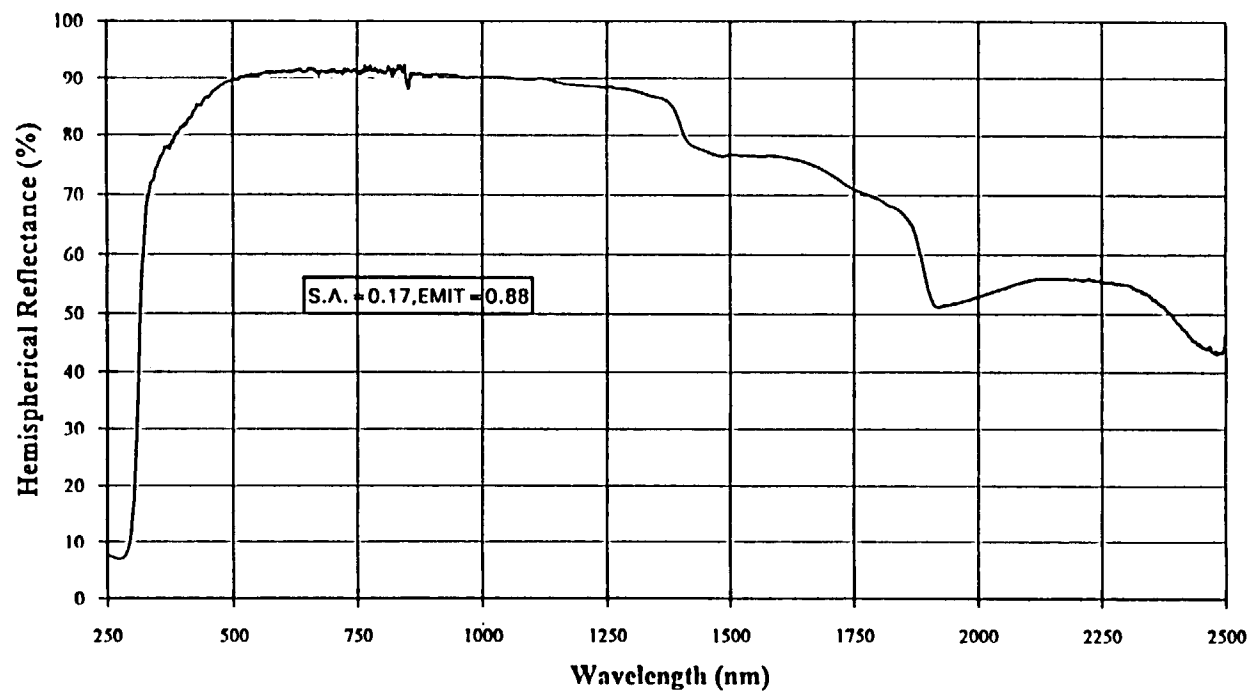
Figure 3-45. Reflectance Spectrum of Ta_2O_5/SS-55 (RT Cure) Sample #IH-21, Batch #U-359.
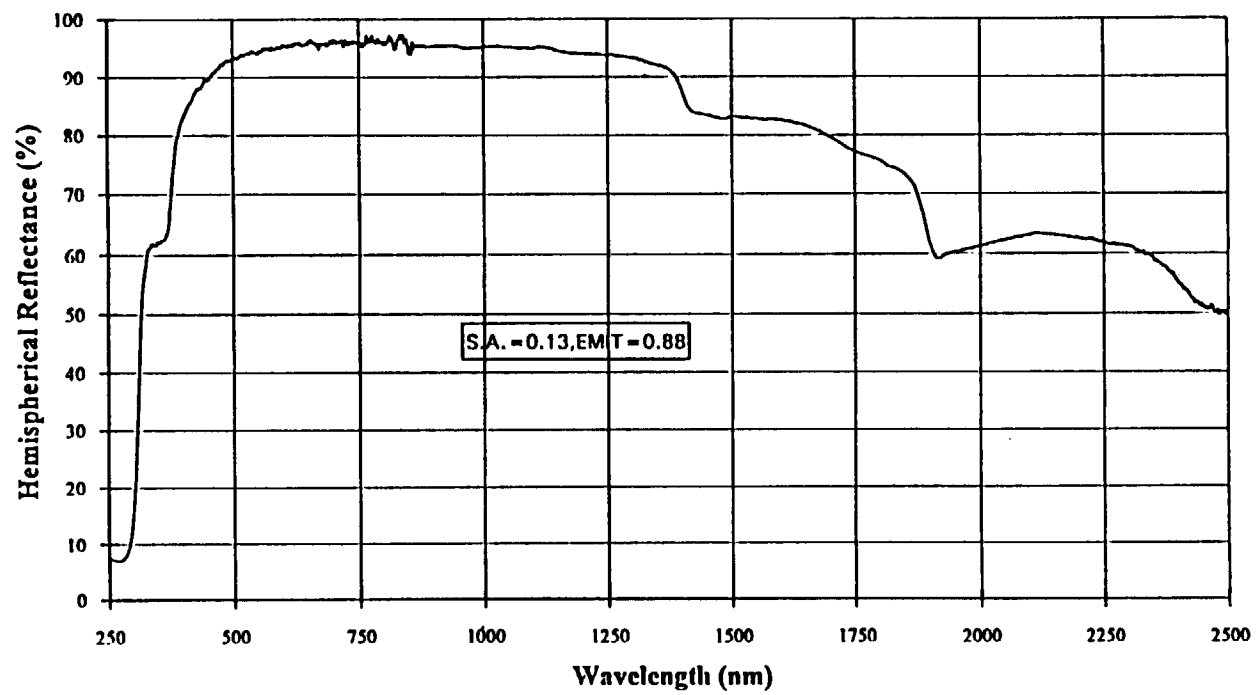
Figure 3-46. Reflectance Spectrum of Ta$_2$O$_5$/DHS-2 (RT Cure) Sample #IB-15, Batch #U-364.
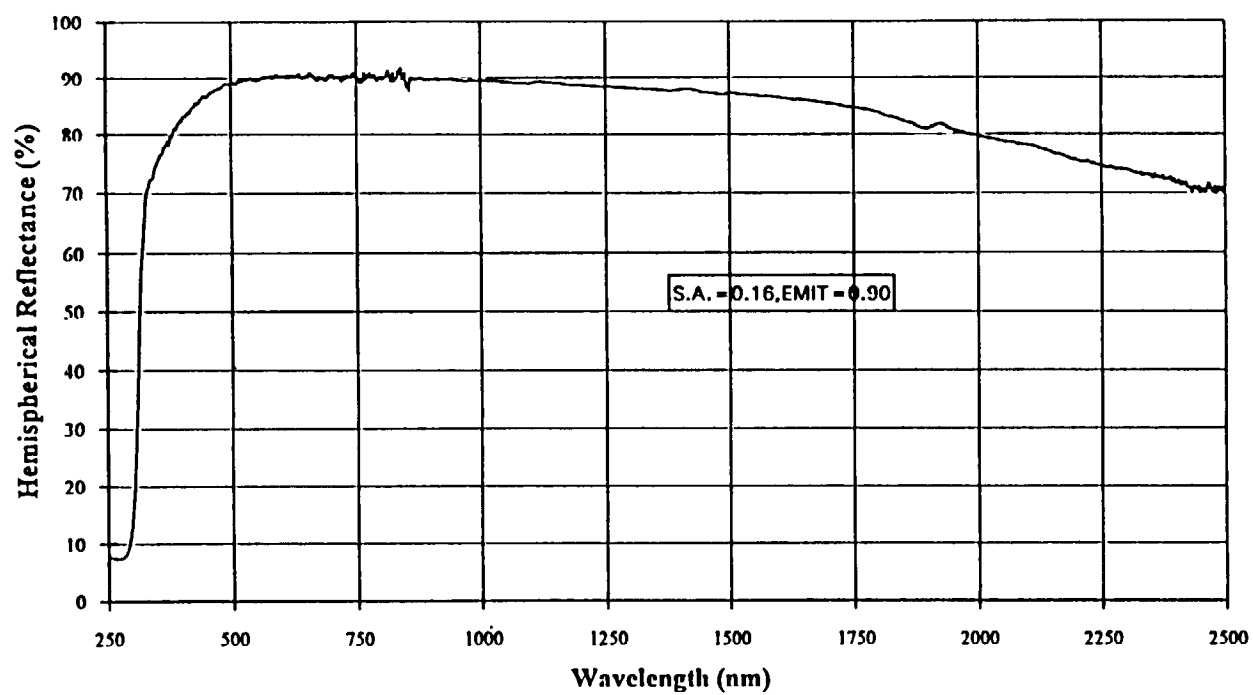
Figure 3-47. Reflectance Spectrum of $Ta_2O_5/2130$ (HT Cure) Sample #IG-13, Batch #U-358.
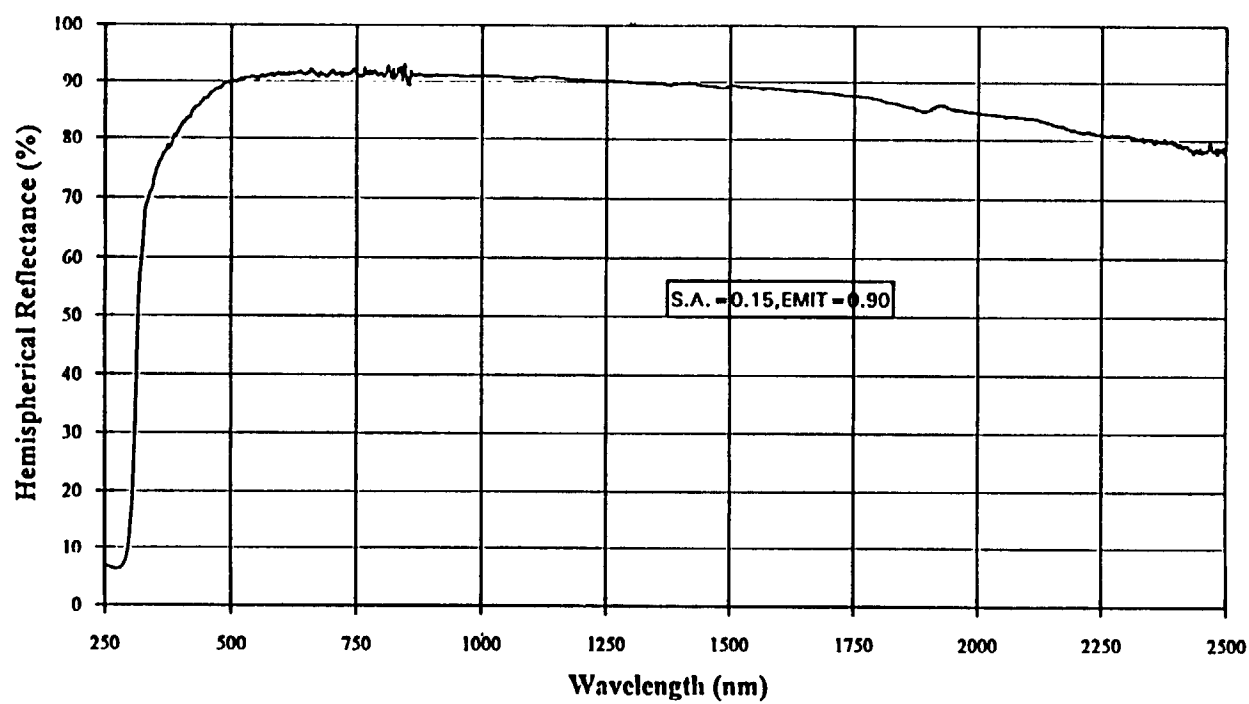
Figure 3-48.   Reflectance Spectrum of Ta$_2$O$_5$/SS-55 (HT Cure) Sample #IH-18, Batch #U-359.
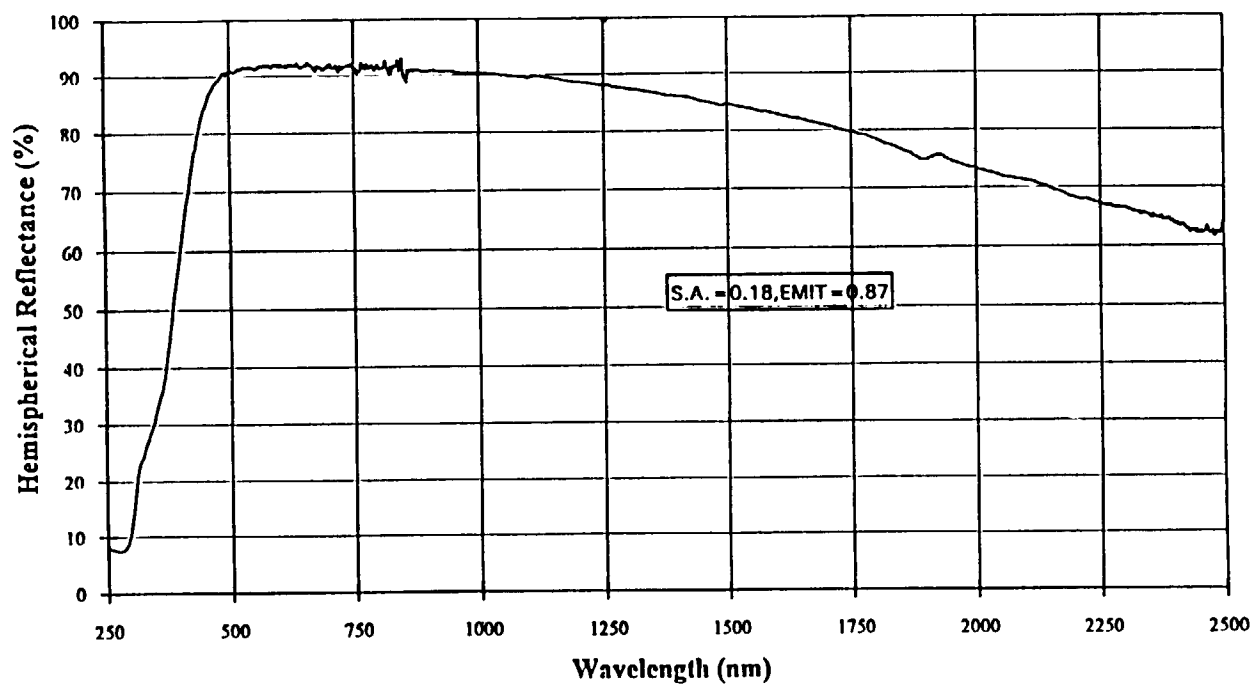
Figure 3-49. Reflectance Spectrum of Ta₂O₅/DHS-2 (HT Cure) Sample #IB-24, Batch #U-364.
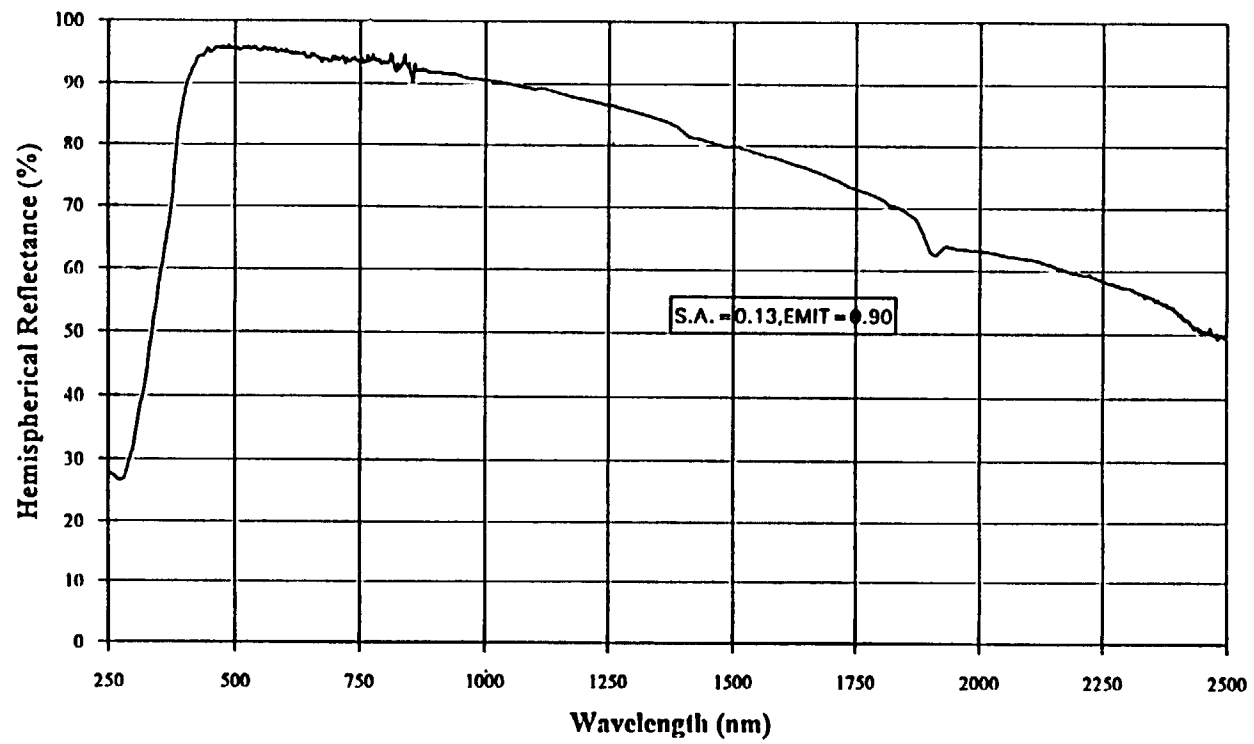
Figure 3-50. Reflectance Spectrum of Sb Doped Sample #GE-16, Batch #U-252.

3.3.1.5 Relevant Comments on Other Material Design Concepts and Data. The following important observations can be made from data presented in Section 3.3.1.4.

The last flexible material design concept based on antimony doping, was not included in screening studies because of vagarities of availability of experimental Sb.doped tin sol and variations of its electrical properties for each lot received by IITRI. The doped tin sol provided by P.Q. Corporation's R&D Division was no longer available in the same grade. A few different versions are still available. In view of this development, we were forced to end the efforts on this material concept.

From measured reflectance on ZOT pigment based concept, it was observed that the use of protonating phos sol (pH = 4.0 to 5.0) provided complete shift of reflectance spectrum to the left of 400 nanometers, a typical representative of edge for unreacted ZnO in ZOT. Thus, one can conclude that the phos sol has reacted with the unreacted ZnO present in the ZOT the pigment. The binder, phos sol, thus helps to achieve a better reflecting thermal control system. The surface electrical resistance measurements indicated the coating met the program goals, and provided a leaky dielectric. The room temperature cured samples of ZOT/phos sol was tested for adhesion following ASTM-D-3359A tape peel adhesion test. The samples passed the adhesion test with a rating of 5A. Heat treatment may provide more toughness. This binder system (phos sol) demands further attention for its use as a viable component to the TCMS.

3.3.1.6 Flexible White (Low α_S/ϵ_N) White TCMS. In this material design, we are totally dependent on the pigment to provide charge transfer processes. The pigment solid-state chemistry and pigment surface chemistry play a major role in tailoring resistances for such a material design. The binder represents a dielectric layer on the pigment. The cured polydimethyl siloxane (without catalyst) acts as a dielectric and has very high volumetric resistivity. The surface resistances are usually in the range of 10^{14} to 10^{15} $\Omega/\square$. When used with a catalyst such as dibutyl-tin-dilaurate used at IITRI in all silicone formulations, the surface resistance decreases to 10^{12} to 10^{13} $\Omega/\square$. Petrach Chemicals has introduced organo zirconates and organo titanates as alternate catalyst agents. Petrach Chemicals claims that these catalysts can bring surface resistance down to 10^{10} to 10^{11} $\Omega/\square$, but may have adverse impact on pot life and cure kinetics of the resin system used in thermal control coatings along with some penalties in α_S. In view of the limited scope of this screening study, emphasis was placed on the use of

doped pigment alone, with the highest possible pigment-to-volume ratio to formulate the flexible TCMS. No attempts were made to manipulate flexible binder dielectric system so that it can participate in the charge transfer process as a leaky dielectric. Such a manipulation calls for an entire research program devoted towards such a goal.

The screening study efforts were very limited in producing the needed resistance tailoring results. Our dependence on pigment to tailor surface resistance required the material design to depend on very high dopant levels to meet the surface resistance goals. This was more apparent when interested industrial parties evaluated RF losses of candidate flexible and silicate-based TCMS, and gave qualitative feedback. The DS13N/LO-41 was a border line acceptable compared to Sb-doped versions. The RF losses in $Sb:Zn_2SnO_4$ were very high.[33] Thus, only DS13N/LO-41 was included in the screening study.

The comments made to us[33] citing European Space Agency (ESA) studies on S13GP/LO-1 for inquiring reasons for electroluminescence were very important from material design issues. There has been no effort to evaluate the behavior of this material under charged conditions. Such behavior needs to be fully characterized along with the electrical performance. It may be worthwhile to visit this phenomenon of electroluminescence in a qualitative way.

3.3.1.7 Electroluminescence (EL) in Thermal Control Systems. The phenomenon of EL means conversion of electrical energy directly into light. The word direct is important, because it means no intermediate process (or mechanism). Many textbooks can give detailed definitions, candidate mechanisms, and lists of materials that show such characteristics. All pigments used in the candidate TCMS are either ZnO based or titanate (ZOT) based, which can be found on such lists. Thus, all are capable of showing EL performance under favorable charging conditions.

The essential element of EL grain in the thermal control system can be stated briefly as follows: The electric energy imparted to grain is used to excite the grain into a more energetic state. This stored energy tends to relax by a variety of processes. One of which is radiative recombination, i.e., that free electrons and holes combine and fraction of liberated energy is emitted as photon. The two essential mechanisms are then electrical excitation and radiative

recombination. They both need to be studied. Radiative recombination competes with the other process which are bulk and are nonradiative-relaxation type to lose excitation energy.

In the case of candidate electrically conductive TCMS with doped silicate or soda silicate binders, the relaxation process is built into the binder system. In the case of flexible candidate thermal control systems, the polydimethyl siloxane cannot participate in a relaxation process until one alters the polymer chemically to make it as a leaky dielectric. The impact of such a manipulation on space environment stability of siloxane polymer is not known. Hence, the approach taken here was not to alter polymer chemistry. This leads to providing limits on relaxation processes available as a mechanism of charge dissipation in flexible conductive thermal control coatings.

The EL effects also need to be studied for the state-of-the-art TCMS and for the conductive versions where we provide doped relaxation paths. The time constants of recombination and relaxation processes and nature of incoming space irradiation (UV, e', P^+) determines resultant charge development. From this discussion, one can conclude that it is essential to characterize baseline and candidate material designs for their response to pulses. No such study was planned during this effort. The goal for this screening study was to provide candidate engineering material system, and to check its response to select promising candidates for future scaleup and validation and use on space hardware.

Lastly, interested researcher should refer to the treaties on EL to assess role of dielectric behavior, interface effects, contact formation and junctions and their impact on radiative recombination. We expect that EL does play a role for the inorganic version of the conductive concepts investigated in this study as well as a significant role for flexible versions. Future studies need to address these issues, if they are important for the hardware. If EL serves as an effective mechanism, one can consider incorporating EL effect enhancing efficient whisker-type innovative material forms (e.g., ZnS whiskers) in existing flexible TCMS for innovative material designs and formulations.

(This page intentionally left blank.)

4. RESULTS OF SPACE ENVIRONMENT SIMULATIONS STUDIES

The space environment simulation did not happen as planned for this screening study. Samples for simulations were submitted as opportunities were made available during this research program. At times, we were ready to submit samples per requests, and at times, we were not completely ready to take advantage of such an opportunity. The detailed screening study on all candidate samples was carried out later at the Aerospace Corporation. In this chapter, results are presented from space environment simulation studies carried out on the candidates material concepts and baseline materials presented earlier in Chapter 3.

4.1 SPACE SIMULATION STUDIES AT AEROSPACE CORPORATION

The space environment simulation at Aerospace Corporation was conducted as a combined radiation test, typically representing low earth orbit (LEO) mission like the DMSP orbit consisting of 2000 ESH of UV + 8.26 x 10^{13} e'/cm^2 (100 KeV) + 5.18 x 10^{13} e'/cm^2 (35 KeV). The detailed report of exposures, and results of pre- and post-total hemispherical solar absorptance measurements were generated under a sub-contract for this material design and screening study. The report is provided in Appendix A for completeness.

The results are summarized here on baseline materials and candidate conductive material design concepts, and presented here in tabular form (Tables 4-1 to 4-5) for completeness and ease of comparison.

Table 4-1. Results of Vacuum-UV, Electron Irradiation of Black TCMS at Aerospace Corporation							
TCMS	Pigment	Binder	Batch #	Sample #	Pretest α_S	Post Test α_S	$\Delta\alpha_S$
Baseline Nonconducting TCMS Candidates							
MH21IP[a]	Black Glass	Kasil 2130	U-284	GZ-21	0.981	0.981	0
MH21S/LO[a]	Black Glass	LO-1	U-360	HZ-18	0.982	0.982	0
D21S/LO[a]	Cosmic Black WB-500	LO-1	T-023	BA-8	0.98	0.98	0
Conductive TCMS Candidates							
DBG-IP[a]	In Doped Black Glass	Kasil 2130	U021	EO-7	0.974	0.975	0.001
DBG-IP[b]	In Doped Black Glass	Kasil 2130	U021	EO-8	0.973	0.974	0.001
MH55IC[a]	Black Glass, Graphite	Kasil 2130	S-024	Z-9	0.94	0.939	-0.001
MH55ICP[b]	Black Glass, Graphite	Kasil 2130	S-024	Z-10	0.942	0.941	-0.001
DBG/DHS[a]	Doped Black Glass	DHS-1	U-283	GU-13	0.958	0.957	-0.001
DBG/DHS[b]	Doped Black Glass	DHS-1	U-283	GU-14	0.956	0.956	0
MH21SC/LO[a]	Black Glass, Graphite	LO-1	U-166	FD-20	0.963	0.964	0.001
MH21SC/LO[b]	Black Glass, Graphite	LO-1	U-166	FD-21	0.965	0.965	0
MH41SC/LO[a]	Black Glass/B4C	LO-1	U-053	FD-5	0.951	0.95	-0.001
MH41SC/LO[b]	Black Glass/B4C	LO-1	U-053	FD-6	0.95	0.953	0.003
D21SC/LO[a]	Cosmic Black, Graphite	LO-1	T-026	BJ-1	0.955	0.956	0.001
D21SC/LO[b]	Cosmic Black, Graphite	LO-1	T-026	BJ-2	0.956	0.957	0.001

(a) UV intensity (0.94 to 0.98 Suns): 2000 ESH + 5.18×10^{13} e'/cm^2 (35 KeV) + 8.26×10^{13} e'/cm^2 (100 KeV).
(b) UV intensity (0.60 to 0.90 Suns): 1500 to 1800 ESH + 5.18×10^{13} e'/cm^2 (35 KeV) + 8.26×10^{13} e'/cm^2 (100 KeV).

TCMS	Pigment	Binder	Batch #	Sample #	Pretest α_S	Post Test α_S	$\Delta\alpha_S$
Table 4-2. Results of Vacuum-UV, Electron Irradiation of White (Low α_S/ϵ_N) TCMS at Aerospace Corporation for Baseline Material Systems and Z-93CZY							
Baseline Nonconducting TCMS							
ZOT[a]	ZOT #98790	None	9890	ZOT#1	0.079	0.104	0.025
Z-93P[a]	Zinc Oxide	Kasil 2130	U-347	HX-10	0.133	0.14	0.007
YB-71[a]	ZOT #98790	Kasil 2130	U-348	HW-3	0.107	0.14	0.033
YB-71P[a]	ZOT #98790	Kasil 2130	U-376	IM-27	0.112	0.123	0.011
S13GP/LO-1[a]	S13GP	LO-1	U-310	IJ-27	0.167	0.177	0.01
S13GP/LO-41[a]	S13GP	LO-41	U-276	HC-20	0.149	0.156	0.007
DZSS/LO-41[a]	DZSS	LO-41	U-208	GH-8	0.077	0.243	0.166
ZOTS/LO-41[a]	ZOT #98790	LO-41	U-343	28	0.133	0.196	0.063
Eu203/2130[a]	Eu203	Kasil 2130	U-352	IF-18	0.092	0.12	0.028
Eu203/LO-41[a]	Eu203	LO-41	U-403	IS-19	0.136	0.178	0.042
Conductive Concept Z-93CXY-Based TCMS							
ZnO(FC)/2130[a]	ZnO(FC)	Kasil 2130	U-321	HM-14	0.148	0.154	0.006
ZnO(FC)/2130[b]	ZnO(FC)	Kasil 2130	U-321	HM-15	0.148	0.149	0.001
ZnO(FC)/SS-55[a]	ZnO(FC)	SS-55	U-322	HF-26	0.147	0.144	-0.003
ZnO(FC)/SS-55[b]	ZnO(FC)	SS-55	U-322	HF-27	0.146	0.144	-0.002
ZnO(FC)/DHS-1[a]	ZnO(FC)	DHS-1	U-323	HG-23	0.157	0.164	0.007
ZnO(FC)/DHS-1[b]	ZnO(FC)	DHS-1	U-323	HG-22	0.149	0.156	0.007
ZnO(FC)/DHS-2[a]	ZnO(FC)	DHS-2	U-327	HL-14	0.139	0.141	0.002
ZnO(FC)/DHS-2[b]	ZnO(FC)	DHS-2	U-327	HL-25	0.146	0.146	0

(a) UV intensity (0.94 to 0.98 Suns): 2000 ESH + 5.18×10^{13} e'/cm^2 (35 KeV) + 8.26×10^{13} e'/cm^2 (100 KeV).

(b) UV intensity (0.60 to 0.90 Suns): 1500 to 1800 ESH + 5.18×10^{13} e'/cm^2 (35 KeV) + 8.26×10^{13} e'/cm^2 (100 KeV).

Table 4-3. Results of Vacuum-UV, Electron Irradiation of White (Low α_S/ϵ_N) TCMS at Aerospace Corporation for Baseline Material Systems and Z-93SCZY							
TCMS	Pigment	Binder	Batch #	Sample #	Pretest α_S	Post Test α_S	$\Delta\alpha_S$
Conductive Concept Z-93SCXY-Based TCMS							
S13GP/2130[a]	S13GP	Kasil 2130	NA	FM-18	0.131	0.148	0.017
S13GP/2130[b]	S13GP	Kasil 2130	NA	FM-21	0.129	0.137	0.008
S13GP/SS-55[a]	S13GP	SS-55	U-405	IU-22	0.125	0.14	0.015
S13GP/SS-55[b]	S13GP	SS-55	U-405	IU-25	0.127	0.134	0.007
S13GP/DHS-1[a]	S13GP	DHS-1	U-279	GS-16	0.147	0.153	0.006
S13GP/DHS-1[b]	S13GP	DHS-1	U-279	GS-17	0.142	0.148	0.006
S13GP/DHS-2[a]	S13GP	DHS-2	U-328	HH-20	0.13	0.155	0.025
S13GP/DHS-2[b]	S13GP	DHS-2	U-328	HH-27	0.134	0.146	0.012
S13N/SS-55[a]	S13N	SS-55	U-260	GR-3	0.115	0.141	0.026
S13N/SS-55[b]	S13N	SS-55	U-260	GR-7	0.114	0.119	0.005
S13N/DHS-1[a]	S13N	DHS-1	U-317	HE-19	0.15	0.173	0.023
S13N/DHS-1[b]	S13N	DHS-1	U-317	HE-23	0.143	0.16	0.017
S13N/DHS-2[a]	S13N	DHS-2	U-329	HI-14	0.134	0.161	0.027
S13N/DHS-2[b]	S13N	DHS-2	U-329	HI-27	0.132	0.16	0.028

(a) UV intensity (0.94 to 0.98 Suns): 2000 ESH + 5.18×10^{13} e'/cm^2 (35 KeV) + 8.26×10^{13} e'/cm^2 (100 KeV).
(b) UV intensity (0.60 to 0.90 Suns): 1500 to 1800 ESH + 5.18×10^{13} e'/cm^2 (35 KeV) + 8.26×10^{13} e'/cm^2 (100 KeV).

Table 4-4. Results of Vacuum-UV, Electron Irradiation of White (Low α_s/ϵ_N) TCMS at Aerospace Corporation for Baseline Material Systems and Z-93SCLMXY							
TCMS	**Pigment**	**Binder**	**Batch #**	**Sample #**	**Pretest α_2**	**Post Test α_s**	**$\Delta\alpha_s$**
Conductive Concept Z-93SCLMXY-Based TCMS							
DZS/2130[a]	DZS	Kasil 2130	T-244	DK-11	0.077	0.132	0.055
DZS/2130[b]	DZS	Kasil 2130	T-244	DK-10	0.081	0.122	0.041
DZS/SS-55[a]	DZS	SS-55	U-207	FO-20	0.107	0.204	0.097
DZS/SS-55[b]	DZS	SS-55	U-207	FO-23	0.1	0.185	0.085
DZS/DHS-1[a]	DZS	DHS-1	U-278	GQ-4	0.075	0.202	0.127
DZS/DHS-1[b]	DZS	DHS-1	U-278	GQ-8	0.078	0.163	0.085
DZS/DHS-2[a]	DZS	DHS-2	U-331	HK-15	0.086	0.189	0.103
DZS/DHS-2[b]	DZS	DHS-2	U-331	HK-27	0.089	0.18	0.091
DS13N/SS-55[a]	DS13N	SS-55	U-315	P-26	0.138	0.173	0.035
DS13N/SS-55[b]	DS13N	SS-55	U-315	P-27	0.137	0.153	0.016
DS13N/DHS-1[a]	DS13N	DHS-1	U-316	S-7	0.123	0.133	0.01
DS13N/DHS-1[b]	DS13N	DHS-1	U-316	S-1	0.124	0.161	0.037
DS13N/DHS-2[a]	DS13N	DHS-2	U-330	HJ-20	0.122	0.128	0.006
DS13N/DHS-2[b]	DS13N	DHS-2	U-330	HJ-20	0.129	0.149	0.02

(a) UV intensity (0.94 to 0.98 Suns): 2000 ESH + 5.18×10^{13} e'/cm^2 (35 KeV) + 8.26×10^{13} e'/cm^2 (100 KeV).

(b) UV intensity (0.60 to 0.90 Suns): 1500 to 1800 ESH + 5.18×10^{13} e'/cm^2 (35 KeV) + 8.26×10^{13} e'/cm^2 (100 KeV).

Table 4-5. Results of Vacuum-UV, Electron Irradiation of White (Low α_S/ϵ_N) TCMS at Aerospace Corporation for Baseline Material Systems for Other Conductive Concepts

TCMS	Pigment	Binder	Batch #	Sample #	Pretest α_S	Post Test α_S	$\Delta\alpha_S$
Other Conductive Concepts Based TCMS							
ZOT/Phos. Sol.[a]	ZOT #98790	Phos. Sol	U-377	HT-21	0.131	0.149	0.018
ZOT/Phos. Sol.[b]	ZOT #98790	Phos. Sol	U-377	HT-22	0.128	0.151	0.023
ZOT/SS-55[a]	ZOT #98790	SS-55	U-379	IN-13	0.117	0.156	0.039
ZOT/SS-55[b]	ZOT #98790	SS-55	U-379	IN-15	0.112	0.156	0.044
ZOT/DHS-2[a]	ZOT #98790	DHS-2	U-378	IO-21	0.125	0.158	0.033
ZOT/DHS-2[b]	ZOT #98790	DHS-2	U-378	IO-28	0.122	0.181	0.059
Eu203/SS-55[a]	Eu203	SS-55	U-353	ID-11	0.087	0.138	0.051
Eu203/SS-55[b]	Eu203	SS-55	U-353	ID-20	0.1	0.126	0.026
Eu203/DHS-2[a]	Eu203	DHS-2	U-381	II-12	0.093	0.158	0.065
Eu203/DHS-2[b]	Eu203	DHS-2	U-381	II-15	0.076	0.108	0.032
Ta205/2130[a]	Ta205	Kasil 2130/RT	U-358	IG-11	0.163	0.304	0.141
Ta205/2130[b]	Ta205	Kasil 2130/RT	U-358	IG-25	0.18	0.286	0.106
Ta205/2130[a]	Ta205	Kasil 2130/HT	U-358	IG-12	0.165	0.232	0.067
Ta205/2130[b]	Ta205	Kasil 2130/HT	U-358	IG-22	0.181	0.231	0.05
Ta205/SS-55[a]	Ta205	SS-55/RT	U-359	IH-19	0.137	0.222	0.085
Ta205/SS-55[b]	Ta205	SS-55/RT	U-359	IH-20	0.143	0.226	0.083
Ta205/SS-55[a]	Ta205	SS-55/HT	U-359	IH-17	0.149	0.199	0.05
Ta205/SS-55[b]	Ta205	SS-55/HT	U-359	IH-27	0.167	0.216	0.049
Sb Doped[a]	ZnO + Sb:Zn2SnO4	Kasil 2130	U-252	GE-9	0.141	0.159	0.018
Sb Doped[b]	ZnO + Sb:Zn2SnO4	Kasil 2130	U-252	GE-8	0.144	0.176	0.032
Flexible Conductive Concept Based TCMS							
DS13N/LO-41[a]	DS13N	LO-41	U-334	HQ-10	0.161	0.278	0.117
DS13N/LO-41[b]	DS13N	LO-41	U-334	HQ-12	0.163	0.239	0.076

(a) UV intensity (0.94 to 0.98 Suns): 2000 ESH + 5.18×10^{13} e'/cm^2 (35 KeV) + 8.26×10^{13} e'/cm^2 (100 KeV).
(b) UV intensity (0.60 to 0.90 Suns): 1500 to 1800 ESH + 5.18×10^{13} e'/cm^2 (35 KeV) + 8.26×10^{13} e'/cm^2 (100 KeV).

4.2 SPACE ENVIRONMENT AT GODDARD SPACE FLIGHT CENTER (GSFC)

The space environment simulation at GSFC was conducted for UV-vacuum in situ reflectance degradation studies for 1000 ESH exposure. It refers to the original research plan, the screening study at the Aerospace Corporation which was to provide candidate concepts for this simulation exercise, but the program and scheduling did happen as originally planned. Dr. Lon Kauder offered additional test spots very early in the program to insert Z-93SC55 (S13GP/DHS) samples into the UV-vacuum test that was being carried out at GSFC. The Z-93SCXY:Z-93SC55 (S13GP/DHS) samples from GPS Block IIR hardware witness samples were provided along with samples based on the material design concept Z93SCLMXY (Z93SC1655:[DZS/SS-55]). GSFC (thermal branch) also processed Z93SC55 samples (T-251). The following samples were submitted to GSFC and were included in UV-vacuum exposure tests for up to 4300 ESH. In situ reflectances were measured at every 500 ESH. The report on this testing can be found in Appendix B, titled "Ultraviolet Degradation of IITRI's Six White Paints." The results from this study can be summarized in a tabular form (Tables 4-6 and 4-7) as follows.

Table 4-6. Candidate Baseline and Conductive Concepts for 4000 ESH Study					
Item No.	Material Concept	Pigment	Binder	Batch # Sample #	PBR
1	Z-93SCXY: (Z-93SC55)	S13GP	DHS 2130 + SS-55 (50:50)	EI-2 (T-342)	5.5
2	Z-93SC55	S13GP	DHS 2130 + SS-55 (50:50)	T-251 processed by GSFC	5.5
3	Z-93SCLMXY: (Z-93SC1655)	DCS	SS-55	EK-20 (T-344)	5.5
4	Z-93P	calcined ZnO	2130	N/A	4.3
5	S13GP/LO-1	S13GP	MHS/LO stripped polydimethyl siloxane	N/A	2.1

Table 4-7. Results of In Situ Reflectance Degradation Study [4300 ESH (UV-Vacuum)] for Baseline TCMS						
Sample Description	Optical Properties	0 ESH	1010 ESH	2041 ESH	3042 ESH	4331 ESH
Nonconductive White TCMS						
S13GP/LO-1	α_S	.181	.186	.184	.195	.192
	ϵ_N	.922	No Measurement	.919	.917	.918
Z93P (Kasil 2130)	α_S	.172	.175	.178	.181	.189
	ϵ_N	.930	.931	.929	.928	.929

Table 4-8. Results of In Situ Reflectance Degradation Study [4300 ESH (UV-Vacuum)] for Conductive TCMS						
Sample Description	Optical Properties	0 ESH	1010 ESH	2041 ESH	3042 ESH	4331 ESH
Conductive White TCMS						
Z93SC55 (T251)	α_S	.140	.151	.157	.175	.177
	ϵ_N	.935	.929	.930	.931	.929
Z93SC55 (EI-2)	α_S	.151	.164	.177	.200	.207
	ϵ_N	.934	.928	.926	.928	.929
Z93SC1655 (EK-20)	α_S	.128	.220	.261	.304	sample removed
	ϵ_N	.935	.926	.927	.925	sample removed

The SEE Project Office has also contracted GSFC to assist this screening study to study reflectance degradation for 1000 ESH exposure of UV-vacuum irradiation. Dr. Lon Kauder and Ms. Wanda Peters at GSFC received companion samples of the selected material concepts that were also submitted to Aerospace Corporation. The material concepts submitted to GSFC are listed here in Table 4-9.

Unfortunately, selection of conductive concepts for this study do not benefit from the input from the screening test at Aerospace Corporation as planned. The scheduling conflicts precluded us from doing that. Thus, the choices were made strictly based on conservative

Table 4-9. Electrically Conductive TCMS for 1000 ESH UV-Vacuum Exposure Induced Reflectance Degradation Study			
Concept Name	Sample #	Pigment	Binder
Black Conductive TCMS			
DBG-IP	GTM-29	Doped black glass (Indium doped)	Kasil 2130
MH55-ICP	Z-6	Black glass, Graphite 9035, ZnO	Kasil 2130
MH21SC/LO	GX-16	Black glass, graphite fiber, Graphite 9035	MHS/LO stripped polydimethyl siloxane
MS41SCB/LO	U-356 IC-20	Black glass/B_4C	MHS/LO stripped polydimethyl siloxane
D36SCB/LO	JV-17	Cosmic black WB-500, B_4C	MHS/LO stripped polydimethyl siloxane
White Conductive TCMS			
ZnO(FC)/DHS-2	HL-26	ZnO(FC)	DHS-2
S13GP/DHS-2	HH-19	S13GP	DHS-2
S13N/DHS-2	HI-21	S13LN	DHS-2
DS13N/DHS-2	HJ-25	DS13N	DHS-2
DS13N/SS-55	P-31	DS13N	SS-55
DS13N/LO-51	JX-16	DS13N	MHS/LO stripped polydimethyl siloxane
ZOT/SS-55	IW-19	ZOT #98790	SS-55
Eu_2O_3*/SS-55	HD-26	Eu_2O_3	SS-55
Sb Doped	GE-12	ZnO + Sb doped Zn_2SnO_4	Kasil 2130

engineering judgement where electrical resistance behavior was more reproducible. We could have also picked candidates like ZOT/Phos. Sol and D21SC/LO from reproducibility results, but the space limitations in the chamber did not allow more samples. In conclusion, one should not assume that these concepts were considered as promising candidates.

The report for the degradation behavior results can be found in Appendix C titled, "Ultraviolet Degradation on Study of IITRI Electrically Conductive Thermal Control

Formulations". The summary of their results is given here in Table 4-10 for quick comparison purposes.

Table 4-10. Results of UV-Vacuum (1000 ESH) Exposure Induced Degradation of Candidate TCMS at GSFC				
TCMS/Sample # Description	Optical Properties	0 ESH	1068 ESH	$\Delta\alpha_S$
DBG-IP/[GTM-29]	α_S	.957	.951	-0.006
	ϵ_N	.911	.914	
MH55-IC/[Z-6]	α_S	.928	.938	0.010
	ϵ_N	.886	.885	
MH21SC/LO/[GX-16]	α_S	.951	.955	0.004
	ϵ_N	.862	.864	
MS41SCB/LO/[IC-20]	α_S	.939	.947	0.008
	ϵ_N	.866	.867	
D36SCB/LO/[JV-17]	α_S	.962	.967	0.005
	ϵ_N	.908	.909	
ZnO(FC)/DHS-2/[HL-26]	α_S	.158	.168	0.010
	ϵ_N	.925	.925	
S13GP/DHS-2/[HH-19]	α_S	.148	.165	0.017
	ϵ_N	.934	.932	
S13N/DHS-2/[HI-21]	α_S	.152	.162	0.010
	ϵ_N	.935	.932	
DS13N/DHS-2/[HJ-25]	α_S	.148	.154	0.006
	ϵ_N	.937	.935	
DS13N/SS-55/[P-31]	α_S	.152	.172	0.020
	ϵ_N	.930	.930	
DS13N/LO-51/[JX-16]	α_S	.210	.434	0.224
	ϵ_N	.926	.926	
ZOT/SS-55/[IW-19]	α_S	.129	.180	0.051
	ϵ_N	.881	.881	
Eu_2O_3/SS-55/[HD-26]	α_S	.096	.129	0.033
	ϵ_N	.923	.921	
Sb Doped Concept/[GE-12]	α_S	.156	.243	0.087
	ϵ_N	.930	.931	

4.3. SPACE ENVIRONMENT SIMULATION AT AIR FORCE MATERIALS LABORATORY, (AFML) SCEPTRE RESULTS

During the very beginning of the program, interest was also shown by Mr. P. Carlin of AFML to provide assistance for some in situ reflectance degradation studies of the selected concept in the SCEPTRE facility. The program had not progressed enough to make the best possible judgements and to select concepts and samples to provide to AFML. Mr. P. Carlin (AFML) and Mr. C. Cerbus (UDRI) requested two candidates of doped conductive TCMS concept for the space environment simulations and offered to provide six spots for passive samples, where EUV intensities were high. The material concepts submitted to the Air Force Materials Laboratory for their test 96QV01 are described in Table 4-11 for ready reference, along with the tabulated results in Table 4-12. The exposure consists of irradiation in vacuum (5.0E-08 torr) with UV exposure at 2 suns and 1.6 suns along with electrons of 1.0 KeV at a flux of 6.0E+09 e'/cm²/sec and electrons of 10.0 KeV at a flux of 3.0E+09 e'/cm²/sec for total fluence of 1.2E+16e'/cm². The sample temperature was maintained from 135° to 146°F with loss of chiller cooling causing temperatures to rise up to 185°F for 12 hr. period. The total exposure happened over 314 hours. The report provided by Mr. C. Cerbus can be found in Appendix D.

Table 4-11. Material Design Concepts Provided to AFML for In Situ and Passive Reflectance Degradation Study in SCEPTRE Facility

Material Concept	Pigment	Binder	PBR
Conductive Concepts for "In Situ" Studies			
DS13N/LO-51	DS13N	MHS/LO stripped polydimethyl siloxane	5.0
DS13N/SS-55	DS13N	SS-55	5.5
Black Conductive TCMS for "Passive" Tests			
DGB/IP	Doped Black Glass DBG	Kasil 2130	2.0
D36SCB/LO	Cosmic Black WB-500 graphite 9035 B₄C	MHS/LO stripped polydimethyl Siloxane	3.6
White Conductive TCMS for "Passive" Test			
Z-93CXY:Z9355	ZnO(FC)	DHS-2	5.5
Z-93SCXY:Z-93SC55	S13N	DHS-2	5.5
Z-93SCLMXY:Z-931655	DS13N	DHS-2	5.5
Other Conductive White TCMS for "Passive" Test			
Eu₂O₃*	Eu₂O₃	SS-55	5.5

Table 4-12. Summary of Results from SCEPTRE Screening Test 96QV01

TCMS	Batch	Specimen ID	UV Exposure	Pretest α_s	Post Test α_s	$\Delta\alpha_s$
Measured In Situ Conductive White Coatings						
DS13N/LO-51	V-032	JZ-17	1.6 EUVS	0.193	0.423	0.230
DS13N/LO-51	U-315	P-25	2.1 EUVS	0.157	0.267	0.110
Passively Exposed Conductive Black TCMS						
DGB-IP	U-021	EO-17	4.0 EUVS	0.970	0.978	0.008
D36SCB/LO	V-036	JV-15	3.9 EUVS	0.966	0.956	-0.010
Conductive White TCMS						
Z-93CXY						
ZnO(FC/DHS-2	U-327	HL-23	1.1 EUVS	0.143	0.225	0.082
Z-93SCXY						
S13N/DHS-2	U-329	HI-17	1.0 EUVS	0.130	0.196	0.066
Z-93SCLMXY						
DS13N/DHS-2	U-330	HJ-16	3.3 EUVS	0.117	0.237	0.120
Other Conductive White Coatings						
Eu2O3/SS-55	U-353	ID-19	3.6 EUVS	0.076	0.161	0.085

Test Environment Parameters:

Vacuum: 5.0E-08 tour
Total Exposure Time: 314 hrs.

1.0 KeV electron flux   6.0E+09 e'/cm2/sec
10.0 KeV electron flux 3.0E+09 e'/cm2/sec

Total Fluence: 1.2E+16 e-/cm2

Temperature Range:

In Situ*:   135°-146°F
Passive: 185°F

*Lost chiller for 12 hrs and temperatures reached 182°-185°F

4.4 IRRADIATION INDUCED CHARGE DEVELOPMENT [ESD] TESTING

Dr. Lon Kauder at GSFC was also contracted by the SEE Project Office to perform ESD testing on the selected candidates from the screening study conducted at IITRI/AMCL. The samples used for the ESD testing are described below.

IITRI submitted 4"x4" coated samples on Al6061-T6 substrates. The Al-6061-T6 substrates were chosen to assure good electrical contact to substrate. The sample were exposed

to vacuum for several hours to ensure minimum moisture contributions. The electron gun(s) were used to carry out required exposure of the samples to electrons of various energy for various fluxes (currents). The energies used were from 5 KeV to 20 KeV and currents used were from 1.0 nanoamps/cm^2 to 10 nanoamps/cm^2. The charge induced potential (volts) developed on the sample was measured by tracking with a voltage trek probe over the sample. These measurements were carried out at various temperatures between the range of 77 to 325K. The results received from Dr. L. Kauder can be found in Appendix E. The conductive material concepts tested are summarized here in Table 4-13.

Table 4-13. Conductive Material Concepts for ESD Testing at GSFC			
Conductive Material TCMS	**Pigment**	**Binder**	**PBR**
Black Conductive TCMS			
DBG-IP	Doped Black, Glass	Kasil 2130	2.0
MH55ICP	Black Glass, Graphite 9035	Kasil 2130	5.5
MH41SCB/LO	Black Glass, Graphite 9035 B$_4$C	MHS/LO stripped polydimethyl siloxane	4.0
D36SCB/LO	WB-500 Cosmic Black graphite 9035 B$_4$C	MHS/LO stripped polydimethyl siloxane	3.6
MH21SC/LO	Black Glass, Graphite fibers	MHS/LO stripped polydimethyl siloxane	2.5
White Conductive TCMS			
Z-93CXY:Z-93C55	ZnO (FC)	DHS-2	5.5
Z-93SCXY:Z-93SC55	S13GP	DHS-2	5.5
Z-93SCLMXY:Z-93SC1255	DS13N	DHS-2	5.5
Flexible Conductive TCMS			
DS13N/LO-51	DS13N	MHS/LO stripped polydimethyl siloxane	5.0
Other Conductive TCMS			
DZS/SS-55	DZS	SS-55	5.5
ZOT/SS-55	ZOT	SS-55	5.5
Eu$_2$O$_3$/SS-55	Eu$_2$O$_3$	SS-55	5.5

The flexible conductive white sample charged to very high voltages (at 77K) in this study. The results of DS13N/LO-51 are hence, discouraging. The material design does not charge at room temperature. Further investigations are necessary for carrying out root cause analysis, and concurrently carrying out volumetric and surface resistance measurements on the conductive candidate material concepts. The results from GSFC for the ESD test on DS13N/LO-51 are given in Appendix E.

From review of the data from Appendix E, one can conclude that all conductive black coating concepts do not charge under irradiation of electrons for the studied energies and current at the selected temperatures which are representative of typical mission conditions. Table 4-14 summarizes the data. All conductive coatings concepts charged to maximum voltage at 77K and were conductive at room temperature showing charging below 20 volts.

The candidates concepts for the ESD charging testing studies were selected and sent for testing at GSFC without having knowledge of results for $\Delta\alpha_s$ from screening studies done at Aerospace Corporation. Because of this, we took a very conservative approach in selecting candidates for ESD testing. The concepts that are resistive, but have less dopant concentration, were expected to be more stable. Therefore, ESD testing was carried out only on those that were slightly resistive. In light of the screening study results and the charging study, we are very hopeful about the next phase of work. We recommend that more effort be devoted to ESD testing. The limited ESD testing in this program has shown that the conservative material designs also performed satisfactorily. We need to carry out testing on more conductive concepts that have shown remarkable stability to the space environment. Thus, much more remains to be done in this area for the identified promising candidates.

Table 4-14. Results of ESD Test at GSFC

DBG-IP
Date Tested: 11/26/96
Charging Potential Developed on Sample (Volts)

Temperature (K)	Electron Flux				
	5KeV @ 1.0nA/cm²	5KeV @ 10nA/cm²	10KeV @ 1.0nA/cm²	10KeV @ 10nA/cm²	20KeV @ 10nA/cm²
130	-17	-39	-66	-71	-87
179	-20	-32	-63	-70	-80
227	-25	-30	-51	-64	-74
273	-10	-16	-16	-28	-17
320	-1	-5.9	-3.5	-8.1	-3

MH55IC
Date Tested: 11/24/96
Charging Potential Developed on Sample (Volts)

Temperature (K)	Electron Flux				
	5KeV @ 1.0nA/cm²	5KeV @ 10nA/cm²	10KeV @ 1.0nA/cm²	10KeV @ 10nA/cm²	20KeV @ 10nA/cm²
129	-33	-35	-71	-68	-68
178	-30	-30	-60	-56	-61
226	-22	-31	-60	-60	-60
273	-18	-22	-22	-44	
321	-3	-7.3	-3.9	-9.5	

MH41SCB/LO1
Date Tested: 11/30/96
Charging Potential Developed on Sample (Volts)

Temperature (K)	Electron Flux				
	5KeV @ 1.0nA/cm²	5KeV @ 10nA/cm²	10KeV @ 1.0nA/cm²	10KeV @ 10nA/cm²	20KeV @ 10nA/cm²
128	-10	-12.6	-55	-60	-62
173	-13	-13	-62	-60	-61
224	-16	-16	-61	-63	-63
268	-17	-17	-65	-62	
323	-22	-22	-65	-73	-60

Table 4-14. Results of ESD Test at GSFC (Continued)

D36SCBB/LO
Date Tested: 11/20/96
Charging Potential Developed on Sample (Volts)

Temperature (K)	Electron Flux			
	5KeV @ 1.0nA/cm²	5KeV @ 10nA/cm²	10KeV @ 1.0nA/cm²	10KeV @ 10nA/cm²
133	-6.3	-8.5	-8.4	-9.9
178	-6.1	-6.2	-6.5	-7
226	-5.8	-6.1	-5.6	-6.3
275	-4.1	-4.9	-3.9	-4.8
321	-2.4	-3.4	-3	-3.7

MH21SC/LO
Date Tested: 10/28/96
Charging Potential Developed on Sample (Volts)

Temperature (K)	Electron Flux
	5KeV @ 1.0nA/cm²
275	-190
322	-175

ZnO(CF)/DHS-2
Date Tested: 11/13/96
Non-contact Charging Potential Developed on Sample (Volts)

Temperature (K)	Electron Flux			
	5KeV @ 1.0nA/cm²	5KeV @ 10nA/cm²	10KeV @ 1.0nA/cm²	10KeV @ 10nA/cm²
130	-7	-11	-7	-17
179	-8	-15	-9	-14
228	-13	-22	-17	-25
275	-9		-35	-56
322	-3		-3	-20

Table 4-14. Results of ESD Test at GSFC (Continued)

S13GP/DHS-2
Date Tested: 10/23/96
Non-contact Charging Potential Developed on Sample (Volts)

Temperature (K)	Electron Flux		
	5KeV @ 1.0nA/cm²	5KeV @ 10nA/cm²	10KeV @ 1.0nA/cm²
128			
178	-160		
225	-123		
275	-60	-190	-130
321	-2.5	-13	-70

S13GP/DHS-2
Date Tested: 10/31/96
Non-contact Charging Potential Developed on Sample (Volts)

Temperature (K)	Electron Flux				
	5KeV @ 0.44n	5KeV @ 4.4nA	10KeV @ 0.44nA	10KeV @ 4.4nA	20KeV @ 0.44nA
275	-80	-130			
323	-45	-56			

S13GP/DHS-2
Date Tested: 11/4/96
Non-contact Charging Potential Developed on Sample (Volts)

Temperature (K)	Electron Flux				
	5KeV @ 1.0nA/cm²	5KeV @ 10nA/cm²	10KeV @ 1.0nA/cm²	10KeV @ 10nA/cm²	20KeV @ 10nA/cm²
129	-60	-180	-120		-120
179	-45	-170	-110		
228	-70	-160	-110		
275	-30	-100	-65	-160	-60
322	-6	-27	-20	-70	-30

Table 4-14. Results of ESD Test at GSFC (Continued)

ZOT/SS-55
Date Tested: 1/7/97
Non-contact Charging Potential Developed on Sample (Volts)

Temperature (K)	Electron Flux			
	5KeV @ 0.44nA	10KeV @ 0.44nA	10KeV @ 4.4nA	20KeV @ 0.44nA
129	-174			
179	-160			
227	-100	-170		
271	-1.7	-2		-100
319	-0.5	-0.6		0

Eu_2O_3/SS-55
Date Tested: 11/19/96
Charging Potential Developed on Sample (Volts)

Temperature (K)	Electron Flux				
	5KeV @ 0.44nA/cm²	5KeV @ 4.4nA/cm²	10KeV @ 0.44nA/cm²	10KeV @ 4.4nA/cm²	20KeV @ 10nA/cm²
273	-180				
322	-25				

ZnO + Sb doped Zn_2SnOx in Kasil 2130
Date tested 12/2/96
Charging Potential Developed on Sample (Volts)

Temperature (K)	Electron Flux				
	Flux 5KeV @ 0.44nA/cm²	5KeV @ 4.4nA/cm²	10KeV @ 0.44nA/cm²	10KeV @ 4.4nA/cm²	20KeV @ 0.44nA/cm²
129	-77	-134	-143		-140
179	-73	-110	-120		-163
227	-66	-105	-100		-137
275	-30	-120	-60	-160	-70
323	-14	-19	-34	-36	-48

Table 4-14. Results of ESD Test at GSFC (Concluded)

DS13N/LO-41
Date tested 12/4/96
Charging Potential Developed on Sample (Volts)

Temperature (K)	Electron Flux				
	Flux 5KeV @ 0.44nA/cm²	5KeV @ 4.4nA/cm²	10KeV @ 0.44nA/cm²	10KeV @ 4.4nA/cm²	20KeV @ 0.44nA/cm²
274					
320	-20	-76	-41	-145	-40

In the ESD tests carried out, the charging observed for MH21SC/LO and DS13N/LO-41 was not expected. These concepts need further investigation. We expect better ESD performance from these formulations based on their surface electrical resistances. ESD testing carried out for this program was very limited and could not provide information on some more conductive concepts that have shown excellent space environment stability. Thus, it may be premature to carry out data analysis and provide conclusions just based on these tests. Tests are expensive and time consuming and need to be carried out on the full spectrum of material design concepts, so that these results can be used for future material selection - Our approach to tailor steady-state electrical surface resistance at room temperature may also need to be modified for material design. The approach of resistance tailoring may need to consider RF properties in the material design issue. Thus, the material design attempt made for the screening study was limited and has not been completely tested for ESD performance.

4.5 DISCUSSION OF RESULTS

In this section, we present observations, comparison of data, and qualitative comments as applied to the thermal control material system design. Each material design concept was addressed attention in this discussion. For testing and related issues detailed comments were made by each collaborating researcher in their report. One can refer to their reports in the appendices of this final reports. (Appendices A through E).

4.5.1 High Absorptivity Conductive TCMS

The comparison of baseline and conductive concepts reveals that all of the conductive concepts behaved satisfactorily showing excellent stability to the space environment, and satisfactorily mitigating charging for the tested conditions. Table 4-15 provides summary of the typical performance of the promising conductive candidates that are inorganic and flexible with low outgassing siloxane polymer as a vehicle. The thermal designers can use them on spare hardware. The following qualitative comments can be made for the evaluated concepts:

- Candidate conductive thermal control materials systems behaved very similar to the baseline materials and are recommended as space environment stable in low earth orbit (LEO) type exposures studied in this screening effort.

- Doping of black glass provides the ability to tailor surface resistance values without compromising α_S or ϵ_N of the TCMS. This concept should be studied further with emphasis on dopant cost issues and processing issues. This provides material designers additional flexibility to tailor surface resistances along with BRDF.

- If component design and location of hardware on the spacecraft demands that the conductive TCMS should need to depend on tailoring percolating leaky paths only. Then, the use of semi-conducting grade B_4C is a viable option as a conductive phase. It provides the ability to provide percolating path along with additional ability to control RF losses.

- AO resistance studies are recommended on all of the electrically conductive TCMS candidates, with emphasis on cost reducing processing steps. The role of processing steps in AO resistance of TCMS needs to receive attention.

Table 4-15. Typical Performance of Promising Conductive Absorber Optical Coatings in Low Earth Orbit (LEO)				
Material	Pre-exposure α_s	Post-exposure α_s	$\Delta\alpha_s$	Tested By
Inorganic-Conductive				
MH55-IC	0.940	0.938	-0.001	Aerospace Corporation
MH55-IC	0.942	0.941	-0.001	Aerospace Corporation
MH55-IC	0.928	0.938	0.010	GSFC
DBG-IP	0.974	0.975	0.001	Aerospace Corporation
DBG-IP	0.973	0.974	0.001	Aerospace Corporation
DBG-IP	0.957	0.951	-0.006	GSFC
DBG-IP	0.970	0.978	0.008	AFML/SCEPTRE
DBG-DHS	0.958	0.957	-0.001	Aerospace Corporation
DBG-DHS	0.956	0.956	0	Aerospace Corporation
Organic-Flexible-Conductive				
D21S/LO	0.980	0.980	0	Aerospace Corporation
D21SC/LO	0.956	0.957	0.001	Aerospace Corporation
D21SC/LO	0.955	0.956	0.001	Aerospace Corporation
MH21SC/LO	0.963	0.964	0.001	Aerospace Corporation
MH21SC/LO	0.965	0.965	0	Aerospace Corporation
MH41SCB/LO	0.951	0.950	-0.001	Aerospace Corporation
D36SCB/LO	0.962	0.967	0.005	GSFC
D36SCBLO	0.966	0.956	-0.010	AFML/SCEPTRE
MH41SCB/LO	0.939	0.947	0.008	GSFC
MH21SC/LO	0.951	0.955	0.004	GSFC

All tests at GSFC involved exposure to 1000 ESH of UV and Vacuum.

All tests at AFML/SCEPTRE involved exposure at 2.0 Suns of EUV and 6.78 x 10^{15} e'/cm^2 (1 KeV) + 3.39 x 10^{15} e'/cm^2 (10 KeV) and Vacuum.

All tests carried out at Aerospace Corporation involved exposure to 2000 ESH of UV + 8.26 x 10^{13} e'/cm^2 [35 KeV] (typical DMSP orbit) and Vacuum.

• The ESD performance for MH21SC/LO does not correlate with the low steady-state surface resistance value of the sample. The material design (MH21SC/LO) should receive more attention during the next phase to verify this. The comparable surface resistance formulations of other concepts show no charging, hence the sample may be suspect. No surface or sample analysis was carried out to identify root cause of this charging behavior.

4.5.2 Low (α_S/ϵ_N) TCMS

In the area of white thermal control material systems, this screening study has provided significant input in two areas. First, it has provided new insight on baseline nonconducting materials by testing them one more time after recent reformulation study (AFML-TR-94-4126), and secondly, it has evaluated proposed conductive material design concepts to provide guidance to electro-ceramists on designing required surface resistance values in the TCMS.

First, we discuss the nonconducting baseline material systems and their degradation in space environment. The following observations are important.

(1) S13GP/LO-1 and S13GP/LO-41 showed excellent stability in studies carried out at Aerospace Corp and GSFC approaching very close to performance of Z-93P.

(2) Zn_2TiO_4 (ZOT) containing thermal control material systems showed excellent space environment stability. YB-71P turns out to be slightly more stable than YB-71. This is an encouraging result.

(3) All Zn_2TiO_4 (ZOT) pigmented nonconducting and conductive material designs showed an interesting phenomena. They show a reverse correlation of degradation with solar exposure. That is, the samples exposed in intense area of beam showed lesser degradation than their counterparts placed in weaker area of beam in the Aerospace Corporation study. The differences in $\Delta\alpha_S$ are significant. This phenomena needs to receive further attention. If this is true, it has more importance from a material selection point of view for orbits that have significant electron fluxes (e.g., GEO, polar). The other implication of this finding may relate to ground simulation testing. If electron exposure causes degradation and UV acts as a healing or restoring means for reflectance, then during accelerated test one needs to keep ratio of one radiation flux to other as a constant for

simulating similar synergism for a given orbit. If exposures are to be limited to 2 suns to avoid contributions from thermal effects in degradation of reflectance, then from the similarity principles in acceleration and to achieve correct synergism for a given orbit, there needs to be a limit on e' or particulate radiation acceleration. The same opinion has been expressed by Zerlaut and Gilligan[22], Zerlaut et al.[31] in the past while discussing the combined radiation exposures study for ZOT type materials using UV and protons. Their study concluded that radiation flux ratios and rates are important.

(4) Among the baseline nonconducting TCMS concepts, two pigments were studied that can provide beginning of life solar absorptance less than 0.10. The Eu_2O_3 was promising. Although $\Delta\alpha_s$ for Eu_2O_3 were greater than that of Z-93P, one can observe that α_s after [2000 ESH UV + 5.18 x 10^3 e'/cm^2 (35 KeV) + 8.26 x 10^{13} e'/cm^2 (100 KeV] exposure was 0.12 in the Aerospace Corporation study, and 0.16 in AFML's in situ degradation study. The α_s for Z-93P for the same exposure was also 0.16. Thus, future study should include baseline Eu_2O_3/2130 nonconducting material along with its conducting versions to explore if Eu_2O_3 can provide this performance consistently. The Eu_2O_3 may also provide additional flexibility of processing for thermal spraying or plasma spraying of the pigment. Eu_2O_3 is not semiconducting in nature and, hence, should be more conducive to thermal or plasma spraying via microencapsulation.

(5) DZS high temperature route doped (Zn_2SiO_4) based nonconducting baseline material system processed in Kasil 2130 showed extraordinary degradation, thus ruling out its use in any future study.

Among electrically conducting thermal control material systems designs, there were several encouraging observations, as well as a few that are difficult to rationalize. The root causes can either be in material concept or in the selection of the parameters for processing. Table 4-16 is presented here to provide insight on space environment stability. The following qualitative remarks can help us to appropriately assess the material design issues.

Table 4-16. Typical Performance of Promising Conductive White Thermal Control Coatings in Low Earth Orbit (LEO)				
TCMS	Pre-exposure α_s	Post-exposure α_s	$\Delta\alpha_s$	Tested By
Concept:	Flash Calcination of ZnO (SP-500) to retain controlled Zn interstitials, and stabilization with doped hybrid, silicate binder.			
ZnO(FC)/DHS-2	0.139	0.141	0.002	Aerospace Corporation
ZnO(FC)/DHS-2	0.146	0.146	0.000	Aerospace Corporation
ZnO(FC)/DHS-2	0.168	0.168	0.010	GSFC*
ZnO(FC)/DHS-2	0.143	0.225	0.082	AFML/SCEPTRE[1]
Concept:	Z-93SC55 - Stabilization of Zn interstitials via microencapsulation and incorporation in hybrid silicate and doped hybrid silicate binders.			
S13GP/DHS-1	0.147	0.153	0.006	Aerospace Corporation
S13GP/DHS-1	0.142	0.148	0.006	Aerospace Corporation
S13GP/SS-55	0.125	0.140	0.015	Aerospace Corporation
S13GP/SS-55	0.127	0.137	0.010	Aerospace Corporation
S13GP/SS-55	0.140	0.177	0.037	GSFC**
S13GP/SS-55	0.151	0.206	0.055	GSFC**
S13N/DHS-2	0.13	0.196	0.066	AFML/SCEPTRE[1]
Concept:	Z-93SCLMXY - Stabilization of Zn interstitials via microencapsulation using doped hybrid silicate binders and incorporation in hybrid silicate binder or doped hybrid silicate binder.			
DS13N/SS-55	0.136	0.173	0.037	Aerospace Corporation
DS13N/SS-55	0.137	0.153	0.016	Aerospace Corporation
DS13N/DHS-2	0.124	0.161	0.037	Aerospace Corporation
DS13N/DHS-2	0.122	0.128	0.006	Aerospace Corporation
DS13N/DHS-2	0.148	0.154	0.006	GSFC*
DS13N/DHS-2	0.12	0.24	0.120	AFML/SCEPTRE[2]
DS13N/SS-55	0.16	0.27	0.11	AFML/SCEPTRE[3]

TCMS	Pre-exposure α_S	Post-exposure α_S	$\Delta\alpha_S$	Tested By

Table 4-16. Typical Performance of Promising Conductive White Thermal Coatings in Low Earth Orbit (LEO) (Continued)

TCMS	Pre-exposure α_S	Post-exposure α_S	$\Delta\alpha_S$	Tested By
Concept: Flexible Conductive White TCC with DS13N in stripped silicone				
DS13N/LO-41	0.161	0.278	0.117	Aerospace Corporation
DS13N/LO-41	0.163	0.239	0.076	Aerospace Corporation
DS13N/LO-41	0.210	0.430	0.22	GSFC*
DS13N/LO-51	0.193	0.423	0.230	AFML/SCEPTRE[3]
Conductive Concepts with Other Candidate Pigments				
ZOT/Phos. Sol.	0.131	0.149	0.018	Aerospace Corporation
ZOT/Phos. Sol.	0.128	0.151	0.023	Aerospace Corporation
ZOT/SS-55	0.117	0.156	0.039	Aerospace Corporation
ZOT/SS-55	0.112	0.156	0.044	Aerospace Corporation
ZOT/SS-55	0.129	0.180	0.051	Aerospace Corporation
Eu_2O_3*/SS-55	0.087	0.138	0.051	Aerospace Corporation
Eu_2O_3*/SS-55	0.100	0.126	0.028	Aerospace Corporation
Eu_2O_3*/DHS-2	0.093	0.158	0.065	Aerospace Corporation
Eu_2O_3*/DHS-2	0.076	0.108	0.032	Aerospace Corporation
Eu_2O_3*/SS-55	0.096	0.129	0.033	GSFC*
Eu_2O_3*/SS-55	0.076	0.161	0.085	AFML/SCEPTRE[2]

*GSFC test involved exposure to 1000 ESH of UV-Vacuum.
**This GSFC test involves exposure to 4300 ESH of UV-Vacuum.

All tests carried out at Aerospace Corporation involved exposure to 2000 ESH of UV + 8.26 x 10^{13} e'/cm² (100 KeV) + 5.18 x 10^{13} e'/cm² (35 KeV) (typical DMSP orbit) and Vacuum.

(1) Test at AFML/SCEPTRE involved exposure at 1 Sun of EUV-Vacuum (for Z-93CXY and Z-93SCXY) + 6.78 x 10^{15} e'/cm² (1 KeV) + 3.39 x 10^{15} e'/cm² (10 KeV).

(2) Test at AFML/SCEPTRE involved exposure at 3.3 to 3.6 Suns of EUV-Vacuum (for DS13N/DHS-2 and Eu_2O_3*/SS-55) + 6.78 x 10^{15} e'/cm² (1 KeV) + 3.39 x 10^{15} e'/cm² (10 KeV).

(3) The in situ test at AFML/SCEPTRE involved exposure at 1.6 to 2.1 Suns of EUV-Vacuum + 6.78 x 10^{15} e'/cm² (1 KeV) + 3.39 x 10^{15} e'/cm² (10 KeV).

The first concept suggested for the screening study was of flash calcination of ZnO (SP-500) to retain Zn interstitials in grain so as to tailor grain resistivity, and hence, the resultant surface resistance. The material resistivity tailoring exercise showed that the concept met the program goals with all candidate binder systems (i.e., SS-55, DHS-1, DHS-2). The conductive concept Z-93C55: ZnO(FC)/DHS-2, and Z-93(FC)/DHS-1 showed best reproducibility in surface resistance values along with compatibility with ambient storage conditions. Studies at Aerospace Corporation, GSFC, and AFML/SCEPTRE show that both concept have acceptable stability to the space environment, along with acceptable ESD performance. Concept ZnO(FC)/DHS-1 and ZnO(FC)/DHS-2 both should receive attention for further scale up, validation and reliability studies.

The second concept suggested was to microencapsulate ZnO(SP-500) following well know S13G processing steps and to incorporate them in candidate silicate binder systems. GSFC studied this for up to 4300 ESH exposure of UV-Vacuum. The study at Aerospace Corporation (Appendix A), and the study at AFML/SCEPTRE (Appendix D) show that the concept has the required stability to the space environment. The ESD behavior studied shows promising characteristics along with the required RF properties. The concepts Z93SC55:S13GP/DHS-1 and S13GP/SS-55 are suggested for further studies of scaleup, validation and reliability, since they show excellent stability in resistance values for ambient dry storage conditions.

The third concept was stabilization of Zn particles via microencapsulation using doped silicate binder and incorporation of pigment in doped hybrid silicate binders. The screening studies have showed excellent reproducibility for the electrical resistivity values and surface resistance values. The ambient storage had no effect on the observed surface resistance values. The degradation observed for this system at Aerospace Corporation, GSFC, and AFML provide guidance in selecting candidates for the future study of scaleup, validation, and reliability. The pigment/binder couples DS13N/SS-55, DS13N/DHS-1, and DS13N/DHS-2 are excellent candidate for these further studies. The high temperature doping should not receive any further consideration.

The flexible conductive concept showed an acceptable space environment stability for its use, but it can also be improved. The stability may need to be revisited again, because the formulation showed conflicting results. It charged beyond anticipated design values at cold

temperatures but showed acceptable RF loss behavior at room temperature. These results warrant further investigations. The processing of this coating can be a very tricky art. Primer chemistry poses situations that are not process friendly and interfere with the reproducible surface resistance values. The deposition process specifications development should go hand in hand with future "validation and reliability" analysis studies. The result demands that the program should devote the efforts to design a cured resin system that can act as a "leaky dielectric", and preferably with leakage paths. Such a program should be devoted to chemistry manipulations to achieve this goal of designing a "leaky flexible dielectric". It will fill a material technology gap and have considerable impact on space hardware design.

Among other concepts studied, no future efforts should consider tantalum oxide (Ta_2O_5). The pigment showed unacceptable degradation. The Eu_2O_3 based conductive concepts have acceptable electrical properties, but their space environment induced degradation behavior showed mixed results. One needs to keep this material in future studies to access Eu_2O_3 material technology maturity, only because of the flexibility that this pigment brings to electro-ceramist for tailoring surface resistances, as well as for processing options like plasma spray or thermal spray.

The Zn_2TiO_4 (ZOT) pigmented conductive concept showed great promise with acceptable behavior. The ZOT pigmented materials have been traditionally used in GEO successfully. Their use on long life missions has already been proven (e.g., missions like DSP). Our attempt to measure resistivity of exposed YB-71 or YB-71P revealed that the after exposure surface resistance of ZOT pigmented thermal control material system are ideal for the leakage current requirement [earlier communication with by Dr. Purvis[19]] for typical space hardware. In view of this background, the pigment/binder couples: ZOT/Phos sol, ZOT/SS-55, and ZOT/DHS-2 results are promising for tailoring surface resistance and their stability. The surface resistance manipulation of defected ZOT may also provide additional freedom in material design to electro-ceramists. Based on the results of the screening study, one must revisit solid-state chemistry, surface chemistry, and synthesis of titanate to tailor and stabilize defect structures that are hardened. Thus, chemical stabilization of ZOT may provide the sought "very long life" for reliable conductive TCMS.

Lastly, antimony doping efforts may provide cheaper and stable system that can mitigate charging phenomena, but higher $\Delta\alpha_S$ are to be expected for such materials system than the ZnO based or the ZOT based conductive TCMS. No further effort for such a material design is recommended. Future efforts are worthwhile only if the thermal designers are ready to compromise $\Delta\alpha_S$ for electrical performance at less cost. The Sb-doping precursor chemistry does pose market vagarities and inconsistent lot-to-lot variations. Future SEE program funding will be needed to address "source" related issues for such doping chemistry, if there is interest in Sb doping of TCMS pigments by thermal designers.

5. SUMMARY AND CONCLUDING REMARKS

The objective of this program was to address the material needs for two classes of materials: (1) black thermal control coating, where property goals are $\alpha_s \geq 0.90$, $\epsilon_N \simeq 0.90$, with space environment stability for long term use; and (2) low (α_s/ϵ_N) white thermal control coatings, where property goals are $\alpha_s \sim$ minimum as possible ($\simeq 0.18$, i,e., equivalent to Z-93); $\epsilon_N \simeq 0.90$ with space environment stability for long term use. The resistivity goal was 10^4-10^9 $\Omega/\square$ tailorable. Our screening study on suggested various material designs concept and the findings on them have resulted in the following important conclusions.

5.1 HIGH ABSORPTIVITY CONDUCTIVE TCMS

All electrically conductive TCMS designs proposed for high absorptivity applications met the program goals. New In-doped Black Glass material technology was developed along with three doped silicate binder systems. They provide a much needed flexibility in tailoring electrical performance characteristics without penalties in optical performance. These material technologies are recommended for further scaleup and validation, so that the following conductive material concepts can be offered as products in a cost-effective economic manner. The conductive concepts recommended for scaleup are: DBG-IP, DBG/DHS, MH55ICP, MH21SC/LO, MH41SCB/LO, D21S/LO, D21SC/LO, and D36SCB/LO. They all meet the above program goal, and showed acceptable ESD performance. (See Table 4-15)

5.2 LOW (α_s/ϵ_N) WHITE CONDUCTIVE TCMS

The white, low (α_s/ϵ_N) TCMS designs studied in this screening program fall into two categories. One is a baseline nonconducting TCMS design, and the other, the electrically conducting TCMS design. The following important conclusions can be drawn for each individual category found in Table 4-16.

5.2.1 Nonconducting Baseline TCMS

(1) The reformatted versions of baseline white TCMS were evaluated again. The S13GP/LO-1 and S13GP/LO-41 showed space environment stability approaching that of Z-93P.

(2) YB-71P showed more or less equal stability to that of YB-71. The Kasil 2130 is now recommended as a replacement in this formulation.

(3) Zn_2TiO_4 (ZOT) pigmented coating showed reversal in degradation with UV intensity; this should be investigated further, and may have consequences in material selection for thermal control for orbits like GEO.

(4) Eu_2O_3 showed promise as a simple BCC pigment. This can provide flexibility in material design for using doped binders. This material should receive more attention in future studies, to verify some conflicting data obtained in this screening study.

(5) Surface resistance values of YB-71 and YB-71P TCMS after irradiation are: 5.0E+07 to 8.0E+09 $\Omega/\square$.

5.2.2 Electrically Conductive TCMS (α_S/ϵ_N)

The following material technologies were developed as IR&D at IITRI to meet the goals of the screening program:

(1) Material technologies for new binder systems SS-55 and doped binders (DHS-1 and DHS-2) are now available. They have played a significant role in providing flexibility in tailoring surface resistances in the candidate TCMS along with no interference in optical performance of TCMS.

(2) Material and process technology for doped microencapsulation has been developed to provide new pigment DS13N. This provides a pigment that is essentially a ZnO grain coated with doped silica dielectric layer, that provides hardening for the space environment irradiation, along with freedom to tailor dopant levels and dielectric behavior of coating over the grain.

The above mentioned two material technologies need attention to mature to the required reproducibility and reliability. They are excellent material candidates for scaleup and validation efforts.

Along with these material technologies, the following are important findings on individual conductive material design concepts.

(1) The material concept Z-93CXY calls for the flash calcination of ZnO (SP-500) and use of doped binders. This provides an excellent approach to tailor desired surface resistance values in white TCMS. This material design shows acceptable stability to the space environment along with the required ESD properties. This may be the most amenable to scaleup material design concept, and is recommended for future validation and reliability studies. The pigment/binder couples to be studied are: ZnO(FC)/DHS-1 and ZnO(FC)/DHS-2. Future studies should also include characterization of the RF properties for these couples.

(2) The material concept Z-93SCXY calls for microencapsulated ZnO (SP-500) as a pigment and use of doped binders to tailor resistance values for white TCMS. Although this material design limits tailorability of electrical performance, the concept provides much needed RF properties along with ESD performance. The scaleup of this material concept is recommended. The concept needs to be considered in the future validation and reliability studies. The pigment/binder couples to be studied are: S13GP/DHS, S13GP/DHS-1, and S13GP/DHS-2.

(3) The material concept Z-93SCLMXY call for microencapsulation of ZnO (SP-500) with doped silicate binder as pigment and use of doped binders to tailor desired resistance values for white conductive TCMS. Tailorability of resistance values is excellent. The concept provides acceptable ESD performance. RF properties need attention during the next phase of study for this concept. The concept needs to be studied in the future scaleup, validation and reliability studies. The pigment/binder couples to be studied are DS13N/SS-55, DS13N/DHS-1, and DS13N/DHS-2.

(4) ZOT-based conductive TCMS should receive attention based on their performance in the screening studies. The solid-state chemistry of defect structures in ZOT needs attention in processing to improve on our ability to control them, so that tailorability of electrical properties become appealing. Such an understanding of ZOT can provide best, long life electrically conductive TCMS. The pigment/binder couples that should receive attention in scaleup, validation and reliability studies are: ZOT/Phos Sol, ZOT/DHS-2 and chemical stabilization of

ZOT surface defect structures.

(5) Eu_2O_3-based conductive material system provides the ability to use high dopant levels in a binder system. The results of the screening system indicate that Eu_2O_3 is the only non-semiconducting pigment that provides such a ability. Its performance is conflicting, and it remains to be seen if it can mature into an engineering quality material system. The use of Eu_2O_3 provides a different material design regime to electro-ceramists for tailoring properties, especially increase in dopant levels without worrying about its impact on band gap and a resultant impact on material properties. Hence, it is recommended for future scaleup, validation and reliability studies. The pigment/binder couples Eu_2O_3/DHS-1, Eu_2O_3/DHS-2, Eu_2O_3/SS-55 along with Eu_2O_3/2130 as baseline material design should be added to such studies.

(6)   DS13N/LO-XY, flexible conductive TCMS showed limited success in its ESD behavior. The TCMS still shows charging behavior at low temperatures. The future developments are now identified for implementation in the next phase of the program. The results demand that the program should devote efforts to design a cured resin system that can act as a "leaky dielectric", preferably with leakage paths. Such a program should be devoted to chemistry manipulations to achieve the goal of designing a "leaky flexible dielectric". It will fill a material technology gap for conductive flexibles and have a considerable impact on space hardware design.

6. RECOMMENDATIONS FOR FUTURE WORK

The work accomplished during this research program was to study thermal control design concepts to tailor resistivity. We have only finished the screening study on the selected conductivity tailoring concepts for two classes of TCMS (black and white). We have identified material design concepts and approaches that promise success or acceptable performance. This work can be transferred to the aerospace community only through a dedicated effort that can help to generate "reliability" and "long life" into the identified concepts along with a systematic approach and commitment to integrating these types of coatings on space hardware and space structures.

For the material design studies carried out here, overall 18 different material designs (pigment/binder couples) have been identified as very promising material concepts for scaleup, validation and reliability studies. [See section 4.5 and Chapter 5 for details] The pigment/binder couples for future effort are discussed in an earlier section along with promising materials and processes. Some of them need attention as a scaleup study to find economic processing routes that can provide reliability. The following materials related technology needs attention for such a scaleup and reliability study.

- Doped hybrid silicate binder technology/large batches

- Black Glass and doped Black Glass economic routes

- ZOT - Reproducibility issues and reliability, including but not limited to chemical stabilization of defect structures that promise "long life" along with electrical performance

- Eu_2O_3 - Bench scale manufacturing and reliability

- Microencapsulation via doped hybrid silicates

- Flash calcination facility development for "large batches"

- Laboratory synthesis capability for producing alkali silicates and/or polydimethyl siloxane polymers.

The testing community also needs to address the needs of test method development. The screening study identifies the following two needs for future development work.

- Laboratory test methods for electrical measurements that co-relates with ESD type test carried out at GSFC. Such methods need to mature for material certification needs (i.e., very cost effective and economical), and not as a research tool, or validation tool.

- Space environment simulation testing requirements of electrically conductive material systems. The role of conduction mechanisms in space environment induced degradation and synergism, and limits posed by them on effective feasible acceleration rates in the laboratory setup.

The above mentioned items are examples of some of the very broad areas that need to be addressed for the new electrically conductive TCMS to mature fully. At IITRI, we are also involved in integrating appealing material concepts on space hardware for the aerospace industry. It may be worthwhile to present some of the ideas on the use of these conductive thermal control material designs on space hardware, for "reliability" and "long life". In Figure 6-1, we have presented a synthesis of our ideas as a block diagram. Although the figure is fairly self-explanatory, the following discussion may provide insight into the system approach necessary to carry out systematic concurrent engineering exercise. The discussion and block diagram may also apply to all types of thermal control material technologies. Such a concurrent approach will help industry to build long term reliable space hardware and space structures.

The figure shows a dotted oblong-shaped zone called "Effects Zone" of the material system. We have listed here three important effects blocks for conductive material systems. The existence of effects depends on the material technology in question. For example, EL effects may not play a role for all material designs. Thus, one needs to be prudent in interpreting and using this flow diagram. The effect zone is fed by several legs which have several elements on them. Each element has either material technology name or testing technology name or system engineering issue listed in them that is relevant. Each leg is also identified with flow of information related arrows. A two-way flow usually provides an opportunity for concurrent engineering exercise which is needed for cost-effective, reliable integration, and design.

From this flow diagram one can easily see that we have just started to generate information that is required for such a reliable integration in this screening study. The information available for traditional nonconducting TCMS is also fragmentary. Efforts would be needed to generate information for each of these blocks, and industry/government may need
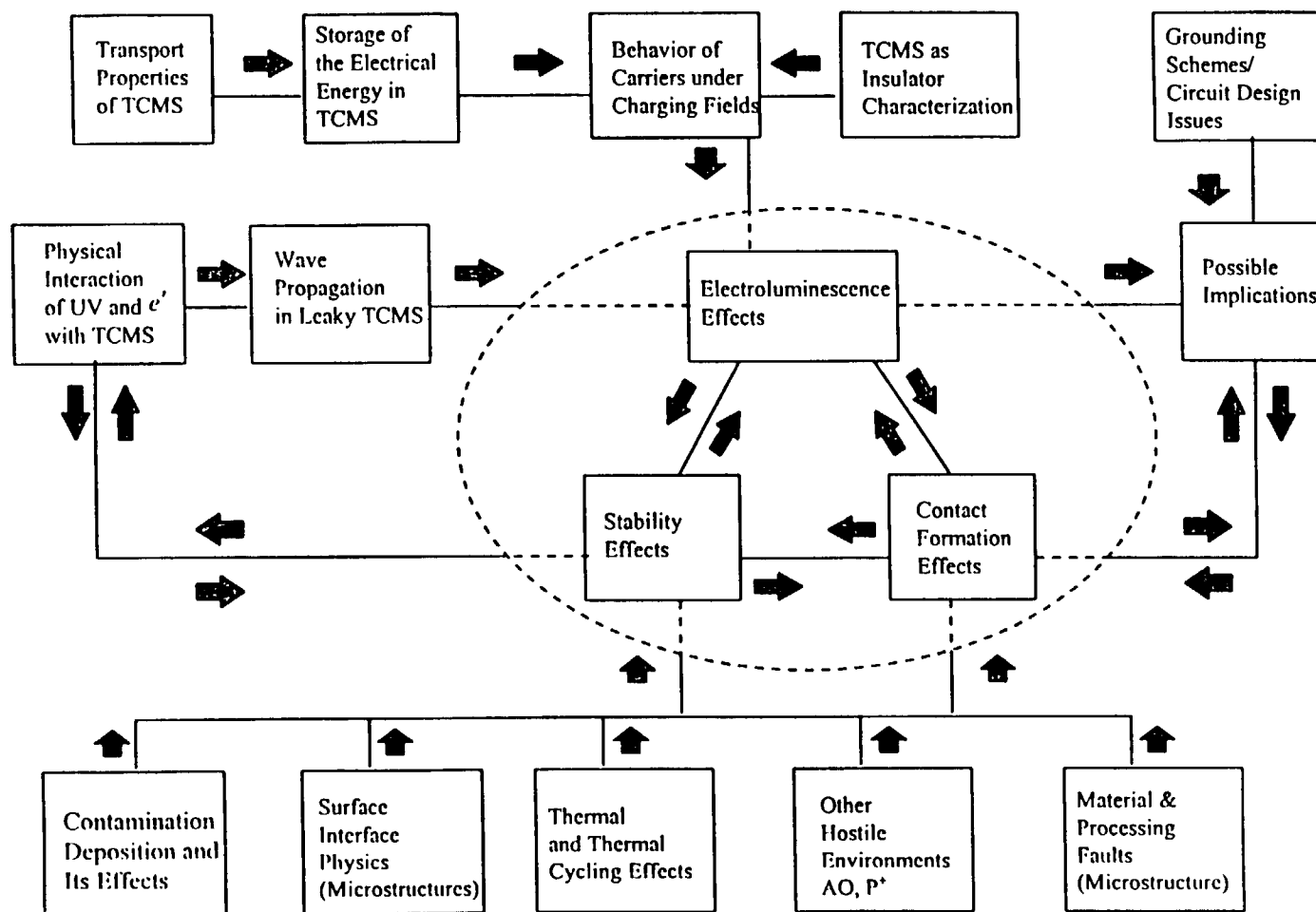
Figure 6-1. Synthesis of Ideas for the Use of Electrically Conductive TCMS on Space Hardware
for Reliability and Long Life.

to cooperate and emphasize sharing of analyzed information for "reliability". SEE Project Office can play a significant role towards these efforts.

In view of the suggested philosophy in the block diagram (Figure 6-1), the following are some of the areas that need to receive attention in future studies of the material design concepts identified here:

- AO resistance testing of conductive TCMS, and impact of AO on dopant chemistry

- UV-VUV-protons-vacuum testing

- Material processing/microstructural features and their role in tailoring electrical properties

- Role of surfaces and contact formations for each applicable material design (formulation) concept

- RF properties of applicable TCMS concepts

- Synergism in UV and e' as applied to semiconducting pigments and acceleration issues in laboratory simulation of space environment

- Thermal cycling effects/life with use of doped hybrid silicate binders

- Behavior of TCMS under charging fields/EL effects

- Electroluminescence of TCMS/if applicable

- Complete characterization of electrical behavior of TCMS [including response to pulses and secondary emission properties as needed in NASCAP charging codes]

- Role of contamination on functional aspects of the electrically conductive TCMS

- Lastly, survivability analysis of conductive TCMS for defense mission needs.

7. REFERENCES

1. L. A. Tiechman and B. A. Stein (Editors), "NASA/SDIO Space Environment Effects on Materials Workshop," Proceedings NASA-CP-3035, pp 621, 1989.

2. Dr. C. Purvis, NASA-LeRC, Private Communication, June 1993.

3. M. S. Deshpande, T. J. Curtis, and Y. Harada, "Conductive Thermal Control Material Systems for GPS Block IIR Hardware", IITRI Report No. C06789, February 1994.

4. S. C. Lockerby, M. V. Barsh, and D. L. Mossman, "ZOT-White Thermal Control Coating for Space Environment: Considerations," in 14th National SAMPE Tech. Conf., pp. 49-57, 1982.

5. A. Mon, C. Gonzales, R. Ross, L. Won, and T. O'Donnell, "Effects of Moisture on Zinc Orthotitanate (ZOT) Paint," JPL Report NPO-17742/7244, March 1991.

6. J. E. Gilligan, "Z-93 - An Estimate of Its Properties and Performance in the Galileo Mission," IITRI Report No. IITRI-C6429-1, January 29, 1979.

7. G. Barry Hillard, "Experimental Measurement of the Plasma Conductivity of Z-93 and Z-93P Thermal Control Paint," Draft Copy, shared by author, to be published as NASA-TM-106132, Private Communication, July 1993.

8. Prof. Hamburger, Cleveland St. Univ., "V-I Characteristics of Z-93 Type Materials," Private Communication, July 1993.

9. M. S. Deshpande, T. Curtis, "SOP on Sample Preparation and Drying Methods for Minimizing Moisture Contributions to the Volumetric and Surface Resistivity Measurements," IITRI Report No. IITRI-C06789, 1993.

10. J. E. Gilligan, Y. Yamauchi, R. E. Wolf, and C. Ray, "Electrically Conductive Paints for Satellites," AFML-TR-76-232, Final Report for Contract No. F33615-76-C-5250, Dec. 1976.

11. C. Hsieh, E. Metzler, G. Forsberg, and J. Cordaro, "Conductive White Thermal Control Paint for Spacecraft," Draft copy shared by Dr. C. Hsieh/G. Forsberg, SAMPE Paper, 1993.

12. G. Forsberg, Private Communication, 1993.

13. E. Metzer, C. Hsieh, "JPL - Material Specification: BS516165, Rev. A," May 25, 1994.

14. G. Forsberg, Private Communication, 1993.

15. M. S. Deshpande, "White Paper - Tailoring Electrical Conductive Thermal Control Materials Systems by Microstructural Engineering," submitted to Dr. Jim C. I. Chang, AFOSR/NASA H.Q., Nov. 1989.

16. Dr. C. Purvis, NASA-LeRC, Private Communication, June 1993.

17. D. S. McLachlan, M. Blasgkiewidz, and R. E. Newnham, "Electrical Resistivity of Composites: Effective Media Theory," J. Am. Ceram. Soc., 73 (8), 2187-2203, (1990).

18. M. S. Deshpande, T. Curtis, and Y. Harada, "Final Report: Conductive Thermal Control Material Systems Development for GPS: Block IIR Hardware," IITRI Report No. IITRI-AMCL-C06789, July 1994.

19. Dr. C. Purvis, NASA-LeRC, Private Communication, June 1994.

20. H. B. Garrett, "Charging of Spacecraft Surfaces," Chapter 7 in Handbook of Geophysics and Space Environment, A. S. Juna, Editor, AD/A167000, 1985.

21. R. H. Bogaard, P. D. Desai, S. K. El Rahaiby, and A. R. Olhoeft, "Selected and Recommended Electrical Properties of Oxides," CINDAS Letter Report, June 1992.

22. G. Zerlaut, J. E. Gilligan, "Stable White Thermal Control Coatings," IITRI Report No. IITRI-C6002-97, (1971).

23. J. C. Guillarman, "New Space Paints," CNES, Toulouse, France in 3rd European Symposium on Spacecraft Materials in Space Environment, p. 239, 1985.

24. Dr. T. Swank, P. Q. Corporation, R&D Laboratories, Private Communication (1993).

25. Dr. S. M. Chitale, Electro Science Laboratory - Manager R&D, Private Communication (1993).

26. L. Levy, D. Sarrail, and J. M. Signair, "Conductivity and Secondary Emission Properties of Dielectrics as Required by NASCAP," Proceeding of 3rd European Symposium on Spacecraft Materials in Space Environment, ESA-SP-232, Nov. 1985.

27. D. Vardin and M. J. Duck, "Conductive Coatings to Minimize the Charging," AERE, Chem. Div., Proc. of 3rd Europena Symposium on Spacecraft Materials in Space Environment, p. 125, 1985.

28. M. Dutat, J. Marco, and A. Paillous, "Space Environment Simulation to Test Satellite Thermal Control Coatings," Vol. 1, ESA-CR-1870, Confer. d'Etudes et de Rechercher de Toulouse, Toulouse, France, Report to Contract ESTEC-4577/81/NL-DG, 122 page, (1985).

29. G. Zerlaut and Y. Harada, "Stable White Coatings," IITRI Report No. IITRI-C207-25,

(1963).

30. Y. Harada, "Space Stable Thermal Control Coatings," IITRI Report No. IITRI-M06020-62, 1982.

31. G. A. Zerlaut, J. E. Gilligan, and N. A. Ashford, "Investigation of Environmental Effects on Coating for Thermal Control of Large Space Vehicles," NASA/MSFC Contract No. NAS8-5379, IITRI Final Report No. IITRI-U6002-97, October 8, 1971.

32. Keithley Instruments, Inc., Private Communication, June 1994.

33. J. Wilson, SPAR Aerospace Ltd., Private Communication, October 1995.

(This page intentionally left blank.)

APPENDIX A

SPACE ENVIRONMENTAL EXPOSURE OF IITRI TAILORABLE ELECTRICALLY CONDUCTIVE THERMAL CONTROL MATERIAL SYSTEMS

FINAL REPORT

THE AEROSPACE CORPORATION

Space Environmental Exposure of IITRI Tailorable Electrically Conductive Thermal Control Material Systems

Final Report

15 September 1996

Prepared by

M. MESHISHNEK
Mechanics and Materials Technology Center
Technology Operations

Prepared for

IIT RESEARCH INSTITUTE
Chicago, IL 60616

Contract No. C06804-S001-00

Engineering and Technology Group

THE AEROSPACE
CORPORATION
El Segundo, California

TECHNOLOGY OPERATIONS

The Aerospace Corporation functions as an "architect-engineer" for national security programs, specializing in advanced military space systems. The Corporation's Technology Operations supports the effective and timely development and operation of national security systems through scientific research and the application of advanced technology. Vital to the success of the Corporation is the technical staff's wide-ranging expertise and its ability to stay abreast of new technological developments and program support issues associated with rapidly evolving space systems. Contributing capabilities are provided by these individual Technology Centers:

Electronics Technology Center: Microelectronics, VLSI reliability, failure analysis, solid-state device physics, compound semiconductors, radiation effects, infrared and CCD detector devices, Micro-Electro-Mechanical Systems (MEMS), and data storage and display technologies; lasers and electro-optics, solid state laser design, micro-optics, optical communications, and fiber optic sensors; atomic frequency standards, applied laser spectroscopy, laser chemistry, atmospheric propagation and beam control, LIDAR/LADAR remote sensing; solar cell and array testing and evaluation, battery electrochemistry, battery testing and evaluation.

Mechanics and Materials Technology Center: Evaluation and characterization of new materials: metals, alloys, ceramics, polymers and composites; development and analysis of advanced materials processing and deposition techniques; nondestructive evaluation, component failure analysis and reliability; fracture mechanics and stress corrosion; analysis and evaluation of materials at cryogenic and elevated temperatures; launch vehicle fluid mechanics, heat transfer and flight dynamics; aerothermodynamics; chemical and electric propulsion; environmental chemistry; combustion processes; spacecraft structural mechanics, space environment effects on materials, hardening and vulnerability assessment; contamination, thermal and structural control; lubrication and surface phenomena; microengineering technology and microinstrument development.

Space and Environment Technology Center: Magnetospheric, auroral and cosmic ray physics, wave-particle interactions, magnetospheric plasma waves; atmospheric and ionospheric physics, density and composition of the upper atmosphere, remote sensing using atmospheric radiation; solar physics, infrared astronomy, infrared signature analysis; effects of solar activity, magnetic storms and nuclear explosions on the earth's atmosphere, ionosphere and magnetosphere; effects of electromagnetic and particulate radiations on space systems; space instrumentation; propellant chemistry, chemical dynamics, environmental chemistry, trace detection; atmospheric chemical reactions, atmospheric optics, light scattering, state-specific chemical reactions and radiative signatures of missile plumes, and sensor out-of-field-of-view rejection.

SPACE ENVIRONMENTAL EXPOSURE OF IITRI TAILORABLE ELECTRICALLY
CONDUCTIVE THERMAL CONTROL MATERIAL SYSTEMS

FINAL REPORT

Prepared by

M. Meshishnek
Mechanics and Materials Technology Center
Technology Operations

15 September 1996

Engineering and Technology Group
THE AEROSPACE CORPORATION
El Segundo, CA 90245-4691

Prepared for

IIT RESEARCH INSTITUTE
Chicago, IL 60616
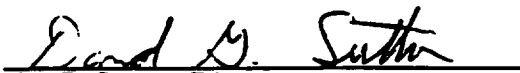
Contract No. C06804-S001-00
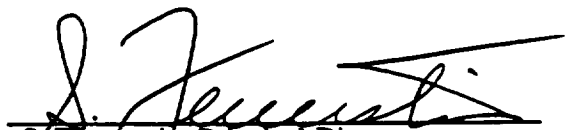
SPACE ENVIRONMENTAL EXPOSURE OF IITRI TAILORABLE ELECTRICALLY
CONDUCTIVE THERMAL CONTROL MATERIAL SYSTEMS

Prepared

M. Meshishnek

Approved

D. G. Sutton, Director
Materials Processing and
Evaluation Department

S. Feuerstein, Principal Director
Mechanics and Materials
Technology Center

Abstract

This report documents the results and data obtained from an extended space simulation test of 85 electrically conductive thermal control paints. This work was performed under a contract with the Illinois Institute of Technology Research Institute (IITRI) and was part of the effort funded by the National Aeronautics and Space Administration/Marshall Space Flight Center (NASA/MSFC) for IITRI to develop new advanced coatings for spacecraft. Part of the IITRI development process involved a simulated exposure of these coatings to ultraviolet (UV) radiation in vacuum. The test was designed to simulate an exposure of a material to low Earth orbit (LEO) conditions. Additionally, since many satellite systems are in polar orbits, a representative dose of electrons was also included in the test. The parameter used to measure the coating performance was the solar absorptance. This parameter was calculated from reflectance spectra measured on each sample pre- and posttest. The results of this test can be used to rank the performance of these materials and their stability to space exposure. While there were clear differences in the response of the various materials to this UV/electron exposure, most, if not all, materials performed well, showing little degradation in reflectance. A control specimen of Chemglaze A-267 polyurethane white paint degraded to a value expected from flight and previous ground test UV data. Contamination monitors included in the test matrix also indicated no appreciable changes due to contamination-radiation effects.

Contents

Table

1. Introduction

In 1994, the Illinois Institute of Technology Research Institute (IITRI) was selected by the National Aeronautics and Space Administration (NASA), under the Space Environment Effects (SEE) program, for a research award to develop new electrically conductive thermal control materials. Part of the award included funds for space environmental exposure testing of the newly developed materials. The Aerospace Corporation, because of its unique large-area exposure capability, was selected by IITRI to perform this testing under a subcontract. This unique capability allows the exposure of up to roughly 90 1 in. specimens in one test. This work was performed in July 1996.

2. Background

The initial purpose of the space environmental test was to evaluate the performance of new advanced electrically conductive thermal control paints, both white and black, under simulated ultraviolet (UV) radiation, typical of a low Earth orbit (LEO) exposure. The performance of the paints was measured against baseline industry standard nonconductive thermal control coatings developed by IITRI. These coatings have been used on several NASA, Department of Defense (DOD), and commercial spacecraft over the last 30 years and continue to be used today. Aerospace suggested that, in addition to the UV exposure, a small dose of electrons, typical of that encountered in a LEO polar orbit commonly used by weather satellites, be included to obtain more information regarding the space radiation stability of the new coatings. The IITRI contract called for a minimum of 500 h exposure of the coatings to an approximate 2 sun level of UV radiation.

3. Description

The candidate developmental coatings tested in the project consisted of 10 baseline nonconductive white thermal control paints and 35 new white thermal control paints exhibiting varying electrical conductivity. One sample of each of the baseline materials was tested, along with two samples of each of the new coatings. Three baseline nonconductive black coatings were submitted for test, along with six new black thermal control coatings exhibiting varying levels of electrical conductivity. Again, one sample of each of the baseline black materials was tested, along with two samples of each of the new black coatings. In addition, two samples of a white porcelain enamel were included in the test at IITRI's request. A sample of Chemglaze A-276 polyurethane white thermal control paint, an optical solar reflector (OSR) from Optical Coating Laboratories, Inc. (OCLI), and a fused silica substrate were also included in the exposure as controls and contamination monitors. The total sample complement was 88 specimens.

The conductive coatings were formulated from either doped pigments and nonconductive binders, from nonconductive pigments using doped binders, or from both doped pigments and doped binders. The coatings were both ceramic, silicate-based, and organic, silicone-based materials. Many of the coatings were derivatives of the existing industry standard IITRI white and black paints currently used on spacecraft.

4. Exposure Conditions

Since the agency funding the development of these new coatings was NASA, and the prime use of the coatings will be in LEO environments, UV radiation was identified as the main component of the space environment that should be simulated. Use of these coatings, in either elliptical or geosynchronous orbits, would require the addition of electrons and protons to the simulation. Both of these orbits have large fluxes of low and high energy particles that cause degradation of the coatings. However, many DOD and National Oceanic and Atmospheric Administration (NOAA) weather satellites, as well as other proposed NASA missions, use polar low earth orbits and hence encounter significant fluxes of electrons. Thus, modeling of the electron radiation environment, and the deposition of energy through the coating, was performed to assess the extent of this type of orbital exposure.

The orbit chosen for simulation was the one used by the Defense Meteorological Satellite Program (DMSP) and is roughly 460 nmi at an inclination of 90°. The model used for the electron environment was AE8 MAX. This model is tabulated in the Appendix. Energy deposition in the coatings was modeled using the code, Integrated Tiger Series (ITS), v. 3.0, available from Oak Ridge National Laboratory. This code was developed at Sandia National Laboratories. The code was run for the two baseline materials, Z-93P and S13GP/LO-1. Dose-depth profiles for a 10 year exposure in a DMSP orbit are given in the Appendix. These curves indicate that the surface dose in these two materials is approximately 25 Mrad for the 10 year exposure.

As the AE8 MAX model indicates, the energies of the electrons vary from less than 40 keV to over 6.5 MeV. The problem that must be solved is how to best simulate this on-orbit exposure in the laboratory using a variable monoenergetic electron beam. Use of the ITS code allows selection of electron energies and fluences that approximate the orbital dose-depth profile. Trial and error selection of energies and fluences are used to fit this profile. The results indicate that energies of 35 and 100 keV produce an adequate simulation. For a 10 year exposure, the corresponding fluences are $5.0 \times 10^{13}/cm^2$ and $8.0 \times 10^{13}/cm^2$, respectively. These results are shown on accompanying graphs included in the Appendix. The two-energy simulation is quite good for the first two mils of coating and is slightly better for the Z-93P material. Since most of the coatings are silicate based, this was the best choice.

The UV simulation source chosen was the xenon high pressure short arc, since it simulates the near-solar UV (200–400 nm) better than any other source. Vacuum UV radiation (<200 nm) was not included in the simulation although it is a significant part of the solar UV spectrum.

8

5. Test Method

Candidate test specimens were received from IITRI in labeled brown envelopes with the sample enclosed in heat-sealed inner plastic bags. Two samples of each material were received, coated on 15/16 in. aluminum disks, with a third specimen of each material on a 2×2 in. square aluminum substrate. Each sample was marked with a code on the back. For this test, only the disk samples were used. The UV-VIS-NIR reflectance of each sample to be tested was measured on a Perkin-Elmer Lambda-9 spectrometer equipped with a 6 in. Labsphere, Inc., Spectralon coated integrating sphere. The diffuse reflectance measurements were made using a 480 nm/min scan rate, 2 nm slit width, 1 s response, with the scan range being 250–2500 nm.

The reflectance spectra were background corrected and referenced to a NIST 2019d white tile diffuse reflectance standard. This procedure references the sample spectrum to a NIST perfect diffuser rather than to the Spectralon integrating sphere coating. Correction factors are calculated and applied to the sample spectrum from the measured NIST standard. The accuracy of the reflectance measurements is ± 2%. The reflectance curves are included in the Appendix to this report.

The calculation of the solar absorptance was made from the reflectance spectrum (assuming that the samples are opaque) over the range of measurement using the trapezoidal rule to approximate the integral in Eq. (1) below:

$$\alpha_s(\lambda_1,\lambda_2) = \frac{\int_{\lambda_1}^{\lambda_2} S_\lambda (1-\rho_\lambda)d\lambda}{\int_{\lambda_1}^{\lambda_2} S_\lambda \, d\lambda} \tag{1}$$

where

$\alpha_s(\lambda_1,\lambda_2)$ = solar absorptance calculated from λ_1 to λ_2 (250–2500 nm)

S_λ = solar air mass zero spectral irradiance curve (ASTM E490)

ρ_λ = measured wavelength-dependent hemispherical reflectance of sample

Inspection of the solar air mass zero spectral irradiance curve in ASTM E490 reveals that 3.9% of the sun's energy falls outside the wavelength region measured by the Lambda-9 spectrometer (250–2500 nm). Depending on the absorptive properties of the samples outside of the measurement range, an error of up to 0.039 (absolute) can be incurred in the solar absorptance calculations. To estimate this error, the calculations using Eq. (1) were also performed, assuming total sample absorption outside the 250–2500 nm measurement range. This worst-case calculation is important for these paints, since the silicate and silicone binders in them absorb strongly in the infrared (IR) region beyond 2500 nm. Similarly, these, like most materials, are also highly absorptive below 250 nm. These calculations indicate that, for the

white materials, the true solar absorptance is approximately +0.03 higher than the value in Table A-2 in the Appendix. There is little difference for the black coatings since they are highly absorptive.

A listing of the samples that were tested, along with their pigment and binder compositions, sample numbers, batch numbers, pretest solar absorptance (250–2500 nm), and corresponding data file is included in Table A-2 in the Appendix to this report.

The exposure test was conducted in the "Deathstar" Facility. A drawing of this facility is included in the Appendix. The chamber is cylindrical, with a 24 in. diameter and a 5 ft length. The chamber is equipped with a water or LN_2 cooled sample table and quartz-halogen IR bake-out heaters. The chamber is pumped with both a turbomolecular pump and a cryopump to achieve a baseline pressure in the mid to high 10^{-9} torr range. The facility is equipped with a data system that monitors temperature, pressure, and electron beam current. The radiation sources used in this test are the xenon solar simulator and the 120 keV electron flood gun. Temperature is measured via five K-type thermocouples, pressure is measured via a nude ion gauge, and the electron beam current is monitored using up to six Faraday cups. The data system integrates the dose rate to obtain the total fluence in real time and estimates the remaining time needed to reach a predetermined dose.

Prior to sample layout, the solar simulator was refurbished, and a new arc lamp was installed. The output UV beam is filtered to remove excess IR radiation with a water filter, cooled via a continuous purge of deionized water. The intensity of the solar irradiance at the table was measured via a calibrated spectroradiometer. Measurements were taken at 5 nm intervals from 200 to 400 nm. These readings were then integrated and normalized to the ASTM E409 solar air mass zero curve to obtain the UV solar intensity in suns, to the nearest 0.1 sun level. The intensity of the source was adjusted to give 3.0 suns at the sample table in the hottest area of the beam. A UV intensity distribution map was generated using a solar cell as an irradiance detector. Short-circuit current was measured for the cell at several locations on the sample table. These readings were then normalized to the highest value to give solar intensity values from 0 to 1. The total solar irradiance, or equivalent UV sun hours (EUVSH) on a sample, is therefore exposure time × 3.0 × intensity factor. The sample layout and the UV intensity map are included in the Appendix. A table of the test specimens with the EUVSH for each sample (Table A-2) is also included. The solar cell was included in the exposure test to monitor UV irradiance during the test and to allow adjustment of the UV source to maintain a 3.0 sun intensity as the lamp degraded.

The electron beam was adjusted for beam size and homogeneity prior to sample introduction. After the samples were laid out, the Faraday cups were added for monitoring of the beam homogeneity, the dose, and the dose rate. During the exposure, several variables are used to maintain the desired flux level: filament power, beam focus, beam divergence, and trap setting. All of these variables are dependent on the electron energy, which is held constant during an exposure. When the energy is changed, all the other variables must also be changed with it. This exposure involved two electrons energies: 100 and 35 keV.

After the reflectance of the samples was measured, they were laid out on the sample table in a hexagonal close-packing arrangement. The samples were arranged so that one each of the candidate new coatings was in the prime area of the UV beam; the corresponding sister sample of each coating was then placed in an area of lesser irradiance. The baseline samples were also placed in a prime area of the beam. Preference was given to the white coatings in the layout, which were placed in a better area of the beam. A videotape record was then started and was updated daily during the test. Roughly 1–3 min of videotape were recorded under varying lighting and exposure conditions.

10

After all necessary adjustments were made, the chamber was evacuated, and the data system was initiated. The samples were pumped on overnight. A plot of the chamber pressure during the test is included in the Appendix. The chamber was vented with GN_2 after roughly 16 h to add the Chemglaze A-276 sample. Pumping was then continued for another day, at which time chamber pressure was in the range of 5×10^{-8} torr, and the solar simulator was started. The chamber was then vented again briefly to adjust the position of the solar cell. Pumping and solar exposure were then continued. After about 4 days' exposure, the 100 keV electrons were started. These electrons were applied only during the normal working hours. After the fluence of $8.26 \times 10^{13}/cm^2$ was reached, the gun settings were changed to allow exposure to 35 keV electrons. This exposure was performed similarly to the first exposure, until the fluence of $5.18 \times 10^{13}/cm^2$ was reached. The test was then continued, with only the UV source running. After roughly 500 h exposure, the arc lamp was replaced, and the exposure was continued. Plots of the sample table temperature and the Faraday cup electron dose and dose rate are shown in the Appendix. The total exposure time for the solar simulator was 722 h. The test time is longer due to pump-down cycles and venting cycles for sample measurements.

At the end of the UV test exposure, the arc lamp was shut down, and the chamber was vented with GN_2. The samples were measured on the Lambda-9 in somewhat random order. The samples that had been in good light were measured first. The white coatings were also measured first. After measurement, the samples were returned to the chamber and held under nitrogen purge. The time that they were each exposed to air was roughly 10 min. The measurements took roughly 2 1/2 days. At the completion of a day's measurements, the chamber was pumped back down to store all samples overnight under vacuum.

After all measurements were taken, the samples were placed in labeled polyethylene bags, and each was stapled to the original brown paper bag for identification. Samples that indicated unusual patterns or colors were photographed.

6. Results

The values for the pretest and posttest solar absorptance are tabulated, together with the sample number and its pigment/binder composition. The solar intensity factor and the corresponding EUVSH values are included in Table A-2 in the Appendix. A curve showing the pretest and posttest reflectance spectrum is given for each sample tested. These 88 curves are presented in the Appendix. In all cases, the posttest reflectance curve is the dashed line.

As can be seen from the data in the table, most samples displayed very little degradation. However, some trends are apparent. The samples containing the DZS pigment generally exhibited higher degradation, as much as a factor of 10, relative to the ZnO pigmented materials. Similar results were seen with the materials that were pigmented with Ta_2O_5. Samples that were pigmented with ZOT or Eu_2O_3 gave mixed values for their degradation. By far, the least degradation was observed in the Z-93P derived materials. Another very positive result is the very small degradation observed with the baseline materials S13GP/LO-1 and S13GP/LO-41. These materials exhibited very small degradation equal to that seen with Z-93P.

One disturbing and peculiar result is the reversal of the degradation in YB-71 and YB-71P. In this exposure, YB-71 indicated three times the degradation of YB-71P, opposite that expected from previous test data.[*] These two samples were exposed side by side in the test; therefore, differences in exposure levels can be ruled out. The other very interesting result observed with only the ZOT-containing materials is the reverse correlation of degradation with solar exposure (EUVSH). That is, the samples exposed in a more intense area of the beam, and therefore received more EUVSH than their counterparts, exhibited less degradation. This result was observed with every ZOT pair tested and with no other pairs. The differences in degradation levels are significant.

The black samples essentially displayed no significant changes due to the exposure. There was also essentially no change for the OSR and the SiO_2 sample. The Chemglaze A-276 sample, which was only one-half exposed at the edge of the beam, gave a degradation, in alpha, of about 0.1 and turned brown, as expected. The white material showing the least degradation is ZnO(FC)/SS-55, and the white material displaying the most degradation is Ta_2O_5/2130 (RT).

---

[*] M. J. Meshishnek, C. S. Hemminger, and S. R. Gyetvay, *Space Environmental Exposure of IITRI White Thermal Control Paints*, TR-95(5904)-2, The Aerospace Corporation, El Segundo, CA (27 April 1995).

13

7. Discussion

Generally, one can conclude from this test that all of the candidate conductive thermal control coatings should perform well optically in a LEO environment. The qualifiers are that the effects of vacuum UV light have not been simulated and hence exposure to this radiation on orbit should increase the degradation. Also, the exposure time is only about 2100 EUVSH in this test, and if the degradation rates of these coatings are slow, they may not be near plateau of the solar absorptance. However, Z-93/Z-93-P has been shown to be stable on orbit. The inference is that these materials performed similarly to Z-93/Z-93P and therefore should also do well on orbit. In some LEO missions, the significant atomic oxygen flux could offset, via bleaching or erosion, UV damage in these materials, providing better overall performance. Previous work on similar coatings has indicated that the performance of materials in an elliptical or geosynchronous orbit may be very poor for those not containing ZnO based pigments.. This is due to the significantly higher charged particle fluxes in these orbits.

After only a few days exposure, and before the electrons were started, some samples (those containing Ta_2O_5 and DZS) began to show changes in color relative to the others on the video. A few samples also developed gray splotches and/or spots. The samples were photographed posttest. The markings did not disappear upon venting or even after air exposure during measurement. The appearance of blemishes or spots on some of the samples would indicate some problem in cleanliness, purity, or processing. These phenomena have been observed in previous IITRI tests, but the cause has never been discovered.

Previous extensive testing of Chemglaze A-276 in this laboratory indicates that a UV exposure of roughly 2000 EUVSH should give a value of 0.38 for solar absorptance. This value compares well with the value of 0.36 that was obtained in this test. Since the sample was only half lit at the edge of the UV beam, this correspondence in values is amazing. The lack of any significant degradation for the mirror or fused silica sample indicates that contamination was essentially nonexistent during this exposure. It would also strongly indicate that cross contamination from outgassing of the IITRI silicone-based materials is exceedingly small. However, surface analysis techniques would be required to validate this assertion, which was beyond the scope of this test.

There may be a possible explanation for the reversal of ZOT pigmented materials' degradation with EUVSH. If the degradation in the ZOT materials is mostly due to electrons and not UV, and if the effects of UV counteract or heal some of the damage due to the electrons, then extended UV exposure will restore the reflectance of the ZOT materials. If this is true, it has important implications for use of these materials in orbits with significant electron fluxes.

Errors involved in the repeatability of the reflectance measurements are estimated at ±0.002. It should be remembered, though, that the reflectance spectrum is measured from 250 to 2500 nm and hence does not include the entire solar spectrum. Thus, the values calculated for solar absorptance will be lower than actual or calorimetric numbers if the sample absorbs above 2500 nm or below 250 nm. This error is roughly + 0.03 in solar absorptance. Since most of the silicate and silicone paints absorb above 2500 nm, this + 0.03 should be added to all pretest and posttest numbers. The delta alpha numbers, however, should not change.

The error in the electron dose is less than 5%. The errors in the UV exposure factors are more difficult to quantify. Since the solar cell exposure area is about 3 in^2 and the test sample area is about 1 in^2, there

15

can be a significant intensity gradient across the area measured by the cell. Thus, the values for the intensity factors are probably only good to ±0.1. This is especially true for the samples placed in the dimmer areas of the beam. Intensity factors for samples that were in good light are probably accurate to ±0.02.

Currently, we do not have a method for determining the amount of recovery of reflectance due to air exposure. Experience has indicated that this recovery is small for the exposure times involved in these tests. In a test designed to screen or rank various candidate materials for relative space environmental stability, this recovery loses much of its importance. Since many materials exhibited significant degradation, wholesale bleaching of radiation damage can be discounted. However, the very small changes that were observed in the zinc oxide pigmented materials are perhaps suspiciously low. To explain this phenomenon, one has to invoke preferential bleaching of only zinc oxide based materials, which is highly unlikely. It should also be remembered that LDEF results indicated a degradation of only about 0.02 for Z-93.* Similar degradation has also been seen in some ground tests.* The very low degradation seen in the S13GP derived materials is somewhat more surprising since large changes in alpha were observed on LDEF. However, the materials that were flown on LDEF used a different silicone binder material, which may account for the difference in degradation. Previous work at Aerospace and other laboratories has shown that ground test data on S13G type materials often underpredicts the flight data. Table 1 presents some of the relevant flight and ground data on these paints:*

Table 1. Selected Flight and Ground Test Data on Z-93/S13G Materials

Paint	Data Type	Time	Delta α
Z-93	LDEF	69 months	0.017
Z-93	Pegasus II	2000 h	0.002
Z-93	Pegasus III	1000 h	0.002
Z-93	OSO III	1580 h	0.005
Z-93	Ground, UV	7067 h	0.02
Z-93P	Ground, UV	3100 h	0.039
Z-93	Ground, UV	5000 h	0.028
Z-93P	UV/e- (This work)	2100 h	0.007
S13G/LO	LDEF	69 months	0.32
S13G/LO-1	Ground, UV/e-	700 h	0.025
S13GP/LO-1	Ground, UV	3100 h	0.036
S13GP/LO-1	UV/e- (This work)	2100 h	0.01

---

* See footnote on page 13.

8. Conclusions

While nearly all of the new material systems tested have shown promise, it would seem that the materials utilizing Ta_2O_5 or DZS should probably be screened out in favor of the other materials. Mixed results seem to have been obtained with the Eu_2O_3 materials; hence, it would seem that they would warrant further investigation before they are discarded.

The conductivity measurements of these samples, pre- and postexposure to UV, are more important than the exposure testing. Careful unambiguous measurements need to be performed to assess the true conductivities of these candidate materials and their relative stability to the space environment. A detailed study of these properties and materials should provide data to focus on a few of the most promising materials for stable conductive thermal control paints.

Future work should focus on the stability of these materials to environments more severe than LEO, such as geosynchronous Earth orbit (GEO) or medium Earth orbit (MEO), where military spacecraft operate. Conductive coatings should prove invaluable for such military systems. These candidate developmental materials may go a long way to solving charging problems for these systems, provided that these materials retain their properties in these higher radiation environments.

Appendix

Test Data, Environmental Model, and
Analytical Predictions for the UV/Electron Exposure

Table A-1. Electron Environment Model AE8 MAX, DMSP Orbit, 460 nmi/90°

E1-E2,MEV	Flux/day>E1	Integral Flux	Flux/day<E1	%<E1
0	9.04E+10	2.50E+10	0.00E+00	.000000
0.04	6.54E+10	1.29E+10	2.50E+10	.276602
0.07	5.25E+10	1.01E+10	3.79E+10	.419328
0.1	4.24E+10	2.39E+10	4.80E+10	.531075
0.2	1.85E+10	1.02E+10	7.19E+10	.795507
0.3	8.29E+10	4.34E+09	8.21E+10	.908360
0.4	3.95E+09	1.85E+09	8.64E+10	.956378
0.5	2.09E+09	6.25E+08	8.83E+10	.976847
0.6	1.47E+09	4.10E+08	8.89E+10	.983762
0.7	1.06E+09	2.47E+08	8.93E+10	.988298
0.8	8.10E+08	1.58E+08	8.96E+10	.991031
0.9	6.52E+08	1.25E+08	8.97E+10	.992779
1	5.27E+08	1.86E+08	8.99E+10	.994162
1.25	3.41E+08	1.19E+08	9.00E+10	.996220
1.5	2.23E+08	7.69E+07	9.02E+10	.997537
1.75	1.46E+08	5.01E+07	9.02E+10	.998388
2	9.56E+07	3.17E+07	9.03E+10	.998942
2.25	6.39E+07	2.10E+07	9.03E+10	.999293
2.5	4.29E+07	1.45E+07	9.03E+10	.999525
2.7	2.84E+07	1.27E+07	9.04E+10	.999685
3	1.57E+07	9.94E+06	9.04E+10	.999826
3.5	5.79E+06	3.86E+06	9.04E+10	.999936
4	1.93E+06	1.36E+06	9.04E+10	.999979
4.5	5.71E+05	4.13E+05	9.04E+10	.999994
5	1.58E+05	1.23E+05	9.04E+10	.999998
5.5	3.51E+04	2.99E+04	9.04E+10	1.000000
6	5.13E+03	5.13E+03	9.04E+10	1.000000
6.5	0.00E+00	0.00E+00	9.04E+10	1.000000
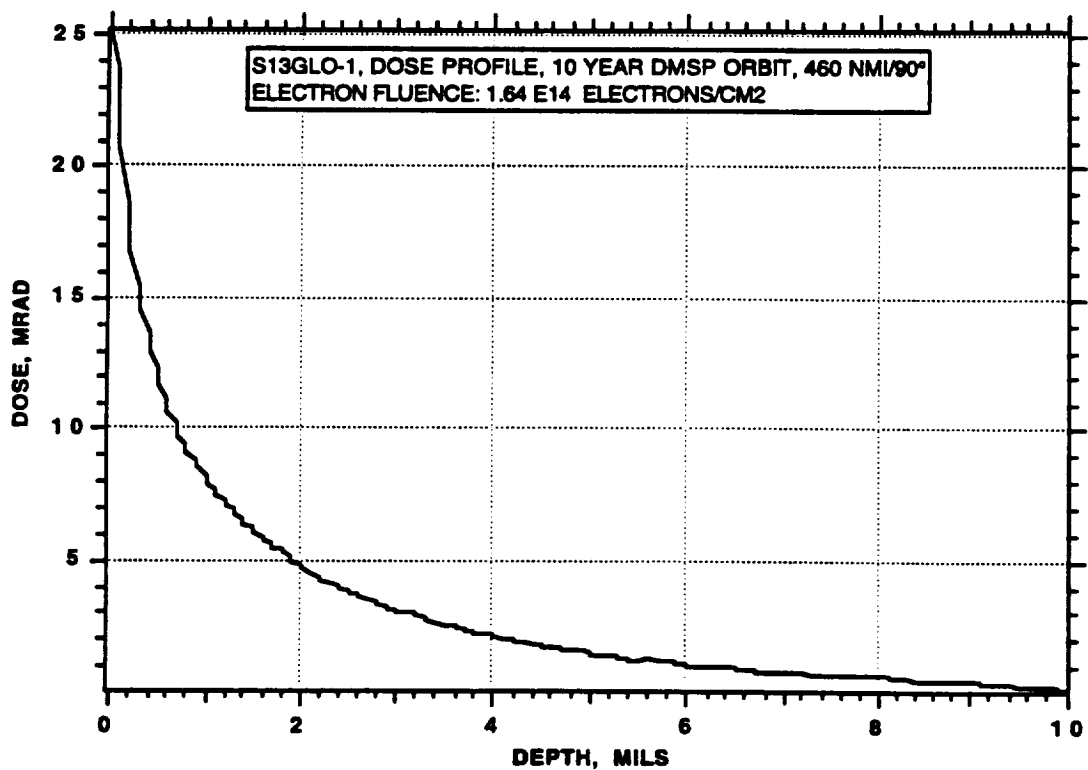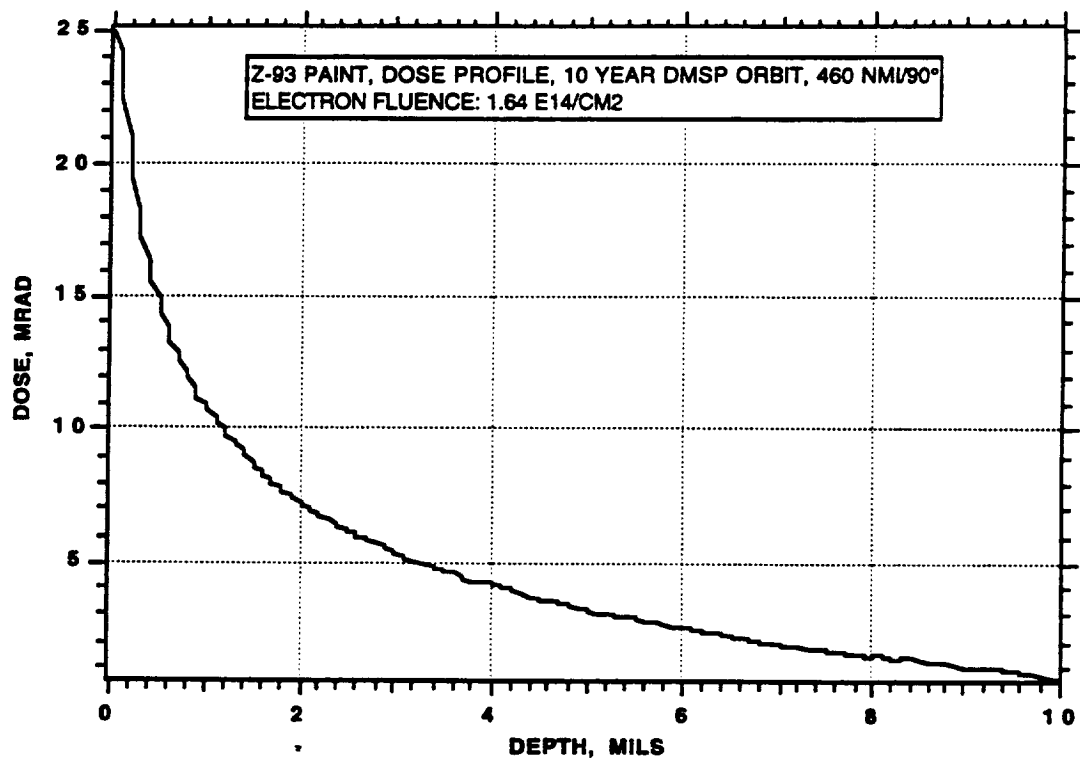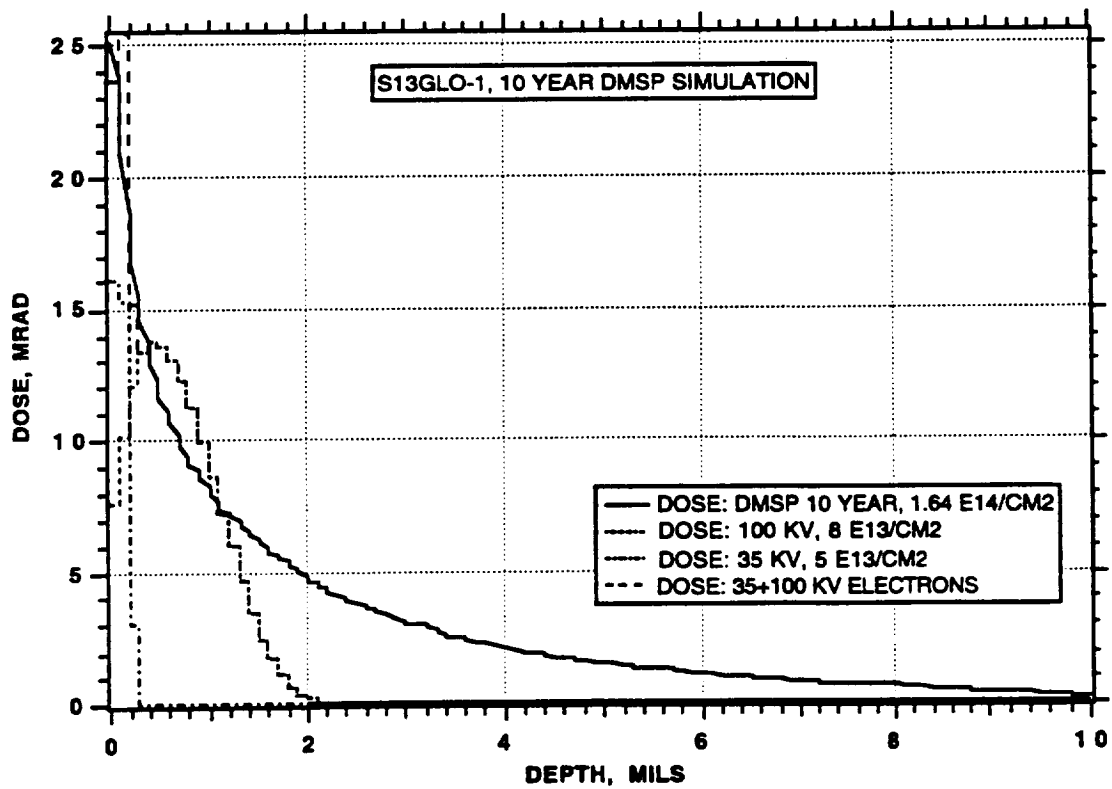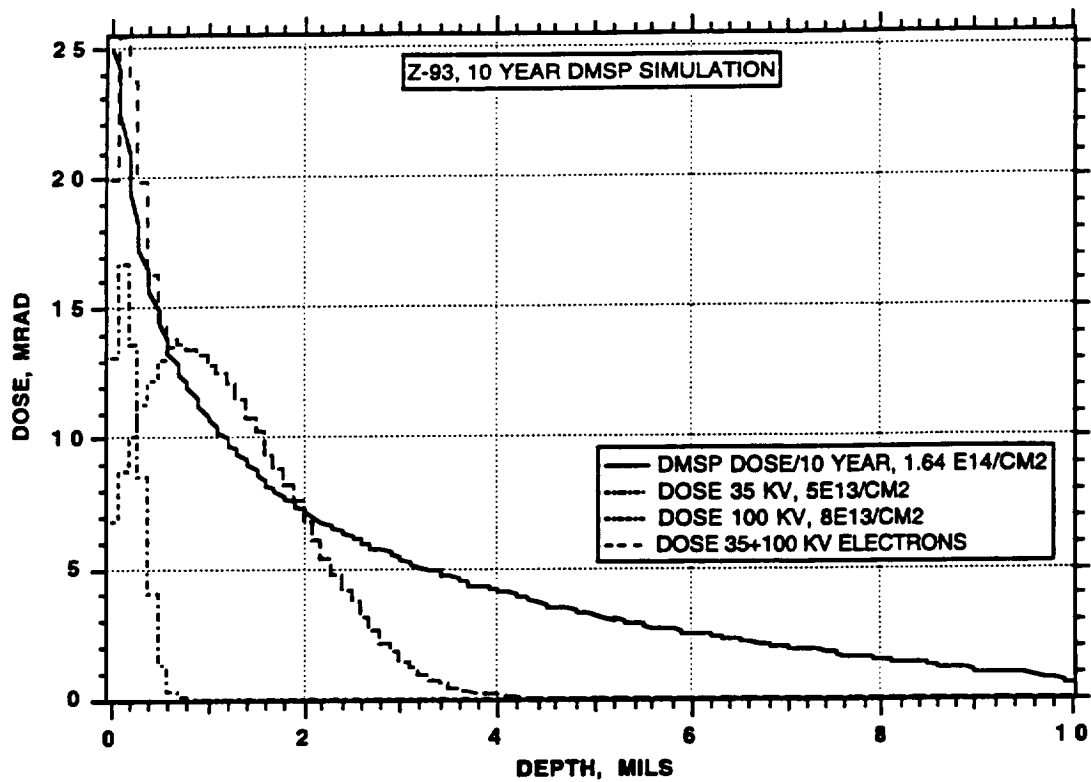
Z-93 PAINT, DOSE PROFILE, 10 YEAR DMSP ORBIT, 460 NMI/90°
ELECTRON FLUENCE: 1.64 E14/CM2

S13GLO-1, DOSE PROFILE, 10 YEAR DMSP ORBIT, 460 NMI/90°
ELECTRON FLUENCE: 1.64 E14 ELECTRONS/CM2

Z-93, 10 YEAR DMSP SIMULATION

DOSE, MRAD (y-axis)
DEPTH, MILS (x-axis)

DMSP DOSE/10 YEAR, 1.64 E14/CM2
DOSE 35 KV, 5E13/CM2
DOSE 100 KV, 8E13/CM2
DOSE 35+100 KV ELECTRONS

S13GLO-1, 10 YEAR DMSP SIMULATION

DOSE, MRAD (y-axis)
DEPTH, MILS (x-axis)

DOSE: DMSP 10 YEAR, 1.64 E14/CM2
DOSE: 100 KV, 8 E13/CM2
DOSE: 35 KV, 5 E13/CM2
DOSE: 35+100 KV ELECTRONS

23

Table A-2. IITRI Test Samples

Coating	Pigment	Binder	Batch #	Sample #	File #	Pretest Alpha	File #	Posttest Alpha	Delta Alpha	UV Factor	EUVSH
ZOT	ZOT #98790	None	98790	ZOT#1	DS40801	0.079	DS41801	0.104	0.025	0.96	2079
Z-93P	Zinc Oxide	Kasil 2130	U-347	HX-10	DS40802	0.133	DS41840	0.14	0.007	0.96	2079
YB-71	ZOT #98790	PS-7	U-348	HW-3	DS40803	0.107	DS41826	0.14	0.033	0.98	2123
YB-71P	ZOT #98790	Kasil 2130	U-376	IM-27	DS40804	0.112	DS41831	0.123	0.011	0.98	2123
S13GP/LO-1	S13GP	LO-1	U-310	IJ-27	DS40805	0.167	DS41814	0.177	0.01	0.99	2144
S13GP/LO-41	S13GP	LO-41	U-276	HC-20	DS40806	0.149	DS41810	0.156	0.007	0.97	2101
DZSS/LO-41	DZSS	LO-41	U-208	GH-8	DS40807	0.077	DS41832	0.243	0.166	0.97	2101
ZOTS/LO-41	ZOT #98790	LO-41	U-343	28	DS40608	0.133	DS41837	0.196	0.063	0.95	2058
Eu2O3/2130	Eu2O3	Kasil 2130	U-352	IF-18	DS40809	0.092	DS41808	0.12	0.028	0.93	2014
Eu2O3/LO-41	Eu2O3	LO-41	U-403	IS-19	DS40810	0.136	DS41813	0.178	0.042	0.96	2079
ZnO(FC)/2130	ZnO(FC)	Kasil 2130	U-321	HM-14	DS40811	0.148	DS41835	0.154	0.006	0.97	2101
ZnO(FC)/2130	ZnO(FC)	Kasil 2130	U-321	HM-15	DS40812	0.148	DS41845	0.149	0.001	0.8	1733
ZnO(FC)/SS-55	ZnO(FC)	SS-55	U-322	HF-26	DS40813	0.147	DS41830	0.144	-0.003	0.98	2123
ZnO(FC)/SS-55	ZnO(FC)	SS-55	U-322	HF-27	DS40814	0.146	DS41846	0.144	-0.002	0.7	1516
ZnO(FC)/DHS-1	ZnO(FC)	DHS-1	U-323	HG-23	DS40815	0.157	DS41847	0.164	0.007	0.64	1386
ZnO(FC)/DHS-1	ZnO(FC)	DHS-1	U-323	HG-22	DS40816	0.149	DS41825	0.156	0.007	0.99	2144
ZnO(FC)/DHS-2	ZnO(FC)	DHS-2	U-327	HL-14	DS40817	0.139	DS41819	0.141	0.002	0.99	2144
ZnO(FC)/DHS-2	ZnO(FC)	DHS-2	U-327	HL-25	DS40818	0.146	DS41850	0.146	0	0.86	1863
S13GP/2130	S13GP	Kasil 2130	NA	FM-18	DS40819	0.131	DS41805	0.148	0.017	0.97	2101
S13GP/2130	S13GP	Kasil 2130	NA	FM-21	DS40820	0.129	DS41851	0.137	0.008	0.78	1689
S13GP/SS-55	S13GP	SS-55	U-405	IU-22	DS40821	0.125	DS41823	0.14	0.015	1	2166
S13GP/SS-55	S13GP	SS-55	U-405	IU-25	DS40822	0.127	DS41852	0.134	0.007	0.78	1689
S13GP/DHS-1	S13GP	DHS-1	U-279	GS-16	DS40823	0.147	DS41803	0.153	0.006	0.94	2036
S13GP/DHS-1	S13GP	DHS-1	U-279	GS-17	DS40824	0.142	DS41854	0.148	0.006	0.8	1733
S13GP/DHS-2	S13GP	DHS-2	U-328	HH-20	DS40825	0.13	DS41806	0.155	0.025	0.96	2079
S13GP/DHS-2	S13GP	DHS-2	U-328	HH-27	DS40826	0.134	DS41856	0.146	0.012	0.91	1971
S13N/SS-55	S13N	SS-55	U-260	GR-3	DS40827	0.115	DS41811	0.141	0.026	0.97	2101
S13N/SS-55	S13N	SS-55	U-260	GR-7	DS40828	0.114	DS41848	0.119	0.005	0.82	1776
S13N/DHS-1	S13N	DHS-1	U-317	HE-19	DS40929	0.15	DS41815	0.173	0.023	0.98	2123
S13N/DHS-1	S13N	DHS-1	U-317	HE-23	DS40830	0.143	DS41867	0.16	0.017	0.85	1841
S13N/DHS-2	S13N	DHS-2	U-329	HI-14	DS40831	0.134	DS41820	0.161	0.027	0.99	2144
S13N/DHS-2	S13N	DHS-2	U-329	HI-27	DS40832	0.132	DS41829	0.16	0.028	1	2166
DZS/2130	DZS	Kasil 2130	T-244	DK-11	DS40833	0.077	DS41727	0.132	0.055	0.96	2079
DZS/2130	DZS	Kasil 2130	T-244	DK-19	DS40834	0.081	DS41844	0.122	0.041	0.78	1689
DZS/SS-55	DZS	SS-55	U-207	FO-20	DS40835	0.107	DS41821	0.204	0.097	0.95	2058
DZS/SS-55	DZS	SS-55	U-207	FO-23	DS40836	0.1	DS41804	0.185	0.085	0.83	1798
DZS/DHS-1	DZS	DHS-1	U-278	GQ-4	DS40837	0.075	DS41816	0.202	0.127	0.95	2058
DZS/DHS-1	DZS	DHS-1	U-278	GQ-8	DS40838	0.078	DS41853	0.163	0.085	0.8	1733
DZS/DHS-2	DZS	DHS-2	U-331	HK-15	DS40839	0.086	DS41812	0.189	0.103	0.96	2079
DZS/DHS-2	DZS	DHS-2	U-331	HK-27	DS40840	0.089	DS41802	0.18	0.091	0.94	2036
DS13N/SS-55	DS13N	SS-55	U-315	P-26	DS40841	0.138	DS41807	0.173	0.035	0.96	2079
DS13N/SS-55	DS13N	SS-55	U-315	P-27	DS40842	0.137	DS41859	0.153	0.016	0.94	2036
DS13N/DHS-1	DS13N	DHS-1	U-316	S-7	DS40843	0.123	DS41849	0.133	0.01	0.7	1516
DS13N/DHS-1	DS13N	DHS-1	U-316	S-1	DS40844	0.124	DS41824	0.161	0.037	0.99	2144
DS13N/DSH-2	DS13N	DHS-2	U-330	HJ-20	DS40845	0.122	DS41868	0.128	0.006	0.8	1733
DS13N/DSH-2	DS13N	DHS-2	U-330	HJ-27	DS40846	0.129	DS41818	0.149	0.02	0.98	2123
ZOT/SS-55	ZOT #98790	SS-55	U-379	IN-13	DS40847	0.117	DS41836	0.156	0.039	0.95	2058
ZOT/SS-55	ZOT #98790	SS-55	U-379	IN-15	DS40848	0.112	DS41865	0.156	0.044	0.8	-1733
ZOT/DHS-2	ZOT #98790	DHS-2	U-378	IO-21	DS40849	0.125	DS41841	0.158	0.033	0.95	2058

Table A-2. IITRI Test Samples

Coating	Pigment	Binder	Batch #	Sample #	File #	Pretest Alpha	File #	Posttest Alpha	Delta Alpha	UV Factor	EUVSH
ZOT/DHS-2	ZOT #98790	DHS-2	U-378	IO-28	DS40850	0.122	DS41862	0.181	0.059	0.8	1733
ZOT/Phos. Sol.	ZOT #98790	Phos. Sol.	U-377	HT-21	DS40851	0.131	DS41842	0.149	0.018	0.94	2036
ZOT/Phos. Sol.	ZOT #98790	Phos. Sol.	U-377	HT-22	DS40852	0.128	DS41860	0.151	0.023	0.8	1733
Eu2O3/SS-55	Eu2O3	SS-55	U-353	ID-11	DS40853	0.087	DS41817	0.138	0.051	0.99	2144
Eu2O3/SS-55	Eu2O3	SS-55	U-353	ID-20	DS40854	0.1	DS41857	0.126	0.026	0.8	1733
Eu2O3DHS-2	Eu2O3	DHS-2	U-381	II-12	DS40855	0.093	DS41822	0.158	0.065	1	2166
Eu2O3/DHS-2	Eu2O3	DHS-2	U-381	II-15	DS40856	0.076	DS41855	0.108	0.032	0.7	1516
Ta2O5/2130	Ta2O5	Kasil 2130/RT	U-358	IG-11	DS40857	0.163	DS41828	0.304	0.141	0.96	2079
Ta2O5/2130	Ta2O5	Kasil 2130/RT	U-358	IG-25	DS40858	0.18	DS41869	0.286	0.106	0.6	1300
Ta2O5/2130	Ta2O5	Kasil 2130/HT	U-358	IG-12	DS40859	0.165	DS41833	0.232	0.067	0.96	2079
Ta2O5/2130	Ta2O5	Kasil 2130/HT	U-358	IG-22	DS40860	0.181	DS41866	0.231	0.05	0.66	1430
Ta2O5/SS-55	Ta2O5	SS-55/RT	U-359	IH-19	DS40861	0.137	DS41838	0.222	0.085	0.92	1993
Ta2O5/SS-55	Ta2O5	SS-55/RT	U-359	IH-20	DS40862	0.143	DS41863	0.226	0.083	0.76	1646
Ta2O5/SS-55	Ta2O5	SS-55/HT	U-359	IH-17	DS40863	0.149	DS41843	0.199	0.05	0.89	1928
Ta2O5/SS-55	Ta2O5	SS-55/HT	U-359	IH-27	DS40864	0.167	DS41861	0.216	0.049	0.79	1711
DS13NSC/LO-41	DS13NSC	LO-41	U-334	HQ-10	DS40865	0.161	DS41839	0.278	0.117	0.9	1949
DS13NSC/LO-41	DS13NSC	LO-41	U-334	HQ-12	DS40866	0.163	DS41858	0.239	0.076	0.69	1495
Sb Doped	ZnO+Sb+Zn2SnO4	Kasil 2130	U-252	GE-9	DS40867	0.141	DS41864	0.159	0.018	0.67	1451
Sb Doped	ZnO+Sb+Zn2SnO4	Kasil 2130	U-252	GE-8	DS40868	0.144	DS41834	0.176	0.032	0.95	2058
Porcelain Enamel			NA	PE-1	DS40869	0.259	DS41809	0.284	0.025	0.92	1993
Porcelain Enamel			NA	PE-2	DS40870	0.265	DS41870	0.289	0.024	0.5	1083
MH21IP	Black Glass	Kasil 2130	U-284	GZ-21	DS40871	0.981	DS41886	0.981	0	0.93	2014
MH21S/LO	Black Glass	LO-1	U-360	HZ-18	DS40872	0.982	DS41883	0.982	0	0.96	2079
D21S/LO	Cosmic Black WB-500	LO-1	T-023	BA-8	DS40873	0.98	DS41887	0.98	0	0.85	1841
DBG-IP	In Doped Black Glass	Kasil 2130	U021	EO-7	DS40874	0.974	DS41882	0.975	0.001	0.95	2058
DBG-IP	In Doped Black Glass	Kasil 2130	U021	EO-8	DS40875	0.973	DS41879	0.974	0.001	0.55	1191
MH55IC	Black Glass, Graphite	Kasil 2130	S-024	Z-9	DS40876	0.94	DS41876	0.939	-0.001	0.94	2036
MH55IC	Black Glass, Graphite	Kasil 2130	S-024	Z-10	DS40877	0.942	DS41880	0.941	-0.001	0.6	1300
DBG/DHS	Doped Black Glass	DHS-1	U-283	GU-13	DS40878	0.958	DS41885	0.957	-0.001	0.93	2014
DBG/DHS	Doped Black Glass	DHS-1	U-283	GU-14	DS40879	0.956	DS41874	0.956	0	0.67	1451
MH21SC/LO	Black Glass, Graphite	LO-1	U-166	FD-20	DS40880	0.963	DS41884	0.964	0.001	0.93	2014
MH21SC/LO	Black Glass, Graphite	LO-1	U-166	FD-21	DS40881	0.965	DS41878	0.965	0	0.55	1191
MH41SC/LO	Black Glass/B4C	LO-1	U-053	FD-5	DS40882	0.951	DS41881	0.95	-0.001	0.93	2014
MH41SC/LO	Black Glass/B4C	LO-1	U-053	FD-6	DS40883	0.95	DS41873	0.953	0.003	0.64	1386
D21SC/LO	Cosmic Black, Graphite	LO-1	T-026	BJ-1	DS40884	0.955	DS41877	0.956	0.001	0.94	2036
D21SC/LO	Cosmic Black, Graphite	LO-1	T-026	BJ-2	DS40885	0.956	DS41875	0.957	0.001	0.55	1191
A-276	TiO2/SiO2	Polyurethane	NA	MM-1	NM11306	0.261	DS41871	0.364	0.103	0.94	2036
OCLI OSR	Coated SiO2/Al	NA	NA	OSR	DS47711	0.065	DS41872	0.064	-0.001	0.85	1841
Fused Silica	Fused SiO2	NA	NA	SiO2	DS42006	0.069	DS41888	0.069	0	0.5	1083

D E A T H S T A R
Space Environment Effects Chamber

A276 OSR

15/16"

HX-10 IO-21 HT-21 IH-17 HL-25 FM-21 IU-25 SiO2

HM-14 IN-13 28 IH-19 HQ-10 GQ-8 GS-17 II-15 FD-21

HF-26 IM-27 GH-8 IG-12 GE-8 Z-9 HH-27 ID-20 HQ-12 EO-8

HG-22 HW-3 DK-11 IG-11 HI-27 BJ-1 P-27 HT-22 IH-27 Z-10

HL-14 HI-14 FO-20 II-12 IU-22 S-1 FD-5 IO-28 IH-20 GE-9

IJ-27 HE-19 GQ-4 ID-11 HJ-27 EO-7 FD-20 IN-15 IG-22 PE-2

HC-20 GR-3 HK-15 IS-19 HZ-18 GU-13 HE-23 HJ-20 IG-25

Solar cell

FM-18 HH-20 P-26 IF-18 GZ-20 BA-8 GR-7 S-7 BJ-2

ZOT GS-16 PE-1 HM-15 HF-27 HG-23 GU-14

HK-27 FO-23 DK-19 FD-6

88 samples

Layout Size:
Approx 9.5x11"

Sample Layout for IITRI UV Test.

27

15/16"

0.94 0.94 0.89 0.86 0.78

0.97 0.97 0.98 0.96 0.96 0.95 0.94 0.91 0.79 0.69 0.52

0.99 0.99 0.98 0.95 1.0 1.0 0.98 0.93 0.89 0.79 0.76 0.57 0.46

0.97 0.97 0.96 0.96 0.96 .096 0.93 0.85 0.80 0.67 0.51

0.94 0.91 0.83 0.78 0.64

87 samples

Layout Size:
Approx 9.5x11"

UV Intensity Map for IITRI Test

Sample Chamber Pressure/Nude Ion Gauge

Sample Table Temperature, TC#1

Sample Table Temperature, TC#3

Electron Dose Rate, Faraday Cup #3

Electron Dose Rate, Faraday Cup #5

31

Electron Dose Profile

Electron Dose Profile

Test Sample Reflectance Plots

Sample: ZOT#1, ZOT #98790, Pellet

Sample: HX-10, Z-93P

33

Sample: HW-3, YB-71

Sample: IM-27, YB-71P

Sample: IJ-27, S13GP/LO-1

Sample: HC-20, S13GP/LO-41

35

Sample: GH-8, DZSS/LO-41

Sample: 28, ZOTS/LO-41

Sample: IF-18, Eu2O3/2130

Sample: IS-19, Eu2O3/LO-41

Sample: HM-14, ZnO(FC)/2130

Sample: HM-15, ZnO(FC)/2130

38

Sample: HF-26, ZnO(FC)/SS-55

Sample: HF-27, ZnO(FC)/SS-55

39

Sample: HG-23, ZnO(FC)/DHS-1

Sample: HG-22, ZnO(FC)/DHS-1

Sample: HL-14, ZnO(FC)/DHS-2

Sample: HL-25, ZnO(FC)/DHS-2

41

Sample: FM-18, S13GP/2130

Sample: FM-21, S13GP/2130

42

Sample: IU-22, S13GP/SS-55

Sample: IU-25, S13GP/SS-55

Sample: GS-16, S13GP/DHS-1

Sample: GS-17, S13GP/DHS-1

Sample: HH-20, S13GP/DHS-2

Sample: HH-27, S13GP/DHS-2

45

Sample: GR-3, S13N/SS-55

Sample: GR-7, S13N/SS-55

46

Sample: HE-19, S13N/DHS-1

Sample: HE-23, S13N/DHS-1

47

Sample: HI-14, S13N/DHS-2

Sample: HI-27, S13N/DHS-2

48

Sample: DK-11, DZS/2130

Sample: DK-19, DZS/2130

Sample: FO-20, DZS/SS-55

Sample: FO-23, DZS/SS-55

50

Sample: GQ-4, DZS/DHS-1

Sample: GQ-8, DZS/DHS-1

51

Sample: HK-15, DZS/DHS-2

Sample: HK-27, DZS/DHS-2

52

Sample: P-26, DS13N/SS-55

Sample: P-27, DS13N/SS-55

53

Sample: S-7, DS13N/DHS-1

Sample: S-1, DS13N/DHS-1

54

Sample: HJ-20, DS13N/DHS-2

Sample: HJ-27, DS13N/DHS-2

Sample: IN-13, ZOT/SS-55

Sample: IN-15, ZOT/SS-55

Sample: IO-21, ZOT/DHS-2

Sample: IO-28, ZOT/DHS-2

57

Sample: HT-21, ZOT/Phos. Sol

Sample: HT-22, ZOT/Phos. Sol

Sample: ID-11, Eu2O3/SS-55

Sample: ID-20, Eu2O3/SS-55

59

Sample: II-12, Eu2O3/DHS-2

Sample: II-15, Eu2O3/DHS-2

Sample: IG-11, Ta2O5/2130 RT cure

Sample: IG-25, Ta2O5/2130 RT cure

61

Sample: IG-12, Ta2O5/2130 HT cure

Sample: IG-22, Ta2O5/2130 HT cure

62

Sample IH-19, Ta2O5/SS-55 RT cure

Sample IH-20, Ta2O5/SS-55 RT cure

63

Sample IH-17, Ta2O5/SS-55 HT cure

Sample: IH-27, Ta2O5/SS-55 HT cure

Sample: HQ-10, DS13NSC/LO-41

Sample: HQ-12, DS13NSC/LO-41

Sample: GE-9, Sb Doped

Sample: GE-8, Sb Doped

66

Sample: PE-1, Porcelain Enamel

Sample: PE-2, Porcelain Enamel

67

Sample: GZ-21, MH21IP

Sample: BA-8, D21S/LO

Sample EO-7, DBG-IP

Sample: EO-8, DBG-IP

69

Sample: GU-13, DBG/DHS-1

Sample: GU-14, DBG/DHS-1

Sample: Z-9, MH55-IC

Sample: Z-10, MH55-IC

71

Sample: FD-20, MH21SC/LO

Sample: FD-21, MH21SC/LO

Sample: FD-5, MH41SC/LO

Sample: FD-6, MH41SC/LO

Sample: BJ-1, D21SC/LO

Sample: BJ-2, D21SC/LO

Sample: MM-1, Chemglaze A-276

Sample: OSR 1, OCLI Coated Optical Solar Reflector

Sample: Fused Silica Witness

APPENDIX B

ULTRAVIOLET DEGRADATION STUDY
OF IITRI'S SIX WHITE PAINTS

SWALES AEROSPACE

Ultraviolet Degradation Study

of

IITRI's Six White Paints

5 Aug 1996

Prepared by:

Wanda C. Peters
Senior Thermal Coatings Engineer
NASA - Goddard Space Flight Center
Mail Code 724.2 - SAI
Greenbelt, Maryland 20771
301-286-5147 (Office)
301-286-1704 (Fax)

SWALES
AEROSPACE
Contamination and Thermal Coatings Department

ULTRAVIOLET DEGRADATION STUDY OF SIX WHITE PAINTS

INTRODUCTION

In July 1995, six (6) formulations of thermal control white paints were selected for ultraviolet (UV) degradation testing by the NASA, Goddard Space Flight Center's (GSFC) Thermal Engineering Branch, Code 724. The purpose of the test was to obtain information on the UV stability of the paints. UV stability is critical to the space application of thermal control white paints. The results of the test will assist in the qualification of the white paints for space flight use. This report contains the test conditions and results of the UV degradation study.

BACKGROUND

The space program uses white paints for controlling temperatures of spacecraft systems and calibrating space optical systems. Some of the commonly used white paints, for space flight missions, are Z93, S13GLO-1, and YB71 (ZOT). These three paints are manufactured by Illinois Institute of Technology Research Institute (IITRI). In 1989, IITRI began researching a replacement for the binder, potassium silicate (PS-7), that was currently used in the formulation of the three white paints. The company, Osram Sylvannia, that supplied IITRI with the binder had discontinued the manufacture of PS-7 for economic reasons. Therefore, a replacement for the binder was necessary because of DOD and NASA current use of the three white paints.

In 1991, the Space and Missile Systems Center's Chief Engineer's Office funded IITRI to reformulate the white paints. The reformulate paints were designated as: Z93P, S13GP/LO-1, and YB71P. At the completion of the first phase of the reformulation process, IITRI with support from Wright Laboratory, Aerospace Corporation, NASA and industry performed test to requalify the reformulated paints. Information obtained from the testing of the reformulated paints were presented at the Aerospace Corporation/Space and Missile Systems Center Industry Briefing for IITRI White Thermal Control Coating Requalification in October 1994. As a result of the requalification process, IITRI decided to replace PS-7 with a potassium silicate binder called Kasil 2130. The requalification process also revealed that further reformulation and testing of the paints was needed. Replacement of Kasil 2130 in Z93P and S13GP/LO-1 gave similar test results to test results of the original formulations. Whereas, testing showed that substitution of Kasil 2130 in YB71P was not an acceptable replacement. During this period, IITRI was also developing a series of conductive paints called Z93SC55 and Z93SC1655.

The IITRI white paints requalification process revealed the need for further simulated space environment testing. Therefore NASA - GSFC's Thermal Engineering Branch, Code 724, requested ultraviolet testing of all newly formulated and reformulated white paints.
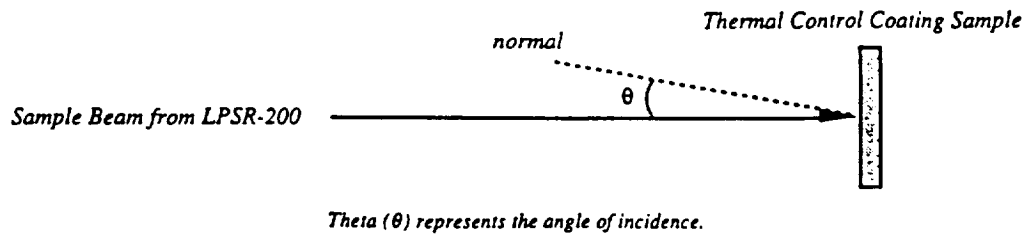
normal

Sample Beam from LPSR-200

θ

Thermal Control Coating Sample

Theta (θ) represents the angle of incidence.

Diagram 1: Reflectance Measurement's Angle of Incidence

The Geir-Dünkle DB-100 InfraRed Reflectometer was used to measure the normal emittance of the samples. The Geir-Dünkle DB-100 measures the normal emittance of the surface from 5 to 40 microns. This measurement is made at room temperature.

The Perkin-Elmer Lambda 9 NearIR/Vis/UV Spectrophotometer was used to measure all "in-situ" measurements. The Lambda 9 measures the reflectance of the sample's surface from 250 to 2500 nm. The light source of the Lambda 9 passes through the sapphire chamber window in order to measure the reflectance of the sample while in the Multisedes chamber. Therefore, these reflectance measurements made by the Lambda 9, while the samples are located in the Multisedes sample chamber, are influenced by the reflectance of the sapphire window.

The Spectrolab X25 solar simulator was used to simulate solar UV light. The X25 solar simulator has a two sun capability. The level of sun intensity radiated by the X25 is used to determines the number.of equivalent sun hours (ESH) during a specified period of time. The IL1700 Radiometer is used to measure the sun intensity level of the X25 solar simulator. From the IL1700 reading, the ESH is calculated as a function of time.

AZ Technology's LPSR-200 was used to perform the post-vacuum reflectance measurements and solar absorptance calculations. The solar absorptance is calculated in accordance with ASTM E903-82. The LPSR-200 measures the reflectance from 250 to 2500 nm of the sample's surface at a 15° angle of incidence. The instrument measurement accuracy is +/. .02 for both α and ε_n values.

TEST PROCEDURE

Before the sample is placed in the Multisedes chamber, the sample's reflectance is measured using the AZ Technology's LPSR-200 to obtained the pre-vacuum solar absorptance value. The reflectance data is graphed and the solar absorptance (α) is calculated and recorded. The normal emittance (ε_n) of the sample is measured and recorded.

At the completion of the pre-vacuum measurements, the samples are then placed into the Multisedes sample chamber. The samples are mounted against a metal cold plate, which has a water reservoir located directly behind the metal plate. The water reservoir is used to maintain the Multisedes' samples at room temperature. When the test samples are all mounted, the chamber is sealed. The following diagram denotes the positions of the samples location in the Multisedes.

2

TEST OBSERVATIONS

Date	Comments
1 Aug 1995	• Six white paint control and test samples' reflectances, solar absorptances, and normal emittances were measured.
7 Aug 1995	• Pre-testing photographs were taken of the control and test samples.
10 Aug 1995	• Test samples were placed in the Multisedes chamber.
16 Aug 1995	• Began "in air" reflectance measurements of six test samples.
17 Aug 1995	• Completed "in air" measurements. • Began evacuating the Multisedes system.
18 Aug 1995	• Began 0 ESH "in-situ" reflectance measurements.
21 Aug 1995	• Completed 0 ESH "in-situ" measurements. • Began UV exposure.
2 Sep 1995	• Made 505 ESH "in-situ" reflectance measurements.
14 Sep 1995	• Made 1010 ESH "in-situ" reflectance measurements.
15 Sep 1995	• Back-filled chamber with gaseous nitrogen and removed samples from Multisedes. Made 1010 ESH reflectance, solar absorptance, and normal emittance measurements. • Visual Examination of Samples: - YB71P*2 showed signs of discoloration (tanish beige) - Z93SC1655 showed discoloration (beige)
15 Sep 1995	• Continued UV exposure of samples.
18 Sep 1995	• UV exposure was halted for recalibration of the lamp and optics.
21 Sep 1995	• S13GP/LO-1 sample was removed for reflectance measurement. During correlation of the data measured on September 15, 1995, it was discovered that this sample had not been measured. The test had reached 1137 ESH of UV exposure. • The S13GP/LO-1 sample was replaced in the chamber and the system was evacuated.

TEST RESULTS

The solar absorptance (α) and normal emittance (ε_n) values of the samples were measured at 0 ESH, 1010 ESH, 2041 ESH, 3042 ESH and 4331 ESH. These measurement were made after removal of the test samples from the Multisedes chamber.

Table 2 contains the measured α and ε_n values of the non-conductive white paint samples. Table 3 contains the measured α and ε_n values of the conductive white paint samples. Table 4 contains the $\Delta\alpha$ of the six white paints. Reflectance curves of each paint test sample are located in the appendix. A comparison curve of the change in solar absorptance over time is also located in the appendix.

Table 2 - Non-Conductive White Paints

Sample Description	Optical Properties	0 ESH	1010 ESH	2041 ESH	3042 ESH	4331 ESH
S13GP/LO-1 (Kasil 2130)	α	.181	.186*	.184	.195	.192
	ε_n	.922	No Measurement	.919	.917	.918
Z93P (Kasil 2130)	α	.172	.175	.178	.181	.189
	ε_n	.930	.931	.929	.928	.929
YB71P*2 (Kasil 2130)	α	.141	.259	.393	.524	sample removed
	ε_n	.933	.932	.927	.928	sample removed

* S13GP/LO-1 was inadvertently not measured at 1010 ESH. The sample was removed at 1137 ESH for measurement.

Table 3 - Conductive White Paints

Sample Description	Optical Properties	0 ESH	1010 ESH	2041 ESH	3042 ESH	4331 ESH
Z93SC55 (T251)	α	.140	.151	.157	.175	.177
	ε_n	.935	.929	.930	.931	.929
Z93SC55 (EI-2)	α	.151	.164	.177	.200	.207
	ε_n	.934	.928	.926	.928	.929
Z93SC1655 (EK-20)	α	.128	.220	.261	.304	sample removed
	ε_n	.935	.926	.927	.925	sample removed

4

APPENDIX

Z93P White Paint (Primer Z93P; Binder Kasil 2130)
UV Degradation Test

0 ESH	a = .172	e = .934	01 Aug 1995
1010 ESH	a = .175	e = .931	15 Sep 1995
2040 ESH	a = .178	e = .929	18 Oct 1995
3042 ESH	a = .181	e = .928	09 Nov 1995
4331 ESH	a = .188	e = .929	28 Feb 1996

Reflectance

Wavelength (nm)
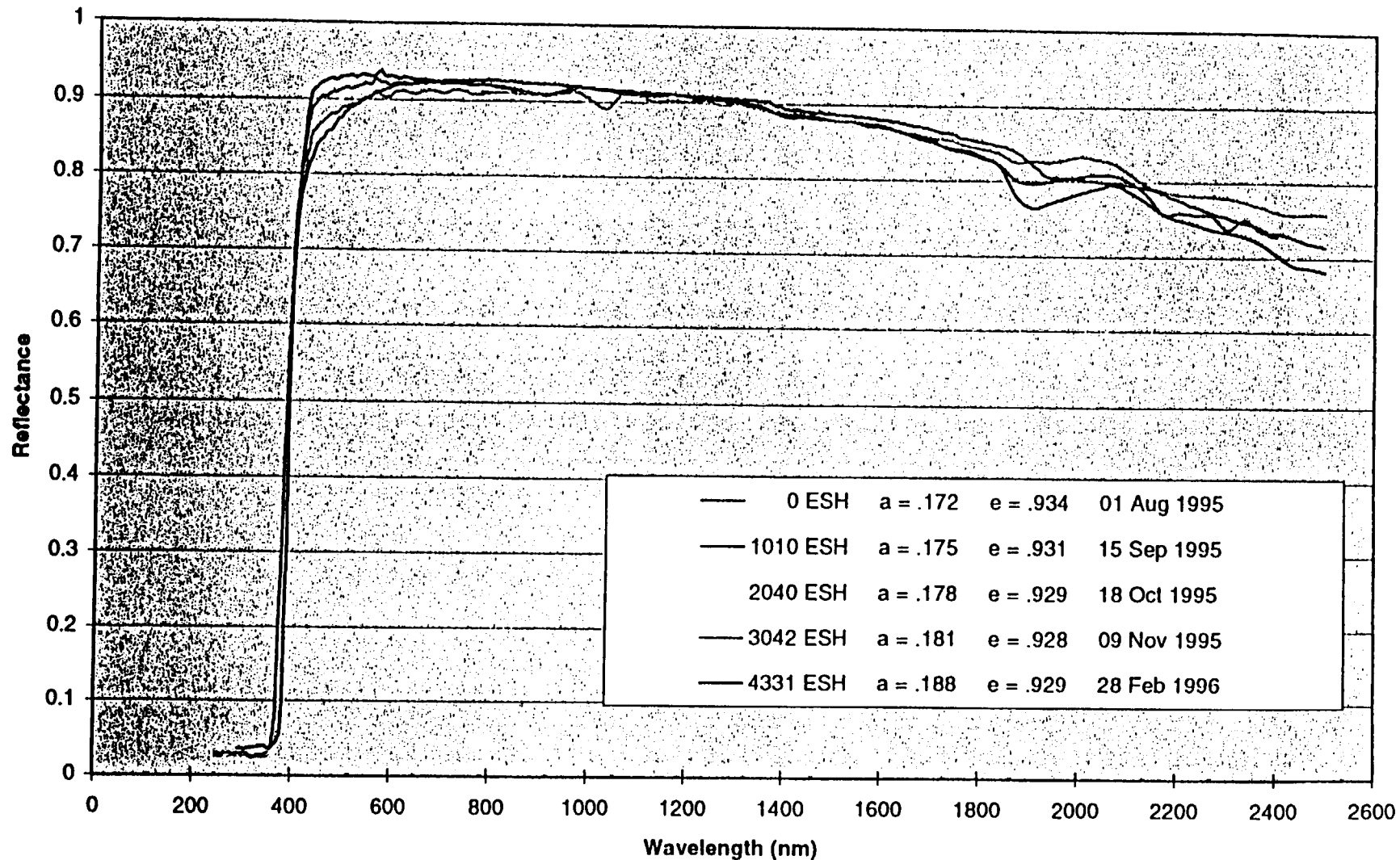
Z93SC55 (T-251) Conductive White Paint
UV Degradation Test

—— 0 ESH	a = .140	e = .935	01 Aug 1995
—— 1010 ESH	a = .151	e = .929	15 Sep 1995
2040 ESH	a = .157	e = .930	18 Oct 1995
—— 3042 ESH	a = .175	e = .931	09 Nov 1995
—— 4331 ESH	a = .177	e = .929	28 Feb 1996

Wavelength (nm)
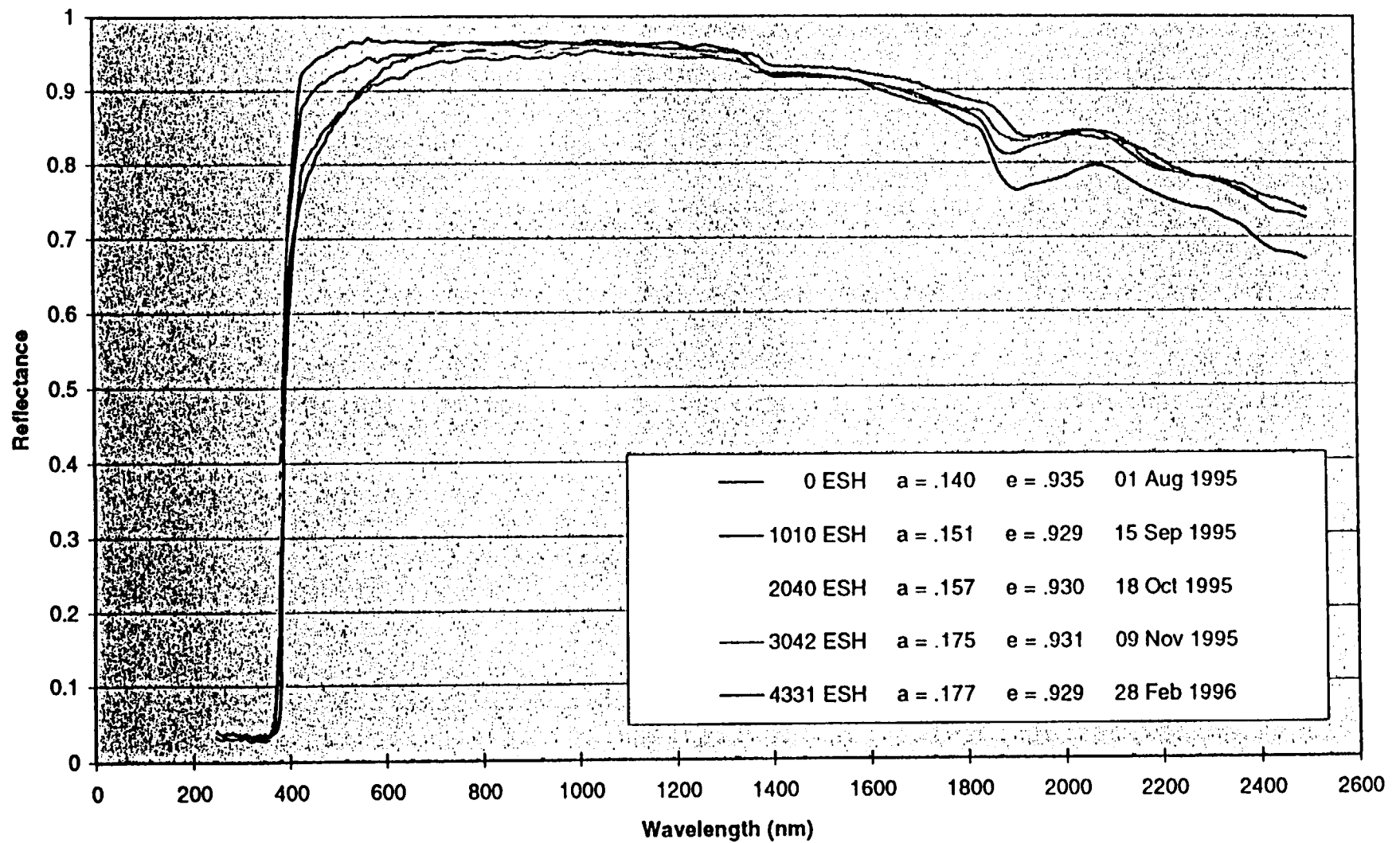
Z93SC1655 #EK-20 Conductive Paint
UV Degradation Test

0 ESH	a = .129	e = .934	01 Aug 1995
1010 ESH	a = .220	e = .926	15 Sep 1995
2040 ESH	a = .261	e = .927	18 Oct 1995
3042 ESH	a = .304	e = .925	09 Nov 1995

Reflectance

Wavelength (nm)

8
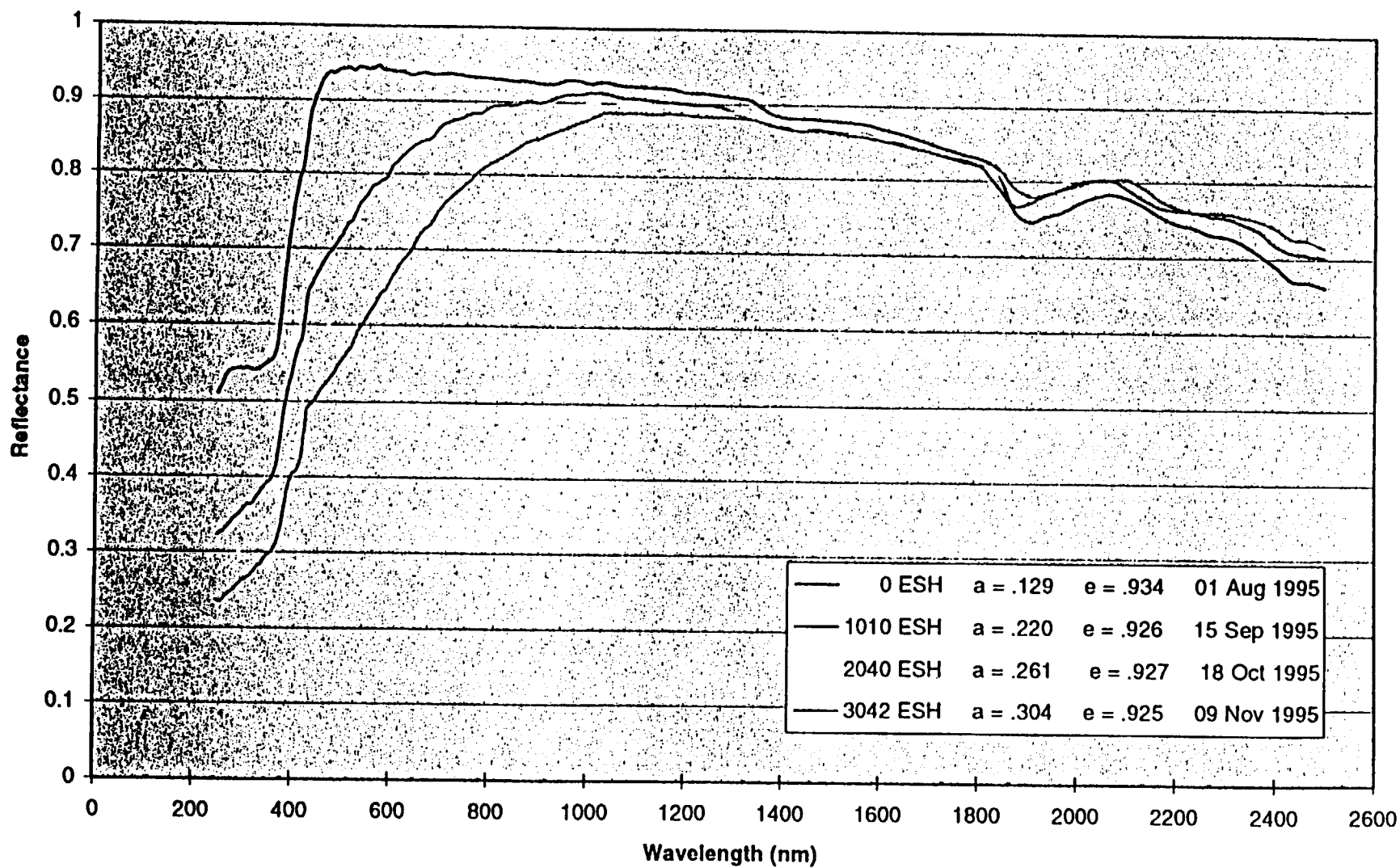
APPENDIX C

ULTRAVIOLET DEGRADATION STUDY
OF IITRI ELECTRICALLY CONDUCTIVE
THERMAL CONTROL FORMULATIONS

SWALES AEROSPACE

Ultraviolet Degradation Study

of

IITRI Electrically Conductive

Thermal Control Formulations

15 October 1996

Prepared by:

Wanda C. Peters

Senior Thermal Coatings Engineer
NASA - Goddard Space Flight Center
Mail Code 724.2 - SAI
Greenbelt, Maryland 20771
301-286-5147 (Office)
301-286-1704 (Fax)

SWALES
AEROSPACE
Contamination and Thermal Coatings Department

Table Of Contents

ULTRAVIOLET DEGRADATION STUDY OF IITRI ELECTRICALLY CONDUCTIVE THERMAL CONTROL FORMULATIONS

INTRODUCTION

In February 1996, fourteen (14) conductive conceptual formulations of thermal control coatings were submitted for ultraviolet (UV) degradation testing by the NASA, Goddard Space Flight Center's (GSFC) Thermal Engineering Branch, Code 724. The fourteen paint samples were developed and supplied by IIT Research Institute (IITRI). The purpose of the test was to obtain information on the UV stability of the paints. UV stability is critical to the space application of thermal control white paints. The results of this test will assist in determining future qualification test. This report contains the test conditions and results of the UV degradation study.

TEST INFORMATION

Test Requestor:	NASA - Marshall Space Flight Center (MSFC)
Project:	None
Type of Test:	Ultraviolet Degradation Study
Test Duration:	1000 Equivalent Sun Hours (ESH)
Results Required:	Reflectance, Solar Absorptance, Normal Emittance
Special Instructions:	Measure reflectance, solar absorptance, and normal emittance "in-situ" reflectance measurement, removal and thermal-optical properties measurements at 1000 ESH.

SAMPLE DESCRIPTION

Table 1: White Coatings.

Concept Name	Batch #	Pigment	Binder
S13GP/DHS-2	HH-19	S13GP	DHS-2[a]
Sb Doped	GE-12	ZnO + Sb doped Zn_2SnO_4[b]	Kasil 2130
S13N/DHS-2	HI-21	S13N[c]	DHS-2
DS13N/LO-51	JX-16	DS13N	MHS/LO stripped polydimethyl siloxane
DS13N/DHS-2	HJ-25	DS13N	DHS-2
DS13N/SS-55	P-31	DS13N[d]	SS-55[e]
ZnO(FC)/DHS-2	HL-26	ZnO (FC)	DHS-2
Eu_2O_3*/SS-55	HD-26	Eu_2O_3[f]	SS-55
ZOT/SS-55	IW-19	ZOT # 98790	SS-55

Table 2: Black Coatings

Concept Name	Batch #	Pigment	Binder
D36SCB/LO	JV-17	Cosmic black-WB-500, B_4C	MHS/LO stripped polydimethyl siloxane
MS41SCB/LO	U-356 IC-20	Black glass/B_4C	MHS/LO stripped polydimethyl siloxane
MH21SC/LO	GX-16	Black glass, graphite fiber, Graphite 9035	MHS/LO stripped polydimethyl siloxane
MH55-IC	Z-6	Black glass, Graphite 9035, ZnO	Kasil 2130
DBG-IP	GTM-29	Doped black glass (Indium doped)	Kasil 2130

Sample Size: One inch diameter circular disc

Control samples are maintained for comparison purposes at the completion of the UV degradation test. The control samples are stored in a dark environment to prevent UV exposure from fluorescent lights.

TEST INSTRUMENTATION

The GSFC Thermal Engineering Branch's Multisedes Vacuum System was used for the UV degradation studies. The system consists of two sorption pumps, a sputter-ion pump, and a sample chamber. The sample chamber consists of 16 testing positions. The system has the capability of testing a maximum of 14 samples at one time. The remaining two testing positions contain a reference mirror and a blank.

The Beckman DK-2 Spectrophotometer was used to perform the pre-vacuum reflectance measurements. The DK-2 measures the reflectance from 290 to 2400 nm of the sample's surface at a 20° angle of incidence. A computer program is used to calculate the solar absorptance in accordance with ASTM E903-82.

Theta (θ) represents the angle of incidence.

Diagram 1: Reflectance Measurement's Angle of Incidence

The Geir-Dünkle DB-100 InfraRed Reflectometer was used to measure the normal emittance of the samples. The Geir-Dünkle DB-100 measures the normal emittance of the surface from 5 to 40 microns. This measurement is made at room temperature.

The Perkin-Elmer Lambda 9 NearIR/Vis/UV Spectrophotometer was used to measure all "in-situ" measurements. The Lambda 9 measures the reflectance of the sample's surface from 250 to 2500 nm. The light source of the Lambda 9 passes through the sapphire chamber window in order to measure the reflectance of the sample while in the Multisedes chamber. Therefore, these reflectance measurements, while the samples are located in the Multisedes sample chamber, are influenced by the reflectance of the sapphire window.

The Spectrolab X25 solar simulator was used to simulate solar UV light. The X25 solar simulator has a two sun capability. The level of sun intensity radiated by the X25 is used to determines the number of equivalent sun hours (ESH) during a specified period of time. The IL1700 Radiometer is used to measure the sun intensity level of the X25 solar simulator. From the IL1700 reading, the ESH is calculated as a function of time.

AZ Technology's LPSR-200 was used to perform the post-vacuum reflectance measurements and solar absorptance calculations. The solar absorptance is calculated in accordance with ASTM E903-82. The LPSR-200 measures the reflectance from 250 to 2500 nm of the sample's surface at a 15° angle of incidence. The instrument measurement accuracy is $+/-$ .02 for both α and ε_n values.

TEST PROCEDURE

Before the sample is placed in the Multisedes chamber, the sample's reflectance is measured using the AZ Technology's LPSR-200 to obtained the pre-vacuum solar absorptance value. The reflectance data is graphed and the solar absorptance (α) is calculated and recorded. The normal emittance (ε_n) of the sample is measured and recorded.

At the completion of the pre-vacuum measurements, the samples are then placed into the Multisedes sample chamber. The samples are mounted against a metal cold plate, which has a water reservoir located directly behind the metal plate. The water reservoir is used to maintain the Multisedes' samples at room temperature. When the test samples are all mounted, the chamber is sealed. The following diagram denotes the positions of the samples location in the Multisedes.

3

Diagram 2: Thermal Coating Samples UV Test Positions

The diagram shows 16 circular sample positions arranged in a 4×4 grid:

Position	Label
1	Reference Mirror
2	Blank
3	D36SCB/LO JV-17
4	MS41SCB/LO U-356 IC-20
5	S13GP/DHS-2 HH-19
6	Sb Doped GE-12
7	S13N/DHS-2 HI-21
8	MH21SC/LO GX-16
9	DS13N/SS-55 P-31
10	DS13N/DHS-2 HJ-25
11	DS13N/LO-51 JX-16
12	MH55-IC Z-6
13	ZnO(FC)/DHS-2 HL-26
14	Eu$_2$O$_3$*/SS-55 ID-26
15	ZOT/SS-55 IW-19
16	DBG-IP GTM-29

Before evacuation begins, an "in air" reflectance measurement is taken of each sample using the Perkin-Elmer Lambda 9 NearIR/Vis/UV Spectrophotometer. At the complete of the "in air" measurement, evacuation of the system is started.

When the system pressure reaches 2×10^{-5} torr, the zero equivalent sun hours (0 ESH) reflectance measurement is made of each sample. The 0 ESH is the first reflectance measurement made of the sample while under vacuum. After the 0 ESH measurements are completed, UV exposure begins.

The X-25 solar simulator is turned on to begin UV exposure. At specified ESH intervals, "in-situ" reflectance measurements are taken of each sample. At 1000 ESH, the reflectance of the samples are measured "in-situ" and then removed from the Multisedes for the post-vacuum reflectance, solar absorptance, and normal emittance measurements. The chamber is back-filled with gaseous nitrogen prior to removal of the samples.

TEST OBSERVATIONS

Date	Comments
22 Mar 1996	• Nine (9) white paint control and test samples' reflectances, solar absorptances, and normal emittances were measured. • Five (5) black paint control and test samples' reflectances, solar absorptances, and normal emittances were measured.
2 Apr 1996	• Test samples were placed in the Multisedes chamber. • Began "in air" measurements of paint samples.
3 Apr 1996	• Completed "in air" measurements. • Began evacuating the Multisedes system.
4 Apr 1996	• Made 0 ESH "in-situ" measurements. • Began UV exposure.
10 Apr 1996	• Made 256 ESH "in-situ" reflectance measurements. • DS13N/LO-51 was beige in color.
3 May 1996	• Made 674 ESH "in-situ" reflectance measurements. • DS13N/LO-51 was brown in color. • Experienced problem with the PE Lambda 9 during "in-situ" reflectance measurements.
9 May 1996	• Corrected PE Lambda 9 problem. Completed 674 ESH "in-situ" reflectance measurements.
20 May 1996	• Made 1068 ESH "in-situ" reflectance measurements. • Back-filled chamber with gaseous nitrogen and removed samples from Multisedes. Made 1068 ESH reflectance, solar absorptance, and normal emittance measurements.

TEST RESULTS

The solar absorptance (α) and normal emittance (ε_n) values of the samples were measured at 0 ESH, 256 ESH, 673 ESH, and 1068 ESH. These measurement were made after removal of the test samples from the Multisede chamber.

Table 2 contains the measured α and ε_n values of the nine white paint samples. Table 3 contains the measured α and ε_n values of the five black paint samples. Table 4 contains the $\Delta\alpha$ of all 14 paints. Reflectance curves of the test samples are located in the appendix.

Table 2 - White Paints

Sample Description	Optical Properties	0 ESH	1068 ESH
S13GP/DHS-2 [HH-19]	α	.148	.165
	ε_n	.934	.932
Sb Doped [GE-12]	α	.156	.243
	ε_n	.930	.931
S13N/DHS-2 [HI-21]	α	.152	.162
	ε_n	.935	.932
DS13N/LO-51 [JX-16]	α	.210	.434
	ε_n	.926	.926
DS13N/DHS-2 [HJ-25]	α	.148	154
	ε_n	.937	.935
DS13N/SS-55 [P-31]	α	.152	.172
	ε_n	.930	.930
ZnO(FC)/DHS-2 [HL-26]	α	.158	.168
	ε_n	.925	.925
Eu$_2$O$_3$*/SS-55 [HD-26]	α	.096	.129
	ε_n	.923	.921
ZOT/SS-55 [IW-19]	α	.129	.180
	ε_n	.881	.881

Table 3 - Black Paints
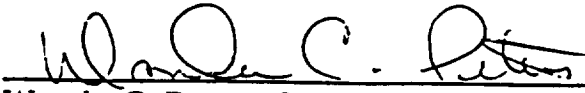
Sample Description	Optical Properties	0 ESH	1068 ESH
D36SCB/LO [JV-17]	α	.962	.967
	ε_n	.908	.909
MS41SCB/LO U-356 [IC-20]	α	.939	.947
	ε_n	.866	.867
MH21SC/LO [GX-16]	α	.951	.955
	ε_n	.862	.864
MH55-IC [Z-6]	α	.928	.938
	ε_n	.886	.885
DBG-IP [GTM-29]	α	.957	.951
	ε_n	.911	.914

Table 4 - Change in Solar Absorptance After UV Exposure

Sample Description	$\Delta\alpha$ after 1068 ESH
S13GP/DHS-2 [HH-19]	.017
Sb Doped [GE-12]	.087
S13N/DHS-2 [HI-21]	.010
DS13N/LO-51 [JX-16]	.224
DS13N/DHS-2 [HJ-25]	.006
DS13N/SS-55 [P-31]	.020
ZnO(FC)/DHS-2 [HL-26]	.010
Eu_2O_3*/SS-55 [HD-26]	.033
ZOT/SS-55 [IW-19]	.051
D36SCB/LO [JV-17]	.005
MS41SCB/LO U-356 [IC-20]	.008
MH21SC/LO [GX-16]	.004
MH55-IC [Z-6]	.010
DBG-IP [GTM-29]	-.006

DATA INTERPRETATION

After 1068 ESH of UV exposure, DS13N/LO-51 [JX-16] and Sb Doped [GE-12] showed significant degradation. Based on repeatability of the measurement ($\pm$ .01), coatings with changes of .02 and greater may display long term instability when life time requirements of greater than ten (10) years are considered.

Wanda C. Peters, Senior Thermal Coatings Engineer

Distribution List:

724/Dennis Hewitt   SAI/Jack Triolo
724/Lonny Kauder   SAI/Grace Miller
724/Ted Swanson   IITRI/Michael Desphande
724/Mark Kobel

APPENDIX

S13GP/DHS-2 White Paint [Batch # HH-19]
UV Degradation Test

Legend:
- 0 ESH — a = .148, e = .934, 26 Mar 1996
- 1068 ESH — a = .165, e = .932, 22 May 1996

Axes: Reflectance (vertical), Wavelength (nm) (horizontal)

10
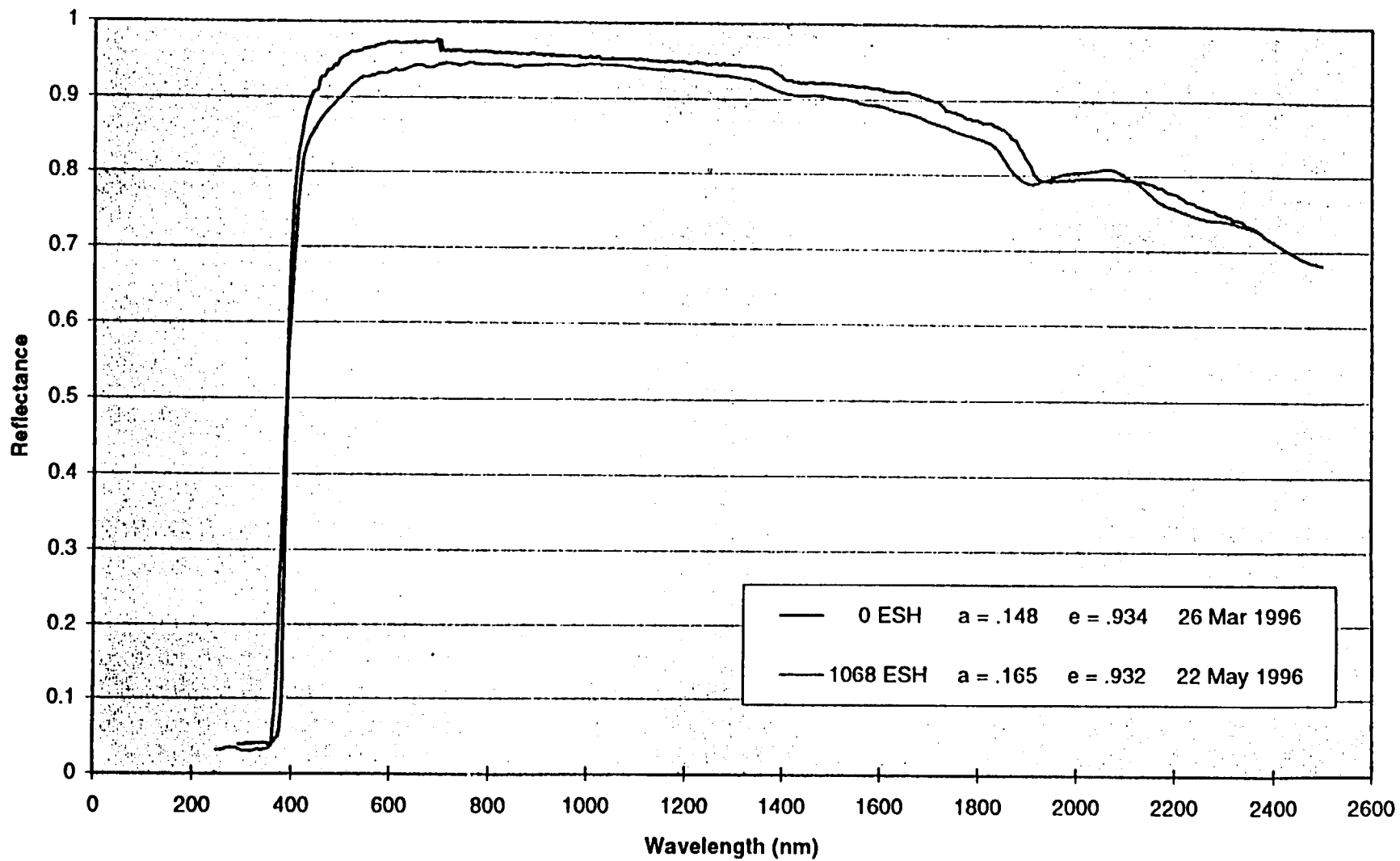
Sb Doped White Paint [Batch # GE-12]
UV Degradation Test
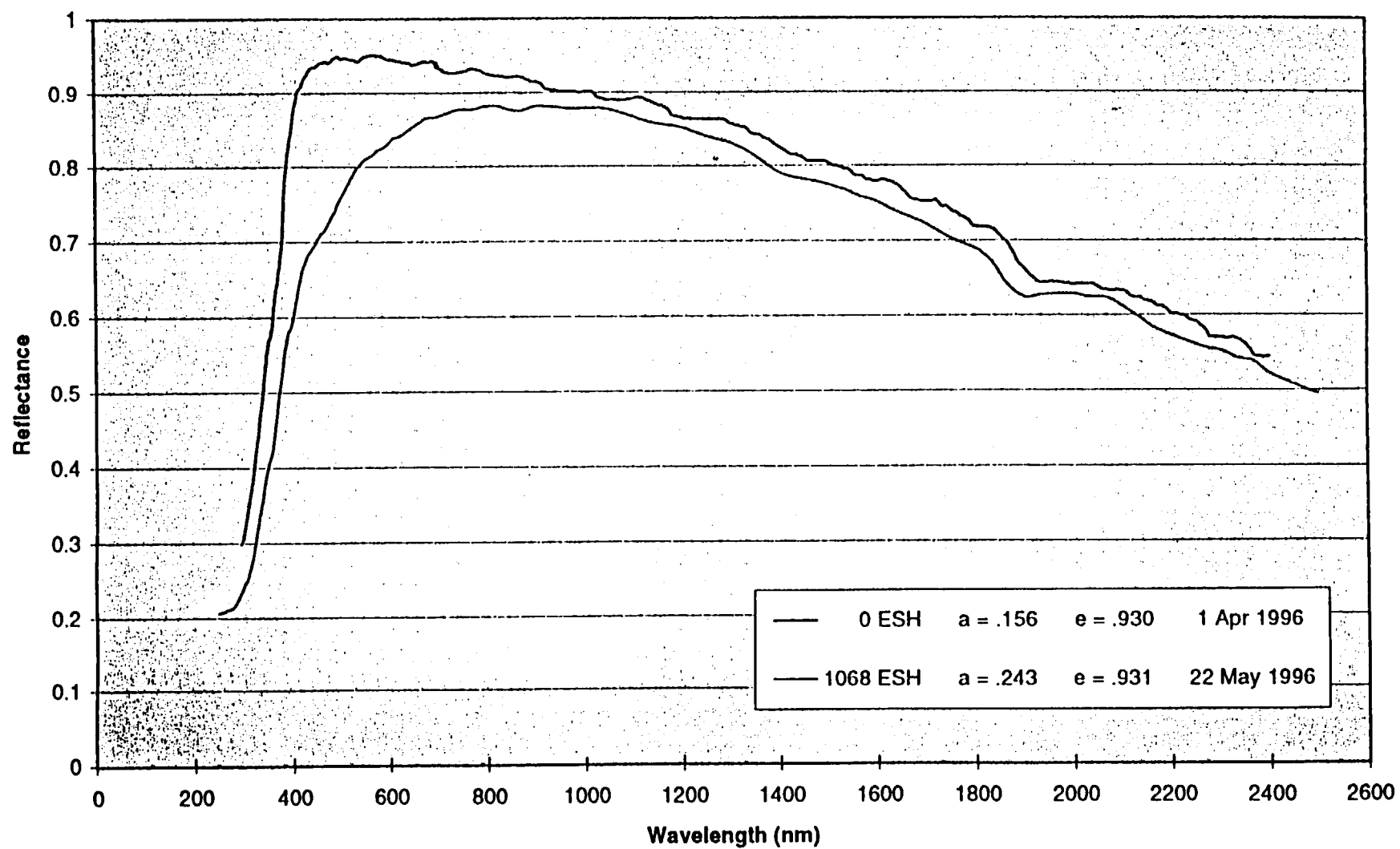
S13N/DHS-2 White Paint [Batch # HI-21]
UV Degradation Test

Legend:
- 0 ESH   a = .152   e = .935   26 Mar 1996
- 1068 ESH   a = .162   e = .931   22 May 1996

Y-axis: Reflectance
X-axis: Wavelength (nm)

-12
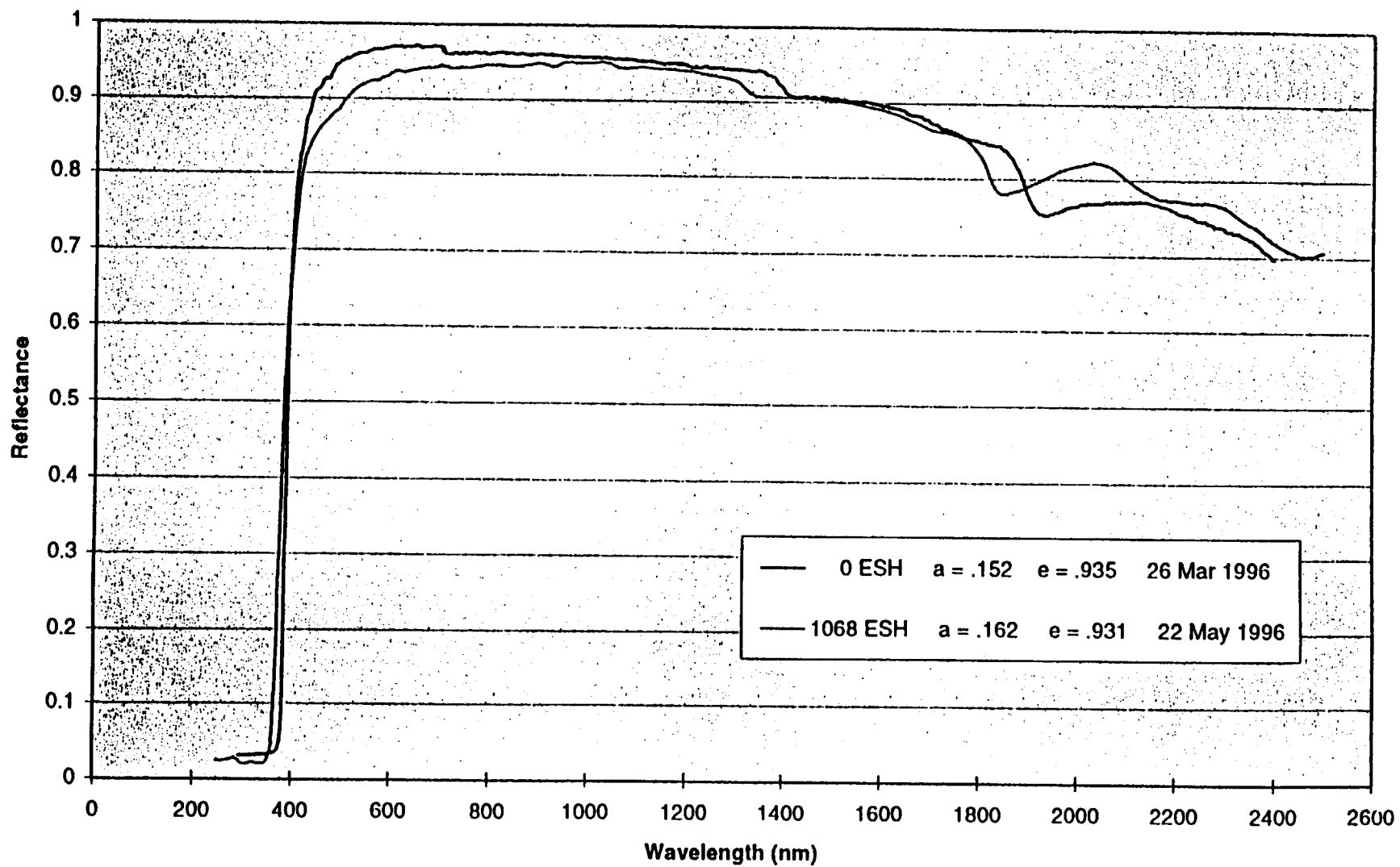
DS13N/LO-51 White Paint [Batch # JX-16]
UV Degradation Test

0 ESH	a = .210	e = .926	27 Mar 1996
1068 ESH	a = .434	e = .926	22 May 1996

Reflectance

Wavelength (nm)

-13-
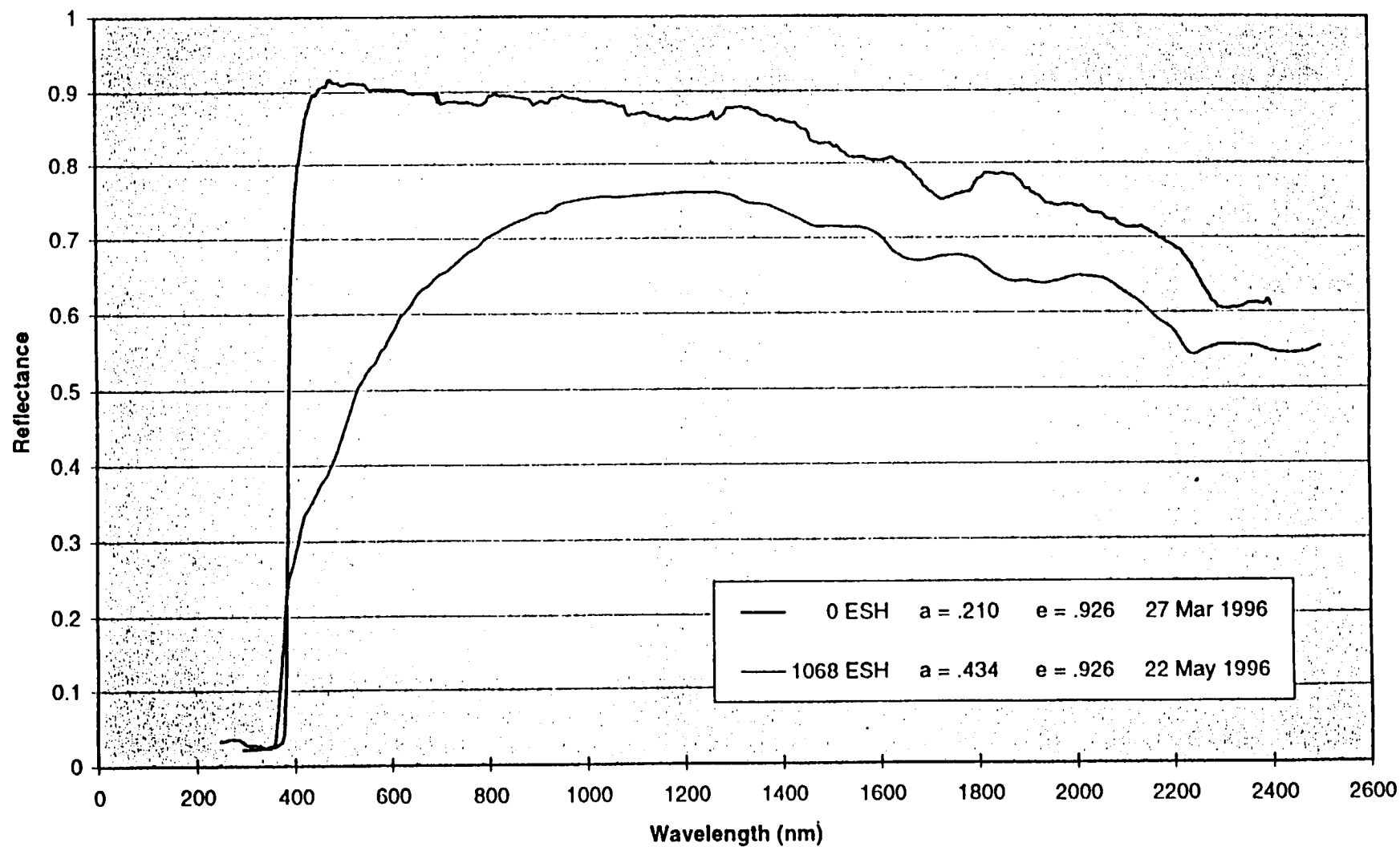
DS13N/DHS-2 White Paint [Batch # HJ-25]
UV Degradation Test

Legend:
— 0 ESH   a = .147   e = .937   26 Mar 1996
— 1068 ESH   a = .154   e = .935   22 May 1996
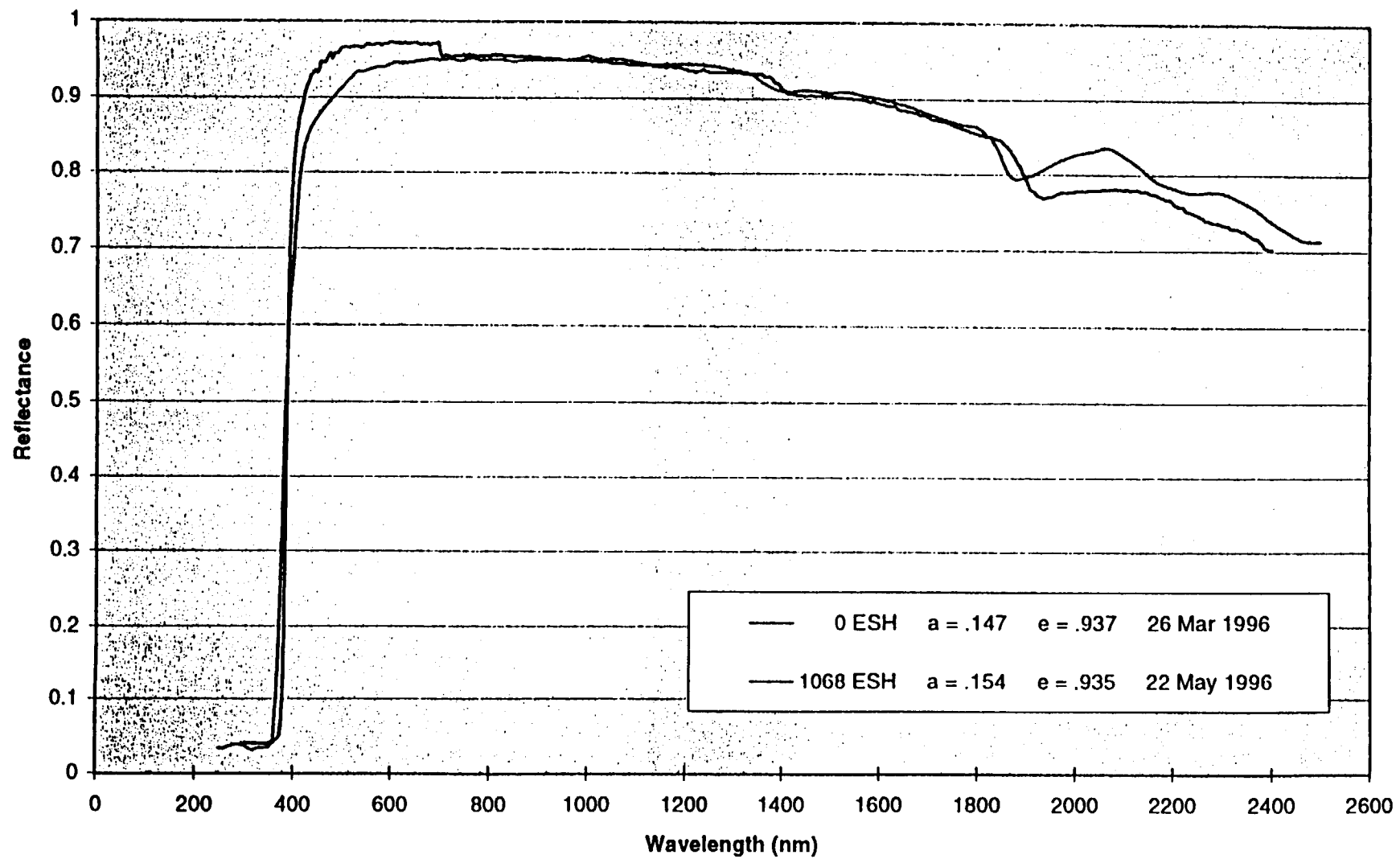
DS13N/SS-55 White Paint [Batch # P-31]
UV Degradation Test

Legend:
- —— 0 ESH   a = .151   e = .930   26 Mar 1996
- —— 1068 ESH   a = .172   e = .930   22 May 1996

Reflectance vs. Wavelength (nm)

15
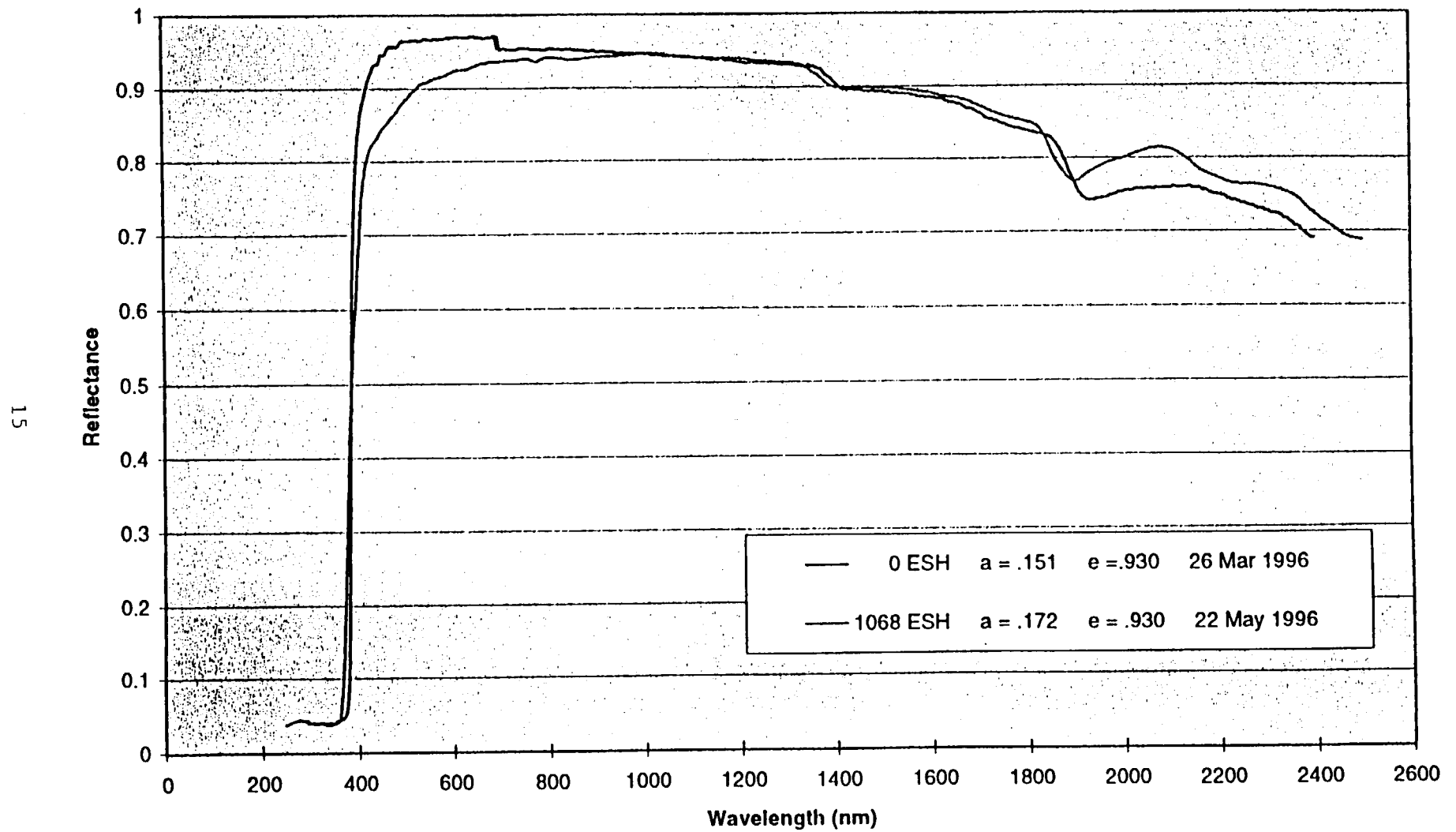
ZnO(FC)/DHS-2 White Paint [Batch # HL-26]
UV Degradation Test

The chart legend shows:

- 0 ESH   a = .158   e = .925   1 Apr 1996
- 1068 ESH   a = .168   e = .925   22 May 1996

Reflectance vs. Wavelength (nm)

16
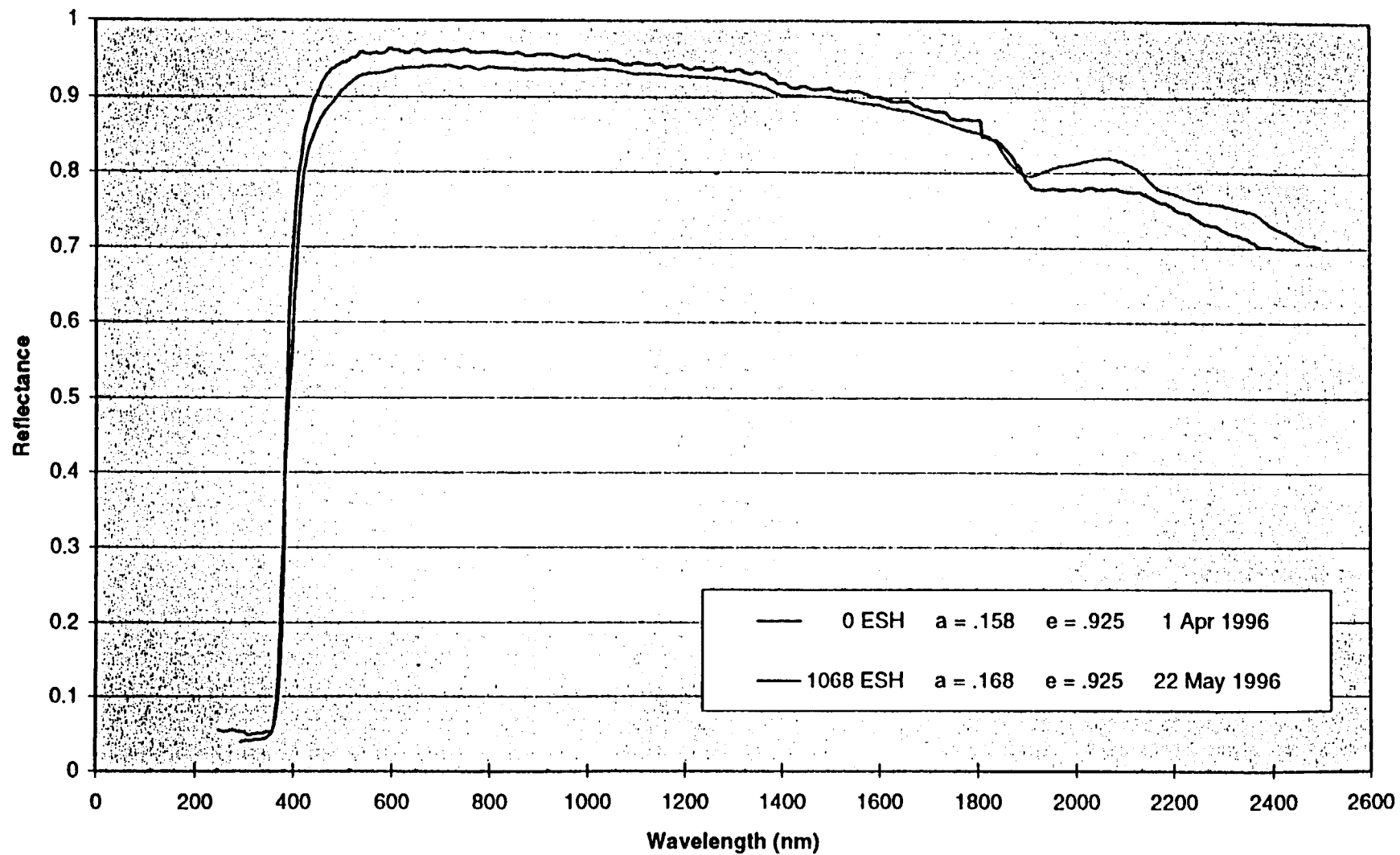
Eu2O3*/SS-55 Whtie Paint [Batch # HD-26]
UV Degradation Test

Legend:
- —— 0 ESH   a = .095   e = .923   1 Apr 1996
- —— 1068 ESH   a = .129   e = .921   22 May 1996

Y-axis: Reflectance
X-axis: Wavelength (nm)

17
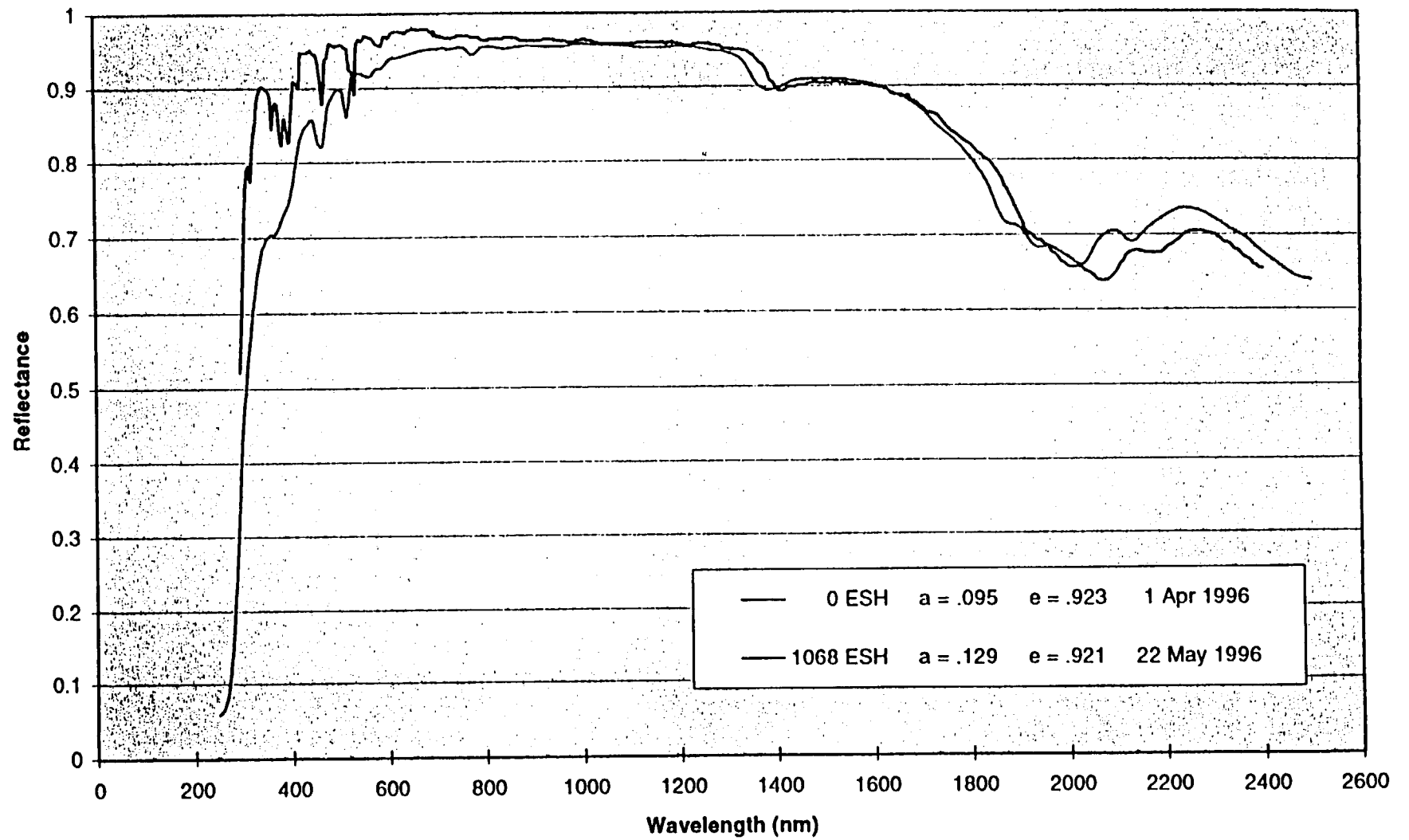
ZOT/SS-55 White Paint [Batch # IW-19]
UV Degradation Test

| | 0 ESH | a = .129 | e = .881 | 1 Apr 1996 |
| 1068 ESH | a = .180 | e = .881 | 22 May 1996 |
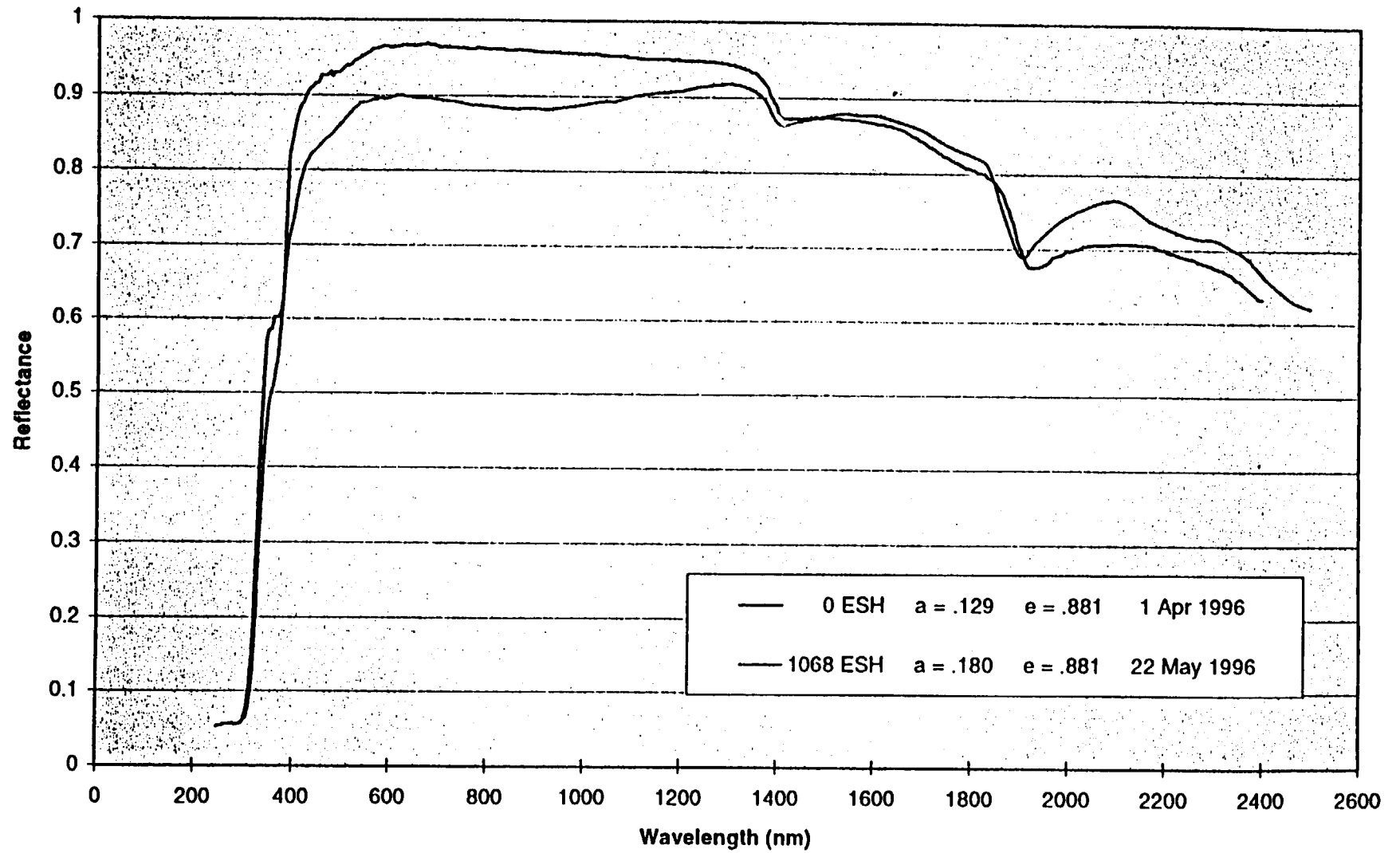
D36SCB/LO Black Paint [Batch # JV-17]
UV Degradation Test

Legend:
- 0 ESH   a = .961   e = .908   23 Mar 1996
- 1068 ESH   a = .967   e = .909   22 May 1996

Axes: Reflectance (y-axis, 0 to 1) vs Wavelength (nm) (x-axis, 0 to 2600)

19
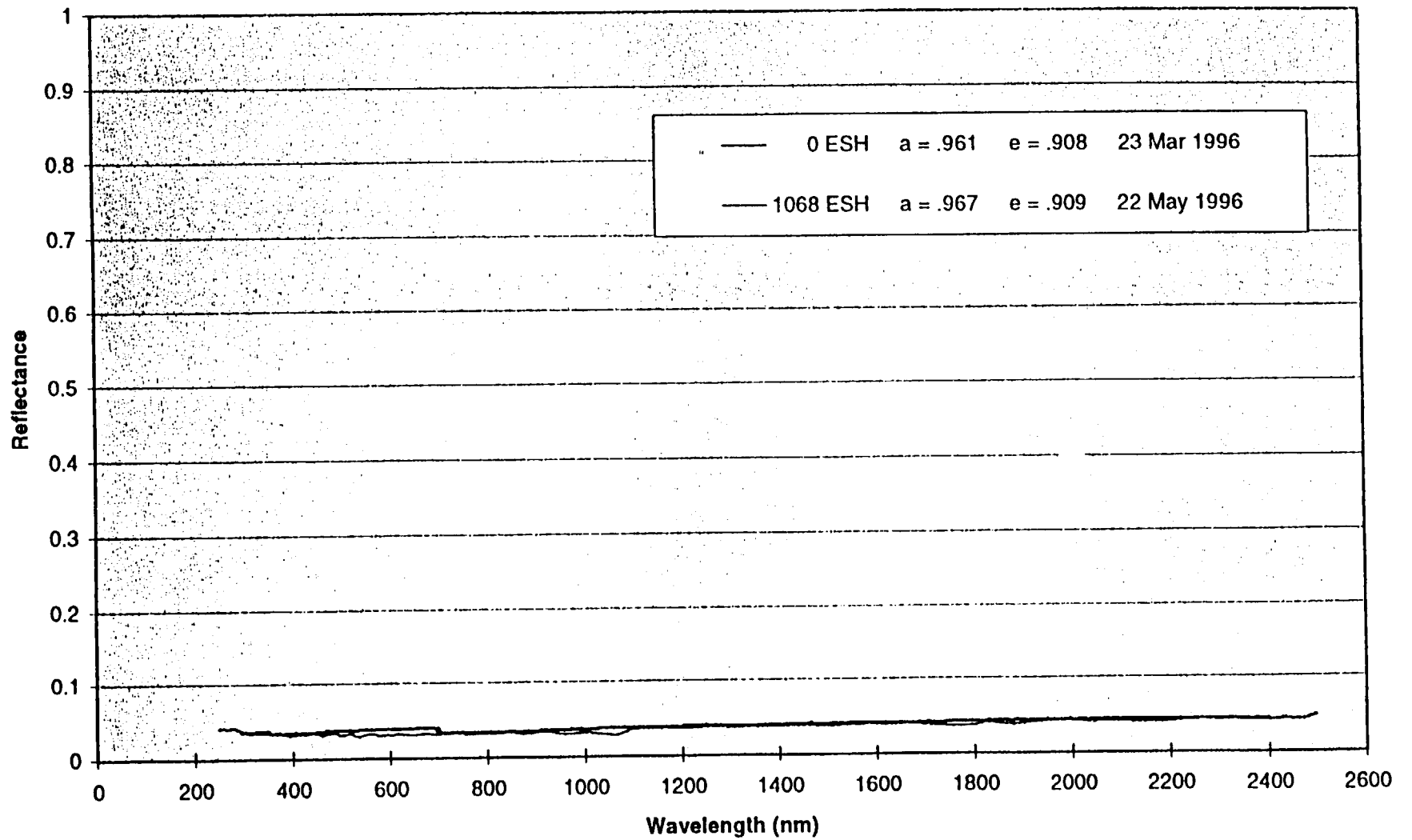
MS41SCB/LO Black Paint [Batch # U-356 IC-20]
UV Degradation Test

Legend:
- 0 ESH   a = .937   e = ,866   23 Mar 1996
- 1068 ESH   a = .947   e = .867   22 May 1996

Y-axis: Reflectance (0 to 1)
X-axis: Wavelength (nm) (0 to 2600)
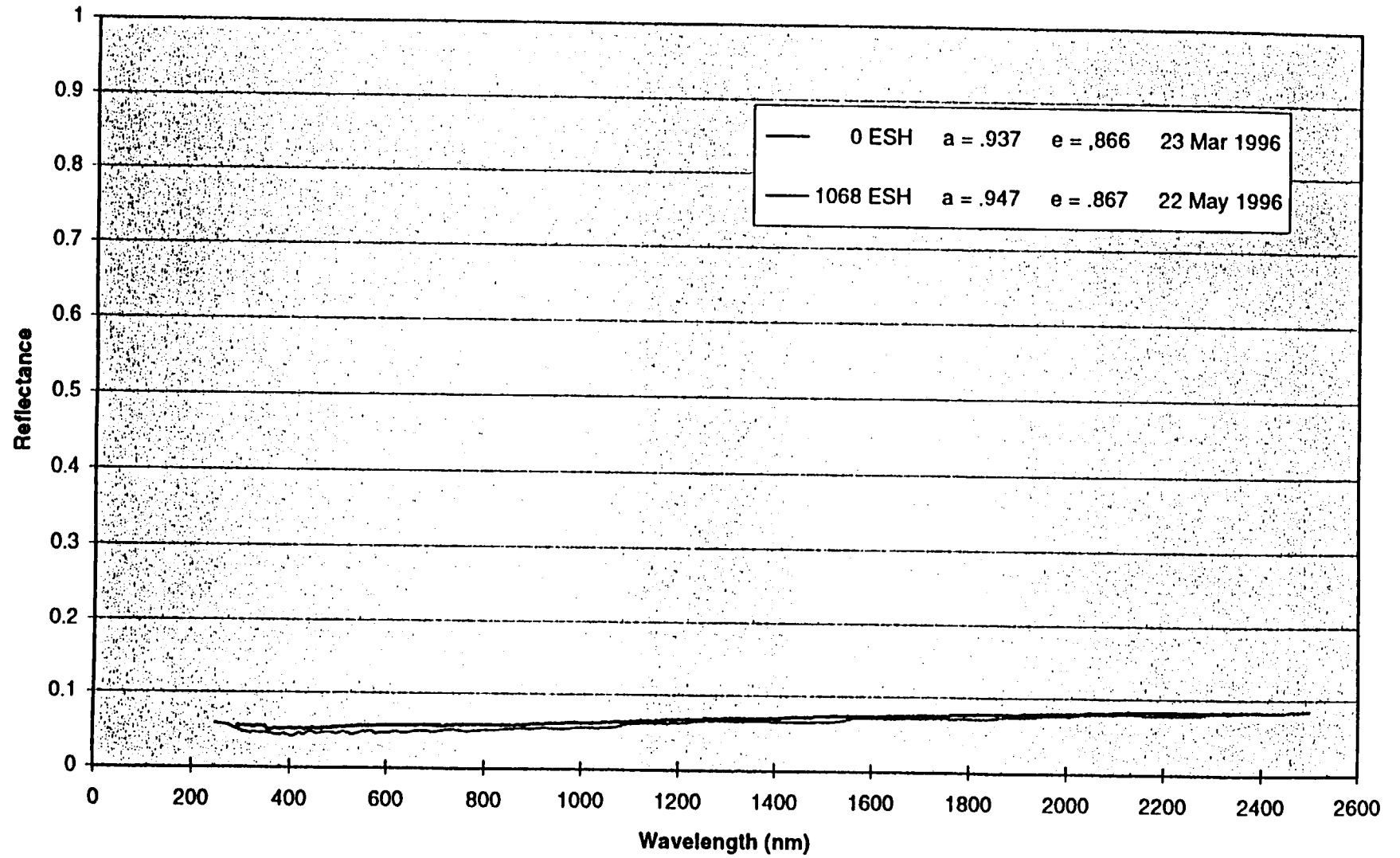
MH21SC/LO Black Paint [Batch # GX-16]
UV Degradation Test

0 ESH	a = .951	e = .862	23 Mar 1996
1068 ESH	a = .955	e = .864	22 May 1996

Reflectance

Wavelength (nm)

21
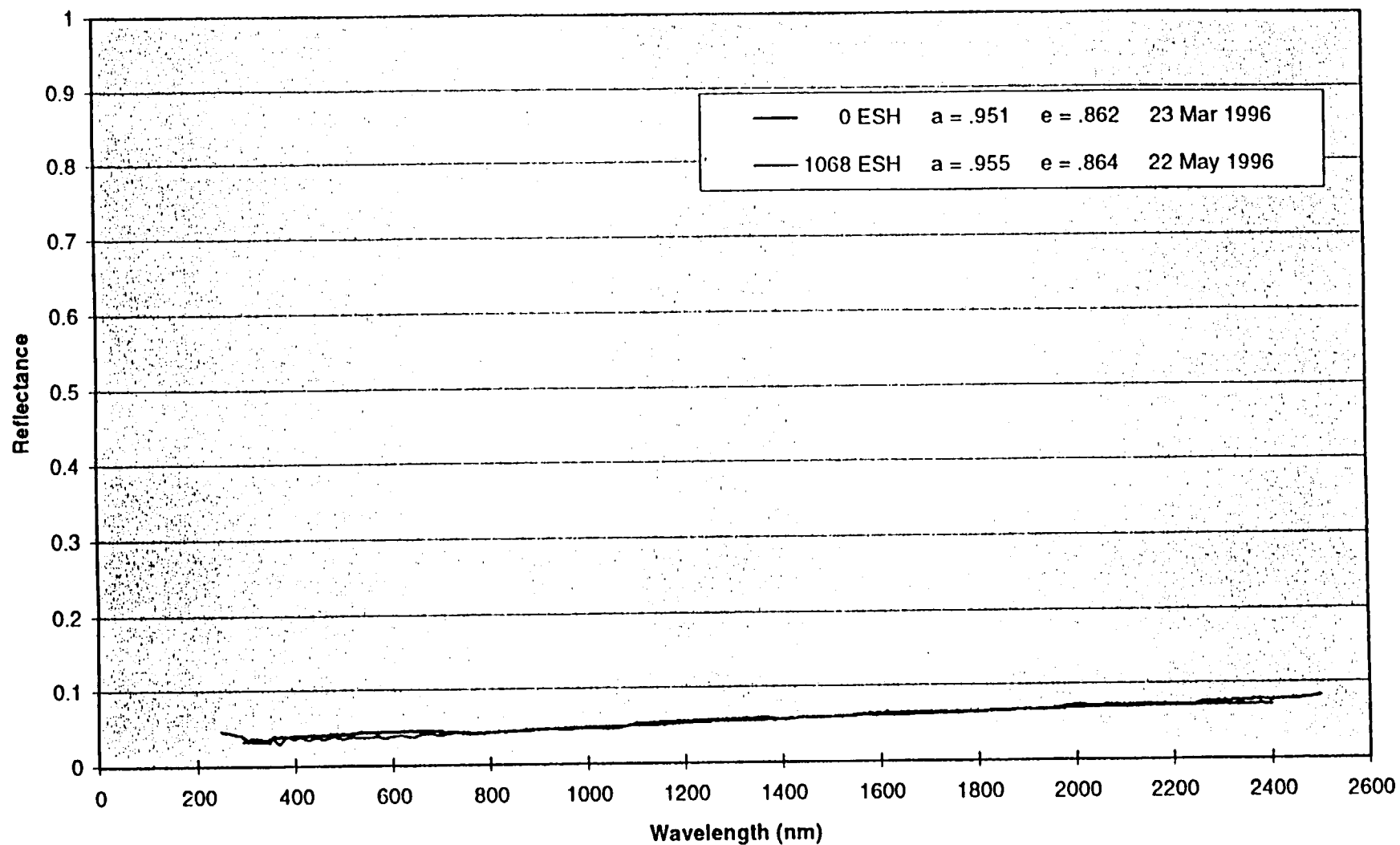
MH55-IC Black Paint [Batch #Z-6]
UV Degradation Test

Legend:
- —— 0 ESH   a = .928   e = .886   23 Mar 1996
- —— 1068 ESH   a = .938   e = .885   22 May 1996

Y-axis: Reflectance (0 to 1)
X-axis: Wavelength (nm) (0 to 2600)

22
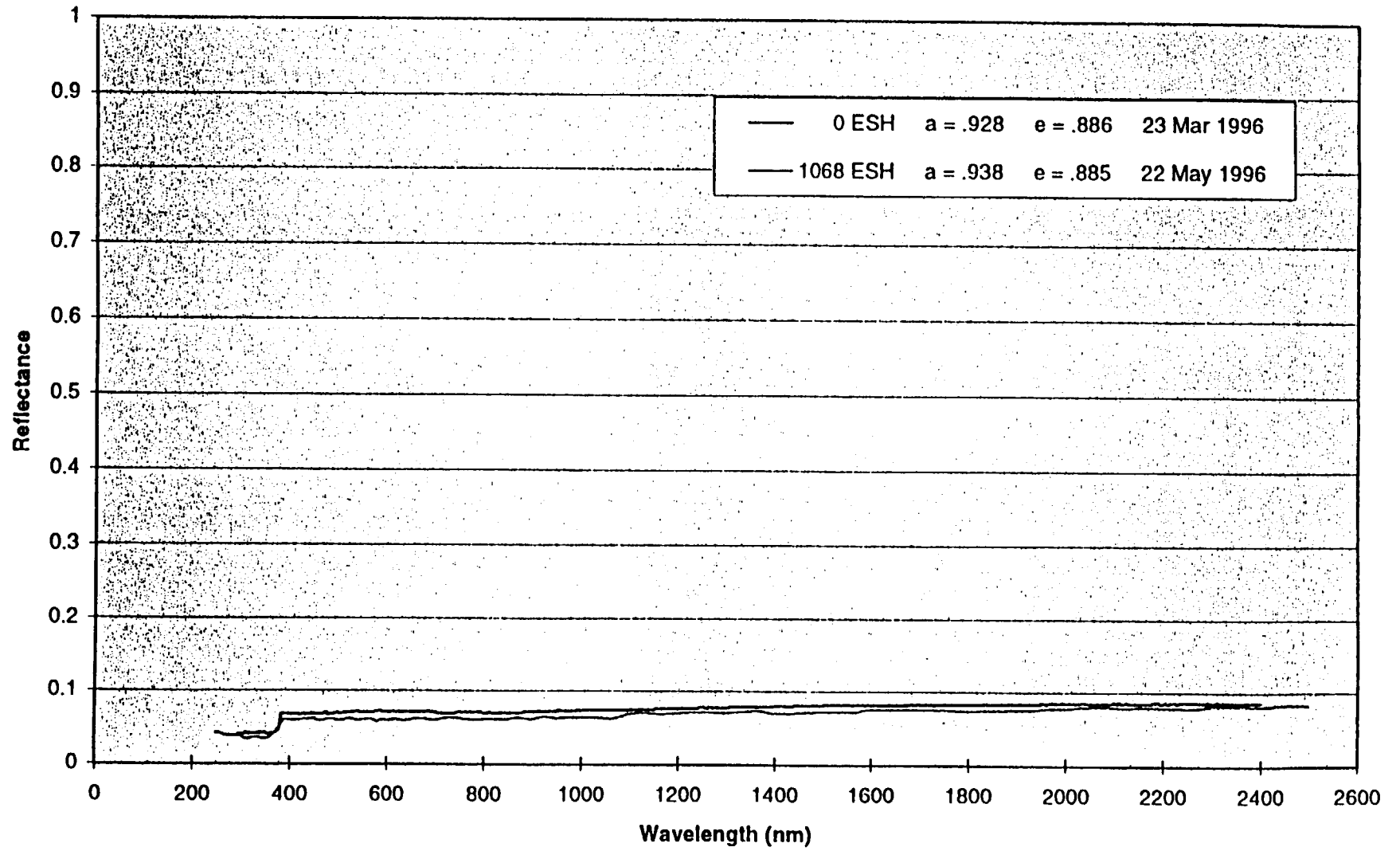
DBG-IP Black Paint [Batch # GTM-29]
UV Degradation Test

0 ESH	a = .961	e = .914	1 Apr 1996
1068 ESH	a = .951	e = .911	22 May 1996

Reflectance

Wavelength (nm)

23
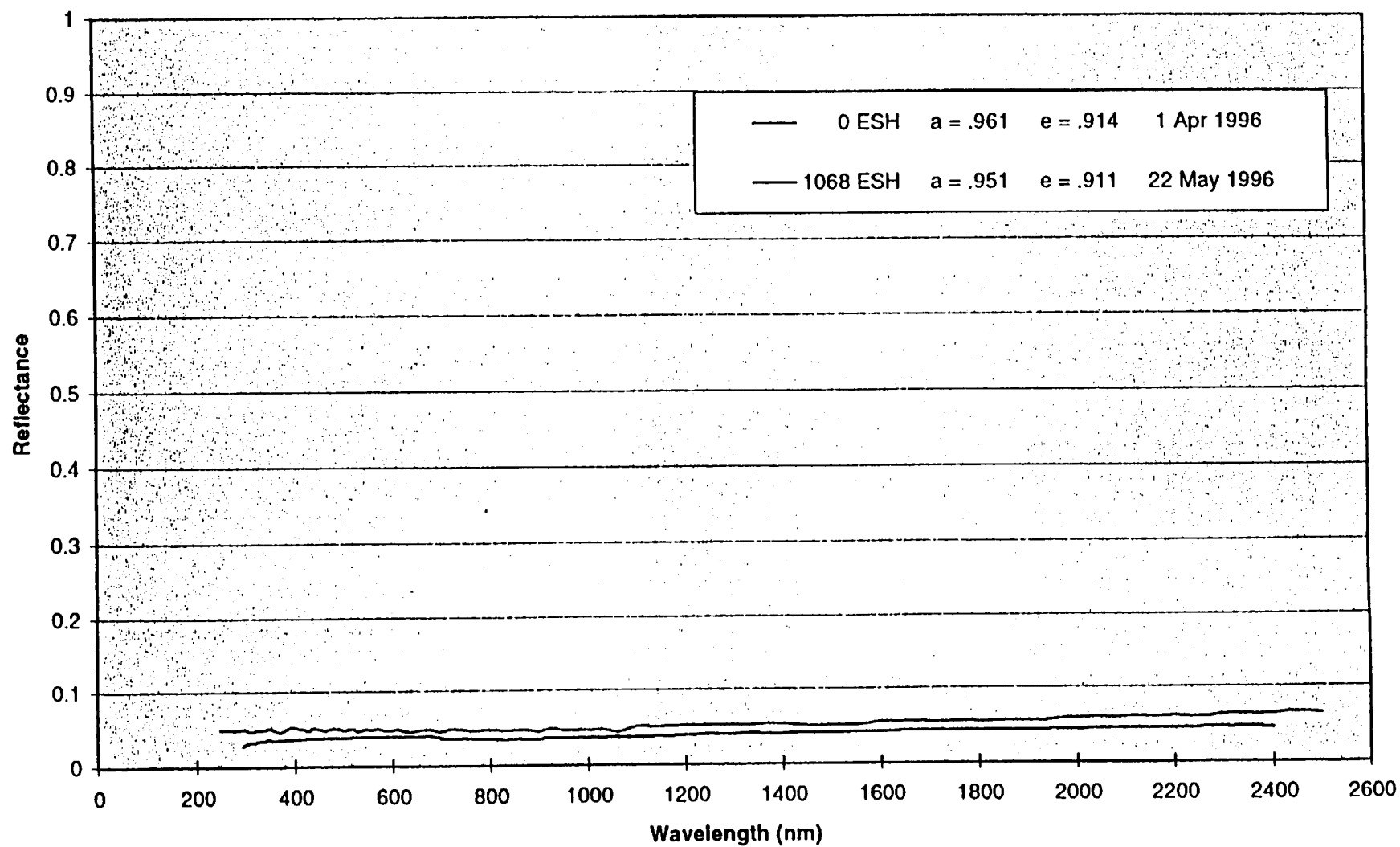
APPENDIX D

USAF WL/ML SCEPTRE SCREENING TEST
96QV01

USAF WL/ML SCEPTRE Screening Test
96QV01
April 9 - May 1, 1996

Test Environmental Parameters

vacuum: 5.0E-08 torr
total exposure time: 314 hrs.

1.0 KeV electron flux - 6.0E+09 e-/cm2/sec
10.0 KeV electron flux - 3.0E+09 e-/cm2/sec

Temperature Range

| In Situ* ·135-146 deg. F |
| Passive = 185 deg. F |
| *lossed chiller for 12 hrs. & tem-peratures reached 182-185 deg. F |

total fluence- 1.2E+16 e-/cm2

Measured In Situ

Conductive White Coatings

Coating	Batch	Specimen ID	UV Exposure	α pretest	α posttest	change in α
DS13N/LO-51	V-032	JX-17	1.6 EUVS	0.193	0.423	0.230
DS13N/SS-55	U-315	P-25	2.1 EUVS	0.157	0.267	0.110

USAF WL/MLBT SCEPTRE Test 96QV01
IITRI Electrically Conductive White Thermal Control Coatings

Solar Absorptance (250-2500 nm)

Equivalent Sun Hours (Exposure Hours X EUVS)

DS-13N/LO-51 (1.6 UEVS)

DS-13N/SS-55 (2.1 EUVS)

USAF WL/ML SCEPTRE Screening Test
96QV01
April 9 - May 1, 1996

Test Environmental Parameters

vacuum: 5.0E-08 torr
total exposure time: 314 hrs.

1.0 KeV electron flux - 6.0E+09 e-/cm2/sec
10.0 KeV electron flux - 3.0E+09 e-/cm2/sec

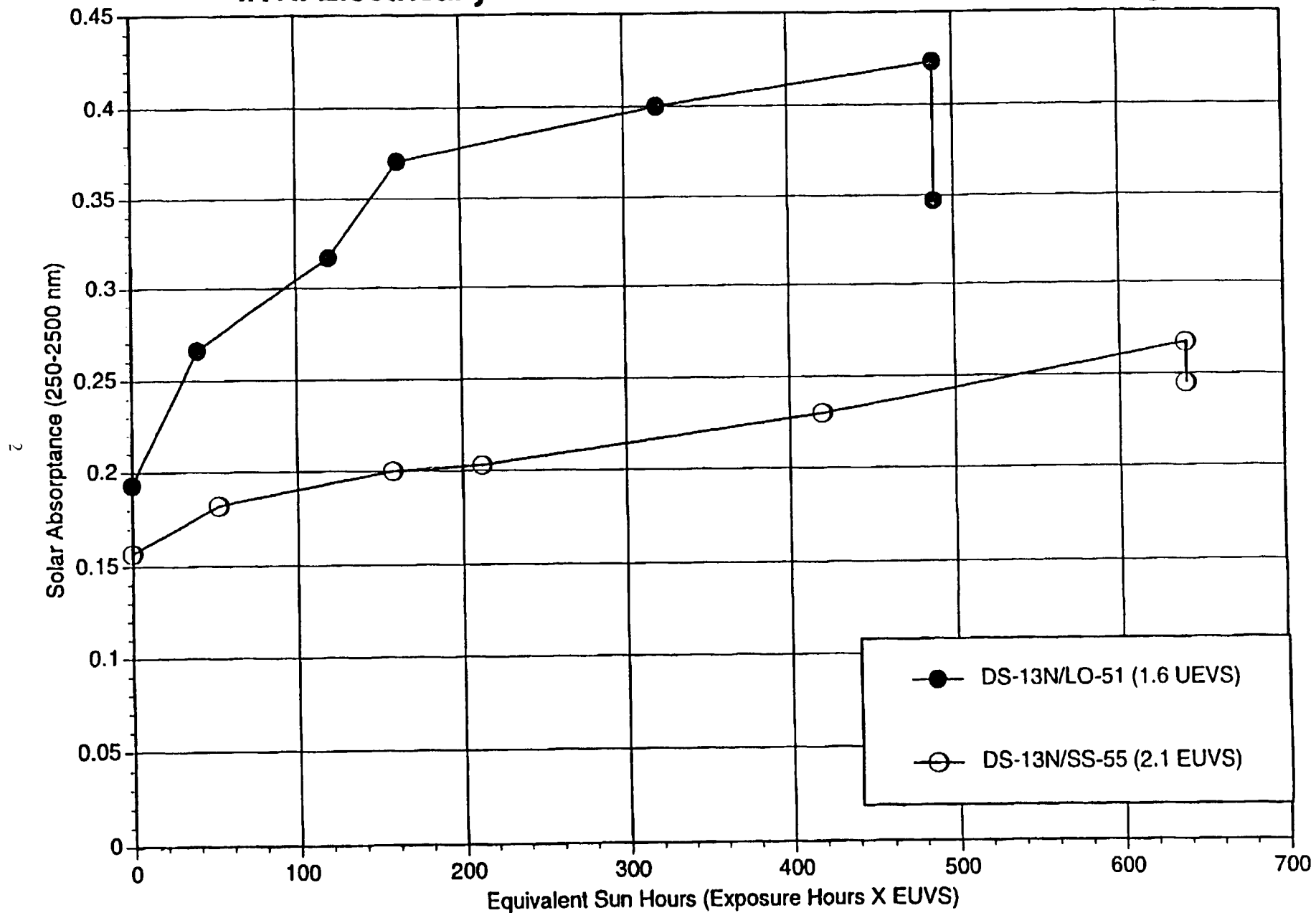total fluence- 1.2E+16 e-/cm2

Temperature Range
In Situ* ·135-146 deg. F
Passive ▪ 185 deg. F
*lossed chiller for 12 hrs. & temperatures reached 182-185 deg. F

Measured. In Situ

Conductive White Coatings

Coating	Batch	Specimen ID	UV Exposure	α pretest	α posttest	change in α
DS13N/LO-51	V-032	JX-17	1.6 EUVS	0.193	0.423	0.230
DS13N/SS-55	U-315	P-25	2.1 EUVS	0.157	0.267	0.110

Passively Exposed

Conductive Black Coatings

Coating	Batch	Specimen ID	UV Exposure	α pretest	α posttest	change in α
DBG-IP	U-021	EO-17	4.0 EUVS	0.970	0.978	0.008
D36SCB/LO	V-036	JV-15	3.9 EUVS	0.966	0.956	-0.010

Conductive White Coatings

Coating	Batch	Specimen ID	UV Exposure	α pretest	α posttest	change in α
Z-93CXY						
ZnO(FC)/DHS-2	U-327	HL-23	1.1 EUVS	0.143	0.225	0.082
Z-93SCXY						
S13N/DHS-2	U-329	HI-17	1.0 EUVS	0.130	0.196	0.066
Z-93SCLMXY						
DS13N/DHS-2	U-330	HJ-16	3.3 EUVS	0.117	0.237	0.120

Other Conductive White Coating

Coating	Batch	Specimen ID	UV Exposure	α pretest	α posttest	change in α
Eu2O3*/SS-55	U-353	ID-19	3.6 EUVS	0.076	0.161	0.085

APPENDIX E

RESULTS OF ELECTROSTATIC DISCHARGE TESTING
AT GODDARD SPACE FLIGHT CENTER

DS13N/LO
Date Tested: 12/4/96

Flux	Non-contact Charging Potential Developed on Sample (Volts)				
	5KeV @ 0.44nA	5KeV @4.4nA	10KeV @ 0.44nA	10KeV @ 4.4nA	20KeV @ 0.44nA
Temperature (K)					
274					
320	-20	-76	-41	-145	-40

ZnO(CF)DHS-2
Date Tested: 11/13/96

Flux	Non-contact Charging Potential Developed on Sample (Volts)			
	5KeV @ 1.0nA/cm^2	5KeV @10nA/cm^2	10KeV @ 1.0nA/cm^2	10KeV @ 10nA/cm^2
Temperature (K)				
130	-7	-11	-7	-17
179	-8	-15	-9	-14
228	-13	-22	-17	-25
275	-9		-35	-56
322	-3		-3	-20

S13GP/DHS-2
Date tested: 10/23/96

Flux	Non-contact Charging Potential Developed on Sample (Volts)		
	5KeV @ 1.0nA/cm^2	5KeV @10nA/cm^2	10KeV @ 1.0nA/cm^2
Temperature (K)			
128			
178	-160		
225	-123		
275	-60	-190	-130
321	-2.5	-13	-70

S13N/DHS-2
Date tested: 10/31/96

Flux	Non-contact Charging Potential Developed on Sample (Volts)	
	5KeV @ 0.44nA	5KeV @4.4nA
Temperature (K)		
275	-80	-130
323	-45	-56

ZnO(CF)DHS-2
Date Tested: 11/13/96

Flux	Non-contact Charging Potential Developed on Sample (Volts)			
	5KeV @ 1.0nA/cm^2	5KeV @10nA/cm^2	10KeV @ 1.0nA/cm^2	10KeV @ 10nA/cm^2
Temperature (K)				
130	-7	-11	-7	-17
179	-8	-15	-9	-14
228	-13	-22	-17	-25
275	-9		-35	-56
322	-3		-3	-20

DS13N/DHS2
Date tested: 11/4/96

Flux	Non-contact Charging Potential Developed on Sample (Volts)				
	5KeV @ 1.0nA/cm^2	5KeV @10nA/cm^2	10KeV @ 1.0nA/cm^2	10KeV @ 10nA/cm^2	20KeV @ 1.0nA/cm^2
Temperature (K)					
129	-60	-180	-120		-120
179	-45	-170	-110		
228	-70	-160	-110		
275	-30	-100	-65	-160	-60
322	-6	-27	-20	-70	-30

ZOT/SS-55
Date tested: 1/7/97

Flux	Non-contact Charging Potential Developed on Sample (Volts)			
	5KeV @ 0.44nA	10KeV @ 0.44nA	10KeV @ 4.4nA	20KeV @ 0.44nA
Temperature (K)				
129	-174			
179	-160			
227	-100	-170		
271	-1.7	-2		-100
319	-0.5	-0.6		0

Eu2O3/SS-55
Date Tested: 11/19/96

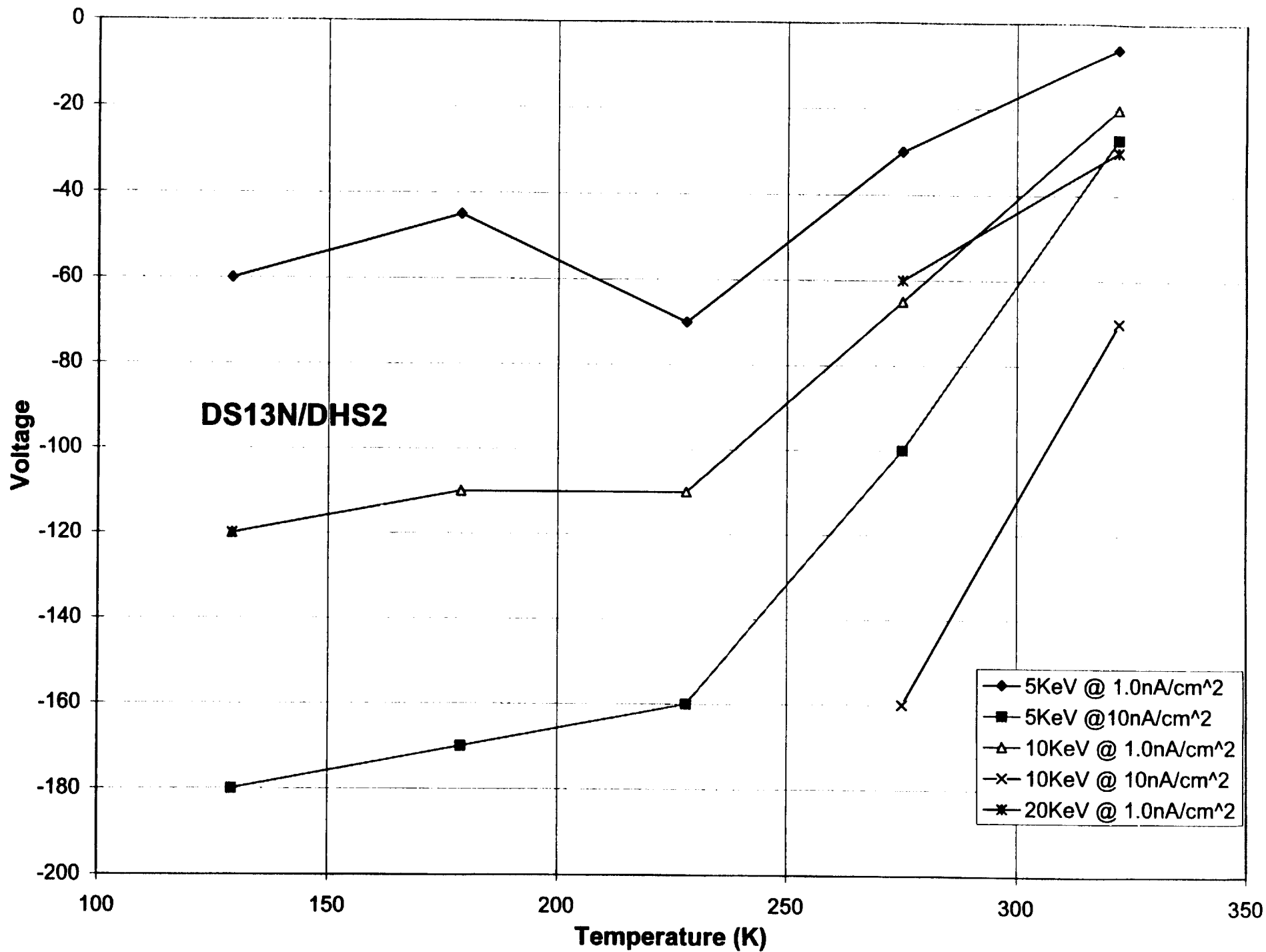| Flux | Non-contact Charging Potential Developed on Sample (Volts) |
	5KeV @ 0.44nA
Temperature (K)	
273	-180
322	-25

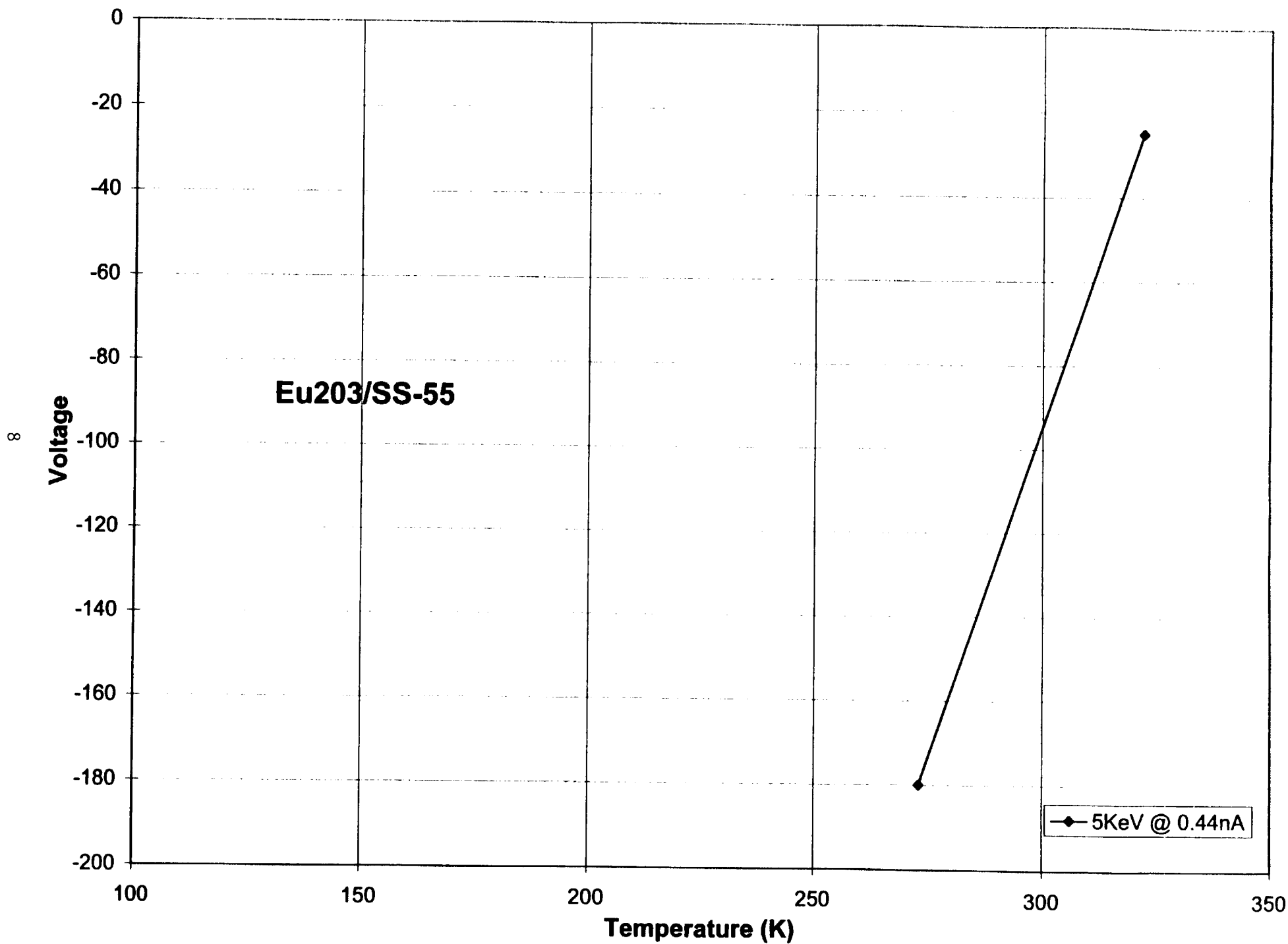**ZnO + Sb : Zn2SnOx**
Date tested: 12/2/96

Flux	Non-contact Charging Potential Developed on Sample (Volts)				
	5KeV @ 0.44nA	5KeV @4.4nA	10KeV @ 0.44nA	10KeV @ 4.4nA	20KeV @ 0.44nA
Temperature (K)					
129	-77	-134	-143		-140
179	-73	-110	-120		-163
227	-66	-105	-100		-137
275	-30	-120	-60	-160	-70
323	-14	-19	-34	-36	-48

S13GP/DHS-2

ZnO + Sb : Zn2SnOx

5KeV @ 0.44nA
5KeV @4.4nA
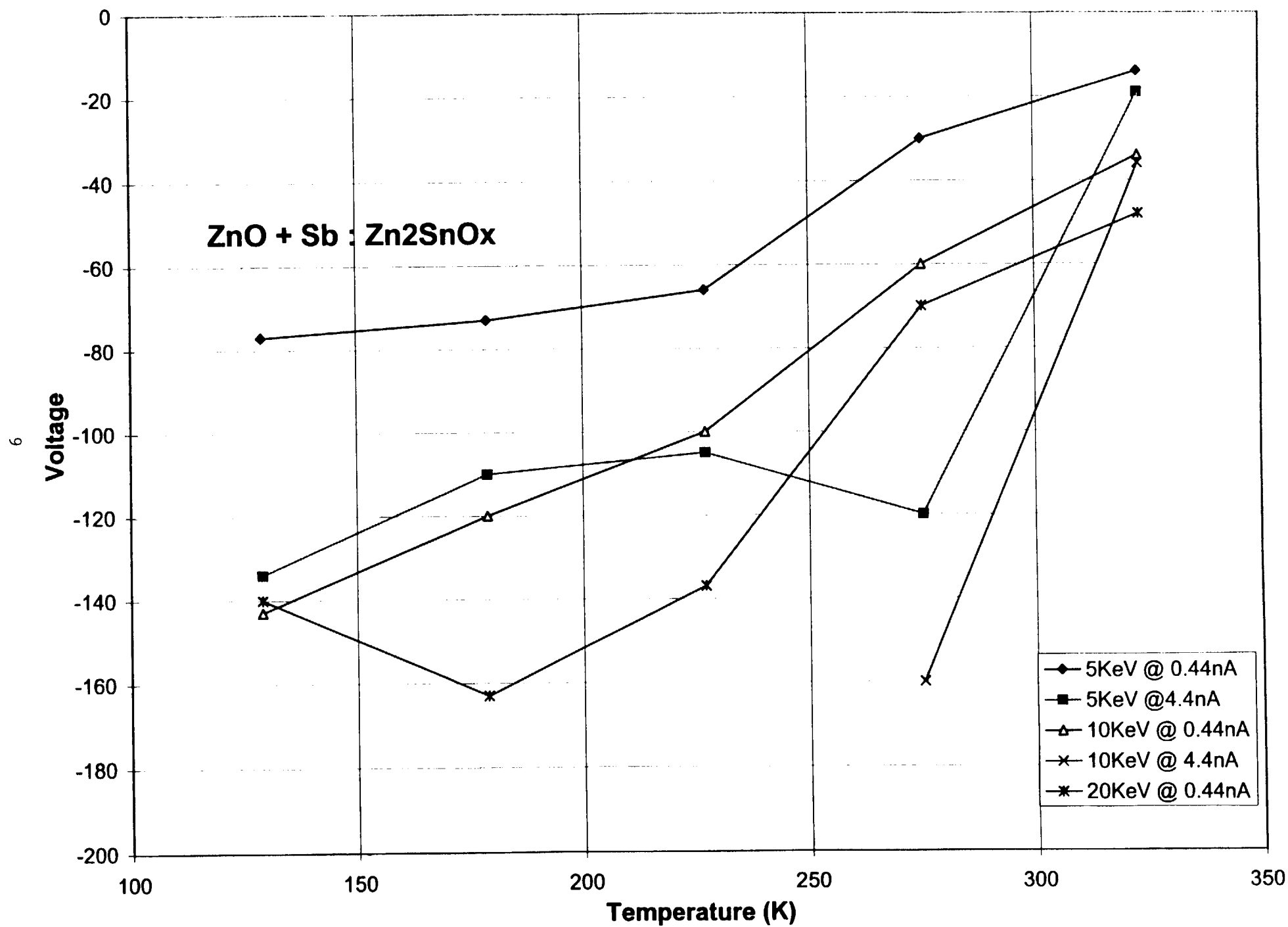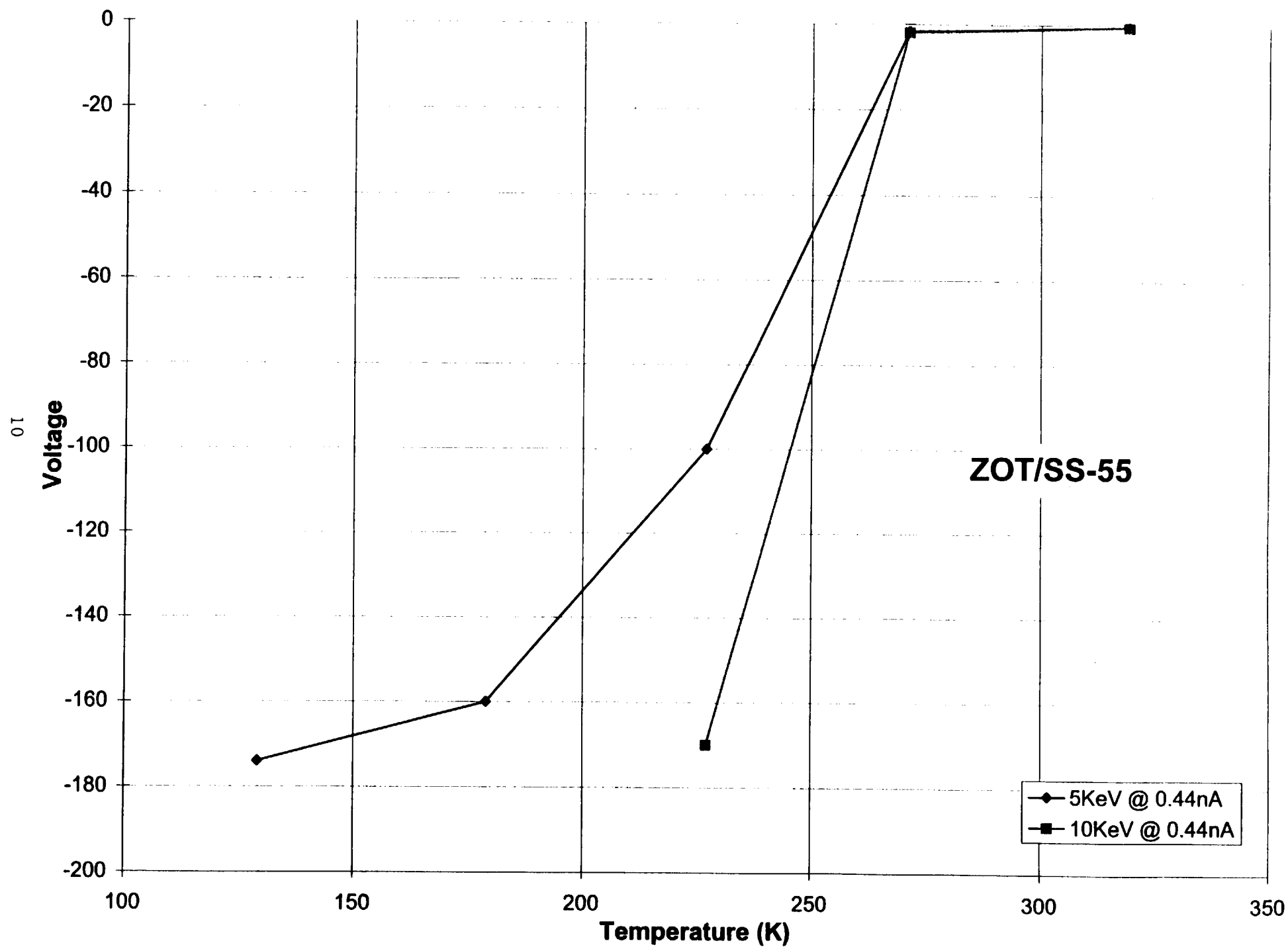10KeV @ 0.44nA
10KeV @ 4.4nA
20KeV @ 0.44nA

MH21SC/LO-2
Date Tested: 10/28/96

Flux	Non-contact Charging Potential Developed on Sample (Volts) 5KeV @ 0.44nA
Temperature (K)	
275	-190
322	-175

D36SCB/LO
Date tested: 11/20/96

Flux	Non-contact Charging Potential Developed on Sample (Volts)			
	5KeV @ 1.0nA/cm^2	5KeV @10nA/cm^2	10KeV @ 1.0nA/cm^2	10KeV @ 10nA/cm^2
Temperature (K)				
133	-6.3	-8.5	-8.4	-9.9
178	-6.1	-6.2	-6.5	-7
226	-5.8	-6.1	-5.6	-6.3
275	-4.1	-4.9	-3.9	-4.8
321	-2.4	-3.4	-3	-3.7

MH55IC
Date Tested: 11/24/96

Flux	Non-contact Charging Potential Developed on Sample (Volts)				
	5KeV @ 1.0nA/cm^2	5KeV @10nA/cm^2	10KeV @ 1.0nA/cm^2	10KeV @ 10nA/cm^2	20KeV @ 1.0nA/cm^2
Temperature (K)					
129	-33	-35	-71	-68	-68
178	-30	-30	-60	-56	-61
226	-22	-31	-60	-60	-60
273	-18	-22	-22	-44	
321	-3	-7.3	-3.9	-9.5	

DBG-IP
Date Tested: 11/26/96

Flux	Non-contact Charging Potential Developed on Sample (Volts)				
	5KeV @ 1.0nA/cm^2	5KeV @10nA/cm^2	10KeV @ 1.0nA/cm^2	10KeV @ 10nA/cm^2	20KeV @ 1.0nA/cm^2
Temperature (K)					
130	-17	-39	-66	-71	-87
179	-20	-32	-63	-70	-80
227	-25	-30	-51	-64	-74
273	-10	-16	-16	-28	-17
320	-1	-5.9	-3.5	-8.1	-3

MH41SCB/LO1
Date Tested: 11/30/96

Flux	Non-contact Charging Potential Developed on Sample (Volts)				
	5KeV @ 1.0nA/cm^2	5KeV @10nA/cm^2	10KeV @ 1.0nA/cm^2	10KeV @ 10nA/cm^2	20KeV @ 1.0nA/cm^2
Temperature (K)					
128	-10	-12.6	-55	-60	-62
173	-13	-13	-62	-60	-61
224	-16	-16	-61	-63	-63
268	-17	-17	-65	-62	
323	-22	-22	-65	-73	-60

DBG-IP

13

MH55IC

Legend:
- 5KeV @ 1.0nA/cm^2
- 5KeV @10nA/cm^2
- 10KeV @ 1.0nA/cm^2
- 10KeV @ 10nA/cm^2
- 20KeV @ 1.0nA/cm^2

Y-axis: Voltage (0, -20, -40, -60, -80, -100, -120, -140, -160, -180, -200)

X-axis: Temperature (K) (100, 150, 200, 250, 300, 350)

D36SCB/LO

MH21SC/LO-2

5KeV @ 0.44nA

MH41SCB/LO

REPORT DOCUMENTATION PAGE

Public reporting burden for this collecton of information is estimated to average 1 hour per response, including the time for reviewing instructions, searching existing data sources, gathering and maintaining the data needed, and completing and reviewing the collection of information. Send comments regarding this burden estimate or any other aspect of this collection of information, including suggestions for reducing this burden, to Washington Headquarters Services, Directorate for Information Operations and Reports, 1215 Jefferson Davis Highway, Suite 1204, Arlington, Va 22202-4302, and to the Office of Management and Budget, Paperwork Reduction Project (0704-0188), Washington, DC 20503.

1. AGENCY USE ONLY (Leave Blank)	2. REPORT DATE June 1998	3. REPORT TYPE AND DATES COVERED Contractor Report (Final)

4. TITLE AND SUBTITLE

Development of Tailorable Electrically Conductive Thermal Control Material Systems

5. FUNDING NUMBERS

NAS8-40580

6. AUTHOR(S)

M. S. Deshpande and Y. Harada

7. PERFORMING ORGANIZATION NAME(S) AND ADDRESS(ES)
IIT Research Institute
10 West 35 Street
Chicago, IL 60616

8. PERFORMING ORGANIZATON REPORT NUMBERS

M-875

9. SPONSORING/MONITORING AGENCY NAME(S) AND ADDRESS(ES)
National Aeronautics and Space Administration
Washington, DC 20546-0001

10. SPONSORING/MONITORING AGENCY REPORT NUMBER

NASA/CR-1998-208474

11. SUPPLEMENTARY NOTES
Prepared for the Marshall Space Flight Center
Technical Monitor: Jason Vaughn

12a. DISTRIBUTION/AVAILABILITY STATEMENT
Unclassified-Unlimited
Subject Category 29
Standard Distribution

12b. DISTRIBUTION CODE

13. ABSTRACT *(Maximum 200 words)*

The optical characteristics of surfaces on spacecraft are fundamental parameters in controlling its temperature. Passive thermal control coatings with designed solar absorptance and infrared emittance properties have been developed and been in use for some time. In this total space environment, the coating must be stable and maintain its desired optical properties for the course of the mission lifetime. The mission lifetimes are increasing and in our quest to save weight, newer substrates are being integrated which limit electrical grounding schemes. All of this has already added to the existing concerns about spacecraft charging and related spacecraft failures or operational failures. The concern is even greater for thermal control surfaces that are very large. One way of alleviating such concerns is to design new thermal control material systems (TCMS) that can help to mitigate charging via providing charge leakage paths.

The object of this program was to develop two types of passive electrically conductive TCMS.

14. SUBJECT TERMS
Materials, Electrically Conductive Materials, Spacecraft Charging

15. NUMBER OF PAGES
311

16. PRICE CODE
A14

17. SECURITY CLASSIFICATION Unclassified	18. SECURITY CLASSIFICATION OF THIS PAGE Unclassified	19. SECURITY CLASSIFICATION OF ABSTRACT Unclassified	20. LIMITATION OF ABSTRACT Unlimited

NSN 7540 - 01 - 280 - 5500

Mac-Computer Generated

Standard Form 298 (Rev 2-89)
Prescribed by ANSI Std. 239-18